Spatio-temporal variation of Tropical Cyclones in Northern Indian Ocean and its impact on marine fisheries

by

Gopika Gopi

(2016-20-025)

THESIS

Submitted in partial fulfilment of the requirements for the degree of

B.Sc. – M.Sc. (Integrated) Climate Change Adaptation

Faculty of Agriculture

Kerala Agricultural University

COLLEGE OF CLIMATE CHANGE AND ENVIRONMENTAL SCIENCE

VELLANIKKARA, THRISSUR – 680

656 KERALA, INDIA

2021

DECLARATION

I, Gopika Gopi (2016-20-025) hereby declare that this thesis entitled **"Spatio-temporal variations of Tropical Cyclones in Northern Indian Ocean and its impact on marine fisheries"** is a bonafide record of research work done by me during the course of research and the thesis has not previously formed the basis for the award to me of any degree, diploma, associateship, fellowship or other similar title, of any other University or Society.

Place: Vellanikkara
Date: 12-11-2021

Gopika Gopi
(2016-20-025)

CERTIFICATE

Certified that this thesis entitled **"Spatio-temporal variations of Tropical Cyclones in Northern Indian Ocean and its impact on marine fisheries"** is a record of research work done independently by Miss. Gopika Gopi under my guidance and supervision and that it has not previously formed the basis for the award of any degree, diploma, fellowship or associateship to her.

Place: Vellanikkara

Date: 12-11-2021

Dr. Shelton Padua
Scientist
Fishery Environment Management Division (FEMD)
Central Marine Fisheries Research Institute (ICAR-CMFRI)
Ernakulam- 682018

CERTIFICATE

We, the undersigned members of the advisory committee of Miss. Gopika Gopi a candidate for the degree of **B.Sc – M.Sc (Integrated) Climate Change Adaptation** agree that the thesis entitled **"Spatio-temporal variations of Tropical Cyclones in Northern Indian Ocean and its impact on marine fisheries"** may be submitted by Miss.Gopika Gopi in partial fulfillment of the requirement for the degree.

Dr. Shelton Padua
(Chairman, Advisory Committee)
Scientist
Fishery Environment Management Division
Central Marine Fisheries Research Institute (ICAR-CMFRI)
Ernakulam- 682018

Dr. P. O. Nameer
(Member, Advisory Committee)
Dean
College of Climate Change and Environmental science,
Kerala Agricultural University
Vellanikkara, Thrissur-680656

Dr. D. Prema
(Member, Advisory Committee
Principal scientist
Fishery Environment Management Division
ICAR-CMFRI, Ernakulam – 682018

Dr. R. Jeyabaskaran
(Member, Advisory Committee)
Principal scientist
Fishery Environment Management Division
ICAR-CMFRI, Ernakulam – 682018

(EXTERNAL EXAMINER)

ACKNOWLEDGEMENT

*First and foremost, I would like to thank **God** Almighty for giving me the strength and opportunity to undertake this research study and complete it satisfactorily.*

*I would like to express my profound gratitude and obligation to **Dr. Shelton Padua**, Scientist, Fisheries Environment and Management Division, ICAR - Central Marine Fisheries Research Institute, and chairman of my advisory committee. Gratefully I acknowledge his exceptional guidance, constant encouragement, support, patience and time throughout the period of my M.Sc. thesis work. It was a great honor and privilege to work under his guidance.*

I must express my very profound gratitude to my advisory committee members Dr. D Prema Principal Scientist, Fishery Environment Management Division, Dr. R Jayabaskaran, Senior Scientist, Fishery Environment Management Division, Dr. P. O Nameer, Dean, College of Climate Change and Environmental Science, KAU for their constant support and encouragement during my work.

*I respectfully thank **Dr. A. Gopalakrishnan**, Director, Central Marine Fisheries Research Institute to permit me to undertake this work. I would also like to extend huge thanks on **Dr.P. Kaladharan**, Principle Scientist & Head in-charge, Fishery Environment Management division. I would also like to extend huge thanks on **Dr. T. V. Sathianandan**, Principle Scientist & Head in-charge, Fishery Resource Assessment Division for providing necessary data for my work. I would also like to thank Smt. Sindhu K. Augustine & Shri. Paulose Jacob Peter, Technical assistants of FRAD in CMFRI for their valuable and timely suggestions given during my work.*

Let me thank, Achuth Haridas E, Punya P, Resna K., Keziya James (JRF), Ros Kooren (SRF), Shameena M.K (JRF), Liya Benjamin (JRF), Parvathy R. (JRF), Dr. Vineetha Gopinath (PDF) for their help, support and generous care throughout the study. Also I would like to thank my beloved classmates of College of Climate

Change and Environmental Science, KAU for their love and support throughout the period of my study.

I am thankful to ***College of Climate change and Environmental Science*** *for providing me the opportunity and all the amenities to complete the research programme. I received generous support from all the teachers, scientists, staff members and field staff of College of Climate Change and Environmental Science and Fishery Environment Management Division.*

Last, but not the least, I would like to thank my parents and my elder brother for their continuous help, support, steady encouragement and love showered on me during the course of my studies as well as my personal life.

Gopika Gopi

TABLE OF CONTENTS

LIST OF TABLES

LIST OF FIGURES

SYMBOLS AND ABBREVIATIONS

AA	Average Area
ACE	Accumulated Cyclone Energy
ARB	Arabian Sea
BOB	Bay of Bengal
CD	Cyclonic Disturbances
Chl	Chlorophyll
CMFRI	Central Marine Fisheries Research Institute
CP	Climatological Period
CPUE	Catch Per Unit Effort
CS	Cyclonic Storms
CSIRO	Commonwealth Scientific and Industrial Research Organisation
D	Depression
DD	Deep Depression
EICC	East India Coastal Current
ENSO	Elnino/Southern Oscillation
ESCS	Extremely Severe Cyclonic Storm
FAO	Food and Agriculture Organisation
GCM	General Circulation Model
GDP	Gross Domestic Product
IMD	India Meteorological Department

IPCC	Intergovermental Panel on Climate Change
JTWC	Joint Typhoon Warning Center
MC	Mean Catch
MDTN	Multi day trawl net
MGN	Mechanized gillnet
MHL	Mechanized hook and lines
MMT	Million Metric Tons
MOES	Ministry of Earth Science
MOTHS	Mechanized other gears
MPS	Mechanized purse seine
MRS	Mechanized ring seine
MTN	Mechanized trawl net
MRV	Modified Rankine Vortex
MSW	Maximum Sustained Winds
MSSW	Maximum Sustained Surface Winds
NIO	Northern Indian Ocean
NFDB	National Fisheries Development Board
OAD	Overall Average Dissimilarity
OBBS	Outboard boat seine
OBBN	Outboard bag net
OBHL	Outboard hook and lines
OBOTHS	Outboard other gears
OBPS	Outboard purse seine

OBRS	Outboard ring seine
OBSS	Outboard shore seine
OCTS	Ocean Colour and Temparature Scanner
OHC	Oceanic Heat Content
PDI	Power Dissipative Index
QP	Quinquennial Period
RH	Relative Humidity
SCS	Severe Cyclonic Storm
SIO	Southern Indian Ocean
SIMPER	Similarity Percentage
SST	Sea Surface Temperature
SuCS	Super Cyclone
TA	Total area
TC	Total catch
VF	Velocity flux
VWS	Vertical wind shear

CHAPTER-1

INTRODUCTION

Throughout history, the climate has varied dramatically around the world. Since pre-industrial times, the average global temperature has risen by about 1 degree Celsius (MoES, 2020). Modifications in marine and terrestrial ecosystems, melting of sea ice and glaciers, global ocean warming and acidification, sea level rise, variations in precipitation and wind patterns (global monsoon shift), and drastic increase in global weather and climate extremes are already contributed by the warming after industrialization. As a result, climatic extremities or severe incidents are clearly one of the most important effects of climate change. Weather events are becoming more intense in recent years as a result of global climate change. Because catastrophic occurrences have such a large impact on society, it is necessary to comprehend and assess the changes. According to the Fourth Assessment Report of the Intergovernmental Panel on Climate Change, warming of the climate system is unequivocal, and it is highly likely (more than 99 percent confidence) that observed changes are the result of anthropogenic activity. As a result, rising carbon dioxide levels in the atmosphere are creating worldwide climatic shifts that are having, and will continue to have, great influences on marine ecosystem (Johnson and Weltch, 2007)

Extreme weather, as defined by the IPCC, is an event that occurs infrequently at a specific location and time of year. It will become a disaster if society and/or ecosystems fail to successfully cope with an extreme weather event. Floods account for the majority of climate extremes, with cyclones having the most severe effects. The total number of climate extremes is steadily rising. (Singh *et al*., 2010). When it comes to global vulnerability, India is the fifth most vulnerable country, while cyclones are the second most common event (Global Climate Risk Index 2020).

Low-pressure systems that form over tropical and subtropical waters are known as tropical cyclones. At the surface, they are distinguished by structured convection and a well-developed cyclonic circulation. Tropical cyclones are recognised to be the most catastrophic of all natural disasters, resulting in the loss

of human lives as well as widespread economic losses. Cyclones are large, spinning, powerful "tropical storms" that are generally accompanied by dangerous thunderstorms that originate over warm tropical seas. It has a low pressure centre and winds of at least 34 knots. As long as it is over warm water, TC draws energy from the sea surface and maintains its strength. It begin as a depression in warm water, then grow into a full-fledged storm and further in to a cyclone. Strong sea surface temperature (SST) (> 26.5 °C), low vertical wind shear (VWS), high low level vorticity, significant Coriolis force, and high mid-tropospheric relative humidity are six critical thermodynamic and dynamic conditions for the formation of TCs. Cyclonic events can be seen in most tropical ocean basins. According to historical archives, there were roughly 80–90 TCs formed annually in global ocean basins (Gray 1968).

The Northern Indian Ocean (NIO), which produces around 5% of all tropical cyclones in the world, produces four TCs per year, three of which originate in the Bay of Bengal (BOB) and one in the Arabian Sea (ARB). These cyclones cause significant loss of life and property in the NIO rim countries due to a variety of socioeconomic reasons. Stronger TCs with maximum sustained winds (MSW) surpassing 95 nautical miles per hour (knots) and above have been more common in the NIO over the last three decades, (Singh *et al*., 2010). Between 1972 and 2020, 379 cyclonic disturbances, including Depression and Cyclonic Storms, occurred in NIO. 112 Depressions, 110 Deep Depressions, 65 Cyclonic Storms, 28 Severe Cyclonic Storms, 28 Very Severe Cyclonic Storms, 31 Extremely Severe Cyclonic Storms, and 5 Super Cyclonic Storms were among them. The tropical Indian Ocean has more statistically significant surface-warming trends than many other tropical basins, including the Northeast Pacific and North Atlantic (Knutson *et al.*, 2006). This raises the prospect that the sea surface warming trends resulting from global warming will have considerable impacts on the cyclogenesis of Indian Ocean region. According to future forecasts based on theory and high-resolution dynamical models, global warming will trigger a change in the global averaged strength of tropical cyclones toward stronger storms, with intensity increases of 2–11% by 2100 (Knutson *et al.,*2010).

Storm surges connected with severe tropical storms threaten most of the countries surrounding the North Indian Ocean. Storm surge flooding has caused significant damages along the coasts of India, Bangladesh, Myanmar, Pakistan, Sri Lanka, and Oman. On a global basis, climate change is expected to increase tropical storm damage and cost between US$28 and US$68 billion per year by 2100, depending on global warming of between 2.7 and 4.5 degrees Celsius. (Thomas *et al*., 2018).

Tropical cyclones have substantial environmental consequences in addition to economic costs, such as damages to coral reefs, which provide vital ecosystem services such as coastal storm protection. Storminess changes pose a serious threat to the worldwide capture fisheries. On a global scale, fisheries are an essential source of nourishment, livelihood, and cultural identity. Fish supply close to 20% of the animal protein consumed by 3.1 billion people, as well as essential micronutrients, which are especially important for the health of children and pregnant women (Sainsbury *et al*., 2018).

Capture fisheries and aquaculture are projected to provide a living for 12% of the world's population, and 38 million fishermen risk their lives on a daily basis in one of the most dangerous vocations on the planet. Fisheries are vital to global food security and nutrition, and they provide development pathways that can help to make the world more affluent, peaceful, and equitable.

Global fish production reached 179 million tonnes in 2018, with a total first-sale value of USD 401 billion and with 82 million tonnes worth USD 250 billion coming from aquaculture. Human consumption accounted for 156 million tonnes of the total, or to an annual supply of 20.5 kg per inhabitant. The remaining 22 million tonnes were allocated for non-food applications, mostly fishmeal and fish oil production (FAO, 2018). The fisheries sector provides 5.23 percent to the agriculture sector's GDP and 0.91 percent to the country's total GDP. The sector's dynamism can be seen in India's astounding 17-fold increase in fish production over the last six and a half decades, from 0.75 million metric tonnes (MMT) in 1950-51 to 12.6 MMT in 2017-18 (NFDB, 2017-2018).

Coastal habitats are very significant since they produce more than 90% of the food produced by marine ecosystems (Johnson and Weltch, 2007). Changes in storminess put fisheries at danger, as storms disrupt fishing efforts and represent a physical threat to fishermen, their vessels, equipment, as well as fishing communities and infrastructure. Climate change forecasts reveal that rising sea surface temperatures, storm severity, sea level rise, changing rainfall patterns, and nutrient cycling will all be affected as a result of the changing climate. Increased cyclonic events as a result of the climate change will have an impact on habitats and has the potential to ruin important fishing grounds in coastal locations. The loss of this coastal nursery grounds resulted in a decrease in the catch of offshore fishery. Freshwater inflows, sediment re-suspension from storms, and upwelling of nutrient-rich seas, on the other hand, contribute to a rise in primary productivity (Poiner *et al*., 1993).

The Odisha coast was hit by the most cyclones in NIO, resulting in both positive and negative impacts on the fish production. The total marine fish landings along the Odisha coast in 2018 were 89177.5 t, a decrease of roughly 30% from the previous year (126958.2 t). The biggest catch of 322683.8 t was recorded in 2011, followed by a slow fall and the lowest in the year 2018, according to a 12-year analysis of landings from 2007 to 2018. This could be owing to fewer fishing days as a result of natural disasters (CMFRI., 2019).

Cyclonic storms have an impact on fish populations in one way or other. Phytoplankton blooms have been observed in several circumstances, resulting in increased fish abundance and, in some cases, a decline due to obstruction in larval recruitment and destruction of nursery grounds (Hobday *et al*, 2008).

Given the importance of marine fisheries and the vulnerability of marine resources to tropical cyclones, a study, titled "**Spatio-temporal variations of tropical cyclones in NIO and its impact on marine fisheries**," is being conducted with the following goals:

1) To analyse the spatio-temporal variations of Tropical Cyclones in Northern Indian Ocean
2) To assess the impacts of tropical cyclones on selected major marine fish resources.

The present study is an attempt to investigate the spatial and temporal variations of tropical cyclone (TC) activity in the Northern Indian Ocean (NIO) and understanding how storms interact with the marine fishery sector. The information generated from the study can evolve into adaptive action and help to reduce the vulnerability of those dependent on fisheries for their livelihood.

CHAPTER 2

REVIEW OF LITERATURE

2.1 Characteristics of tropical cyclones

Tropical cyclones are one of the most catastrophic phenomena that wreak tremendous harm in terms of lives and property in the country (Mckinnon *et al*., 2003; Zhang *et al*., 2011). A Tropical cyclone is defined by strong winds spiralling inwards towards the centre and a low pressure core. When strong winds from a low pressure system with enough energy and travel to shallow coastal areas, the coastal area is flooded as a result of surge (Maneesha *et al*., 2015).Tropical cyclones are known by various names in different parts of world including Hurricanes in Atlantic ocean and Eastern Pacific Ocean, Cyclones in NIO, Typhoons in western pacific ocean and Willy Willies in Australia (McAdie, 2007).

There could be a link between storm activity and sea surface temperature. SST greater than 26℃ is well known as one of the requirements for cyclone generation in theory (Rana *et al*., 2014; Gray 1968; Royer *et al*., 1998). Coriolis force, low-level troposphere vorticity, relative humidity, vertical shear wind shear, and large-scale circulations are all variables that determine cyclone formation (Maneesha *et al*., 2015; Webster *et al*., 2005; Erick *et al*., 2011). Other factors, like as vertical shear and mid-tropospheric moisture, have been suggested to have a role in determining hurricane characteristics.

Several criteria are being assessed in context of the intensification of tropical cyclones. They are the upper ocean heat content (OHC), environmental wind vertical shear, interactions with other weather systems, dry air impacts, and landfall. When considering the influence of wind shear, a TC approaching an area of strong shear should weaken or even vanish (Jenny *et al*., 2010). Strong vertical wind shear (20 m s^{-1}) and quick TC motion (15 m s^{-1}) reduce TC intensification and result in weaker lifetime peak intensities, according to earlier research (Jenny *et al*., 2010). The interaction of the mature TC with an upper tropospheric vorticity centre (e.g. upper-level trough) can result in TC intensification as these "upper" and "lower"

vortices interact, either directly strengthening the primary TC circulation or causing a secondary wind maxima. Finally, in a heavily sheared environment, a TC can produce a strong, long-lived convective event that leads to fresh surface circulation on the downshear flank of the initial TC, a process known as down-shear reformation. The vertical wind shear also affects the wider TC vortex. TC size has been linked to variations in the impact of environmental vertical wind shear. In the presence of the same vertical wind shear, smaller TC weaken more quickly than larger TC, according to Wong and Chan (2004)'s modelling study (Jenny *et al*., 2010). A TC heading toward a high shear location, for example, would be expected to weaken or even vanish.

2.2 Climate change and cyclone formation

Observations show that the average global ocean temperature has increased by approximately 0.5℃ since 1961 because the oceans have absorbed approximately 80% of the additional heat in the global climate system (Webster *et al*., 2009). Tropical cyclones are considered as giant heat engines so the consensus among the scientists is that rising temperature will cause more intense cyclones and coastal areas will experiences heavy rains associated with dust and thunderstorms (Hussain *et al*., 2011). It is predicted that every 1 degree centigrade of temperature could result in 5% increase in the wind speed of the cyclone. If the earth's temperature increases by 1.5℃ – 4.5℃ , the occurrence of category 4 and 5 cyclones will enhance (Hussain *et al*., 2011; Emmanuel 2005). If the observed increase has only been about 0.5℃, these peak winds should have only increased by 2–3%, and the power dissipation therefore by 6–9% (Emmanuel, 2005).

Among geographic areas, the effects of climate change are expected to differ in both magnitude and direction (Adriaan *et al.,* 2009). Due to greenhouse warming, global mean tropical-cyclone-frequency will either decrease or remain essentially unchanged (Knutson *et al*., 2010). During the past several decades, SST have increased by several tenths of a degree celsius in most regions of Tropical cyclone formation. Recent global climate models indicate that the wind speed of tropical cyclones will increase by 5 to 12% with global warming (Johnson *et al*., 2010).

Temperature has been found to directly affect the metabolism of marine fish species, increasing growth rates and reducing egg incubation time plus other physiological effects (Johnson *et al*., 2010). Ocean warming, as measured by increases in sea surface temperature (SST), can thus cause changes in abundance, local distribution, food webs, predator–prey balance, and the extent of species ranges, all of which can affect the composition and value of fisheries. Poleward shifts in distributions are one of the most commonly observed changes in marine fishes and invertebrates as SST rises (Leitao *et al*., 2018). Hydrostatic pressure variations have been shown to have an effect on marine animals, and research on the subject has been reviewed (Flugel., 1972; Naylor ; Atkinson, 1972).

Variability of large-scale atmospheric circulation, instead of SST, is the main cause of variability in TC activity (Erick *et al*., 2011). IOD may also affect the relationship between TC activity and ENSO by influencing the large-scale parameters, which then either enhance or weaken the favourable conditions for TC genesis and development. Instead of SST, a large percentage of the variations is related to the planetary scale atmospheric circulation and thermodynamic structure caused by the El Nino/Southern Oscillation (ENSO) phenomenon.

2.3 Tropical cyclones in NIO

When considering the Northern Indian Ocean, 5-6% of the total cyclone occurred in NIO, produces about four TCs per year out of which three form in the Bay of Bengal (BOB) and one forms in the Arabian Sea (Maneesha *et al*., 2015). Indian Ocean basin can broadly be divided as North Indian Ocean (NIO) in the northern hemisphere and South Indian Ocean (SIO) in the southern hemisphere. The landmass of Indian subcontinent further divides the NIO region into two basins, Bay of Bengal (BoB) to the east and Arabian Sea (ARB) to the west of Indian subcontinent. The Bay of Bengal is a semi-enclosed tropical ocean basin that receives a large volume of freshwater from both river discharge and rainfall. In addition to monsoon winds and freshwater input, the circulation in the BoB (Friedrich *et al*., 2001) is forced by remote effects from the equatorial Indian Ocean. The BoB has a well-developed anticyclonic gyre and a poleward east India coastal

current (EICC) during the premonsoon months (February–May). During the summer monsoon (June–September), the EICC flows poleward along the Indian coast and equatorward further north (Shetye *et al*., 1993).

Tropical cyclones occur over the Bay of Bengal throughout the year with minimal frequency in winter (December to February) and maximal frequency in October–November. Formation of strong surface stratification observed in Bay of Bengal due to the immense fresh water discharge from major rivers, such as Ganges, Brahmaputra, Godavari. Due to light inhibition by water turbidity, low vertical nutrient supply and cloud cover makes BOB biologically less productive than ARB. (Maneesha *et al*., 2015). The phytoplankton bloom reported here is significant because the BOB is thought to be a low-productivity region in comparison to the Arabian Sea. Stratification caused by freshwater influx is thought to limit nutrient upwelling. However, stratification in the southern BoB is weaker than in the north, and is insufficient to prevent nutrient upwelling (Vinayachandran *et al.,* 2003).

A recent statistical analysis of past cyclone frequency revealed a decrease in the frequency of cyclones in BoB and a small increase in the frequency of cyclones in the ARB (Sebastian and Behera., 2015). Though the frequency of cyclones in the NIO is lower than in other basins, the destructive power of cyclones in this region is greater due to its shallow bathymetry and densely populated coastal area (Maneesha *et al*., 2015). Storm surges associated with severe tropical cyclones pose a threat to countries along the Indian Ocean's northern rim. A recent example is Super Cyclone Phet, which churned the Arabian Sea and hit coastal Gujrat, Rajasthan, and Karachi in June 2010 (Hussain *et al*., 2011).

2.4 Quantifying TC activity

Frequency of occurrence, duration, maximum sustained wind intensity, landfall of the cyclone, surge height, rainfall associated and basin integrated quantities like Accumulated Cyclone Energy (ACE) and Power Dissipative Index (PDI) can be used for measuring the Tropical cyclone activity and Velocity Flux

(VF). ACE is calculated as square of maximum sustained wind speed and PDI is the cube of maximum sustained wind speed which measures the destructive potential of a tropical cyclone (Maneesha *et al*., 2015). In the NIO region, the ACE, PDI and VF shows an increasing trend (Mohapatra and Vijayakumar, 2017).

2.5 Recent trends

In terms of global tropical cyclone frequency, it was resolved that there was no significant change in global tropical storm or hurricane numbers from 1970 to 2004. On this time period, the global number of the most severe tropical cyclones (Category 4 and 5 on the Saffir–Simpson scale) increased significantly (nearly doubling). With projected twenty-first-century warming, some increase in the mean maximum wind speed of tropical cyclones is likely, though increases may not occur in all tropical regions. Rainfall associated with tropical cyclone is expected to increase as the planet warms. But, there is no conclusive evidence that any observed changes in tropical cyclone genesis, tracks, duration, and surge flooding exceed the natural variability (Knutson *et al*., 2010).

When considering the Arabian Sea, anthropogenic global warming has increased the likelihood of post-monsoon ESCSs and the results of the GCMs showed an increase in cyclonic intensity while the frequency of the cyclones was either decreased or remained unchanged (Maneesha *et al*., 2015). It was also supported by other literatures like the number and proportion of hurricanes reaching category 4 and 5 have increased significantly (Knutson *et al*., 2010 and Webster *et al*., 2005). Cyclones with wind speeds greater than 100 km/h were labelled as the "most intense cyclones." The study conducted by Emmanuel, 2005 and Webster *et al*., 2005 found a fivefold increase in the occurrence of intense cyclones in the Arabian Sea over the previous 12 years (1995–2007) compared to the previous 25 years (1970–1995) and along with an increase in the "number" of severe cyclone occurrences, the "intensity" of these cyclones increased over time. In a warming environment, such intensification and occurrence of severe cyclones in the tropics has increased (from around 20 percent to around 35 percent, particularly in the Atlantic and Indian Oceans (Emanuel 2005; Webster *et al*., 2005) whereas the sum

of hurricane categories 2 and 3 has a small trend, both in terms of number and percentage (Webster et al.,2005).

Changes in tropical cyclone intensity can be divided into two categories: changes caused by changing environmental conditions and internal fluctuations caused by storm-scale instabilities or the stochastic effects of high-frequency transients such as moist convection. The majority of literature on hurricane intensity focuses on the prestorm thermodynamic environment and specific atmospheric properties, such as vertical shear of the horizontal wind and dynamical features, such as upper troposphere disturbances. It is well known that hurricanes change the surface temperature of the ocean. It has also been noted that a drop in ocean surface temperature near the core of the storm would be enough to completely shut down energy production (Emanuel *et al*., 2004).

Following the passage of Cyclone Sidr, surface cooling of 2°C–3°C was observed in the central Bay of Bengal along the cyclone track. These findings are consistent with previous research, which found a 2°C–7°C decrease in SST. Smitha *et al*. (2006), for example, reported that the May 2003 (11–19) cyclone in the Bay of Bengal cooled SST by 4°C–5°C. The surface layer was cooled as a result of the cyclone Sidr's wind-forced upwelling (Maneesha *et al*.,2015).

2.6 Future predictions

Research on possible future changes in hurricane frequency as a result of global warming is inconclusive, with most studies indicating that future changes will be regionally dependent, with an increase or decrease in total number of storms (Hussain *et al*.,2011).

Globally, the frequency of weak (intense) storms will decrease (increase) in the future (Knutson *et al*., 2010; Webster *et al*., 2005). During the post-monsoon season, the average location of tropical storms may shift westward over the North Indian Ocean, resulting in an increased (decreased) frequency of tropical storms over the ARB (Bay of Bengal). Anthropogenic global warming has increased the

likelihood of post-monsoon ESCSs over the ARB and is a major contributor to recent (2014 and 2015) observations in this regard (Webster *et al*., 2005).

Data from around the world show a 30-year trend toward more frequent and intense TCs. Human-caused environmental changes are expected to affect TC intensity and rainfall, but the effects on TC numbers are still unknown (Zhang *et al*.,2011). The expected average warming in the tropical band as a result of greenhouse gas emissions over the next century can thus be expected to have an impact on the genesis, frequency, and intensity of TCs (Royer *et al*., 1998).

2.7 Impact on fisheries sector

Almost all storms that occur on the world's oceans last only a few days, but the physical and biological effects of the perturbation can last for several weeks (Madhu *et al.*, 2002 ; Sarma *et al*., 2019). Almost 80% of the world's fisheries species are currently considered to be at or near their harvest capacity, and the proportion of overexploited, depleted, and recovering stocks has remained constant over the last 10–15 years. The region up to 200 m depth was assigned as highly productive coastal waters that are likely to serve as spawning sites (for adult fish stock) as swell as feeding grounds for fish larvae, juveniles and adults (George *et al.*, 2019). Overall, global marine fisheries catches decreased by 2.6 million tonnes, supplying approximately 82 million tonnes of food fish to the world, with a per capita supply of 8.9 kg (live weight equivalent; FAO, 2008a). Coastal ecosystems produce more than 90% of the food provided by marine ecosystems, making them especially important given that half of the world's marine fisheries catch is captured in less than 10% of the ocean. Temperature is an important factor in all regions due to its pervasive effect on organisms. Because of the effect of stratification on the vertical structure of marine ecosystems and bottom-up processes, stratification (the result of the interaction between temperature and wind forcing) will be an important factor in all regions. Aside from mixing and water circulation in the open ocean, changes in wind strength and direction influence the strength of the upwelling along the coastal region and shelf (Adriaan *et al*., 2019).

Mangroves have suffered severe damages as a result of Orissa Super Cyclone (Nayak *et al*., 2001). Cyclones also affect the seagrass communities. Rapid changes were observed in shelf waters and pelagic communities on Australia's southern Northwest Shelf as a result of tropical cyclones (McKinnon *et al*., 2003; Poiner *et al*.,1993). Seagrass areas form important habitats for many marine animals, providing protection from predators and strong currents and contributing significantly to the food cycle of coastal ecosystems. According to CSIRO research, seagrass communities are the primary nursery grounds for juvenile tiger prawns (*Penaeus esculentus* and *P. semisulcatus*) and should be protected. Cyclone 'Sandy' removed approximately 183 km of seagrass from the Gulf of Carpentaria, affecting juvenile prawn populations. Tiger prawn catches in this area have consistently been lower than in unaffected areas (Poiner *et al*.,1993). The extreme hydrodynamic force exerted by tropical cyclones has a significant impact on coral reefs. Because of the vulnerable condition of the reef lagoon's unconsolidated sediments, the coral reef system has a long-term impact (Riddle 1988).

More frequent climate and oceanographic extremes may destabilise existing trophic links, favouring shorter-lived, high-turnover fish species at higher trophic levels and resulting in increased spatial and temporal variability of plankton productivity. The impact of changes in plankton communities on the pelagic larvae of important fisheries target species is a critical issue. Fish larvae spend days to months in the plankton, whereas important fishery invertebrates like crustaceans spend months in the plankton before settling (Hobday *et al*., 2008). Starvation is thought to be a major contributor to mortality during the larval period, especially as larval duration increases, and shifts between low-nutrient and high-nutrient plankton communities may have a significant impact on fish larvae survival (McKinnon *et al*., 2003 and Johnson *et al*., 2010). Such a shift is likely to increase variability in population recruitment dynamics. A mismatch between fish reproduction and periods of high plankton productivity could have a significant impact on fish population replenishment (Johnson *et al*., 2010).

In bottom or reef-associated fish communities, cyclones cause increased juvenile mortality and re-distribution of site-attached subadults. These disturbances are temporary, with recovery times ranging from a few weeks for soft sediment infauna (Riddle, 1988) to decades for slow-growing hard coral and seagrass communities (McKinnon *et al*., 2003)

2.8 Some positive impacts

SST cooling is an important effect of TC on the upper ocean. The surface flux of latent and sensible heat in the atmosphere causes 20% of the cooling, whereas vertical mixing of the base of the oceanic mixed layer causes 80% of the cooling (Smitha *et al*.,2006). The Bay of Bengal region is known to be less productive than the Arabian Sea due to cloud cover, light inhibition by water turbidity, and low vertical nutrient supply (Maneesha *et al*., 2015), whereas the Arabian Sea is highly productive due to open ocean upwelling, mixing, and lateral advection, whereas high productivity along India's southwest coast in summer is primarily due to coastal upwelling (Smitha *et al*., 2006; Madhu *et al*., 2002).

On October 29, 1999, the Orissa coast was hit by a severe cyclone with winds exceeding 200 km/hr, and there was an increase in chlorophyll concentration in the post-monsoon period compared to the pre-monsoon period in Orissa. This was due to cyclonic wind stresses and land influxes. The Orissa coast had undergone rapid changes as a result of abnormally high sediment settling from offshore storm surges as well as receding flood water (Nayak *et al*., 2001). Extreme winds and cyclones have an effect on the ocean. It has the potential to improve upwelling, primary production, and, eventually, fish productivity. Deep-water species will also migrate to the shelf seas as a result of this effect. Increased warming will cause earlier stratification of water masses within shelf areas (if not offset by increased wind mixing), affecting the timing of the spring bloom as well as the level and composition of primary production (Adriaan *et al*.,2019).

Nayak *et al*., (2001) discovered that Chl a concentrations increased (5–10 times) along the central west coast of the Bay of Bengal after nutrients were

supplied by a super cyclone (25–29 October 1999). Madhu *et al*., (2002) noted that the super cyclone of 1999 increased nutrient concentrations (nitrate by 1 M) and, as a result, primary production (by 21 to 955 mgC m2 d1) in the southwestern Bay of Bengal. The cyclone's strong winds churn up the upper ocean, increasing the supply of nutrients to the surface. In November 2007, phytoplankton blooms were supported by nutrients supplied by both vertical mixing of water aided by heavy winds and land drainage associated with cyclone Sidr along the west coast of the Bay of Bengal. From this, it can be deduced that cyclones that hit either the east coast or the northern coast (West Bengal and Bangladesh) during the October–December period may cause phytoplankton blooms all along the east Indian coast within a few days, aided by EICC (Maneesha *et al*., 2015 and Vinayachandran *et al*., 2003). Cyclones, which are common during this time, cause intense blooms in the western Bay of Bengal. The extent and intensity of the bloom offshore vary from year to year. Phytoplankton blooms as a result of the cyclonic gyre caused by EP. Cyclones amplify the bloom in their area of influence. In contrast, chl a levels are found to be relatively low during cyclone-free years (Vinayachandran *et al*., 2003).

Cyclonic wind stress promotes vertical mixing and evaporation, lowering surface temperatures along the cyclone's path. Nutrient inputs from sediment disturbance and river runoff frequently cause regional-scale phytoplankton blooms in coastal waters (Delesalle et al., 1993; Furnas, 1989). These post-cyclone blooms have ramifications for pelagic communities. McKinnon (1993) discovered an increase in copepod egg production rates following post-cyclone floods, as well as an increase in zooplankton abundance. The flood plume translocated coastal fish communities, but the effects appear to be taxon-specific and transient (McKinnon *et al*., 2003).

Following the cyclone, the composition of larval fish catches changed at all shelf stations. The appearance of larvae from many families that were underrepresented in light trap catches prior to the cyclone caused the most noticeable changes near the shelfbreak. It was discovered that strong cross-shelf

winds associated with storms in the Bahamas were followed by an increase in settlement by coral reef fishes such as the Nassau grouper (*Epinephelus striatus*). In this case, a single four-day storm was responsible for 86 percent of total annual recruitment (Mckinnon *et al*., 2003)

2.9 Socio-economic impacts

In recent years, tropical cyclones have caused significant increases in economic damage and disruption. Rising coastal populations and the increasing value of coastal infrastructure are the primary causes of this. In developing countries, in particular, population migration to the coast is caused by social factors that are difficult to address. Climate change is thus one of several factors that are likely to influence the future evolution of tropical cyclone damage. The vulnerability of coastal regions to tropical cyclone storm-surge flooding is expected to increase with future sea-level rise and coastal development, though this vulnerability will also depend on future storm characteristics (Knutson *et al*., 2010).

The socioeconomic consequences for countries visited by TCs can be dramatic, resulting in the loss of human life and the destruction of infrastructure and agriculture.

A cyclone struck Bangladesh in 1991, killing 138,000 people. The ecological perturbation caused by large-scale tree destruction by strong winds can alter the structure and composition of some tropical forests (such as those in the Caribbean), and it has been estimated that commercial wood species might be reduced by increased hurricane disturbances. The annual global damage caused by the 80 or so TCs each year is estimated to be around $1.5 billion, with an average death toll of 15,000 to 23,000 human lives, and thus any increase in TC frequency in a warmer climate would have very significant human and economic consequences (Royer *et al*., 1998).

CHAPTER 3

MATERIALS AND METHODS

Tropical cyclones which have occurred in the Northern Indian Ocean region since 1986 and their impacts on marine fisheries have been assessed for the climatological period (CP) from 1986 to 2015 and the quinquennial period (QP) from 2016 to 2020. The strategies used to achieve the goals of this project are mentioned below. The paper is organised into two sections: 1) spatial and temporal variations of tropical cyclones in NIO, and 2) their impacts on marine fisheries along the Odisha coast. The details of data collection and analysis, as well as the statistical packages utilised for various analyses, are described in this chapter.

Study area

The area considered for the study is Northern Indian Ocean between 0° N and 30° N latitudes and 50° E and 100° E longitudes.

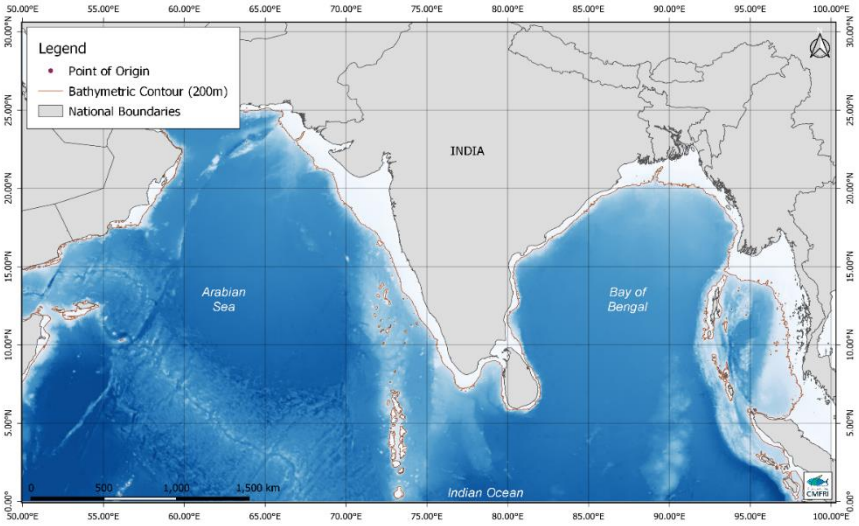

Fig 3.1 Location of study area-Northern Indian Ocean

3.1 Tropical cyclone data

The best track data of tropical cyclones with detailed information about location and intensity for the Northern Indian Ocean with every 6 hr interval from 1986-2020 was downloaded from the Indian Meteorological Department (IMD) available at https://rsmcnewdelhi.imd.gov.in/report.php?internal_menu=MzM=1. This track data was compared with JTWC best track data available at https://www.metoc.navy.mil/jtwc/jtwc.html to avoid the mislaid of any event.

Software used

QGIS 3.16.1, R 4.1.0, PAST 4.03 and MS-EXCEL were used for the analysis. The path of cyclones along the Northern Indian Ocean region was tracked and wind fields of >=52 km/hr were drawn for CDs for the study period using QGIS software.

Parametric modeling of tropical cyclone wind fields

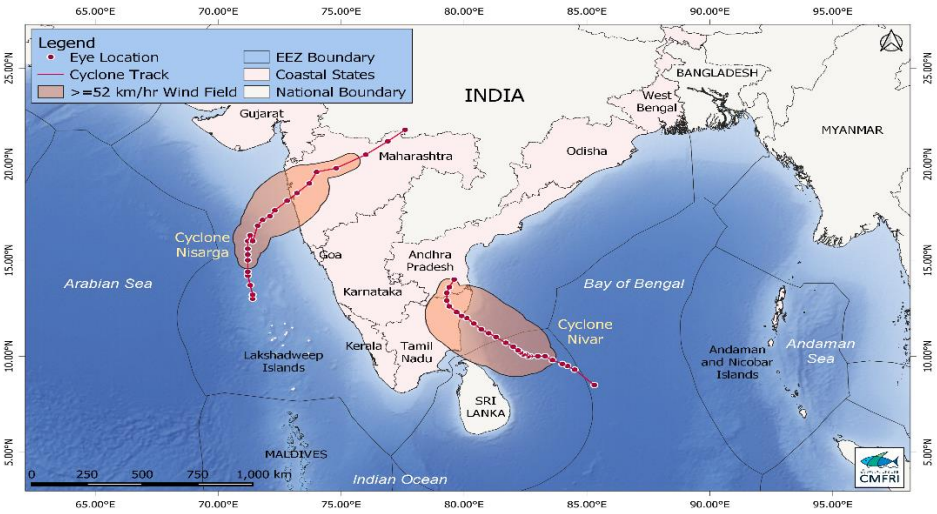

Fig 3.2 Cyclone track and wind field of cylones Nisarga and Nivar in NIO

In a parametric model, the wind field of an apotheosize stationary or real-time moving storm is represented as a wind profile. The wind speed is zero in the storm's core, quickly climbs to its maximum at the R_{mw}, and then drops to zero at wide radii (Das *et al.*, 2018). Various types of wind models are utilised in different places

to generate TC wind fields. For the generation of wind fields in this work, we used Modified Rankine Vortex (MRV).

Modified Rankine Vortex (MRV)

Depperman was the one who first proposed the MRV wind profile parametric model (Das *et al.,* 2018). It is made up of a solid rotating body region with constant vorticity circulation and a centre with zero vorticity circulation (Holland *et al*., 2010). In this model, the value of x is determined to be in the range of 0.4-0.6 for each wind radii threshold (i.e., 34, 50, and 64 kt), where the wind field is a function of the intensity, V_{Max} radius r, and a shape parameter x. x =0.5 was employed in several additional research.

$$V = V_{Max}\left(\frac{R_{mw}}{R}\right)^{x} \quad for\ r \geq R_{mw} \qquad \text{(Das } et\ al.\text{, 2018)}$$

For the majority of historical cyclones, R_{mw} is a unknown input. Therefore Spentza *et al.,* (2012) the first who assumed a general relationship in the following form.

$$R_{mw} = exp(A(V_{Max}) + B(Lat) + C) \qquad \text{(Spentza } et\ al.,\text{ 2012)}$$

Where the values of A, B, and C are determined using error least square minimisation. For the Northern Indian Ocean the values are: A=-0.0142, B=-0.0148, C= 4.1497 (Spentza *et al.,* 2012).

According to IMD classification, TCs are classified into different categories based on Maximum Sustained Wind (MSW) speed, which is listed in Table 3.1.

Table3.1 Categorisation of tropical cyclones by IMD

Type	Wind speed in km/h	Wind speed in knot (mps)
Low Pressure Area	Less than 31	Less than 17
Depression	31-49	17-27
Deep Depression	50-61	28-33
Cyclonic Storm	62-88	34-47

Severe Cyclonic Storm	89-118	48-63
Very Severe Cyclonic Storm	119-165	64-89
Extremely Severe Cyclonic Storm	166-220	90-119
Super Cyclonic storm	221 or more	120 or more

During the period 1986-2020, the number of cyclonic disturbances and total area affected along the Northern Indian Ocean, including the Arabian Sea and Bay of Bengal, are examined. According to the IMD categorization, a year is divided into four seasons: winter (January–February), pre-monsoon (March–May), monsoon (June–September), and post-monsoon (October–December). The Tropical Cyclone Days were calculated by multiplying the duration in days of each CDs by 24 and adding them up for the season.

The full impact of cyclonic disturbances cannot be determined by the number of tropical storms or the region affected. As a result, the overall cyclonic activity is determined using Velocity Flux (VF), Accumulated Cyclone Energy (ACE) and Power Dissipation Index (PDI). The goal of this study was to see if there was a pattern in VF, ACE, and PDI during the CP as well as in the QP in the NIO region.

Velocity Flux

$$VF = V_{max}$$ (Mohapatra *et al.,* 2017)

where V max is intensity (MSW) of TC.

Accumulated Cyclone Energy

The ACE is a metric for expressing tropical cyclone activity.

$$ACE = V^2{}_{max}$$ (Mohapatra *et al.,* 2017)

with units (10^4 kt^2), where V max is the TC's maximum intensity (MSW)

Power Dissipation Index

The destructive power of a tropical cyclone is measured by the cube of the cyclone's maximum sustained wind speed over the course of its life. It aids in determining the cyclonic activity's level of activity.

$$PDI = \sum Vmax^3$$ (Mohapatra *et al.,* 2017)

For each TC/CD, the above parameters were calculated every six hours. Interannual variation of tropical cyclone energy metrics over the North Indian Ocean was divided into two categories: I) all Cyclonic Depressions (including D and DD) and (ii) all Tropical Cyclones (CS, SCS, VSCS, ESCS, and SuCS) in various seasons, including winter, premonsoon, monsoon, and post-monsoon seasons, and the year as a whole over the AS, BOB and NIO. Furthermore, linear trend analyses were performed on the time series of VF, ACE, and PDI of CDs and TCs developed during various seasons and years across the BOB, AS, and NIO. The ACE and PDI calculations provide a more accurate picture of the tropical storm season's strength. For the NIO, including the Bay of Bengal and the Arabian Sea, ACE and PDI were estimated independently for each TC during a month, season, and year. The total distance travelled by a TC was measured from the first (genesis location) to the last observation point (dissipation) in the dataset and the point of origin was extracted and plotted seasonwise to find out the spatial distribution of cyclogenesis location in NIO during CP and QP.

Depth and morphology analysis

The morphology and depth of cyclone formation were plotted by season and monthly to find out the existence of any relationship or trend.

Terrain Ruggedness Index

TRI indicates how jagged or flat the terrain is on average. Ruggedness is measured in metres of elevation difference for grid points 30 arc-seconds (926

metres on the equator or any meridian) apart. Higher the ruggedness, higher will be the TRI.

3.2 Fisheries data

Because the Odisha coast saw the greatest number of cyclones, Odisha coast was chosen for this investigation to assess the impacts of cyclonic storms on marine fisheries. In this study, cyclonic disturbances that crossed Odisha with intensity of >=34 kt are considered and there were 12 cyclones that fall in this category.

The catch variation of fish species in the Odisha coast is analysed from the data supplied by the NMFDC of ICAR-CMFRI. The resource assemblage of the species along the Odisha coast was also analysed from catch data and the abundance of fish species was estimated by calculating the Catch Per Unit Effort (CPUE). The major marine resources considered in the present study include the economically important species in Odisha coast, such as *Sardinella fimbriata, Rastrelliger kanagurta, Trichiurus lepturus, Tenulosa ilisha,* and *Lepturacanthus savala.*

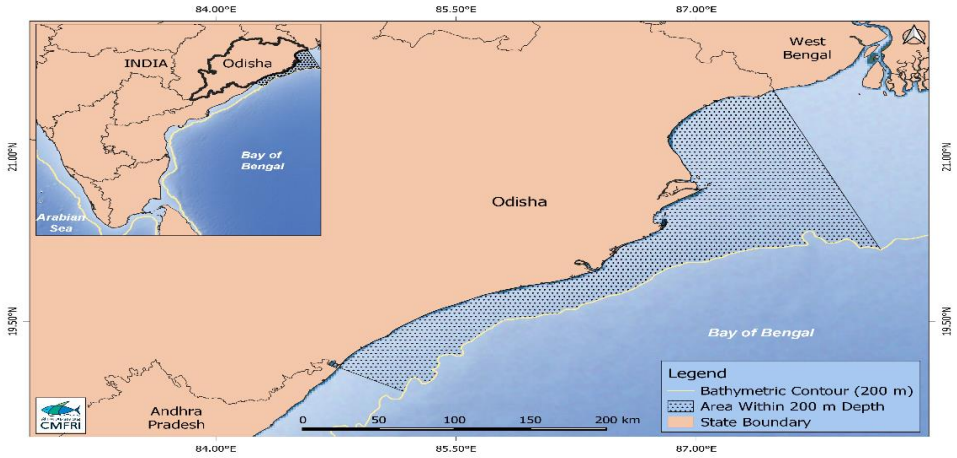

Figure 3.3: Location of the study area- Odisha coast. The study region (stippled area) is enclosed by the coastline on the west and 200 m isobath on the east.

The gears that are considered in this study belong to different groups, which are shown in Table 3.2.

Table 3.2 Types of Gears

Mechanised	**Motorized**
Multi day trawl net	Outboard bag net
Mechanized gillnet	Outboard boat seine
Mechanized hook and lines	Outboard gillnet
Mechanized purse seine	Outboard hook and line
Mechanized ring seine	Outboard purse seine
Mechanised trawl net	Outboard ring seine
	Outboard Shore seine

Apart from these, other gears are sometimes observed and these are mechanized other gears (MOTHS) and outboard other gears (OBOTHS).

The catch varies depending on the area of operation and the type of gear used. The continental shelf region is more productive than any other region in the sea and this region comprises a wide variety of organisms. The catch is caught from nearshore through NM and most outboard crafts and gears differ mechanised crafts such as trawl nets which operates in distant waters and the species caught are different. Depending on the depth of operation, the fish caught can be pelagic, that live in the water column itself, or demersal, that live in the lower water column, or benthic, that live near the sea bed.

The National Marine Fisheries Data Centre (NMFDC) of the Central Marine Fisheries Research Institute (CMFRI), Kochi, India, collects fisheries data such as total catch by resource, gear, and district, number of units operating (Effort), and real fishing hours. This data is gathered using a scientific sampling scheme devised by CMFRI termed stratified multi-stage random sampling design. In this system, trained observers collect data on landings of various resources, the number of fishing days, and the number of units operated per month from all landing centres along the Indian coast from 16 to 18 days of each month and this information is derived to get the monthly estimate of every coast (Srinath *et al*., 2005). The data

for the Odisha Coast from the period 2007-2020 was extracted from this and used for this study.

Catch Per Unit Effort (CPUE)

CPUE is a measure of the abundance of fish resources and their level of utilisation. CPUE indirectly indicates fish stock variation and provides a better understanding of fish resources than catch data alone (Richards *et al*., 1992). It is calculated as the proportion of total catch to total effort.

$$\text{CPUE} = \text{Total Catch} \div \text{Effort}$$

Total catch is the weight of fish biomass in kilogrammes, and effort is the time spent in the water by the fishing vessel. The six districts of Balasore, Bhadrak, Kendrapara, Jagatsingpur, Puri, and Ganjam were chosen from 2007 to 2020 to examine the consequences of Tropical Cyclones on fish resources along the Odisha coast. For the state of Odisha, CPUE was estimated district-by-district and gear-by-gear. During the period 2007-2020, large cyclonic events with wind speed more than or equal to 34 kt occurred along the Odisha coast, and the CPUE of the selected species were calculated to determine the impact of the associated tropical Cyclones, if any.

SIMPER (Similarity Percentage)

This analysis was done to see how the species composition changed before and after the cyclonic event (Demestre *et al*., 2000). For the requisite period, the Bray–Curtis dissimilarity was estimated, as well as the average dissimilarity between all species.

The dissimilariy of the species in A (Month in which cyclone is formed) and A1(cyclone unaffected month), B (next month after cyclone forming month) and B1(corresponding unaffected month), C (the second next month after the cyclone month) and C1(corresponding unaffected month), D (the third next month after the

cyclone month) and D1(corresponding unaffected month). The five major species which had a higher contribution to the Overall Average Dissimilarity were studied.

Spearman correlation test

A statistical measure of the strength of a monotonic link between paired data is Spearman's correlation coefficient. The value of a Spearman correlation coefficient might range from 1 to +1. A positive correlation is indicated by +1, a negative correlation by -1, and no correlation by 0 (Fritz., 1974). In this investigation, the Spearman correlation test was done in R to determine whether or not there was any correlation in the area affected both land and ocean during the cyclonic event and the catch for the selected species in Odisha between 2007-2020.

3.3 Chlorophyll-a concentration (Chl-a)

Global ocean colour data from 2007 to 2020 were obtained from the Ocean Colour Climate Change Initiative (OC-CCI) website (https://www.oceancolour.org/). Chlorophyll data were downloaded as NC files with a spatial resolution of 4x4km.

CHAPTER 4

RESULTS

4.1 Spatial distribution of TC in NIO

4.1.1 Spatial distribution of location of origins of CDs during CP and QP

During the climatological period (1986-2015), the distribution of genesis locations of CDs formed in the NIO region is depicted in fig. 1a. TCs were formed throughout the NIO and made landfall along the shores of India, Bangladesh, Myanmar, Sri Lanka, and Oman. The majority of CDs were produced between 5° N-20° N latitude. In the lower latitudes, a few CDs formed. The formation of CDs increases with latitude and then diminishes. A longitudinal variation could be observed here. Between 85°E-90°E in BOB and 65°-70°E in AS, the most of the CDs were formed. In terms of both latitude and longitude, BOB experienced more CD formation than ARB. A similar pattern may also be seen in QP (Fig.1a and Fig.1b).

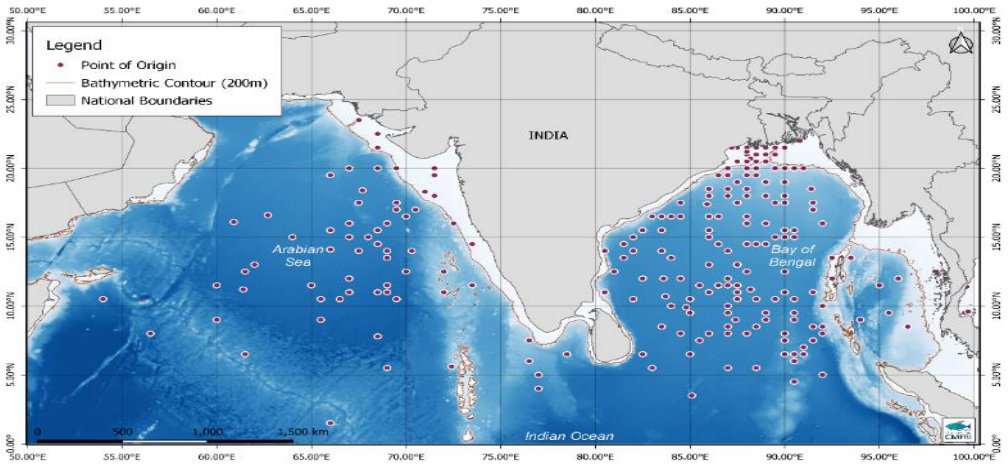

Fig.1a. Annual distribution of genesis locations of CDs formed in the NIO during CP

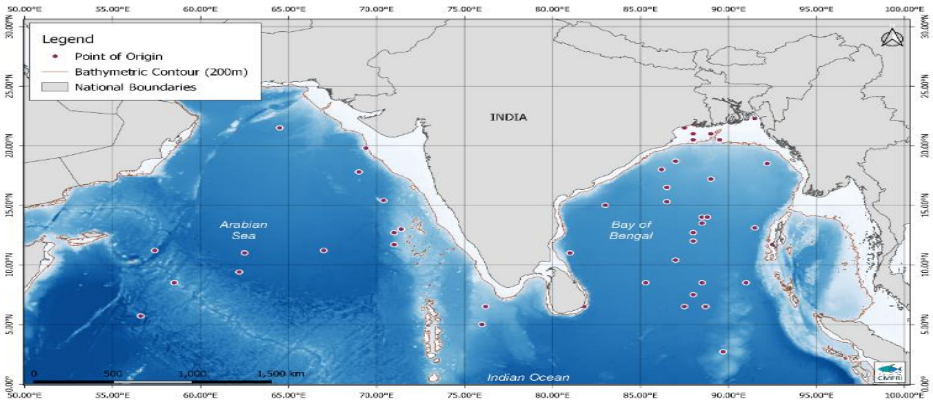

Fig.1b. Annual distribution of genesis locations of CDs formed in the NIO during QP

4.1.2 Seasonal and monthly distribution

The seasonal distribution of CD genesis locations in the NIO is depicted in Figure.2a-d. The frequency of CDs is substantially lower during the winter season, and the most of them are generated in BOB. CDs become more common in the pre-monsoon season, and their genesis place shifts northward. The majority of CDs were generated between 5 and 15^{o} N latitude during this season. This genesis place has again shifted northwards during the monsoon season and there was an increase in the frequency also, with the majority of them forming between 15-20^{o} N latitude in both BOB and AS. The frequency of CDs rises dramatically during the post-monsoon season, forming in all regions of the NIO. Landfall affects the entire eastern and western coasts. The winter season is fully free from CDs during QP (Fig.4a-d) and other seasons follow the same trend as that of CP. Figs.3a-l depicts the monthly distribution of CD genesis locations in NIO during the CP. There were significant variations in the TCs' genesis locations and tracks during different months. The average genesis location of NIO CDs almost exactly followed the Sun's northward and southward shifting (Mohapatra *et al*., 2019). From January to August, the average genesis location of TCs shifted northward, then southward continuously. The smallest number of CDs can be seen in February and March, while the highest frequency can be seen in October and November. (Fig.5.a-l).

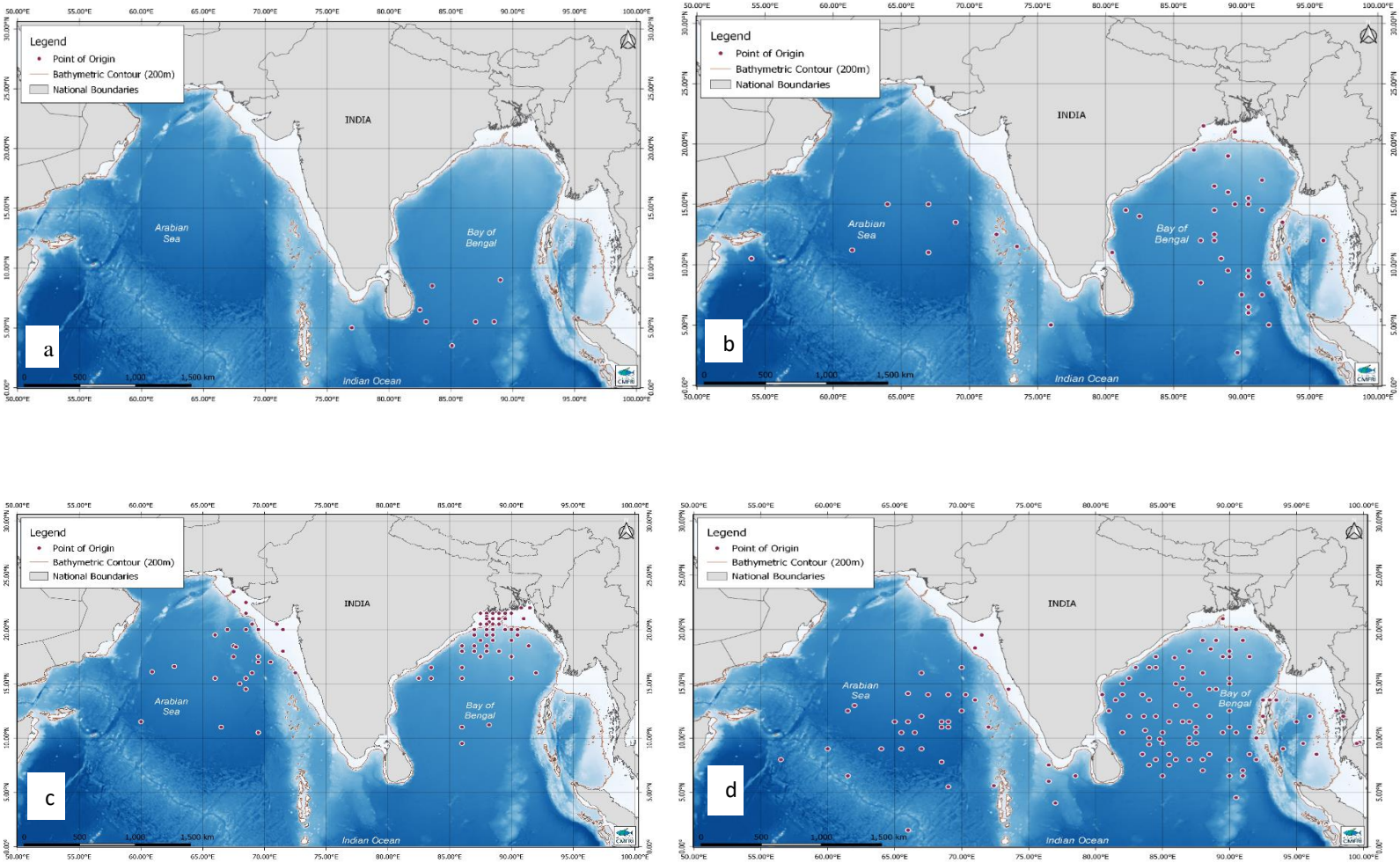

Fig.2. Seasonal distribution of genesis locations of CDs in the NIO during CP- a) Winter, b) Pre- Monsoon, c) Monsoon, d) Post-Monsoon

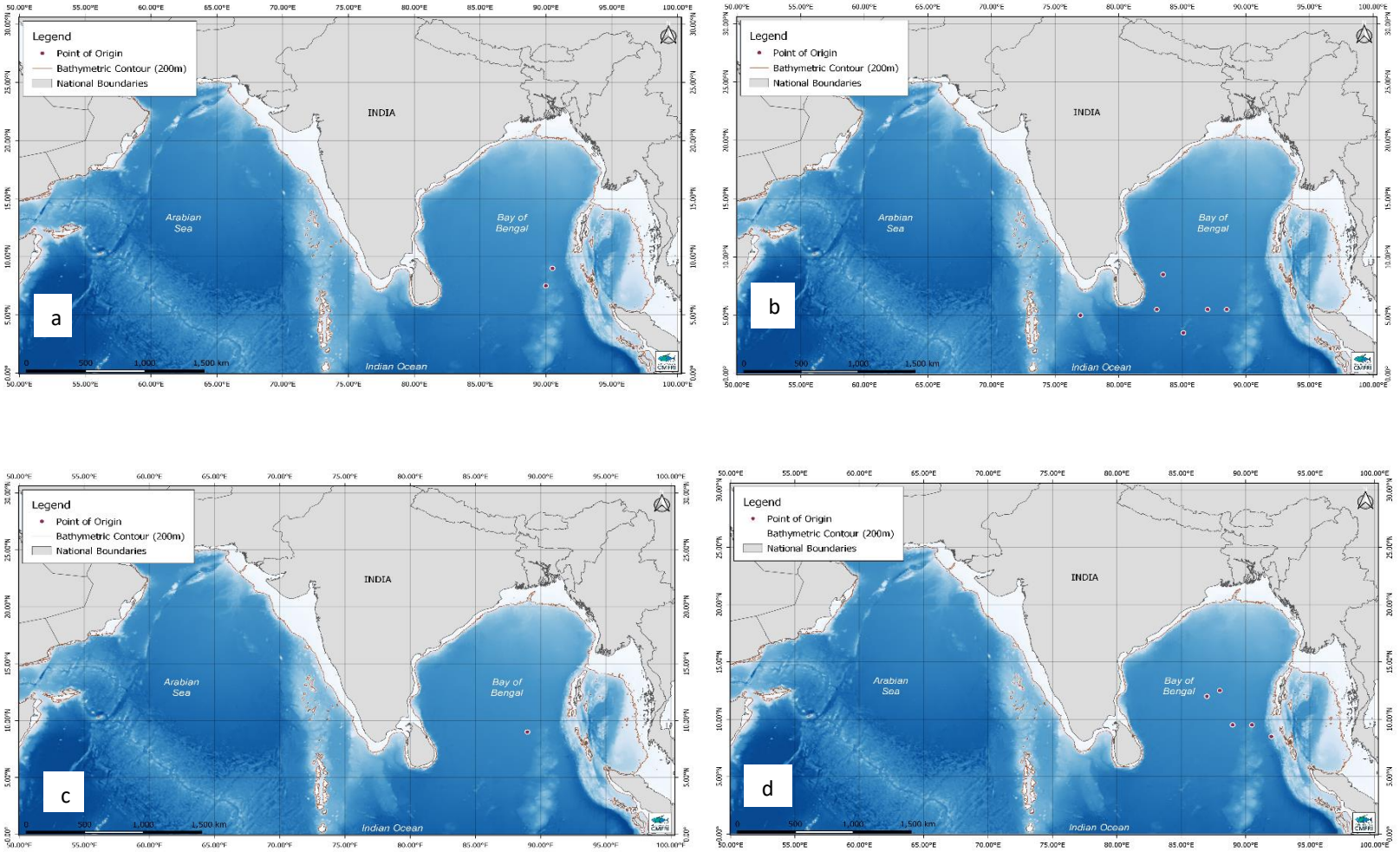

Fig.3 i.Monthly distribution of genesis location of CDs in NIO during CP-a) January, b) February, c) March, d) April

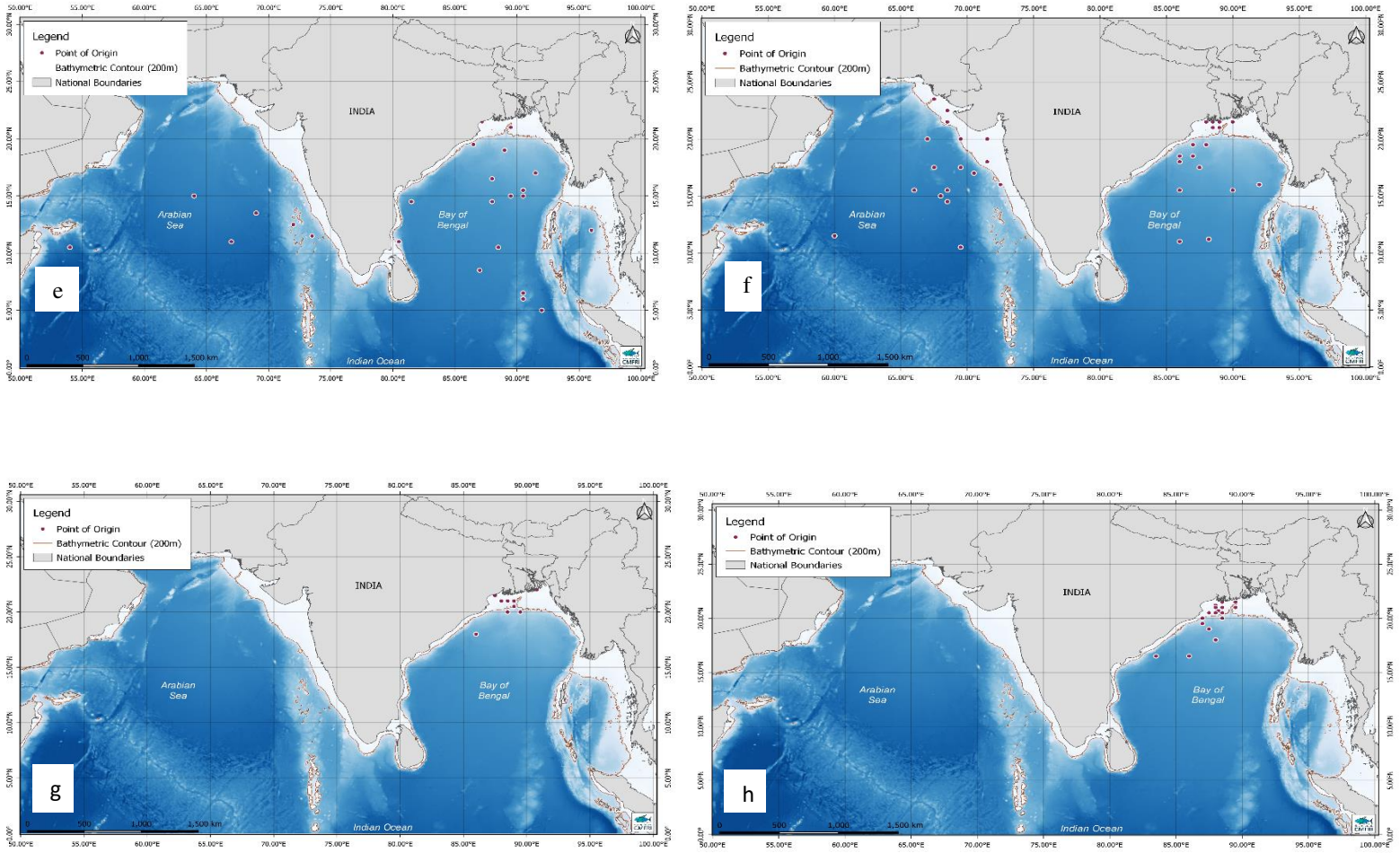

Fig.3 ii.Monthly distribution of genesis location of CDs in NIO during CP - e) May, f) June, g) July, h) August

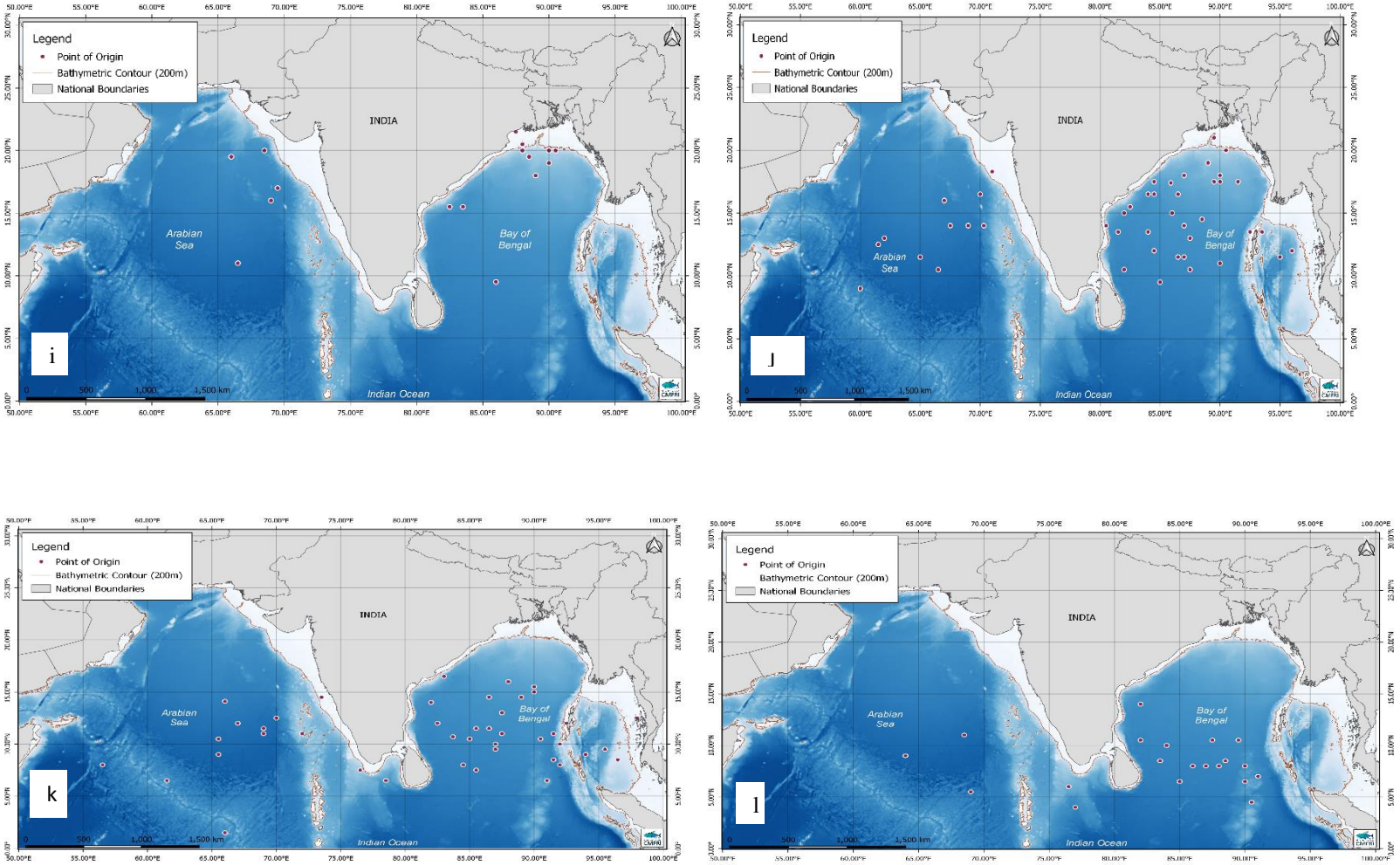

Fig.3 iii.Monthly distribution of genesis location of CDs in NIO during CP i)September, j) October, k) November l) December

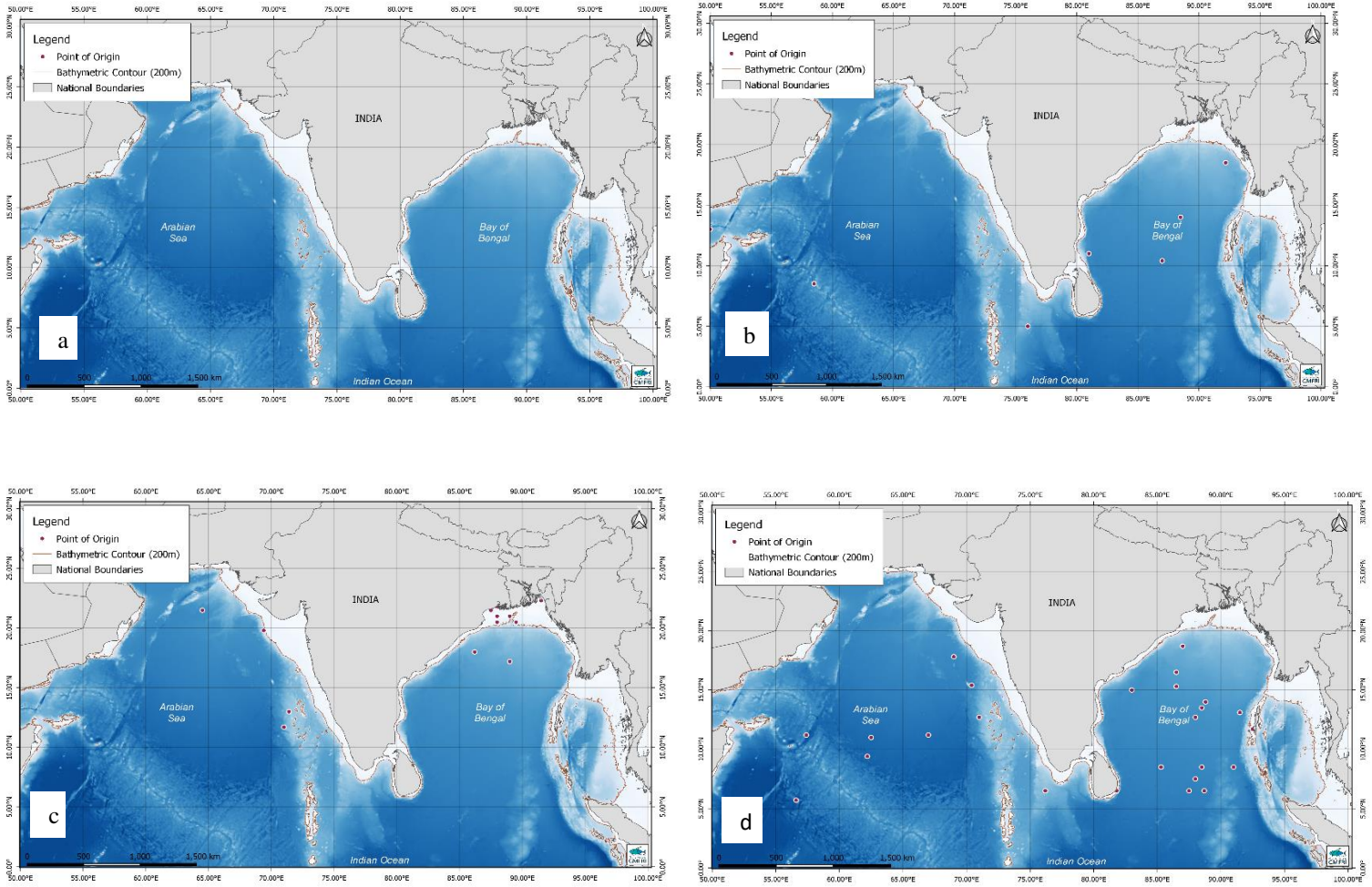

Fig.4. Seasonal distribution of genesis locations of CDs in the NIO during QP- a) Winter, b) Pre- Monsoon, c) Monsoon, d) Post-Monsoon

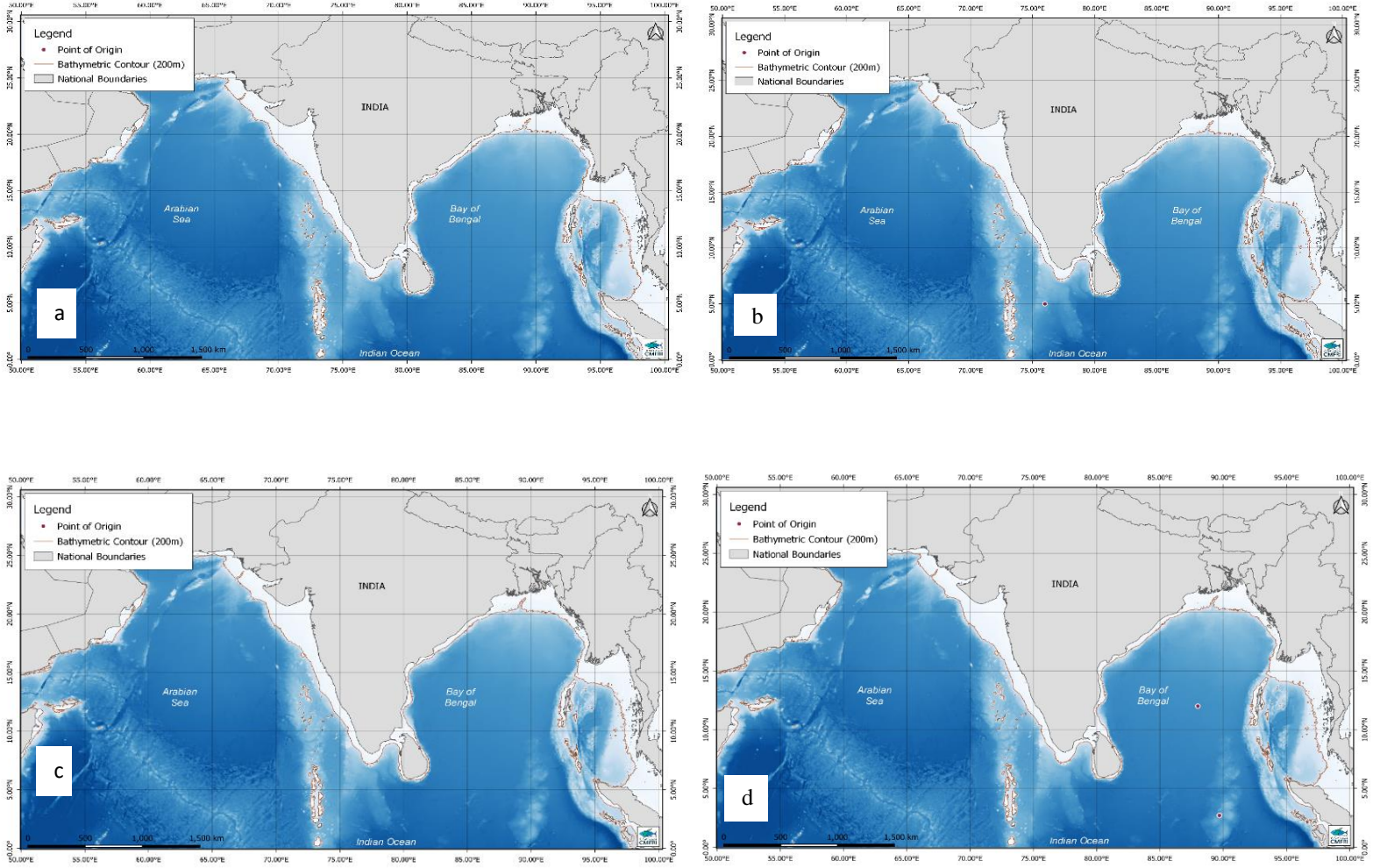

Fig.5 i. Monthly distribution of genesis locations of CDs in the NIO during QP- a)January, b) February, c) March, d) April

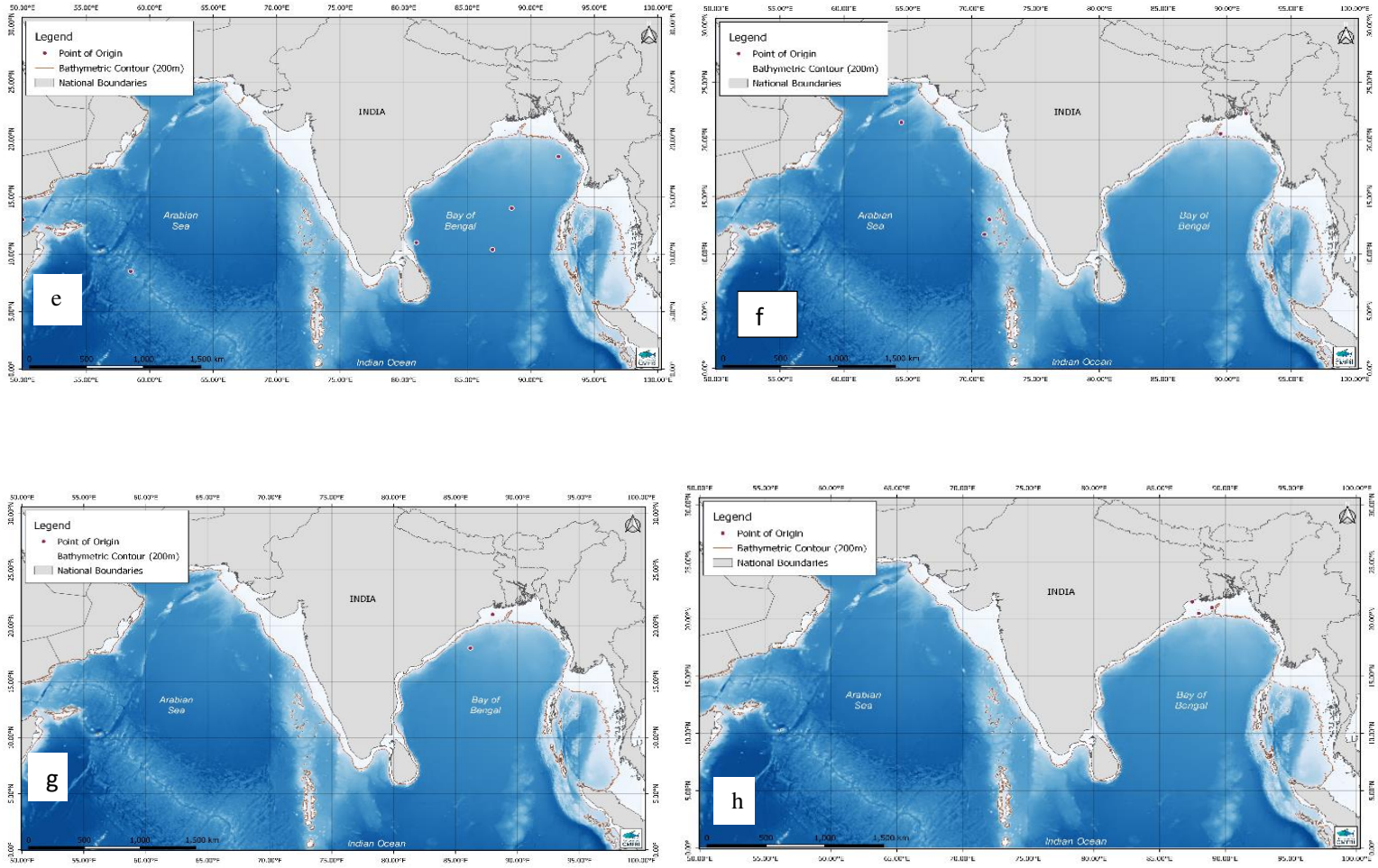

Fig.5 ii. Monthly distribution of genesis locations of CDs in the NIO during QP- e) May, f) June, g) July, h) August

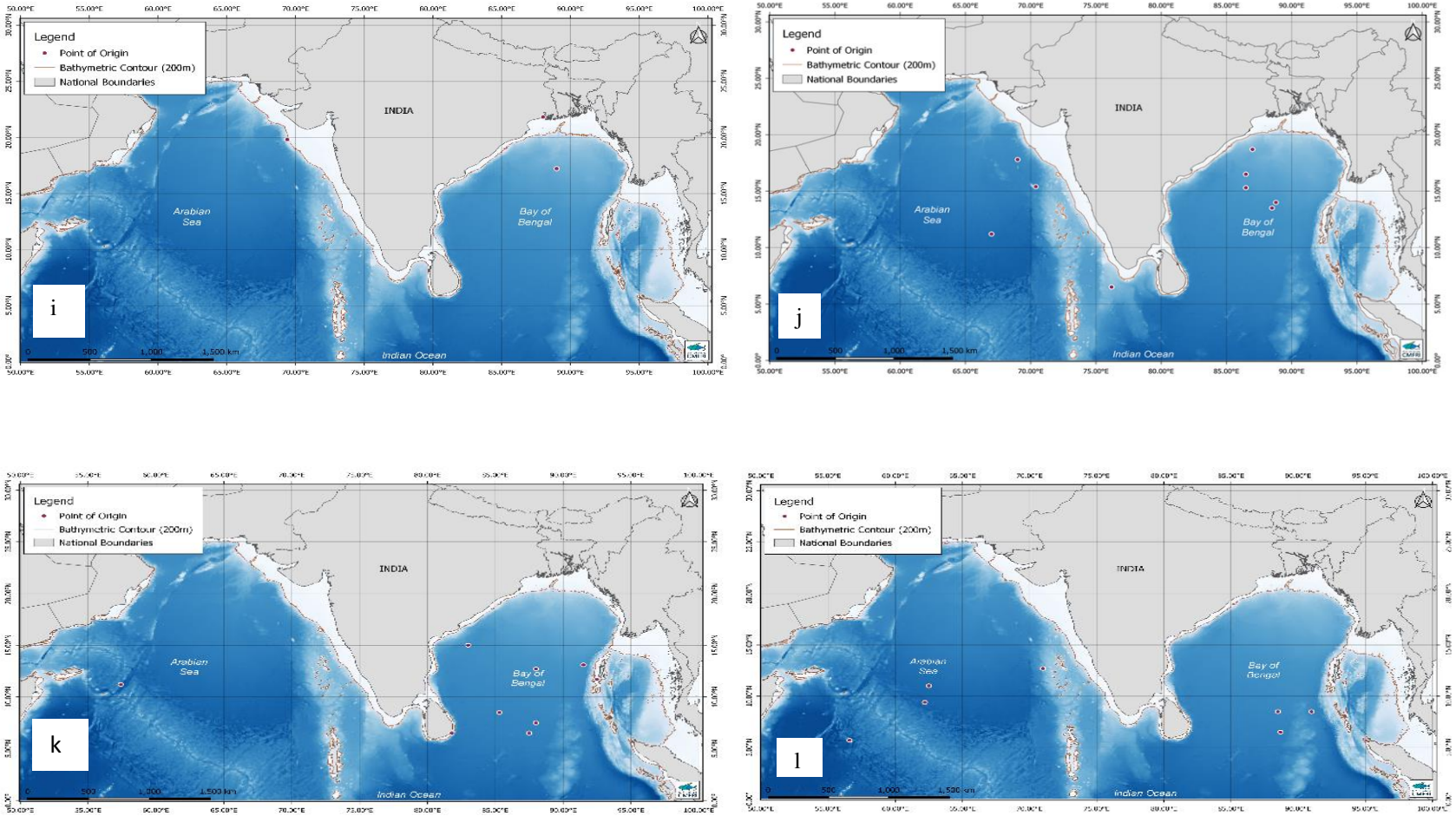

Fig.5 iii. Monthly distribution of genesis locations of CDs in the NIO during QP- i) September, j) October, k) November, l) December

4.2 Temporal distribution of TC in NIO

4.2.1 Annual distribution

The NIO is currently experiencing an increase in the number of CDs, which has a significant impact on the NIO rim countries due to its socioeconomic impacts. The annual frequency of CDs that formed over NIO from 1986 to 2015 is depicted in Fig.6. A total of 275 CDs were formed during this period, frequency was fluctuating between the years, with the highest value in 2005 and the lowest in several years. For the frequency of cyclones, the trendline shows a slightly upward trend. Apart from the frequency of CDs, Fig.7 shows the area affected by CDs during this CP in the NIO region. Similarly, the affected area varies greatly between years, and the trendline shows a decreasing trend. During the QP, the frequency of CDs follows a similar pattern to that of CP (Fig.8), but the total area affected by CDs increases (Fig.9). In general, it could be seen that there has been little increase in the frequency of CDs in NIO when considering CP and QP, whereas the area affected by CDs has increased in recent years.

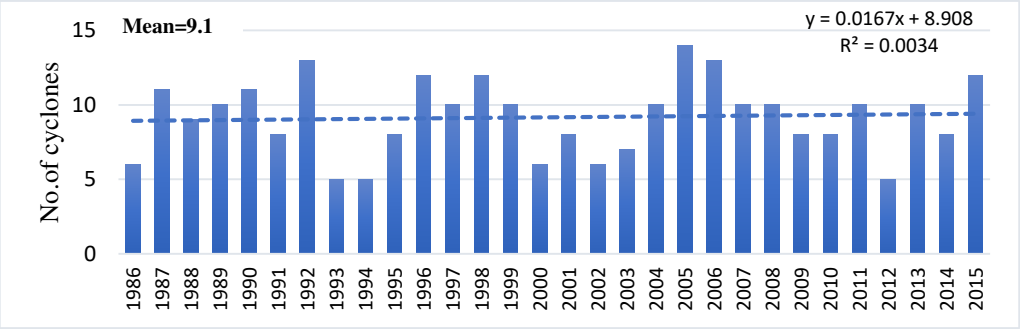

Fig.6.Total no.of cyclones in NIO during CP.

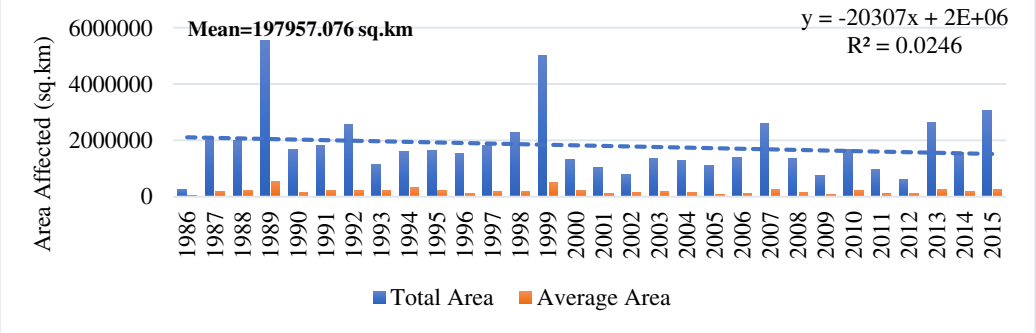

Fig.7 Total area affected by cyclones in NIO during CP.

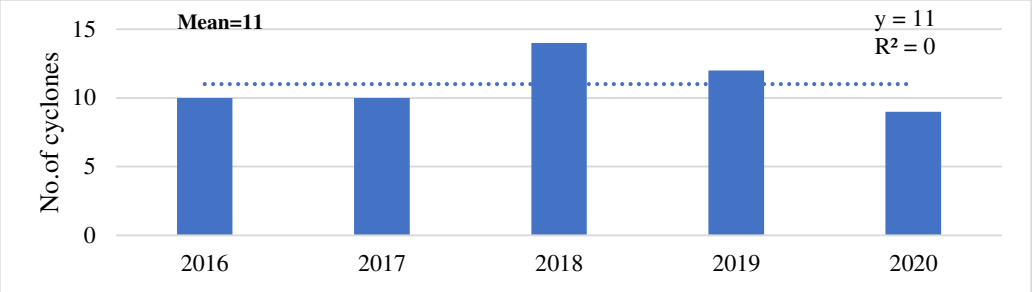

Fig.8 Total no.of cyclones in NIO during QP.

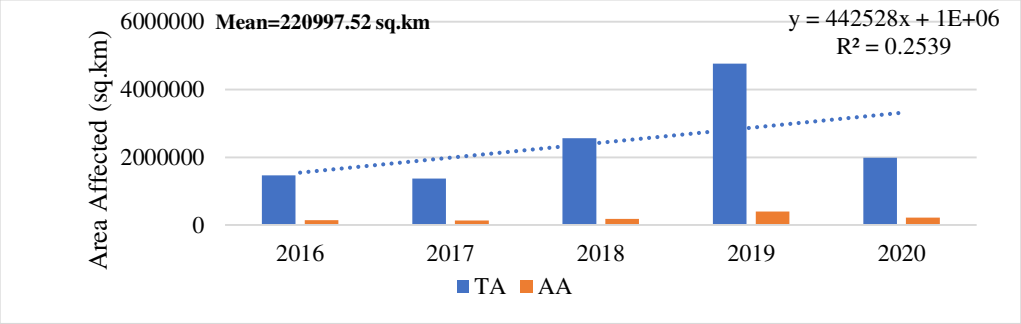

Fig.9 total area affected by cylones in NIO during QP

4.2.2 Intensitywise distribution

4.2.2a Comparison of intensitywise distribution of CDs during CP and QP in NIO

The intensitywise distribution of total CDs that formed over NIO during the CP in terms of frequency and area affected are shown in Fig.10 and Fig.11. There were 73 D, 89 DD, 51 CS, 21 SCS, 17 VSCS, 21 ESCS, and 3 SuCS among the total 275TC formed over the NIO. Overall, DD was the most common and SuCS was the least common The areas affected by different cyclone intensities differ, with VSCS and ESCS affecting roughly the same area which is the highest and D affecting the smallest area. When this result is compared to the QP, which runs from 2016 to 2020 (Fig.12 and Fig.13), 55 TC are formed, including 16 D, 12 DD,9 CS, 3 SCS, 9VSCS, 4 ESCS and 2 SuCS. The D appears more frequent here, while the SuCS appears less frequently.

Despite the fact that only 9 ESCS occurred during this time period, the impacts of these cyclones were felt in more areas.

The frequency of D that formed over NIO during the CP (Fig.14) show higher fluctuations between the years, with a significant increasing trend, while during the QP the frequency showed a decreasing trend (Fig.15). In the case of frequency and area affected by DD during CP (Fig.16 and Fig.17) as well as QP (Fig 18 and Fig.19) it showed a more or less similar negative trend. The cyclonic storms both in CP and QP also showed a decreasing trend (Fig.20, Fig.21, Fig.22, and Fig.23). The Severe cyclonic storm showed a decreasing trend during the CP in terms of both frequency and area (Fig.24 and Fig.25), whereas it did not show any trend for frequency (Fig.26) and a negative trend for the area affected during QP (Fig.27). The frequency of intense cyclones like VSCS and ESCS showed an increasing trend (Fig.28 and Fig.32.). The area affected by VSCS showed an increasing trend (Fig.28) and that of ESCS showed a decreasing trend during the climatological period (Fig.33). But during the QP, an increasing trend is visible for areas affected by both (Fig.30, Fig.31, Fig.34 and Fig.35). In the case of the most intense SuCS, there is no significant trend is visible for both CP and QP (Fig.36, Fig.37, Fig.38a, and Fig.38b in terms of frequency and area. In altogether it can be says that the frequency and area affected by the intense cyclones are increasing in the NIO.

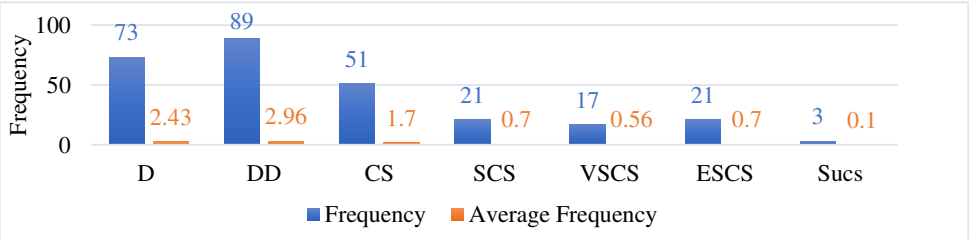

Fig.10 The intensitywise distribution of frequency of CDs that formed in NIO during CP

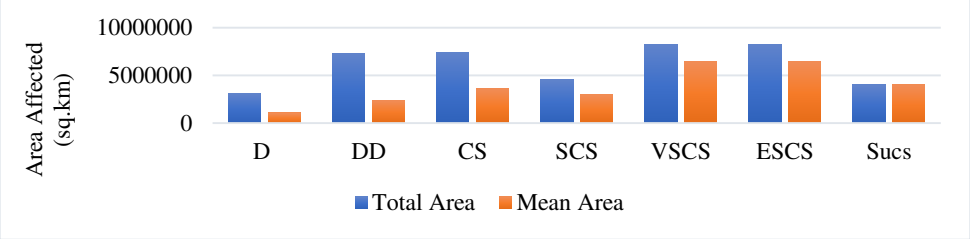

Fig.11 The intensitywise distribution of area affected by the CDs that formed NIO during CP

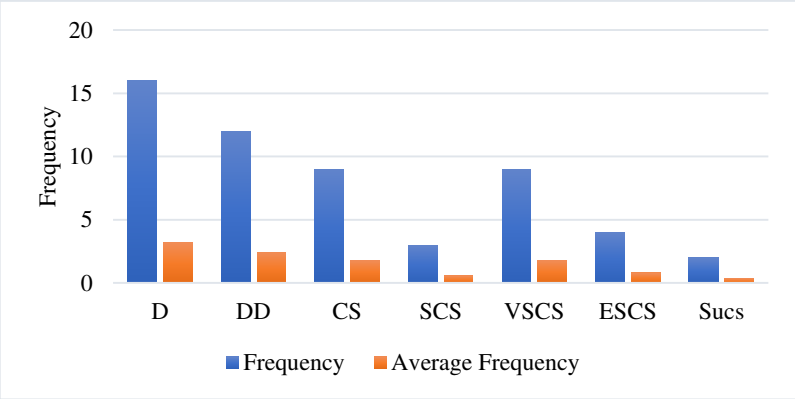

Fig.12 The intensitywise distribution of CDs that formed over NIO during QP in terms of frequency

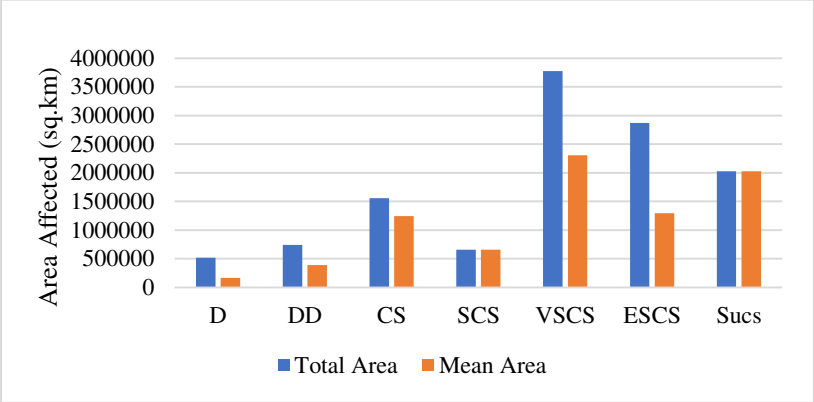

Fig.13 The intensitywise distribution of CDs that formed over NIO during QP in terms of area affected

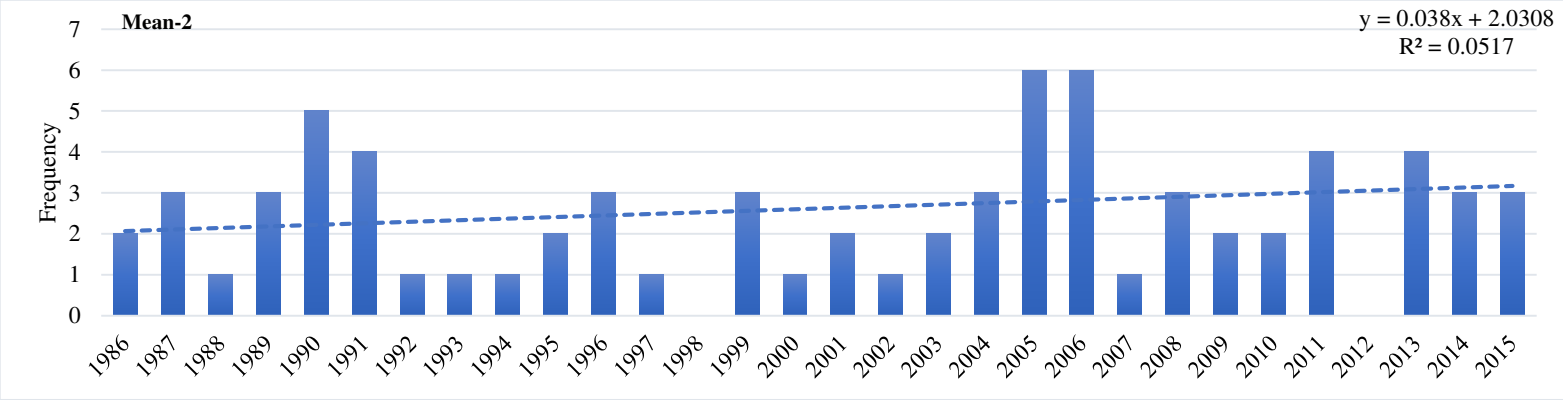

Fig.14 The frequency of D that formed over NIO during the CP

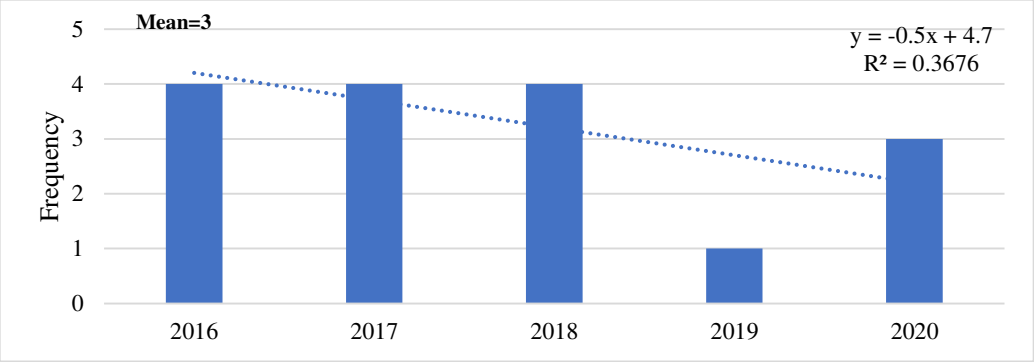

Fig.15 The frequency of D that formed over NIO during the QP

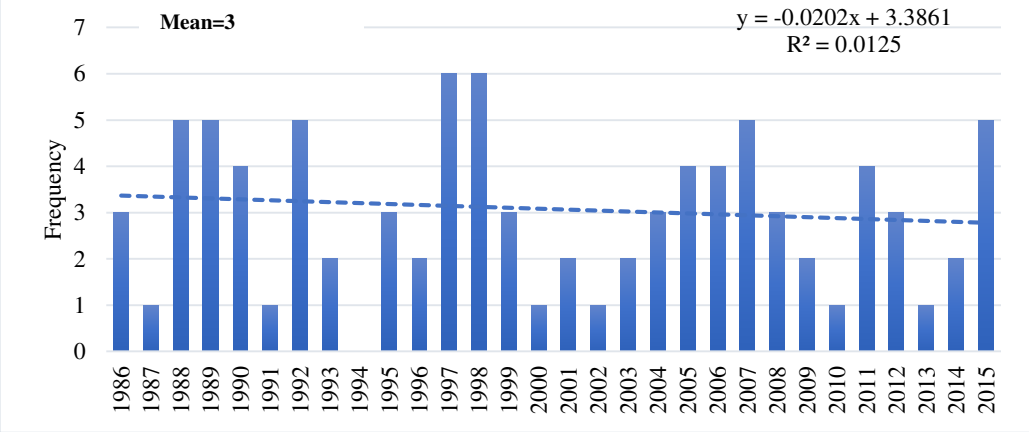

Fig.16 The frequency of DD that formed over NIO during CP

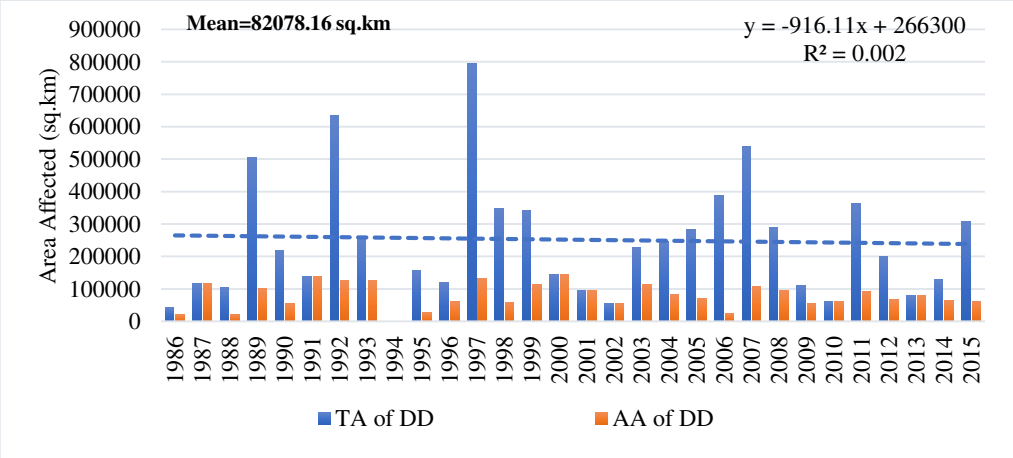

Fig.17 The area affected by DD that formed over NIO during CP.

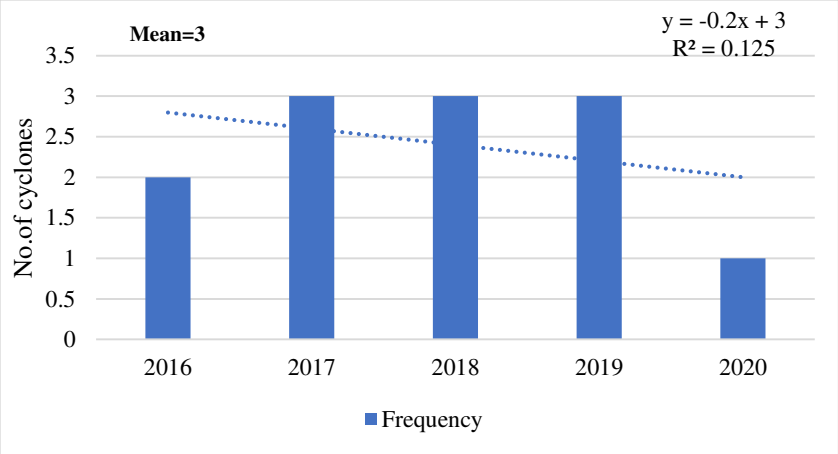

Fig.18 The frequency of DD that formed over NIO during QP

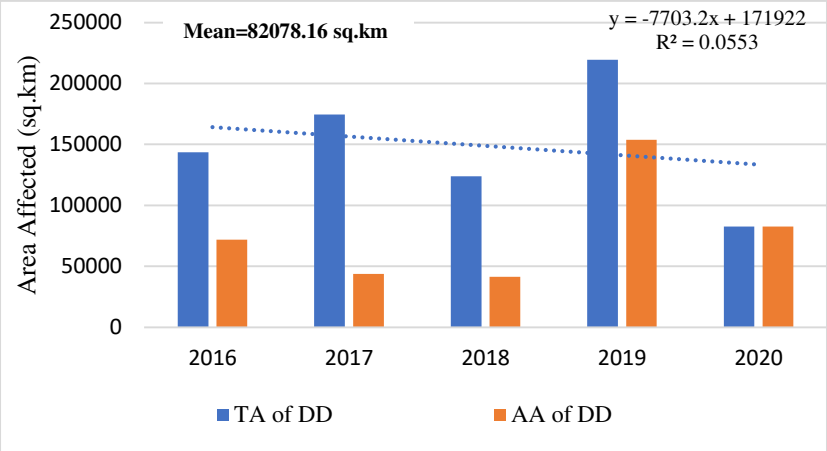

Fig.19 The area affected by DD that formed over NIO during QP

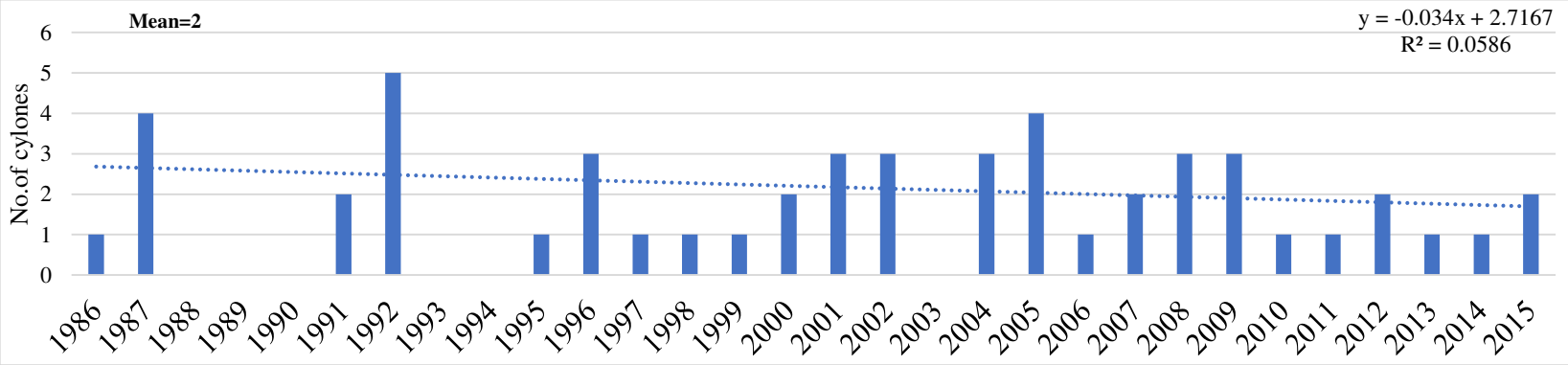

Fig.20 Frequency of CS in NIO during CP

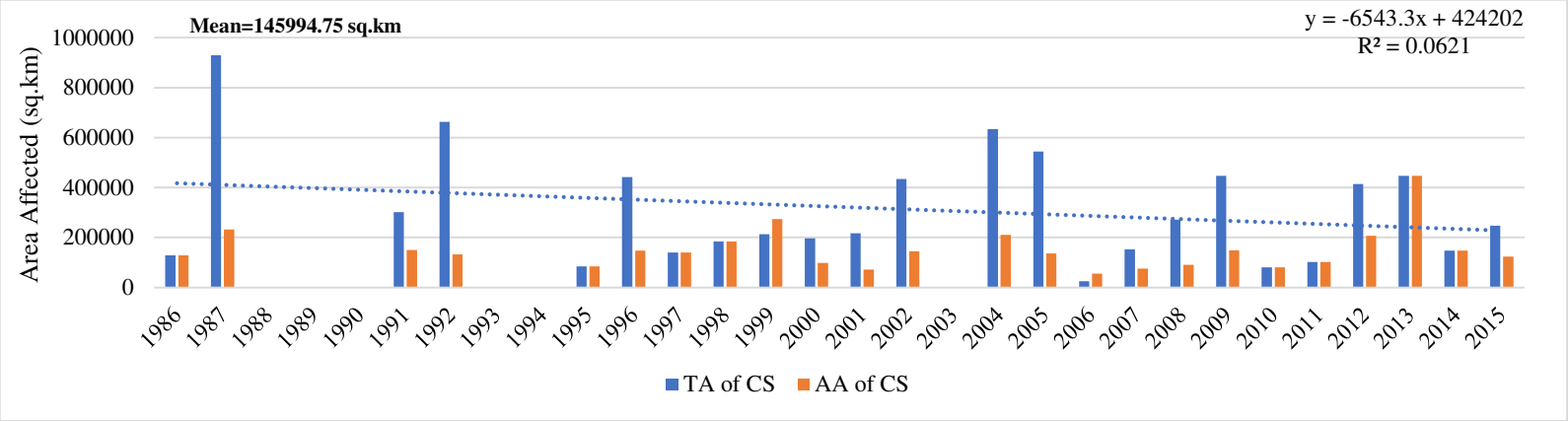

Fig.21 The area affected by CS in NIO during CP

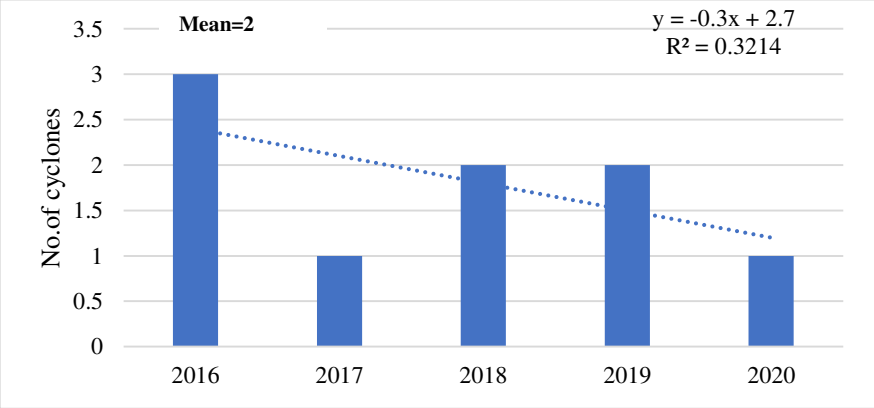

Fig.22 The frequency of CS during QP.

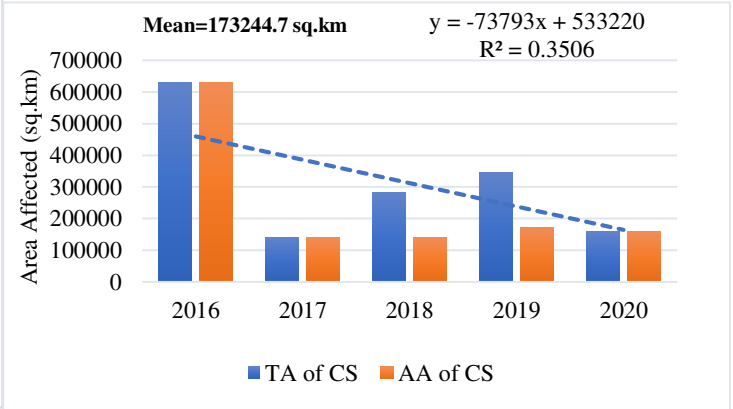

Fig.23 The area affected by CS during QP.

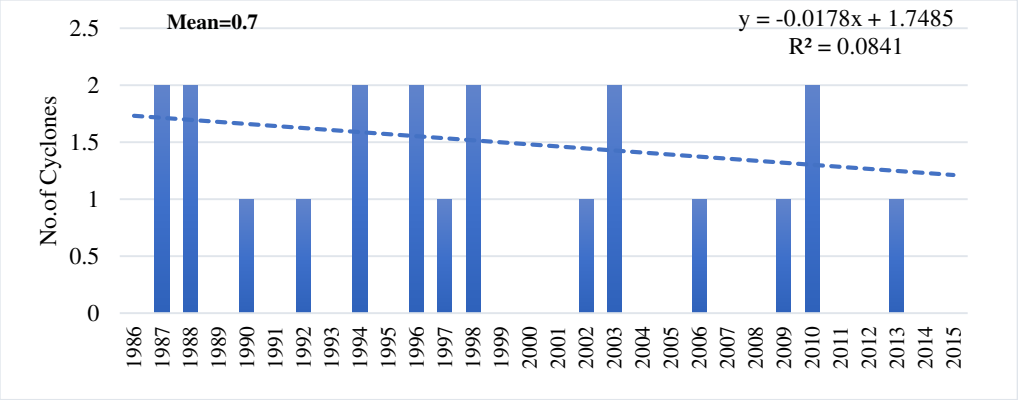

Fig.24 Frequency of SCS in NIO during CP

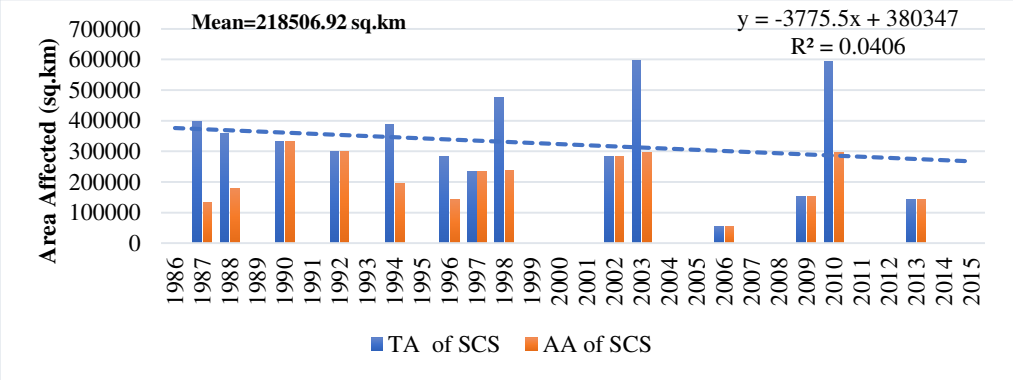

Fig.25 Area affected by SCS in NIO during CP

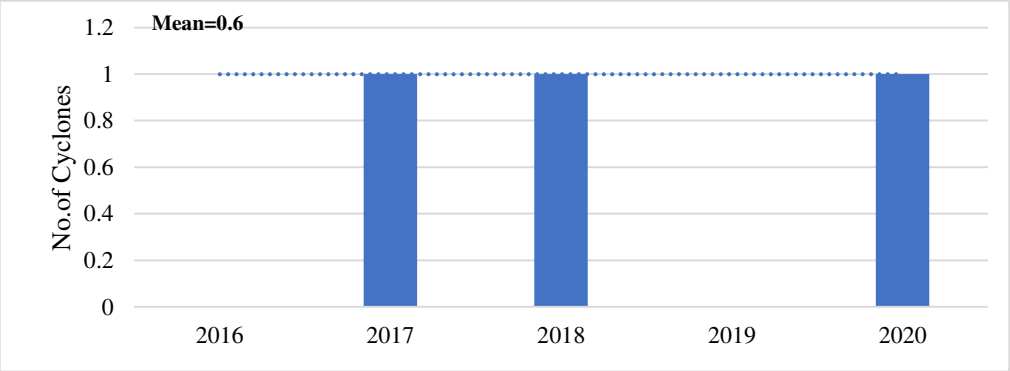

Fig.26 Frequency of SCS in NIO during QP

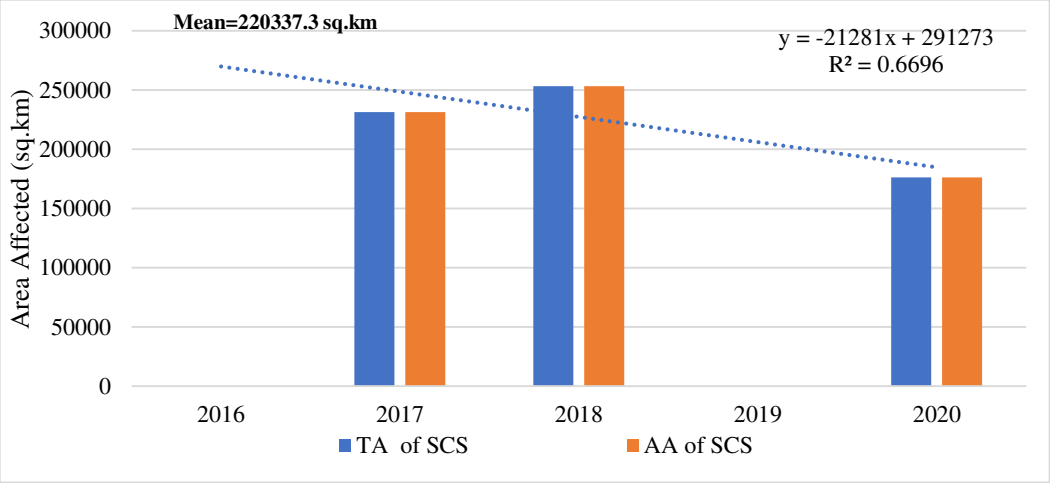

Fig.27 Area affected by SCS in NIO during QP

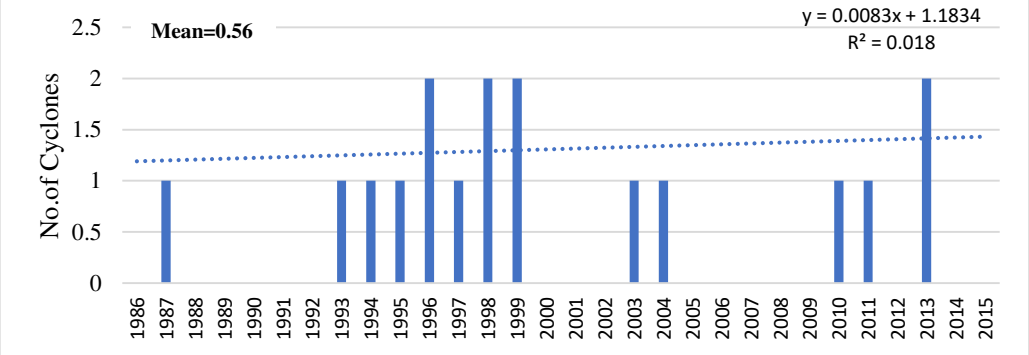

Fig.28 Total No. of VSCS in NIO during CP

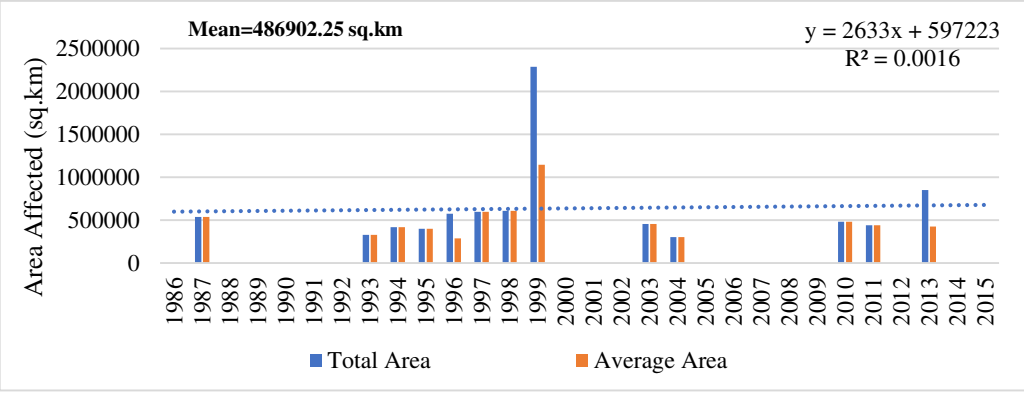

Fig.29 Total area affected by VSCS in NIO during CP

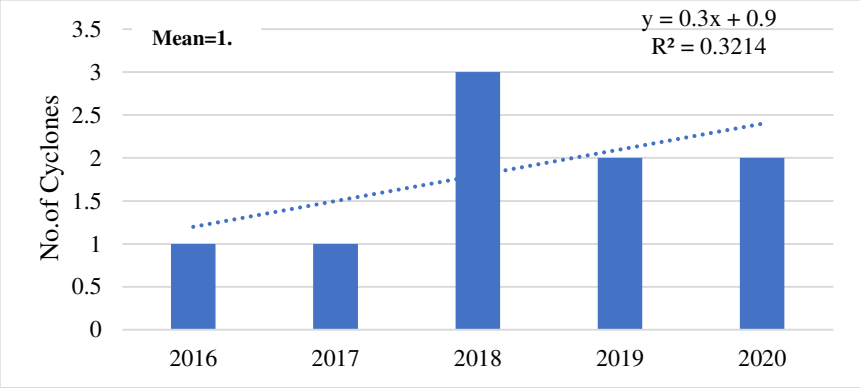

Fig.30 Frequency of VSCS in NIO during QP

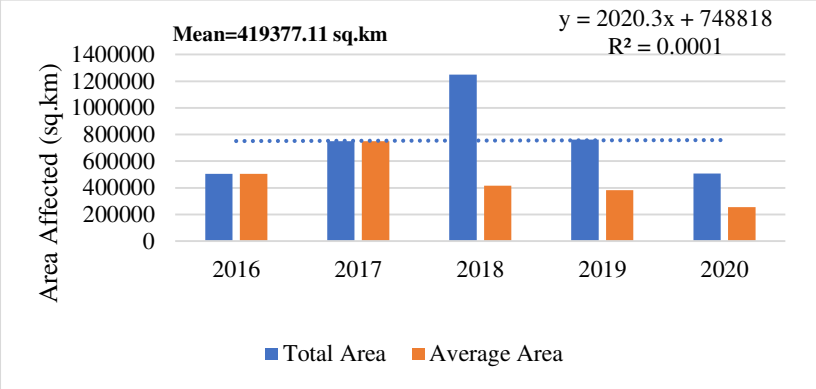

Fig.31 Total area affected by VSCS in NIO during QP

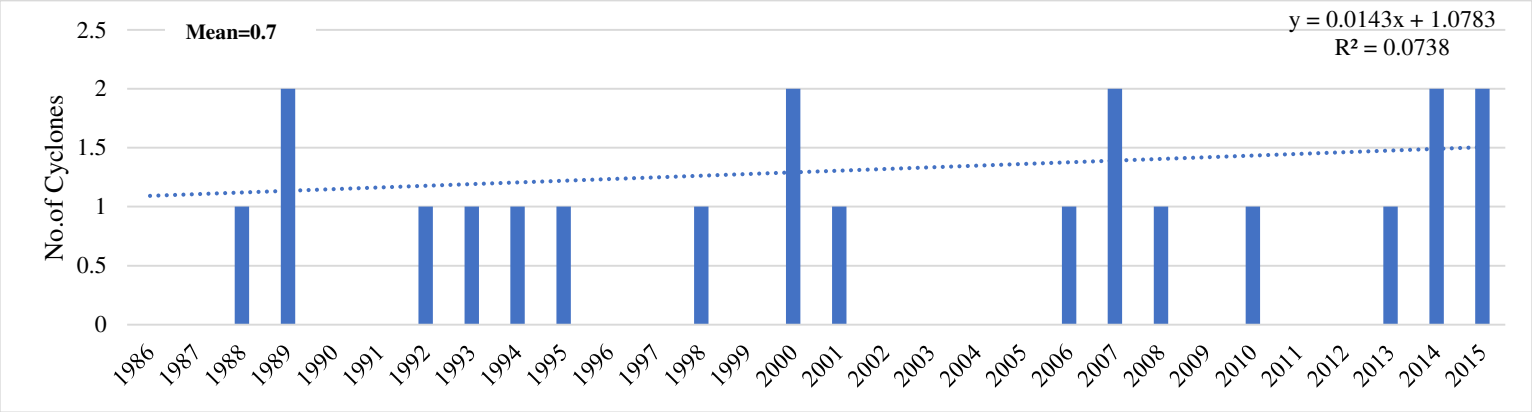

Fig.32 Total No. of ESCS in NIO during CP

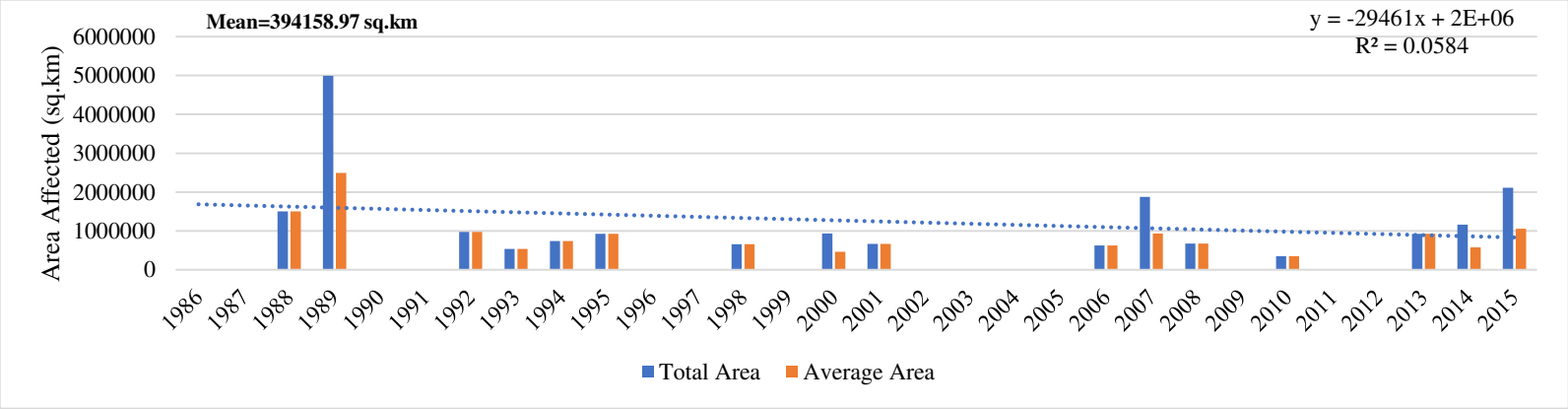

Fig.33 Total area affected by ESCS in NIO during CP

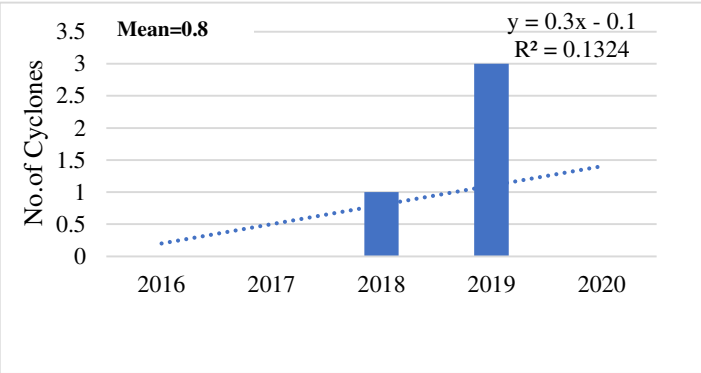

Fig.34 Frequency of ESCS in NIO during QP

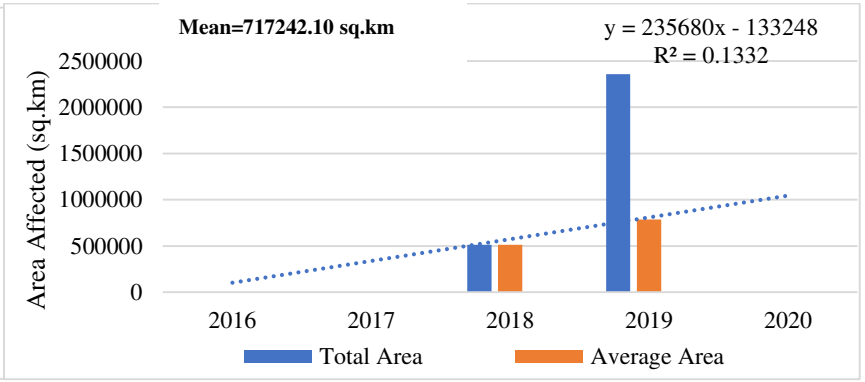

Fig.35 Total area affected by ESCS in NIO during QP

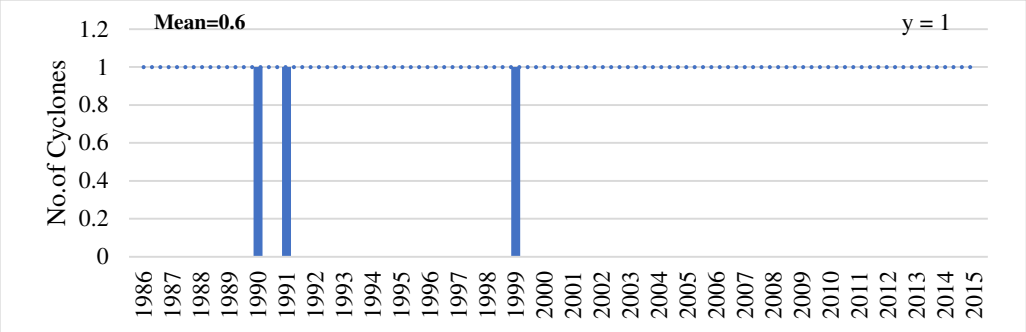

Fig.36 Total No. of SuCS in NIO during CP

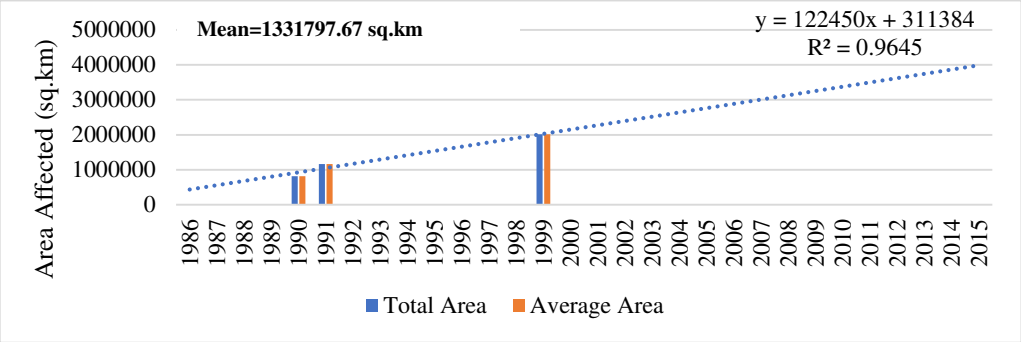

Fig.37 Total area affected by SuCS in NIO during CP

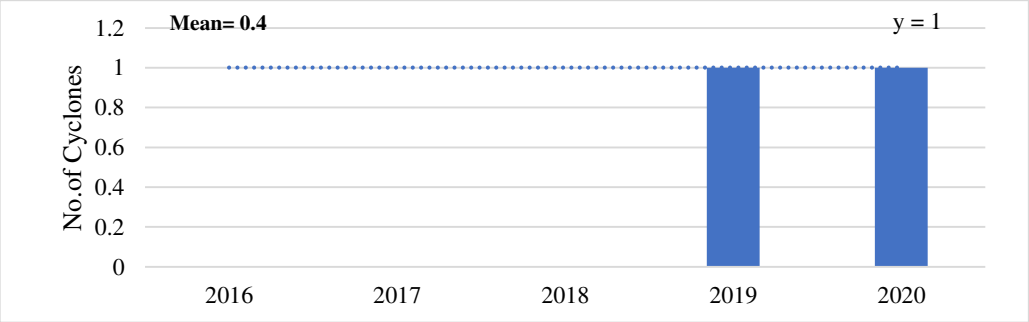

Fig.38.a Frequency of SuCS in NIO during QP

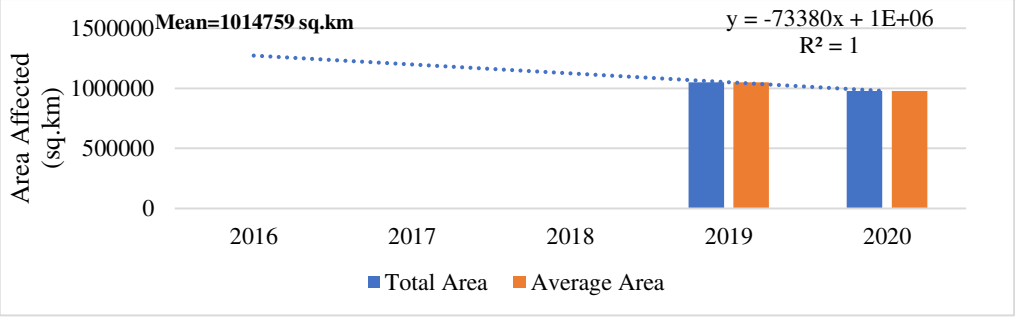

Fig.38.b Total area affected by SuCS in NIO during QP

4.2.3 Seasonal and monthly distribution

4.2.3 (i) Comparison of monthly distribution of TC during CP with QP

The monthly distribution of CDs over the CP and QP, respectively are depicted in Fig.39 and Fig.40. During the CP, November had the most cyclones, followed by October, whereas the QP had more cyclones in both October and November. In the CP, the lowest number was formed in February and March while in the QP, no cyclonic disturbances occurred in February. In both cases, May and June are the months following the highest numbers. NIO experiences the most cyclonic disturbances in October-November and the least in January-February and March.

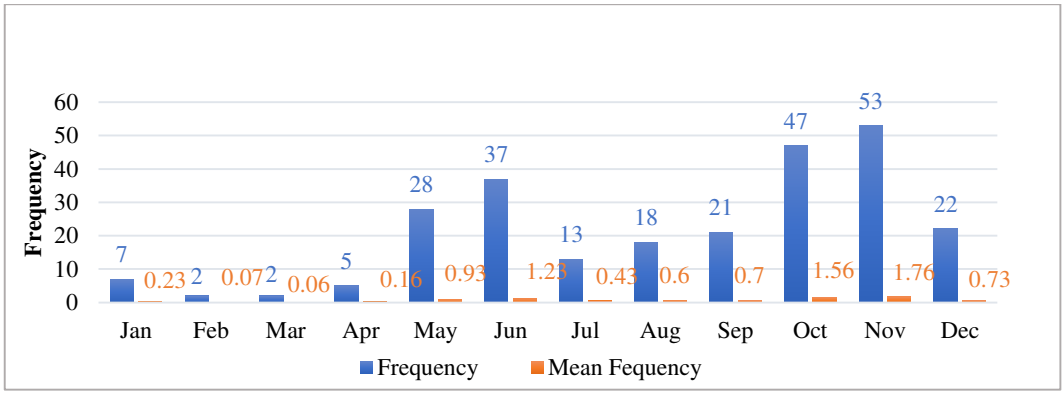

Fig.39 Monthly distribution of CDs in CP

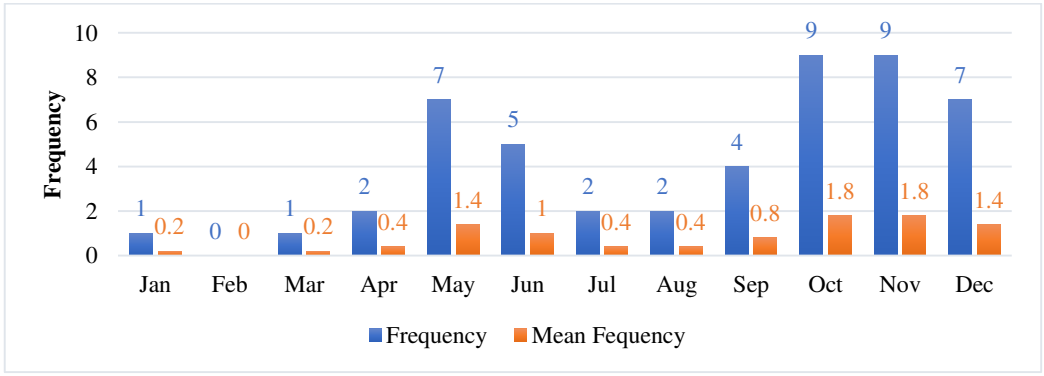

Fig.40 Monthly distribution of CDs in QP

4.2.3 (ii) Comparison of seasonal distribution of TC during CP with QP

Seasonal distribution of CDs in NIO during CP and QP are given in Fig.41 and Fig.42. In both periods, highest number was observed during the Post-Monsoon (Oct-Dec) followed by Monsoon (June-Sep), Pre-Monsoon (March-May) and Winter (Jan-Feb).

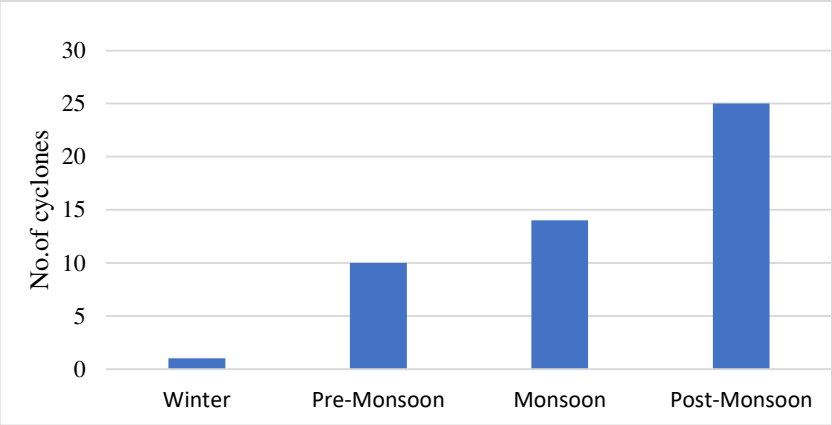

Fig.42 Seasonal distribution of CDs in NIO during CP

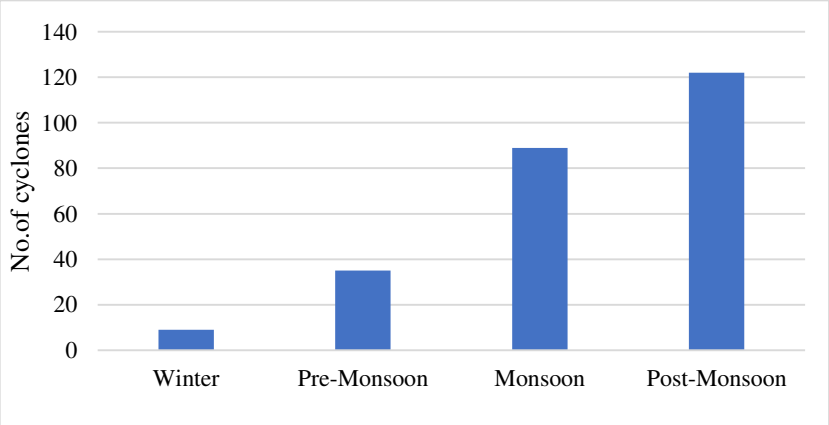

Fig.42 Seasonal distribution of CDs in NIO during QP

4.3.Temporal distribution of cyclonic disturbances in BOB

NIO is subdivided in to BOB and ARB. BOB experienced four times greater number of cyclonic disturbances than the ARB.

4.3.1 Annual distribution

Fig.43 depicts the annual frequency of cyclonic disturbances formed over BOB during the climatological period. It clearly shows a negative trend, indicating that the frequency of Cyclonic disturbances over BOB is decreasing. During the CP, 198 of the 275 cyclonic disturbances formed over NIO were formed over BOB. The frequency varied between the years, with a maximum value in 2005. The area affected by CDs has a negative trend as well (Fig.44). The frequency shows a similar trend in the QP (Fig.45), but the area affected (Fig.46) shows a slightly positive trend, with the highest value in 2019.

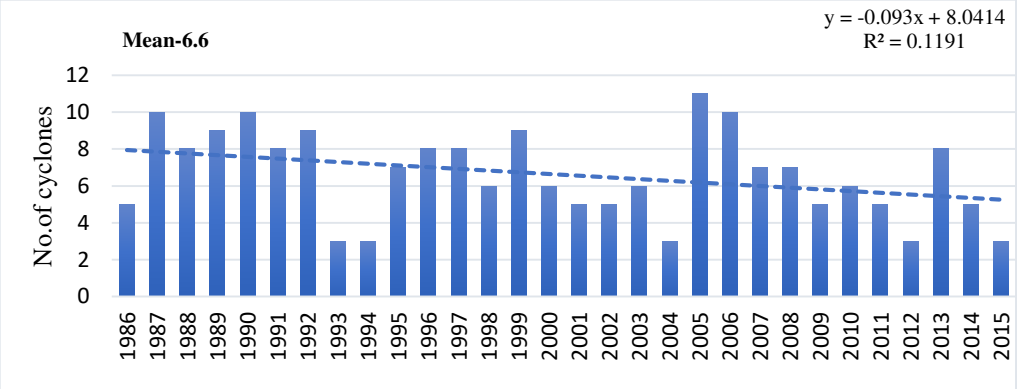

Fig.43 Annual frequency of cyclonic disturbances formed over BOB during the CP

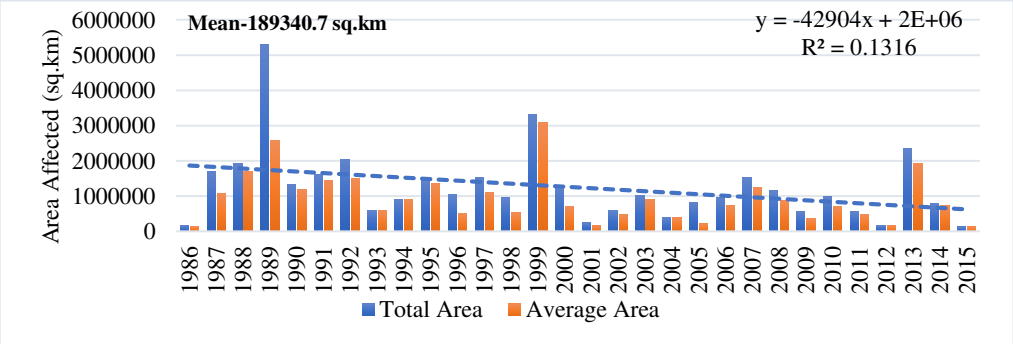

Fig.44 Total area affected by CDs formed over BOB during the CP

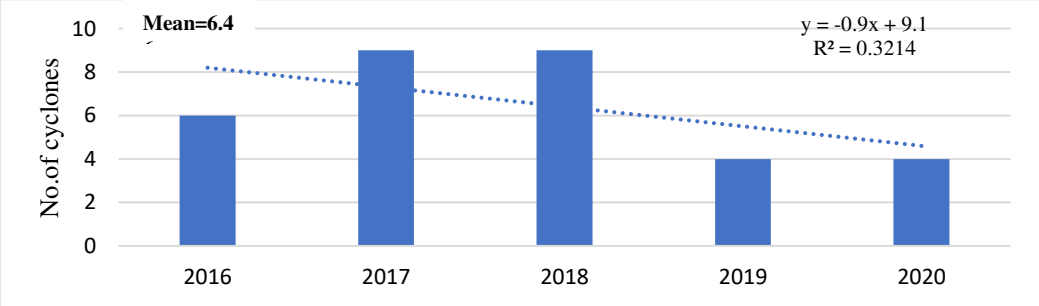

Fig45 Frequency of CDs in BOB during QP

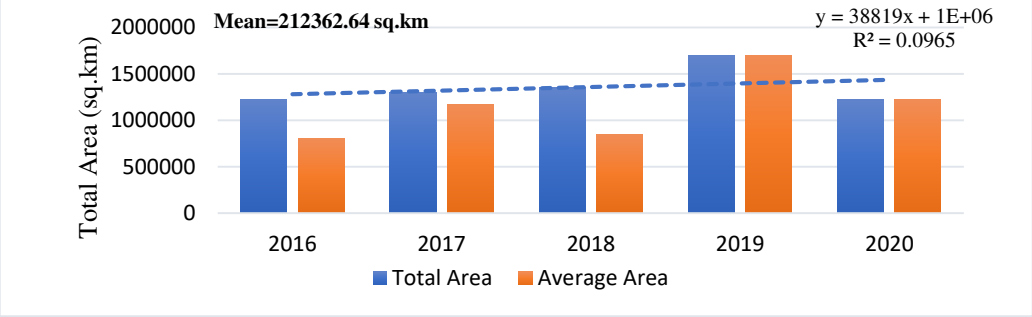

Fig.46 Total area affected by CDs in BOB during QP

4.3.2 Intensitywise distribution

4.3.2 (i) Comparison of intensitywise distribution of TC during CP with the QP

The intensitywise distribution of the frequency of CDs that formed over BOB during the CP and QP are shown in Fig.47 and Fig.48. There were 198 CD, 56 D, 65 DD, 31 CS, 16 SCS, 10 VSCS, 17 ESCS, and 3 SuCS during CP. The frequency of ESCS is higher in QP than in CP, with DD occurring more frequently and SuCS occurring the least. Fig.49 and Fig.50 show the area affected by the CD in both periods. During CP, ESCS affected more areas, whereas VSCS affected more areas during QP. The areas affected by VSCS are significantly more prevalent in the QP than in the CP.

The frequency of D formed over BoB in both CP and QP has a negative trend (Fig.4.15a and Fig.4.15.b). In both periods, the DD shows a negative trend in terms of frequency and area. During CP, the CS and SCS storms showed a negative trend in terms of frequency and area affected (Fig.4.17a, Fig.4.17c, and Fig.4.17d), while SCS showed no trend in terms of frequency (Fig4.17b). The frequency of intense VSCS increases in both CP and QP in BOB (Fig.4.18.a and Fig.4.18.b), but the area affected during the QP period decreases slightly (Fig.4.18.c and Fig.4.18.d). The ESCS showed a negative trend during CP but no trend during QP (Fig.4.19.a, Fig.4.19.b, Fig.4.19.c, and Fig.4.19.d). The most intense SuCS showed no trend in terms of frequency during either period (Fig 4.20.a, Fig.4.20b), but did show a positive trend for areas affected during the CP (Fig.4.20.c and Fig.4.20d) with the majority indicating positive trends, are visible for VSCS in BOB during both periods.

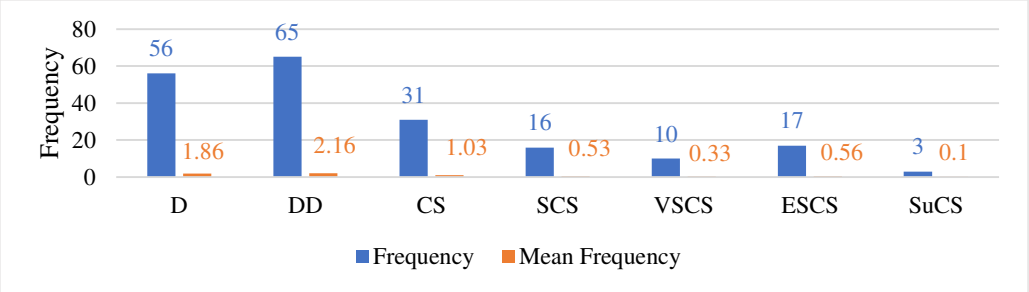

Fig.47 The intensitywise distribution of the frequency of CDs that formed over BOB during the CP

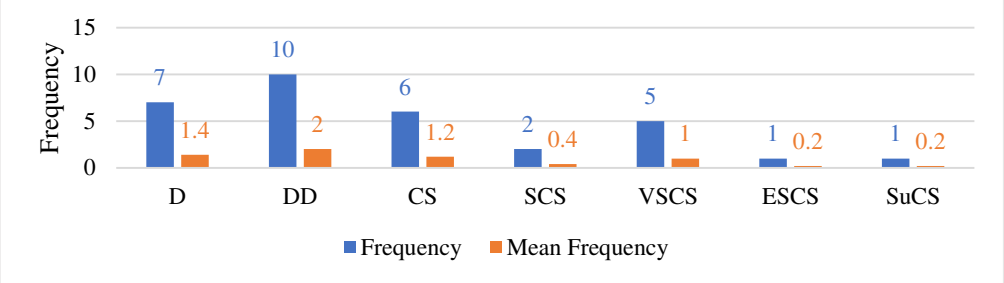

Fig.48 The intensitywise distribution of the frequency of CDs that formed over BOB during QP

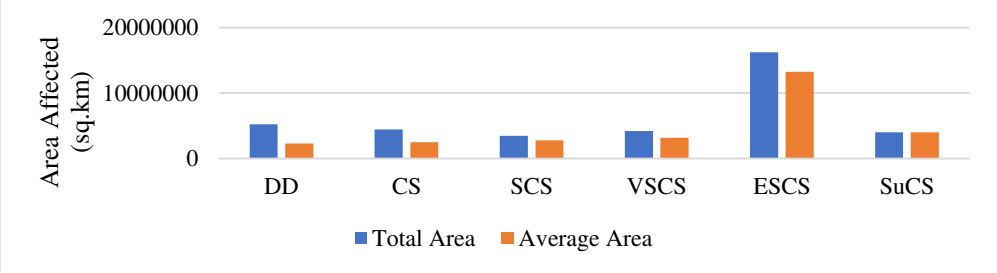

Fig.49 The total area affected by CDs that formed over BOB during CP.

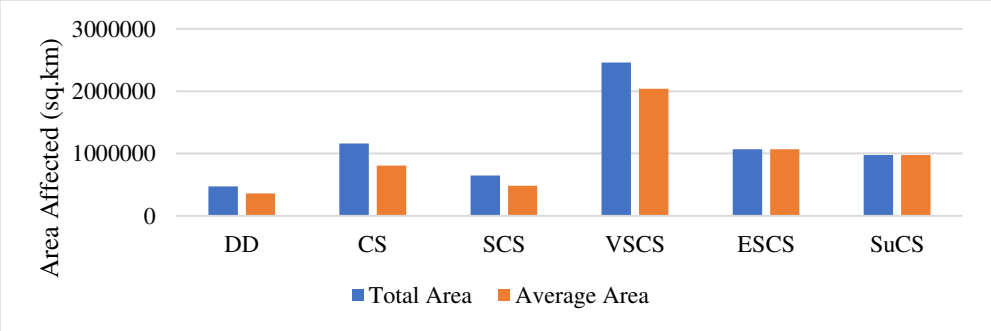

Fig.50 The total area affected by CDs that formed over BOB during QP.

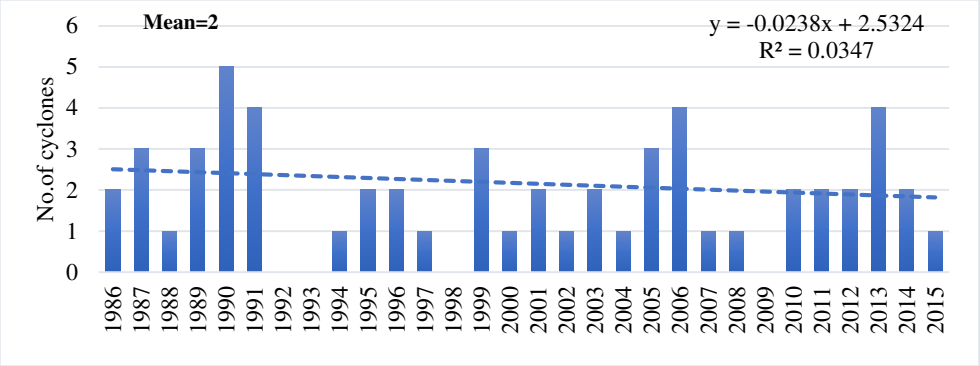

Fig.51 Frequency of D that formed over BOB during CP.

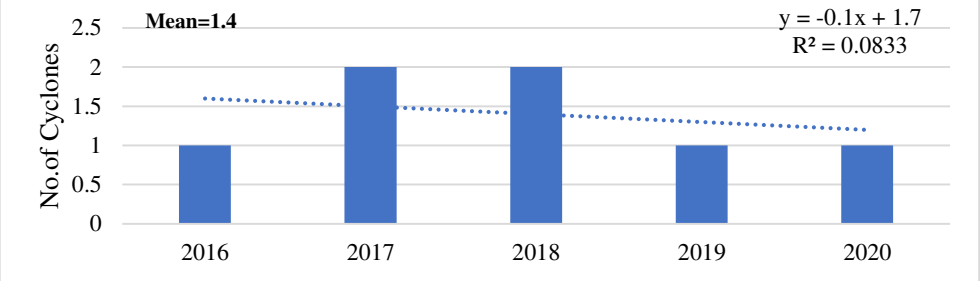

Fig.52 Frequency of D that formed over BOB during QP.

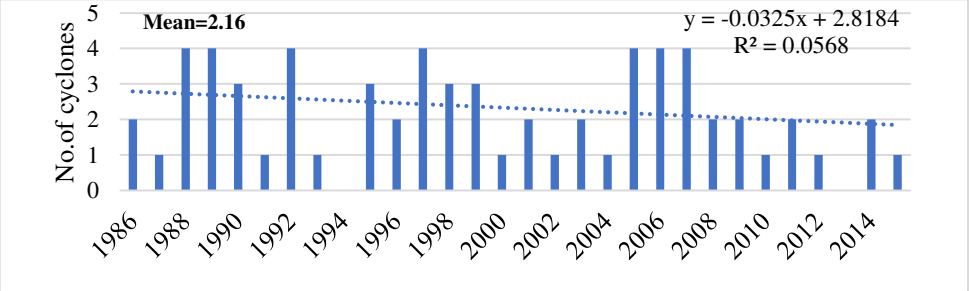

Fig.53 Frequency of DD that formed over BOB during CP.

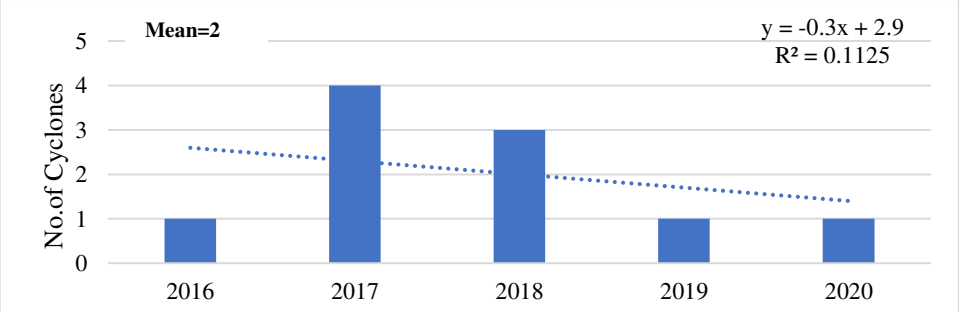

Fig.54 Frequency of DD that formed over BOB during QP.

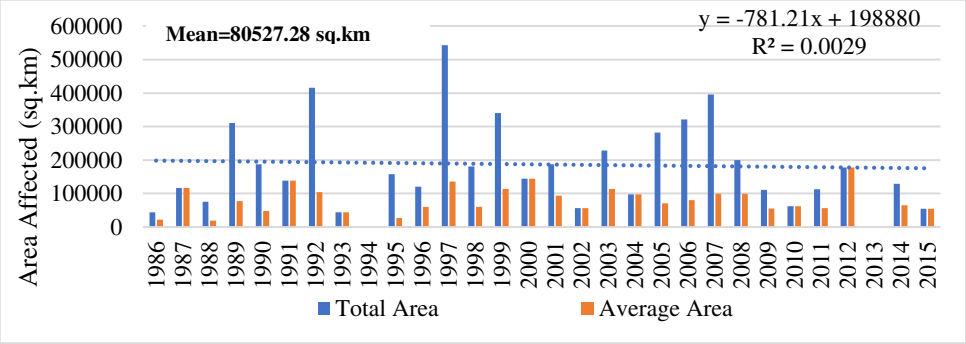

Fig.55 Area affected by DD that formed over BOB during CP.

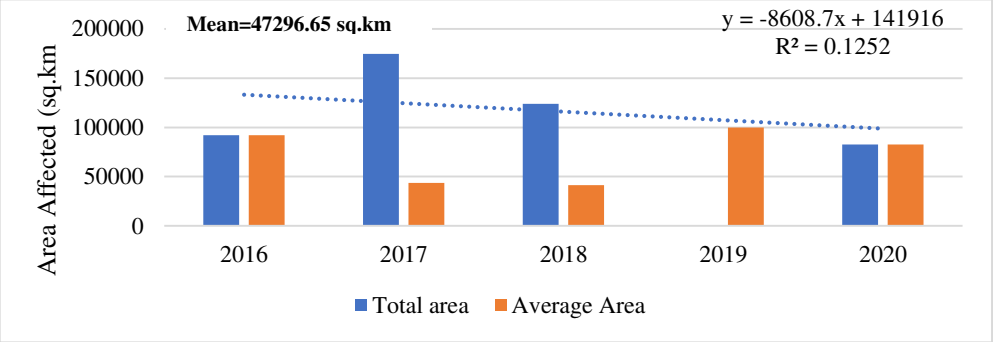

Fig.56 Area affected by DD that formed over BOB during QP.

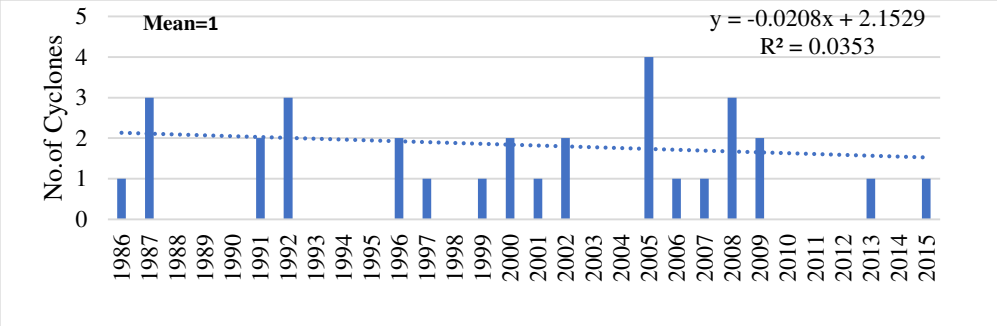

Fig.57 Frequency of CS that formed over BOB during CP

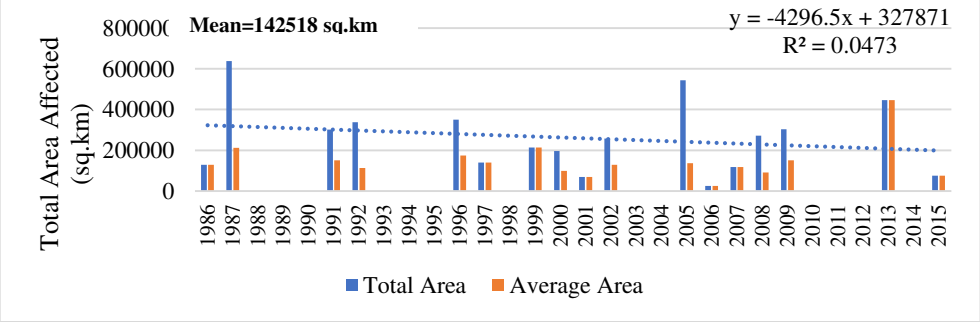

Fig.58 Area affected by CS that formed over BOB during CP

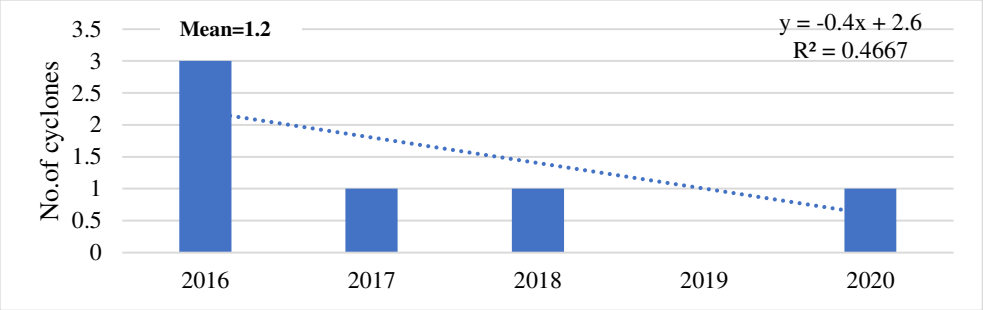

Fig.59 Frequency of CS that formed over BOB during QP

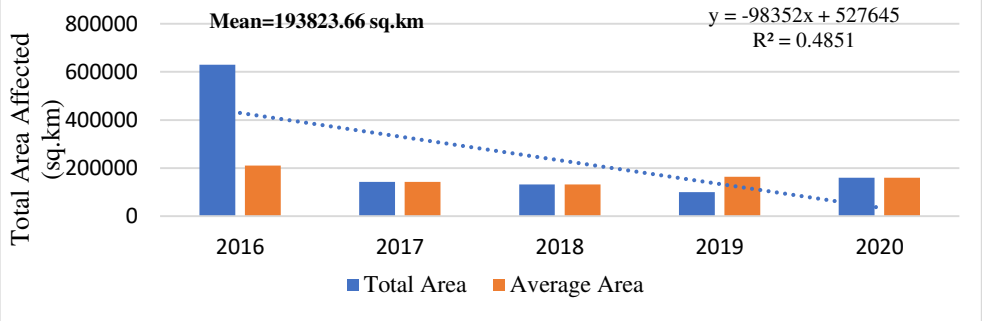

Fig.60 Total area affected by CS that formed over BOB during QP

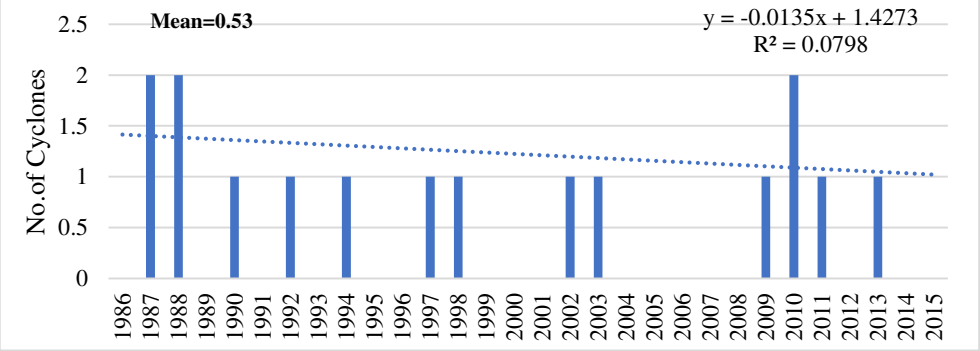

Fig.61 Frequency of SCS that formed over BOB during CP.

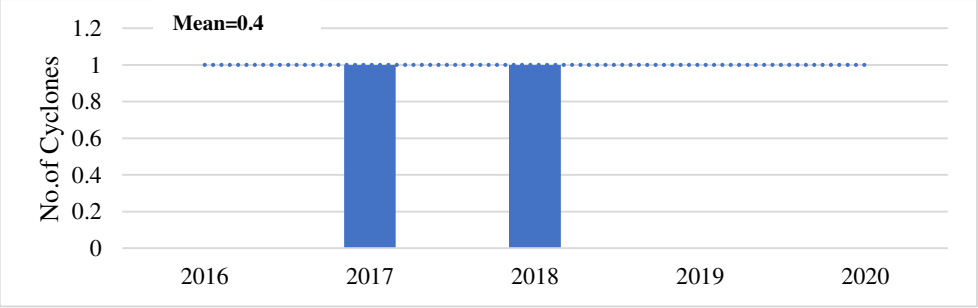

Fig.62 Frequency of SCS that formed over BOB during QP.

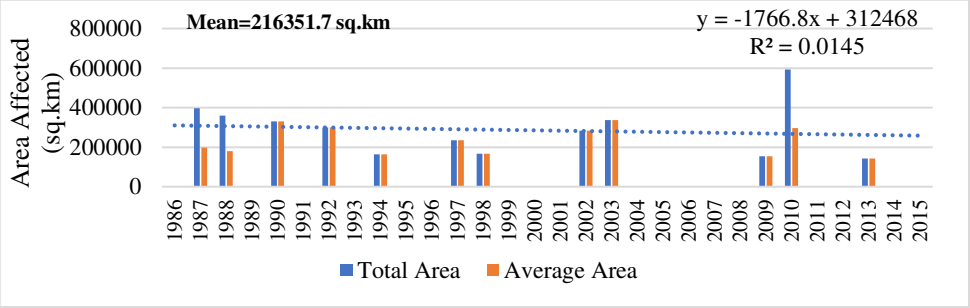

Fig.63Total area affected by SCS that formed over BOB during CP

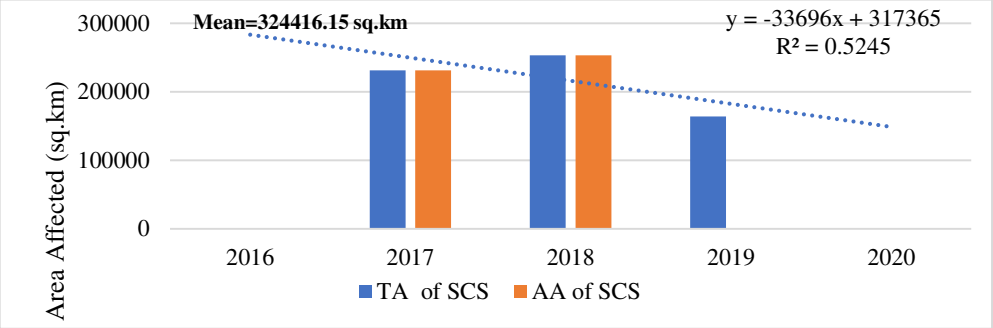

Fig.64 Total area affected by SCS that formed over BOB during QP

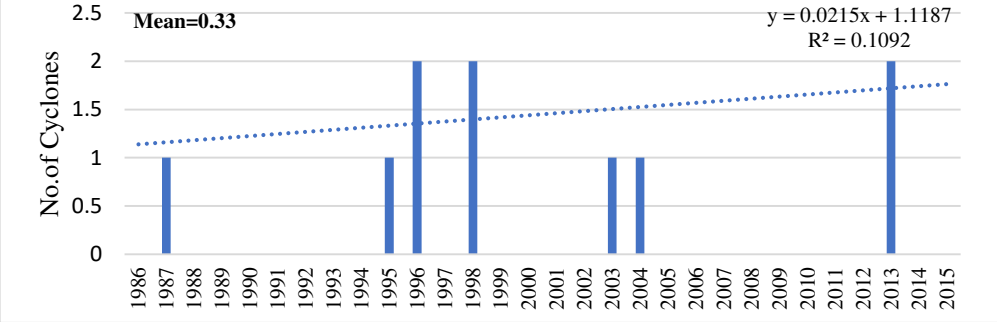

Fig.65 Total frequency of VSCS that formed over BOB during CP

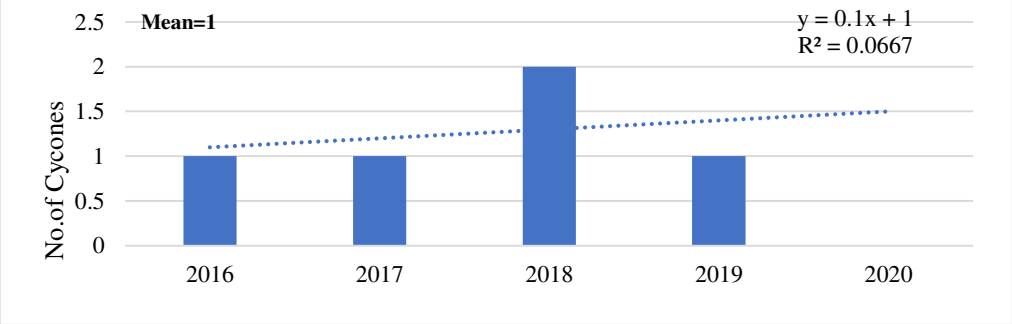

Fig.66 Total frequency of VSCS that formed over BOB during QP

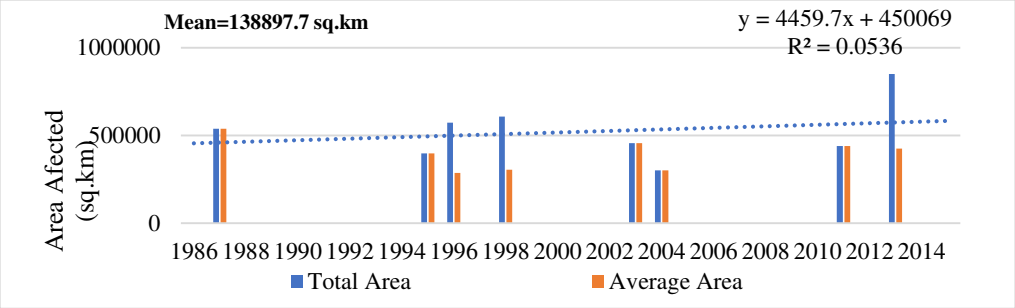

Fig.67 Total area affected by VSCS that formed over BOB during CP

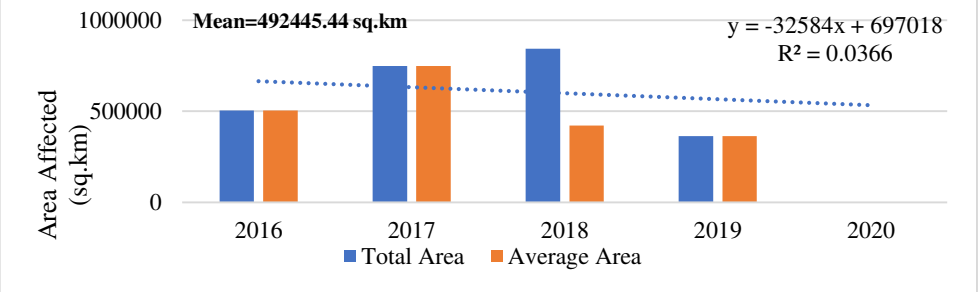

Fig.68 Total area affected by VSCS that formed over BOB during QP

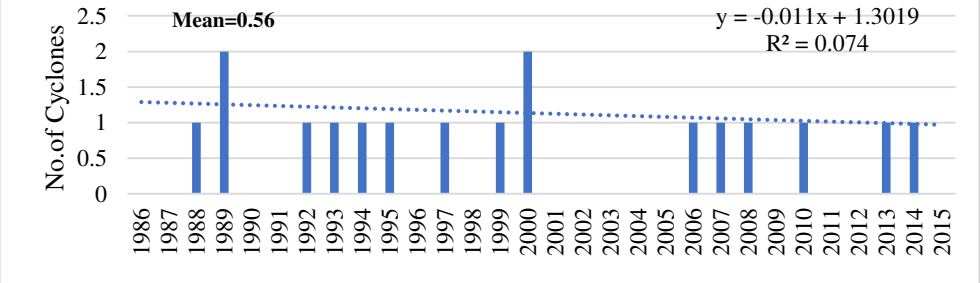

Fig.69 Frequency of ESCS that formed over BOB during CP

Fig.70 Frequency of ESCS that formed over BOB during QP

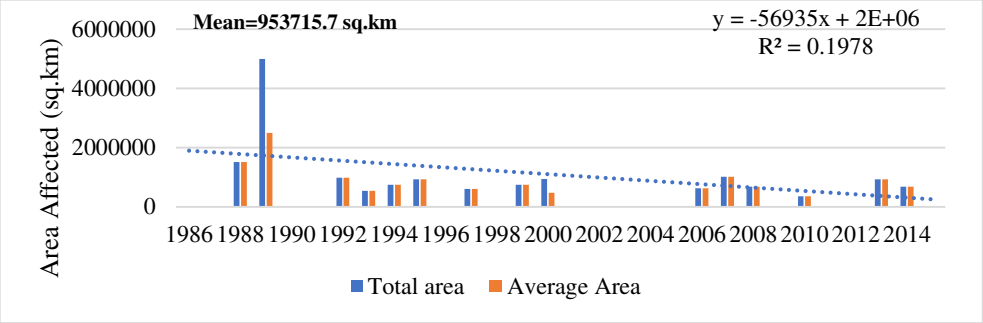

Fig.71 Total area affected by ESCS that formed over BOB during CP

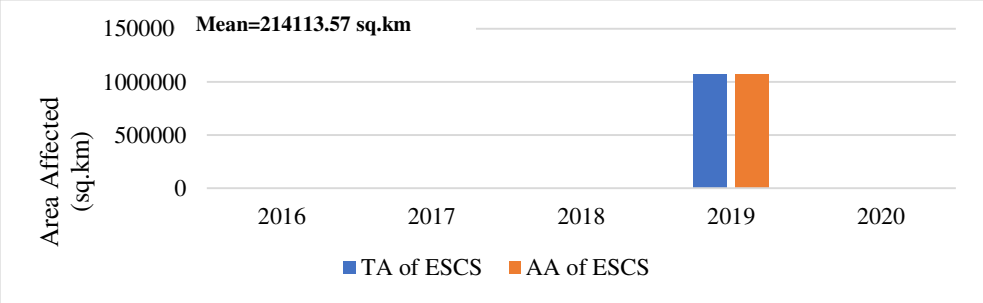

Fig.72 Total area affected by ESCS that formed over BOB during QP

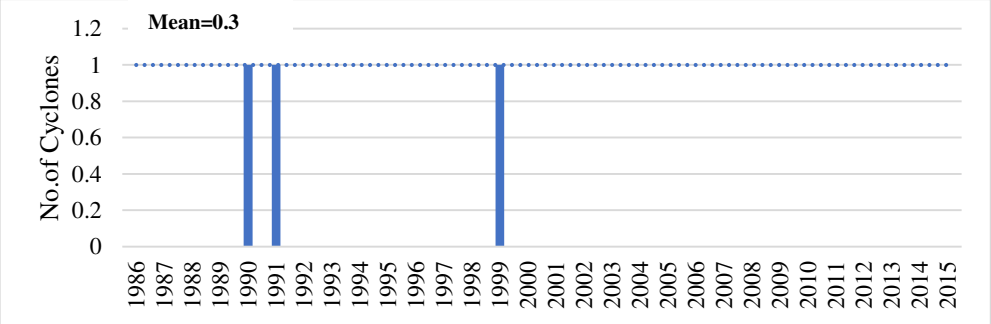

Fig.73 Frequency of SuCS that formed over BOB during CP

Fig.74 Frequency of SuCS that formed over BOB during QP

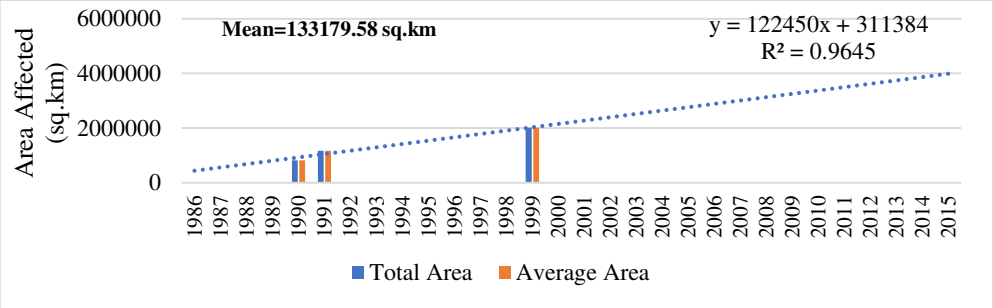

Fig.75 Total area affected by SuCS that formed over BOB during CP

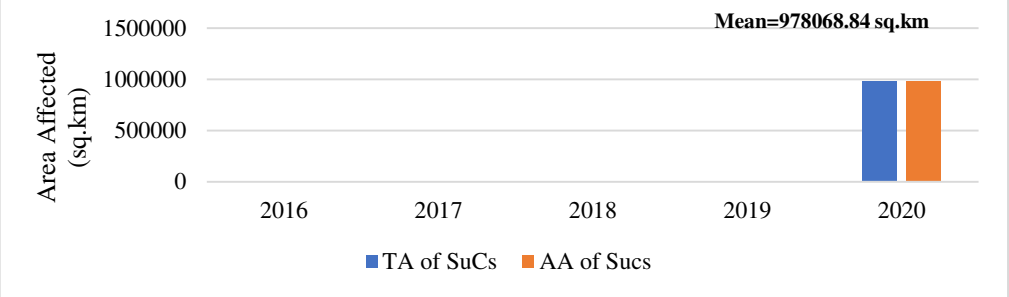

Fig.76 Total area affected by SuCS that formed over BOB during QP

4.3.3 Seasonal and monthly distribution in BOB

4.3.3 (i) Comparison of monthly distribution of CDs during CP with the QP

The monthly distribution of CDs formed over the BOB during CP and QP is depicted in Fig.77 and Fig.78. The highest frequency of CDs was observed in both periods in October and November, and the lowest in February and March. In QP, February and March are completely CD-free. The monthly frequency of cyclonic disturbances in the BOB during the CP clearly shows that the higher frequency of D and DD formed in August and October (Fig.79), while the cyclonic storms formed primarily in November (Fig.80), which is almost identical to the quinquennial period (Fig.81 and Fig.82).

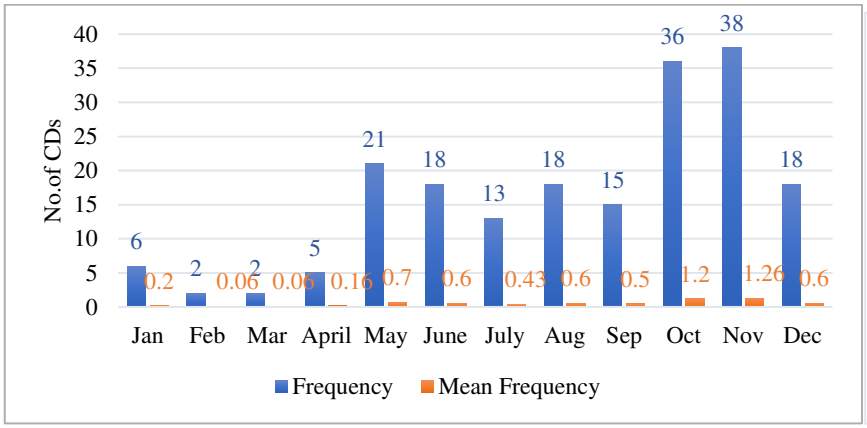

Fig.77 The monthly distribution of CDs formed over the BOB during CP

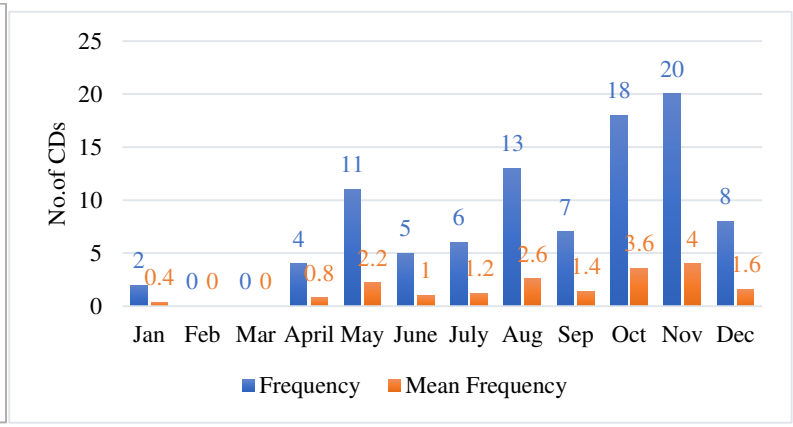

Fig.78 The monthly distribution of CDs formed over the BOB during QP

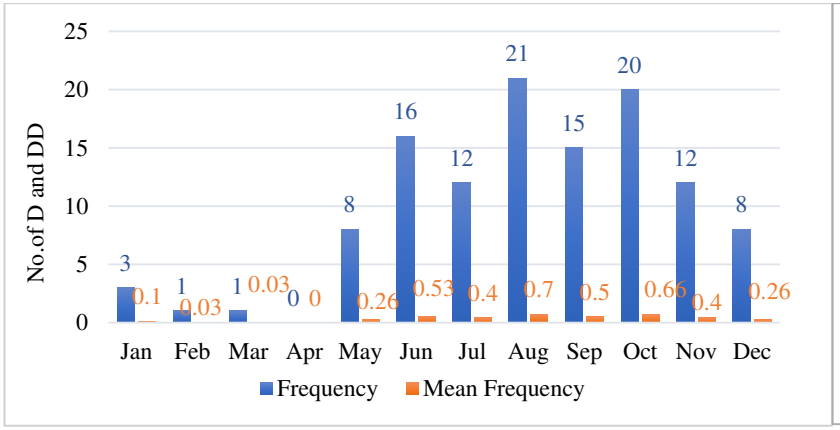

Fig.79 The monthly distribution of D and DD formed over the BOB during CP

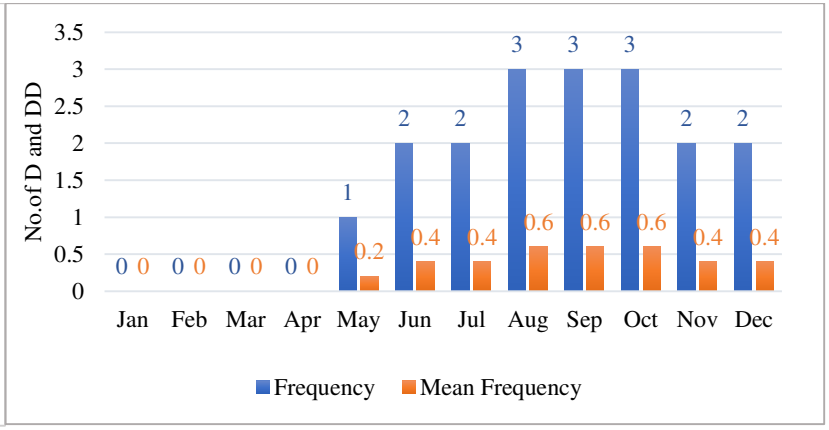

Fig.80 The monthly distribution of D and DD formed over the BOB during QP

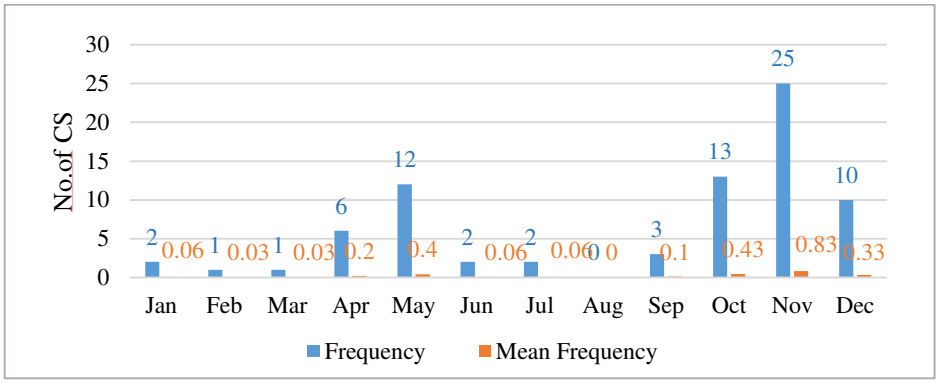

Fig.81 The monthly distribution of CS formed over the BOB during CP

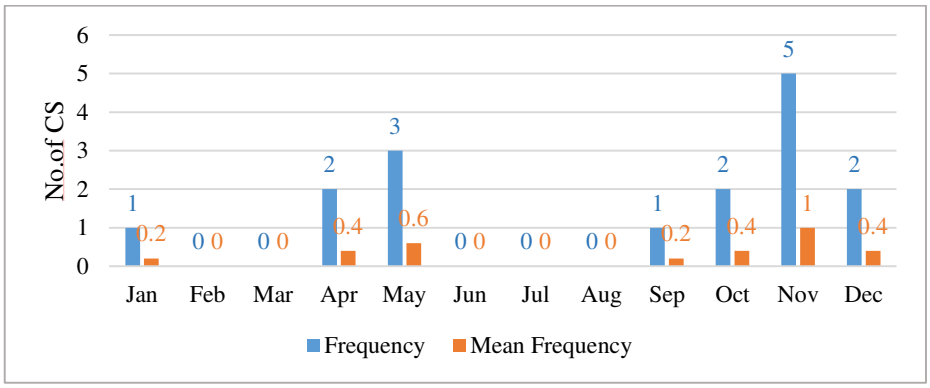

Fig.82 The monthly distribution of CS formed over the BOB during QP

4.3.3 (ii) Comparison of seasonal distribution of TC during CP with QP

When the seasonal distribution of total CD in BOB (Fig.83and Fig.84) was examined, the post monsoon season (Jan-Feb) had the highest number of cyclones, followed by the monsoon (Mar-May), pre-monsoon (June-Sep), and winter (Oct-Dec) in both CP and QP. D and DD are most common during the monsoon season, followed by the post-monsoon, pre-monsoon, and winter seasons in both CP and QP Fi.85 and Fig.87. The frequency of cyclonic storms, including CS, SCS, VSCS, ESCS and SuCS are higher in the post-monsoon followed by the pre-monsoon, monsoon and winter seasons during the CP and QP (Fig.86 and Fig.88).

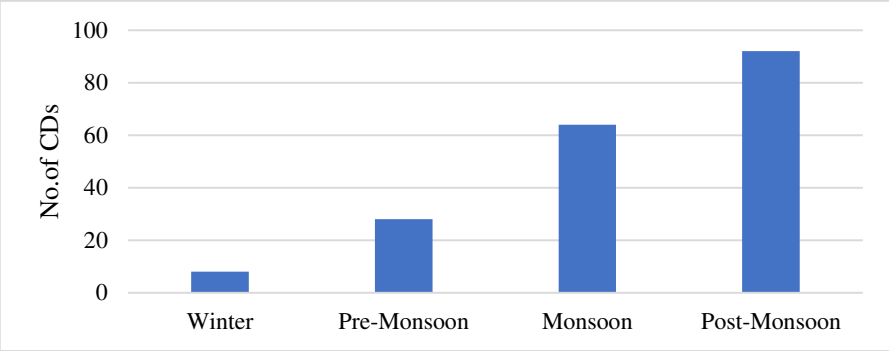

Fig.83 Seasonal distribution of total CDs in BOB in Climatological Period

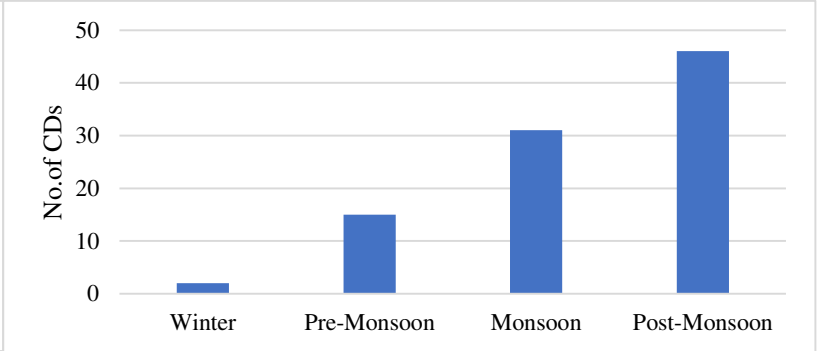

Fig.84 Seasonal distribution of total CDs in BOB in QP

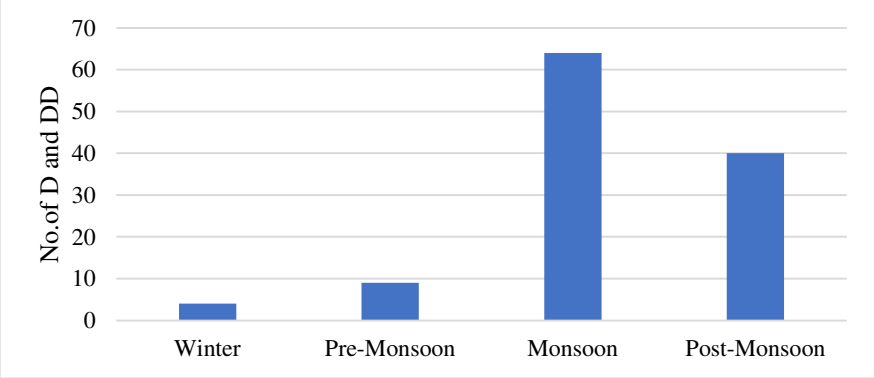

Fig.85 Seasonal distribution of D and DD in BOB during Climatological Period

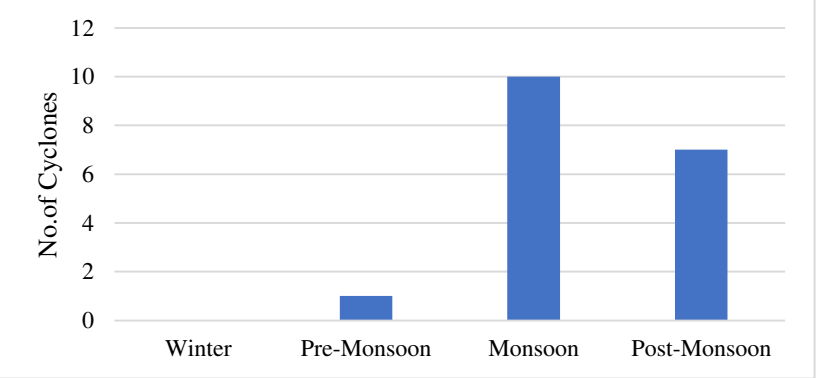

Fig.86 Seasonal distribution of D and DD in BOB during QP

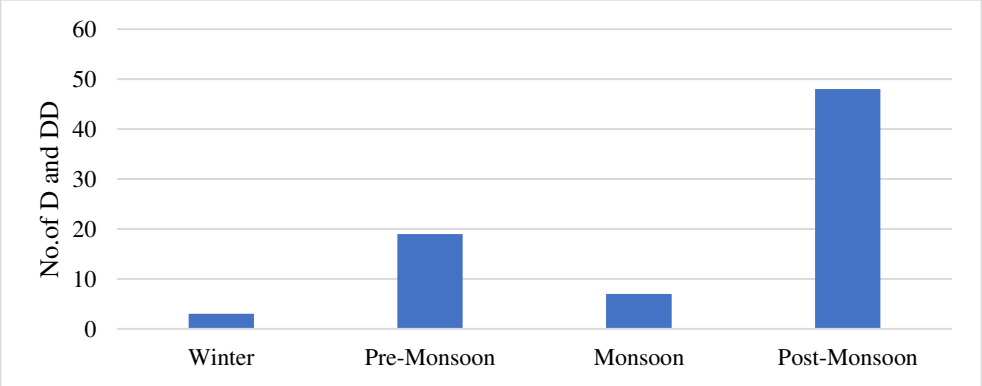

Fig.87 Seasonal distribution of CS in BOB during CP

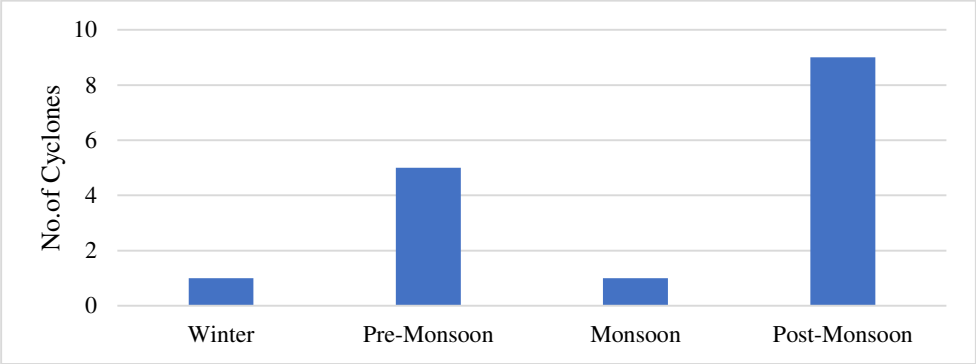

Fig.88 Seasonal distribution of CS in BOB during quinquennial period

4.4. Temporal distribution of cyclonic disturbances in ARB

4.4.1 Annual distribution

The annual distribution of total CD formed over ARB during CP and QP are depicted in Fig.89 and Fig.90. Normally, ARB is less prone to CD than BOB, but it is surprising to note that, while the frequency of BOB CD is decreasing, a significant positive trend was observed for ARB both during CP and QP. In addition, the area affected by the CD in both periods shows an increasing trend (Fig.91 and Fig.92).

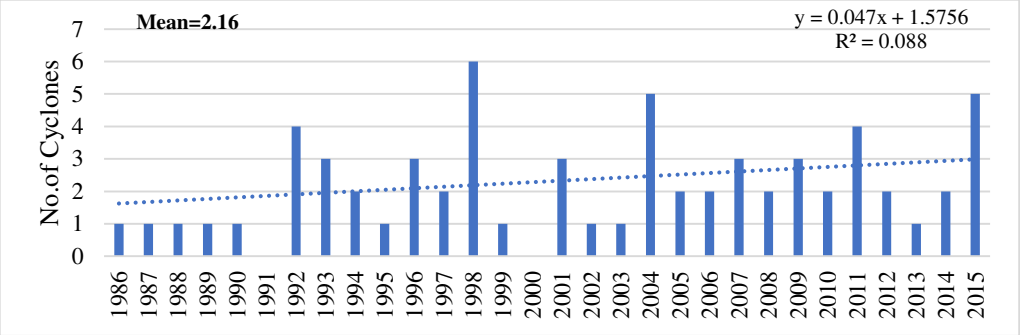

Fig.89 Annual distribution of total CDs formed over ARB during CP

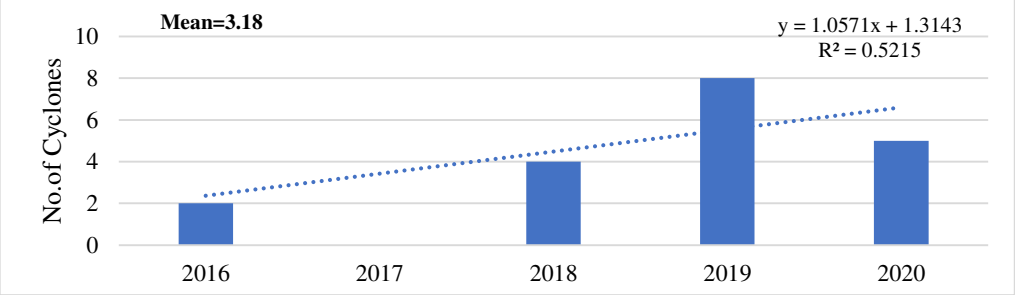

Fig.90 Annual distribution of total CDs formed over ARB during QP

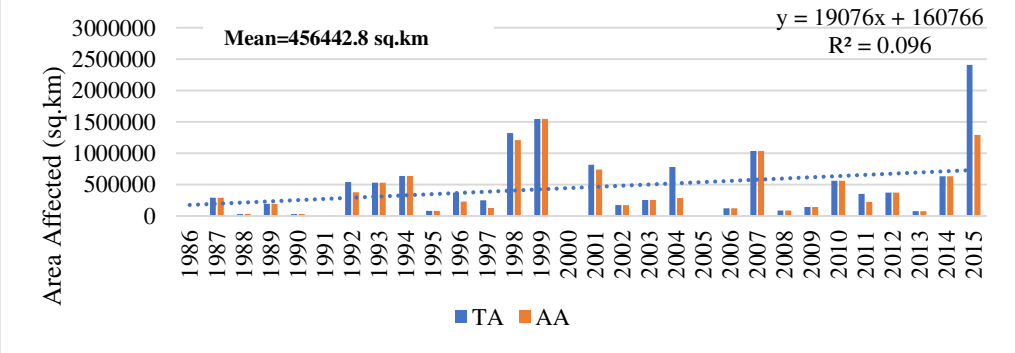

Fig.91Annual distribution of total area affected by CDs formed over ARB during CP

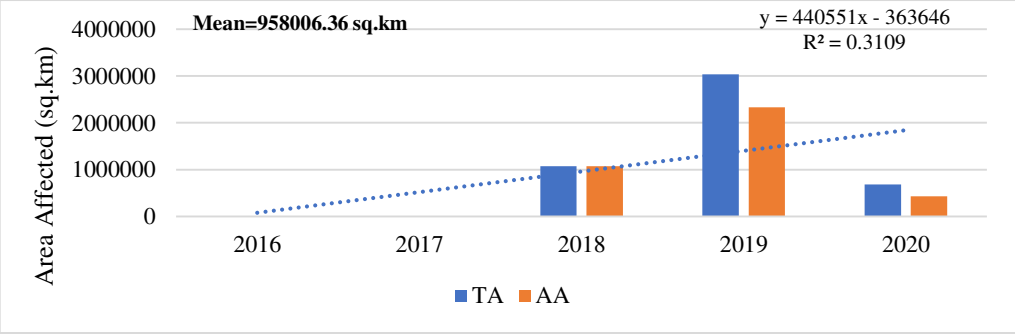

Fig.92Annual distribution of total area affected by CDs formed over ARB during QP

4.4.2 Intensitywise distribution

4.4.2a Comparison of intensitywise distribution of TC during CP with the QP

The intensitywise distribution of Total CDs that formed over ARB during the CP and QP is shown in Fig.93 and Fig.94. There were a total of 65 CDs that formed over ARB during CP, including 9 D, 22 DD, 13CS, 9 SCS, 2VSCS, and 7 ESCS. In QP, the frequency of intense cyclones such as VSCS and ESCS is increasing faster than in CP. D and DD appear to have more occurrences during both periods. Fig.95 and Fig.96 show the area of the ARB affected by the CDs during both periods. The ESCS had a greater impact in both CP and QP. The frequency of occurrence of D increases in CP (Fig.97), whereas it decreases in QP (Fig.98). DD frequency decreased during CP (Fig.99), and DD occurred only twice during the QP. As a result, there was no discernible trend in the frequency or area affected by DD (Fig.100 and Fig.102). The area affected by DD during CP is shrinking (Fig.101). In CP, the frequency and area affected by CS show a decreasing trend (Fig.103and Fig.105), whereas during QP, it occurred only twice, so the frequency and area affected show no significant trend (Fig.104 and Fig.106). The SCS had a positive trend for frequency and area for CP (Fig4.42a and Fig4.43a), but it only occurred once in QP, so it did not show any significant trend during this time period (Fig4.42b and Fig4.43b). Intense cyclonic storms, such as VSCS, show no trend in frequency during the CP, but they do show a significant trend in QP (Fig4.44a, Fig4.44b). In terms of frequency and area, ESCS shows an increasing trend during both CP and QP. Figures 4.46a, 4.46b, 4.47a, and 4.47b). Sucs was not present in ARB during CP, but it did occur once in QP, which was in 2019. Overall, the findings show that the frequency and area affected by intense cyclones is increasing in ARB.

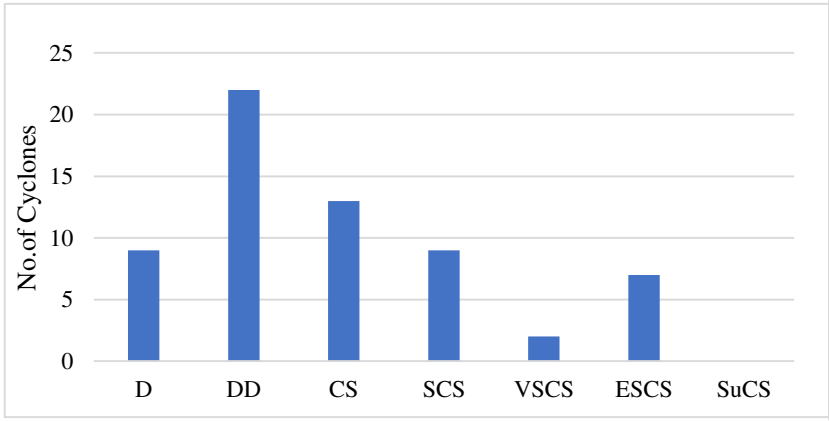

Fig.93 Frequency of CDs that formed over ARB during the CP

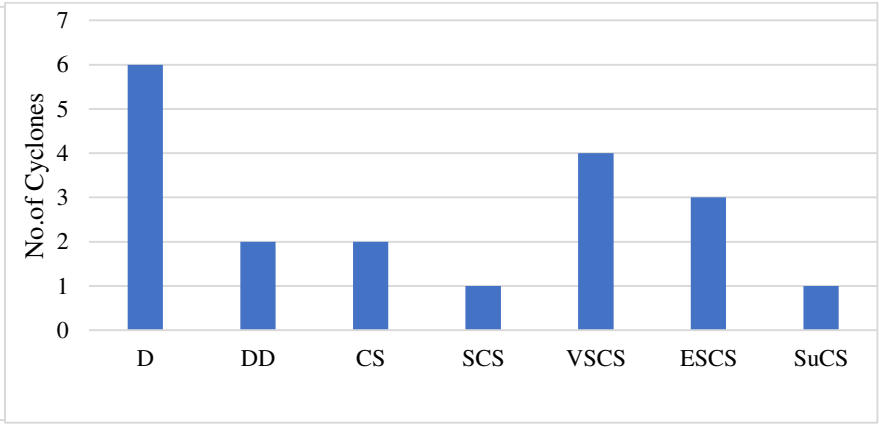

Fig.94 Frequency of CDs that formed over ARB during the QP

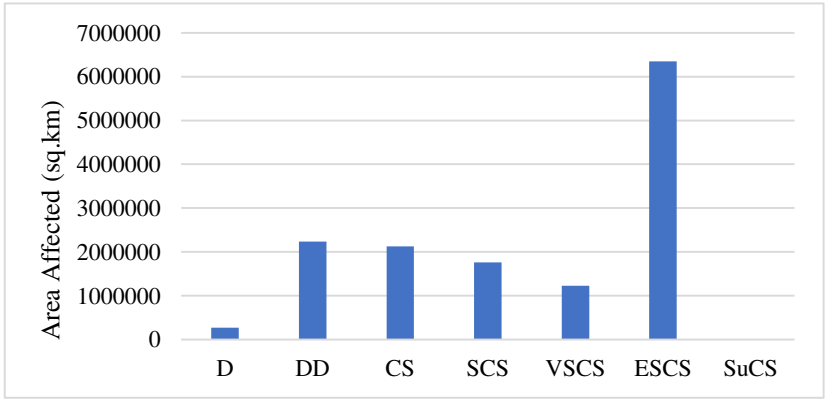

Fig.95 Total area affected by CDs that formed over ARB during the CP

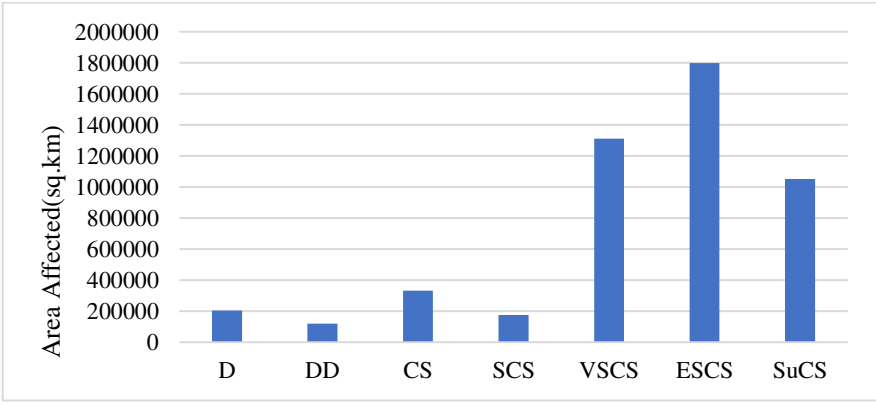

Fig.96 Frequency of CDs that formed over ARB during the QP

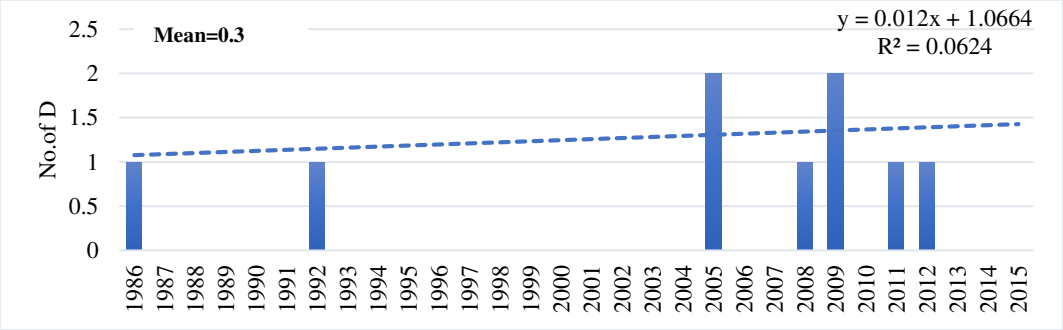

Fig.97 Frequency of D in ARB during CP

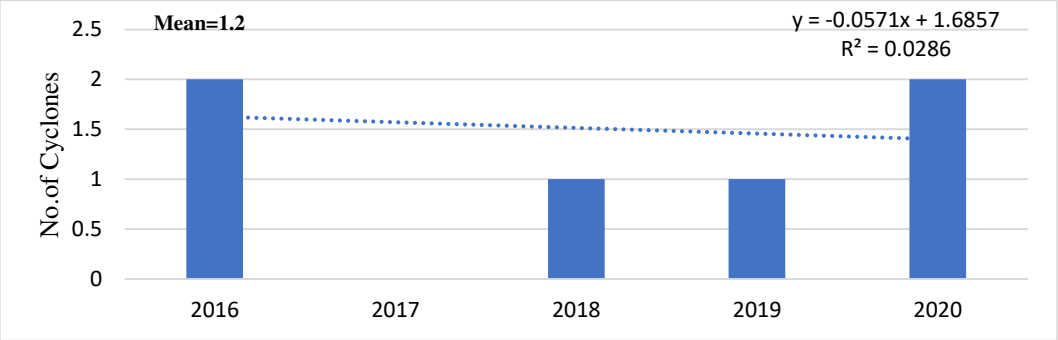

Fig.98 Frequency of D in ARB during QP

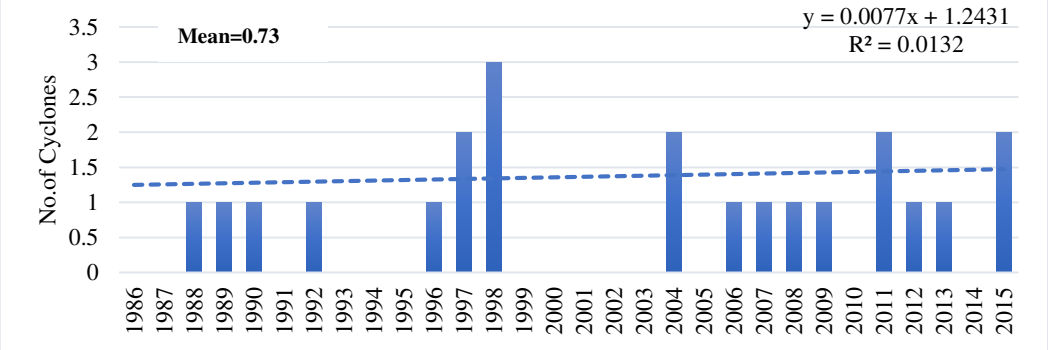

Fig.99 Frequency of DD in ARB during CP

Fig.100 Frequency of DD in ARB during QP

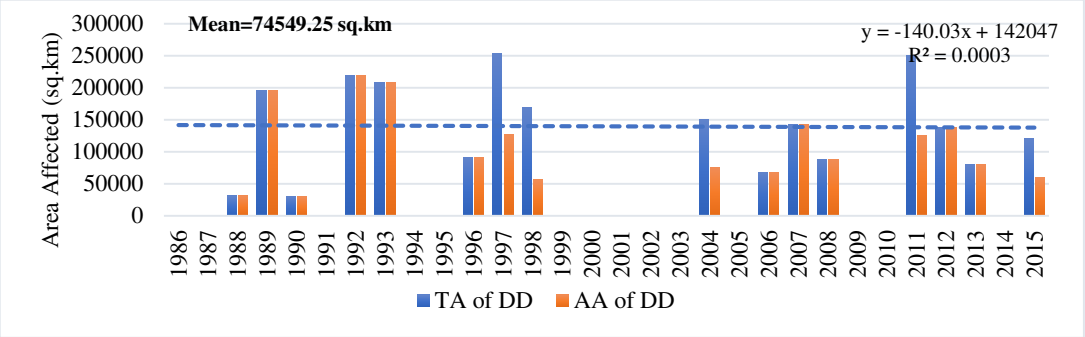

Fig.101 Total area affected by DD in ARB during CP

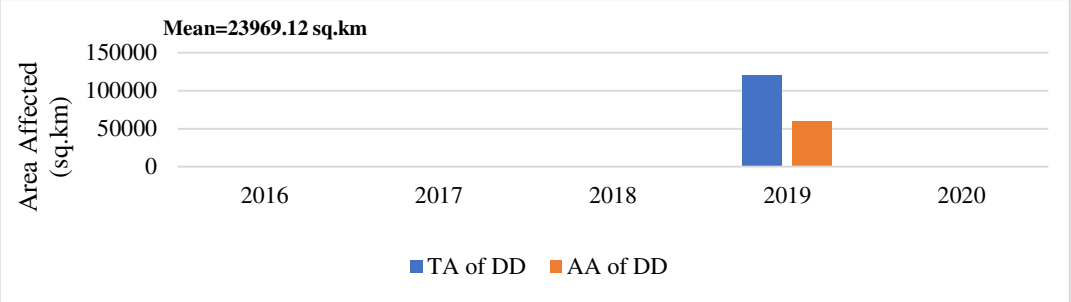

Fig.102 Total area affected by DD in ARB during QP

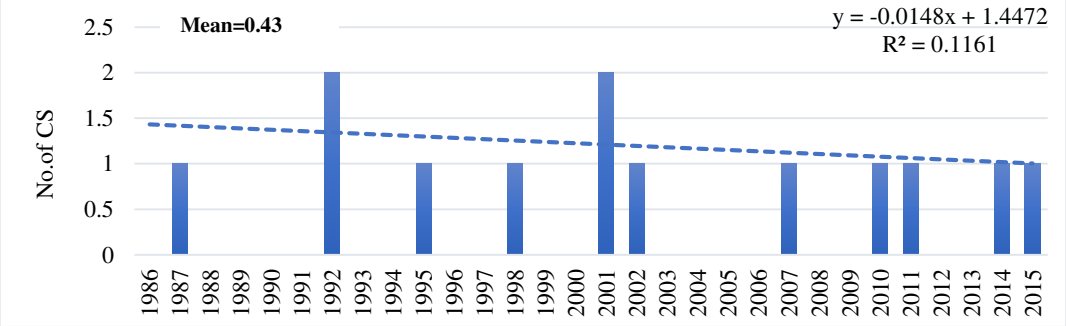

Fig.103 Frequency of CS in ARB during CP

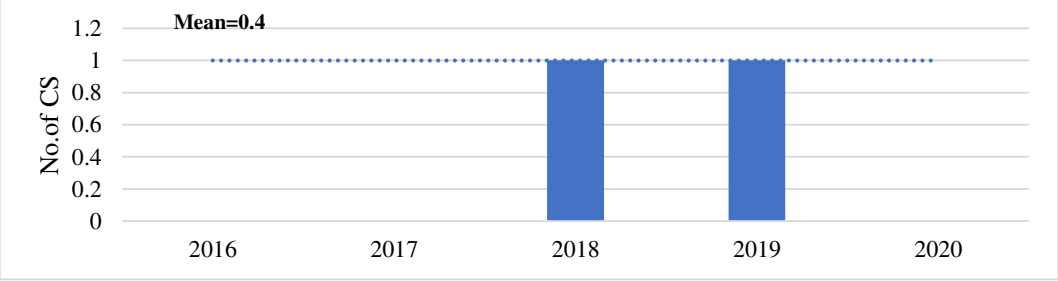

Fig.104 Frequency of CS in ARB during QP

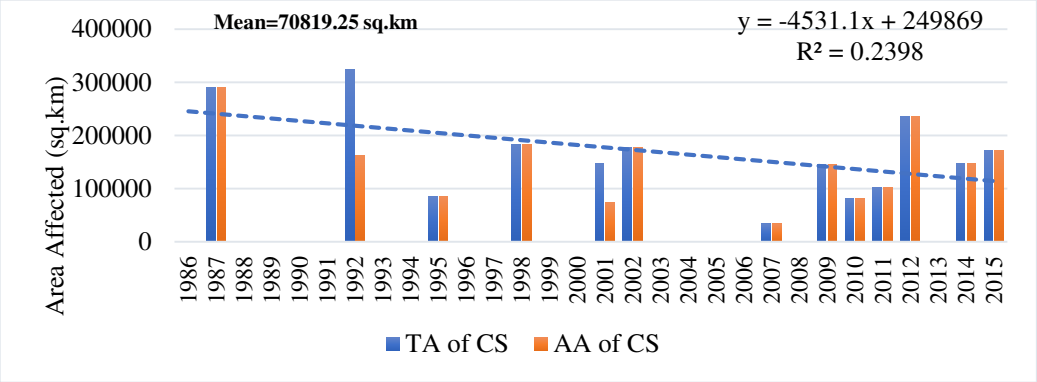

Fig.105 Area affected by CS in ARB during CP

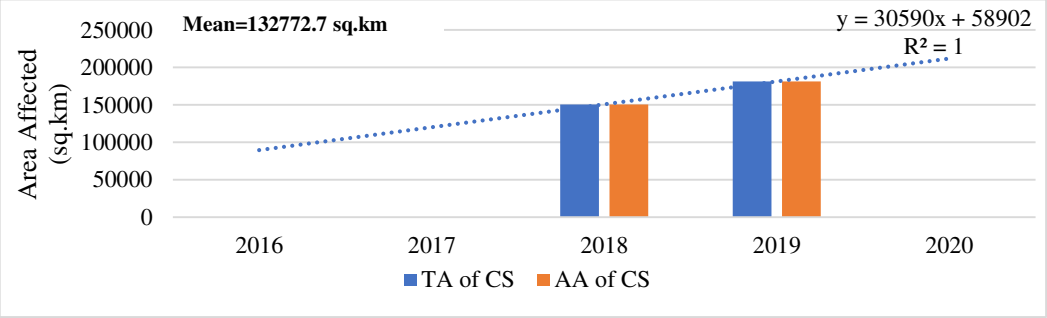

Fig.106 Area affected by CS in ARB during QP

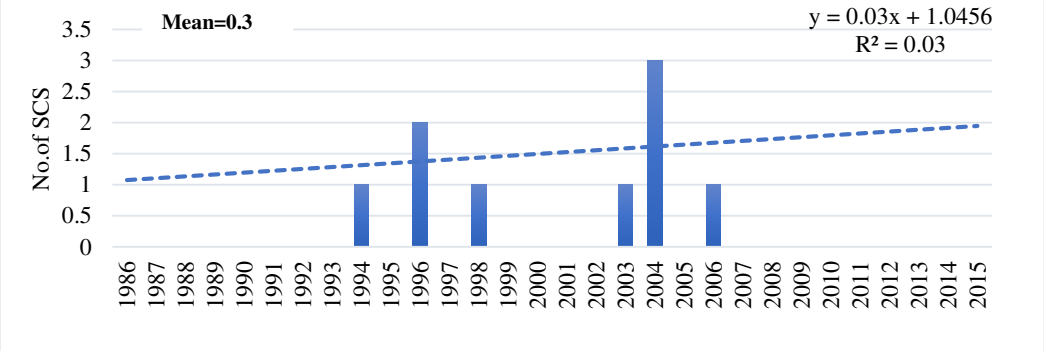

Fig.107 Frequency of SCS in ARB during CP

Fig.108 Frequency of SCS in ARB during QP

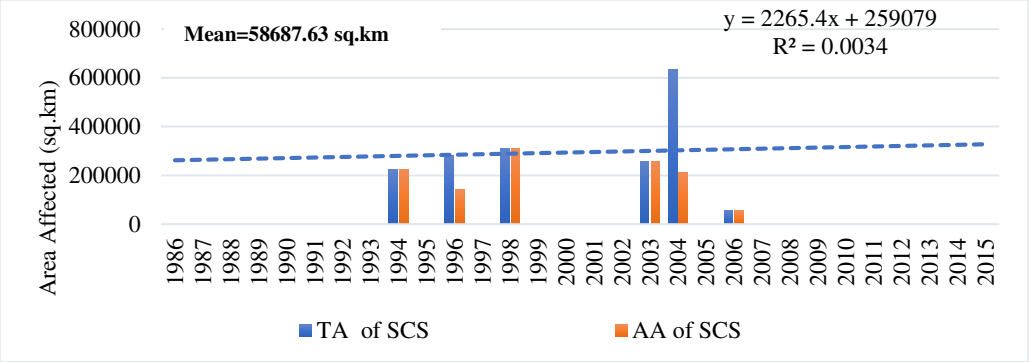

Fig.109 Area affected by SCS in ARB during CP

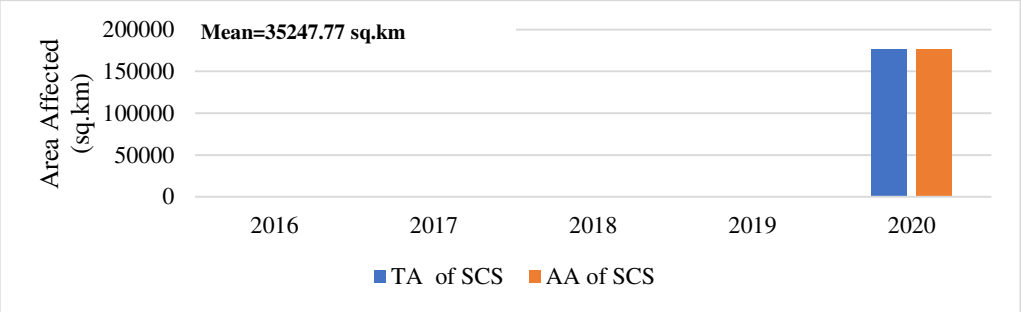

Fig.110 Area affected by SCS in ARB during QP

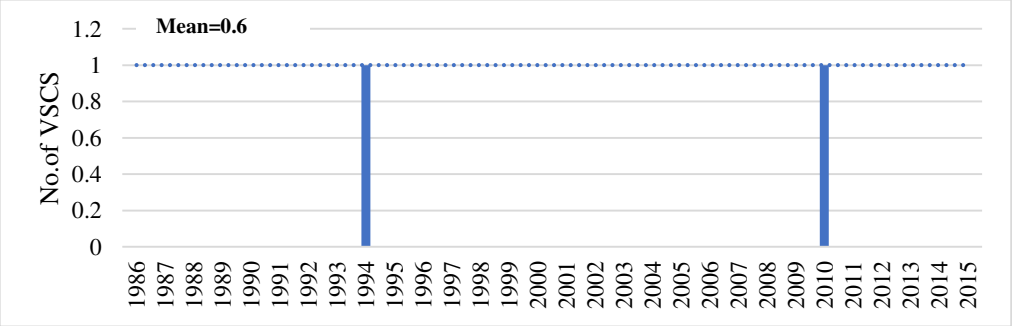

Fig.111 Frequency of VSCS in ARB during CP

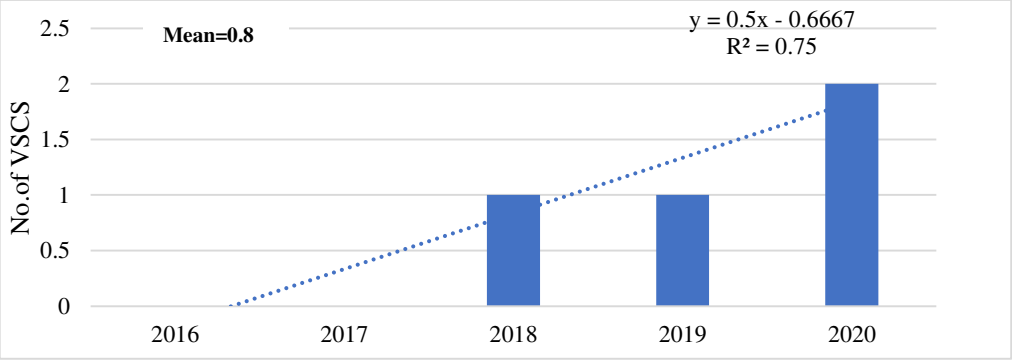

Fig.112 Frequency of VSCS in ARB during QP

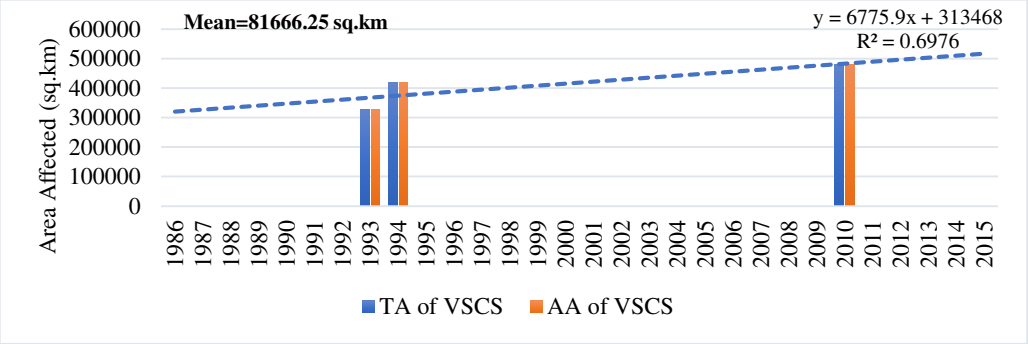

Fig.113 Area affected by VSCS in ARB during CP

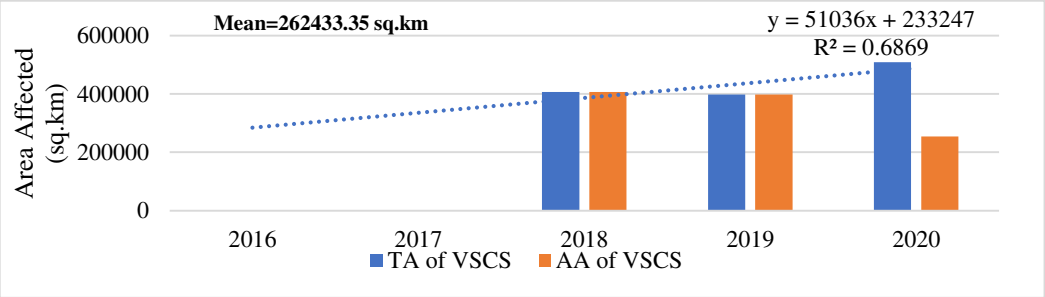

Fig.114 Area affected by VSCS in ARB during QP

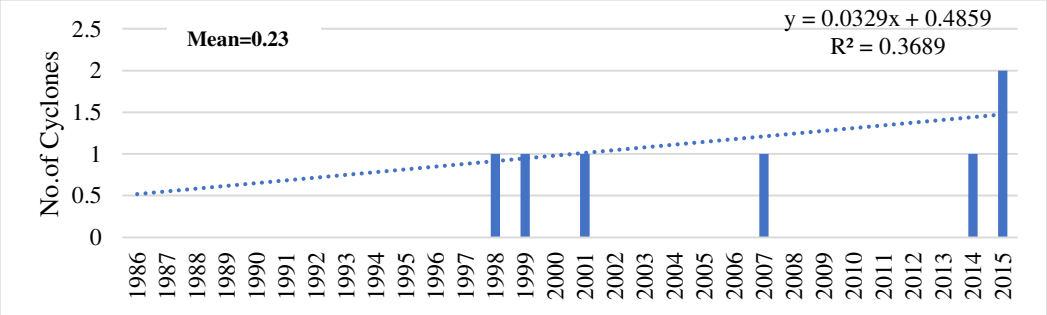

Fig.115 Frequency of ESCS in ARB during CP

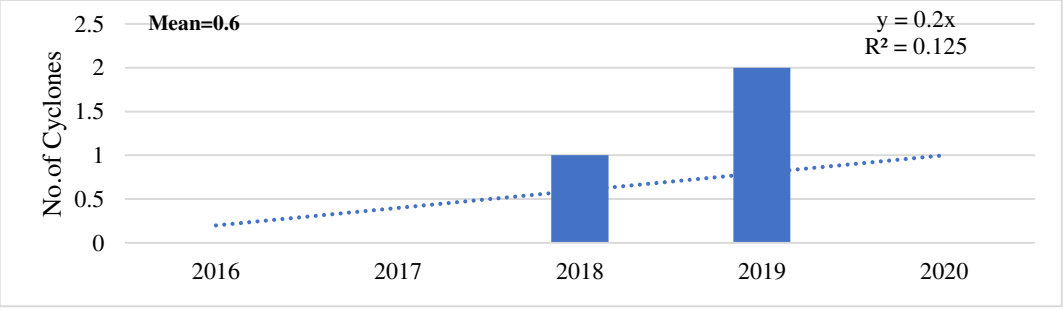

Fig.116 Frequency of ESCS in ARB during QP

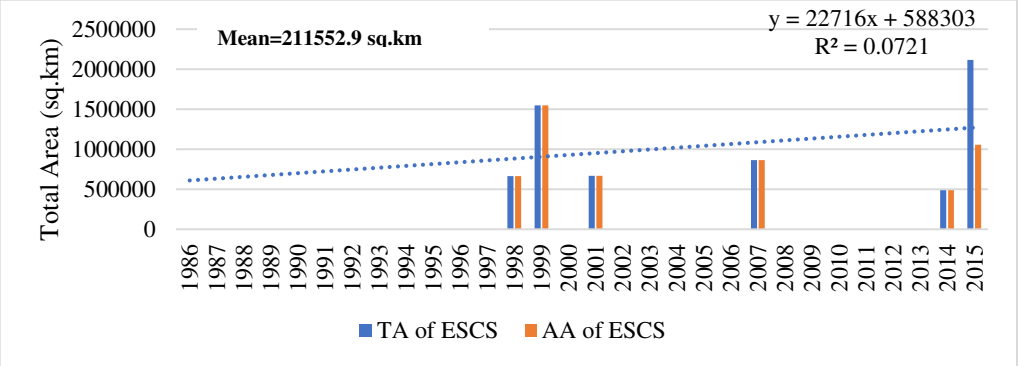

Fig.117 Frequency of ESCS in ARB during CP

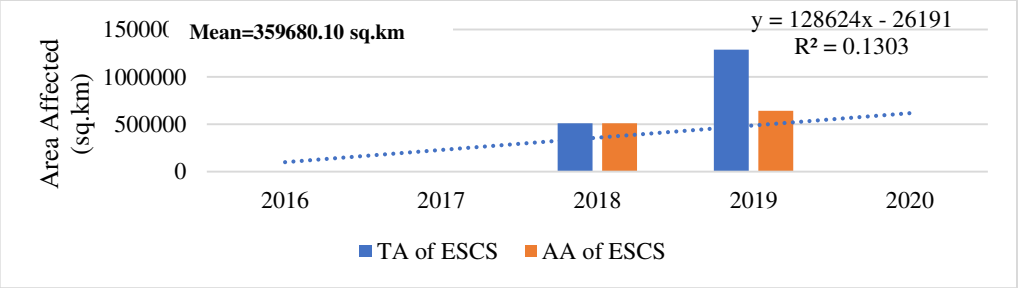

Fig.118 Area affected by ESCS in ARB during QP

4.4.3 Seasonal and monthly distribution

4.4. (i)Comparison of monthly distribution of TC in ARB during CP with QP

The monthly distribution of CDs formed over the ARB during CP and QP is depicted in Fig.119 and Fig.120. Except for March and July, when CDs occurs in the QP but is completely absent in the CP, both of these exhibit more or less similar observations. In both cases, the highest number of CDs occurred in June, while February, March, July, and August were completely free of cyclones during CP. Nov is the second largest month which carries the CDs in both periods. Cyclonic Depressions and Cyclonic Storms are most common in CP during June and November, and in QP during December (Fig.121 and Fig.123). During both periods, February is free of Cyclonic depressions. During both periods, October and November have the highest number of CS (Fig.122 and Fig.124). CS is completely absent during the months of January, February, March, July, and September.

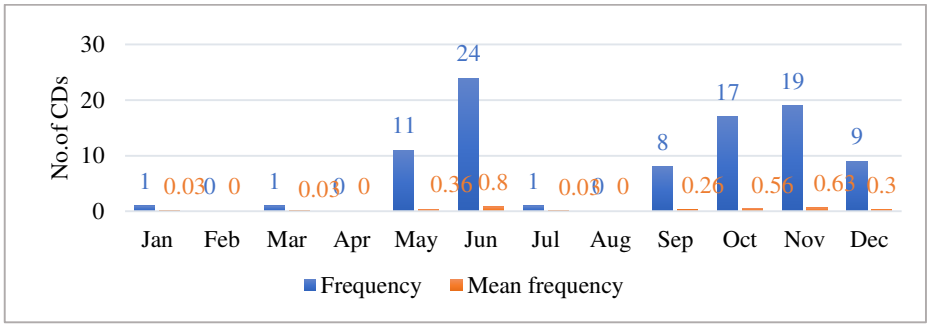

Fig.119 Monthly distribution of CDs formed over the ARB during CP

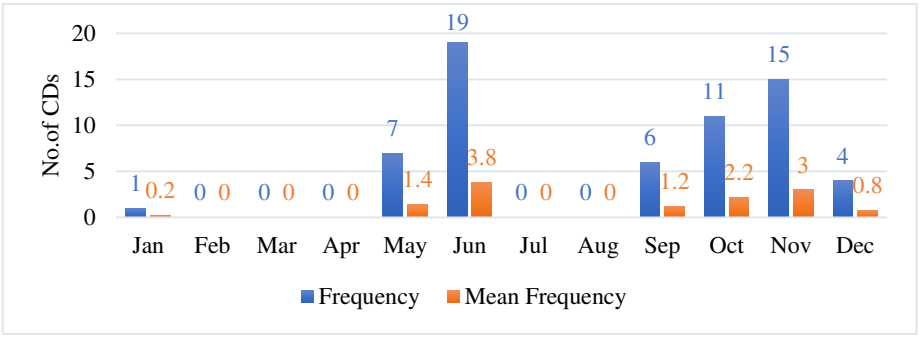

Fig.120 Monthly distribution of CDs formed over the ARB during QP

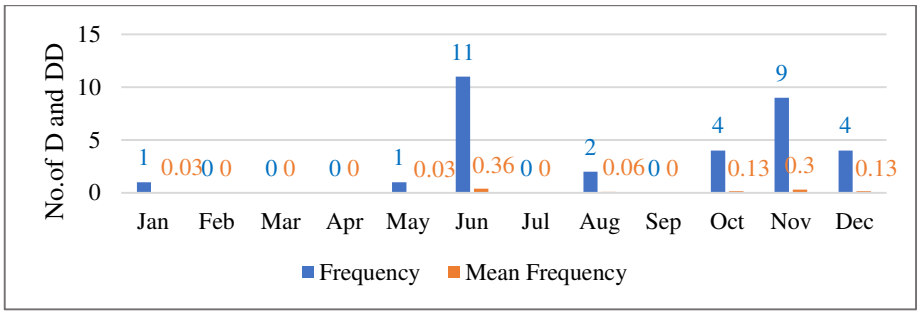

Fig.121 Monthly distribution of D and DD formed over the ARB during CP

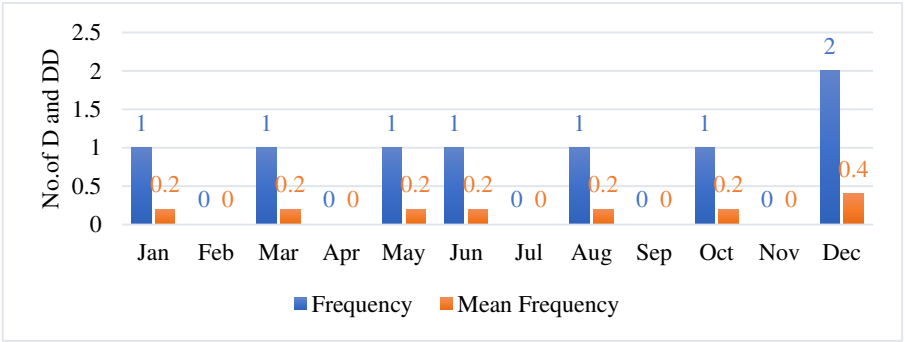

Fig.123 Monthly distribution of D and DD formed over the ARB during QP

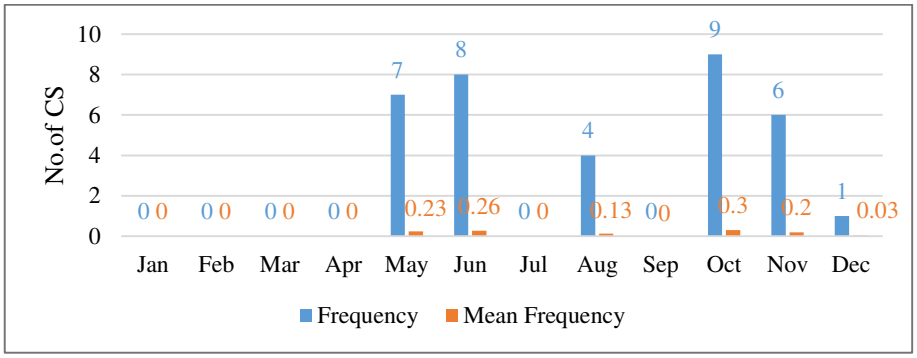

Fig.122 Monthly distribution of CS formed over the ARB during CP

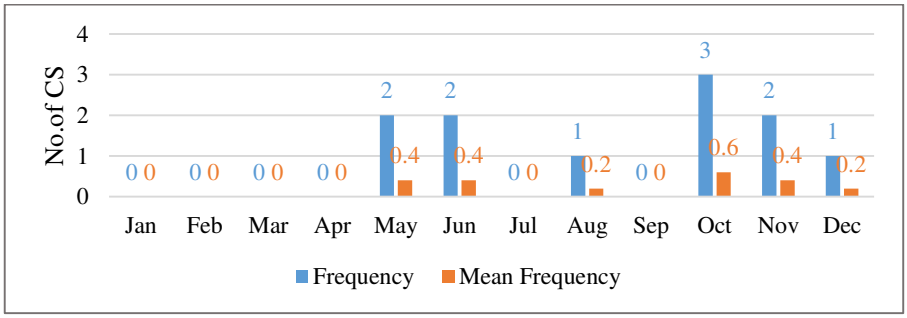

Fig.124 Monthly distribution of CS formed over the ARB during QP

4.4.3 (ii) Comparison of seasonal distribution of TC during CP with QP

When the seasonal distribution of total CDs in ARB was examined (Fig.125 and Fig.126), the post monsoon season (Jan-Feb) had the highest number of cyclones, followed by the monsoon (Mar-May), pre-monsoon (June-Sep), and winter (Oct-Dec) in both CP and QP. When considering the Cyclonic Depressions and Cyclonic storms separately during the CP and QP, the same trend as the above is followed with the winter season being completely free from CS (Fig.127, Fig.128, Fig.129 and Fig.130) in both periods.

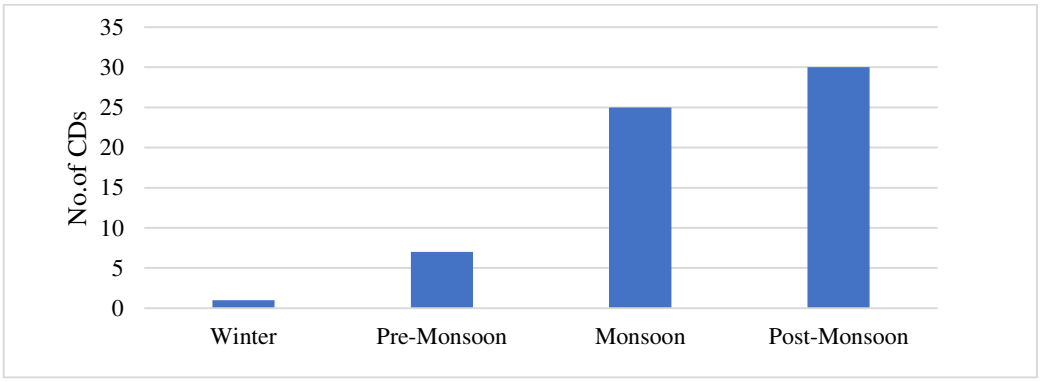

Fig.125 Seasonal distribution of total CDs in ARB during CP

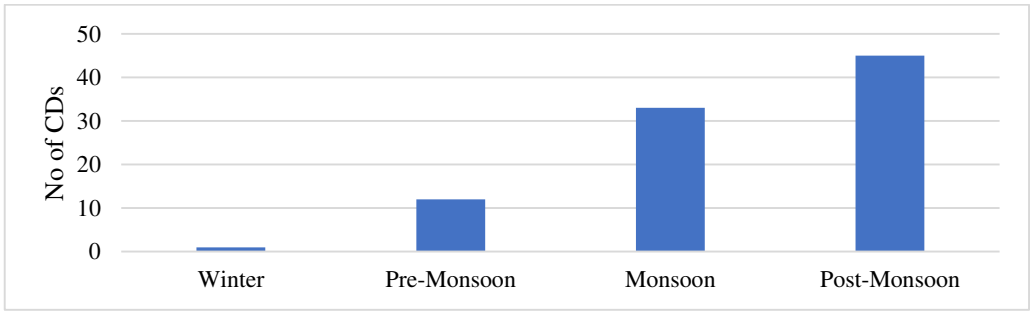

Fig.126 Seasonal distribution of total CDs in ARB during QP

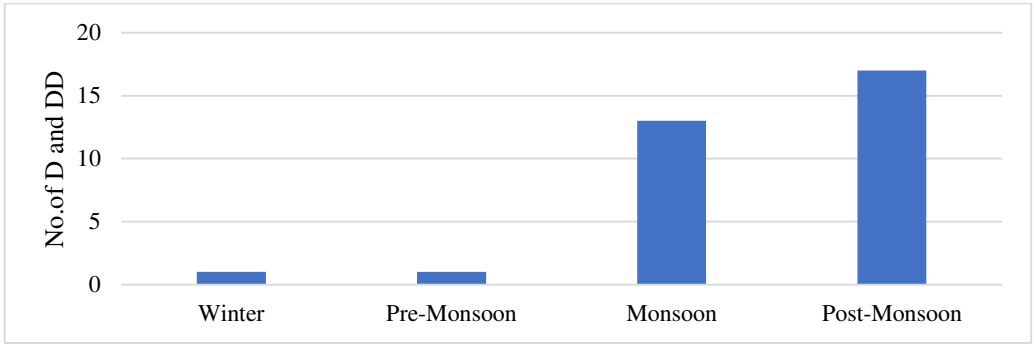

Fig.127 Seasonal distribution of total D and DD in ARB during CP

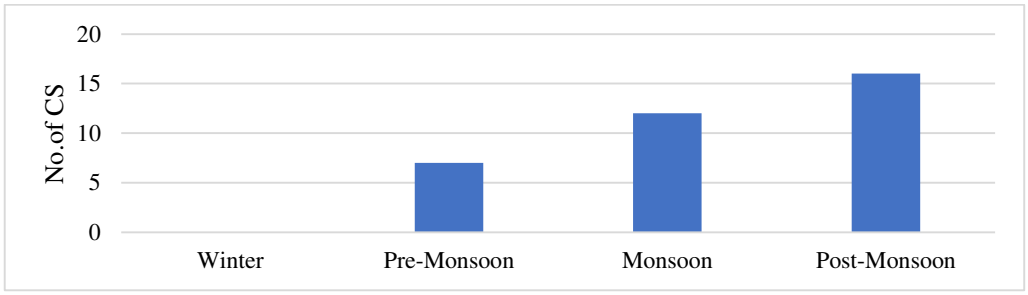

Fig.128 Seasonal distribution of total CS in ARB during CP

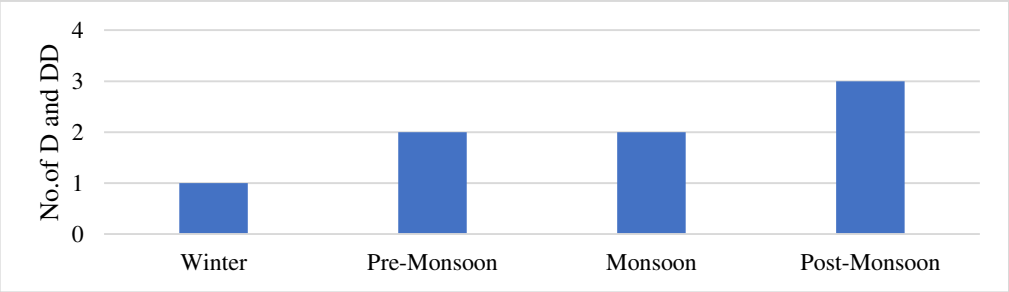

Fig.129 Seasonal distribution of total D and DD in ARB during QP

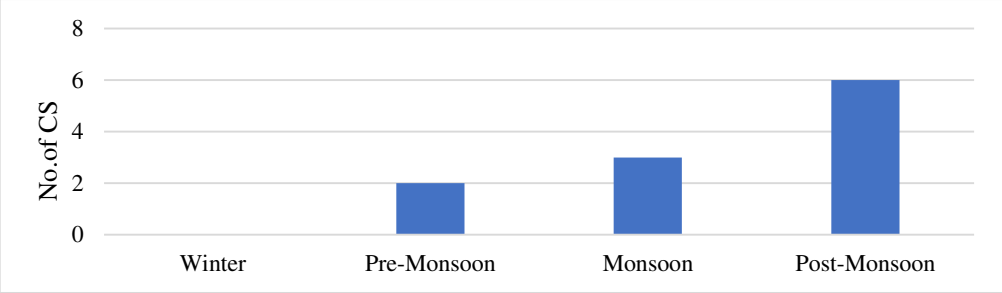

Fig.130 Seasonal distribution of total CS in ARB during QP

4.5 Variation of TC energy metrics in NIO

Different energy metrics such as VF, ACE, and PDI are used to determine the true impact of cyclonic disturbances on the NIO. Each year, they are calculated for different intensities and seasons, and cyclonic activity is defined.

4.5.1(i) Inter annual variation of mean Velocity Flux (VF) during CP and QP

The annual VF (Table 1) for Cyclonic Depressions is 16.26102 ×10^2 kt (36.75102×10^2 kt) in NIO, 11.06102×10^2 kt (25.82102×10^2 kt) in BOB, and 4.37102×10^2 kt (12.39102×10^2 kt) in ARB (Cyclonic Storms). In terms of intra seasonal variation, VF is significantly higher in both BOB and ARB during the Post-Monsoon season, which may be due to the increased frequency and intensity of cyclones during that time. There is no discernible difference in the VF of ARB across seasons. Higher VF is visible on BOB for Cyclonic Storms in both the Pre-Monsoon and Post-Monsoon seasons when compared to ARB. It could be because

the VF is affected by average intensity and frequency, and it is higher on BOB than in ARB. It will be covered in greater detail in subsequent sections. During the monsoon, the VF of CS and CD are lower in BOB than in ARB because the frequency and intensity of cyclones over ARB is higher at that season.

Taking into account the VF over QP (Table4.2), there is a significant increase in the annual VF over NIO, BOB, and ARB as well. This could be due to an increase in the frequency and average intensity of TC during the QP. There isn't much of a difference between BOB's annual VF and ARB like CP's, which could be due to an increase in the frequency and intensity of ARB during QP. In BOB, the Post-monsoon season has the highest VF, followed by Pre-monsoon and Monsoon, while in ARB, the Post-monsoon season has the highest VF, followed by Monsoon. The impact of the monsoon on AS has an impact on the energy metrics of ARB.

The overall changes in VF for D, CS, and total cyclonic disturbances in NIO over the entire study period (Fig.131a, Fig.131b and Fig.131c) show that D and DD have a significant negative trend, whereas VF of cyclonic storms has a significant increasing trend in recent periods. There is a significant increase in the QM than CM in recent periods, indicating an overall increase in the VF of cyclonic storms. In recent periods, the total CD has also shown a positive trend, with a higher value in QM than in CM. The D in the BOB shows a negative trend with a higher value for CM than QM (Fig.132a), but the QM of CS shows a higher value than CM but no positive trend (Fig.132b). When the total VF of BOB, including all Cyclonic Depressions, is combined, there is a negative trend in recent years, with QM having a slightly higher value than CM (Fig.132c). The VF of Cyclonic depression in AS has shown a negative trend in recent years, but its QM is slightly higher than CM (Fig.133a). In recent years, the CS and total cyclonic disturbances of ARB have shown a significant positive trend, with a higher VF in QM than in CM (Fig.133band Fig.133c). Altogether, VF showed an increasing trend in AS and NIO and a decreasing trend in BOB.

Table 4.1 Mean VF (×10^2 kt) during CP and QP

Basin	CP	CD	CS	Total	Basin	QP	CD	CS	Total
NIO	Annual	16.26	36.75	53.02	NIO	Annual	7.38	9.64	6.482
	Winter	1.26	0.206	1.46		Winter	0	1	1.46
	Pre-Monsoon	1.15	16.48	10.69		Pre-Monsoon	1.09	2.34	3.5
	Monsoon	2.33	5.48	13.29		Monsoon	0.683	1.758	2.43
	Post-Monsoon	7.59	21.76	29.35		Post-Monsoon	3.93	5.66	9.6
BOB	Annual	11.06	25.82	36.89	BOB	Annual	7.41	4.55	6.96
	Winter	.968	.206	1.17		Winter	0	1	1
	Pre-Monsoon	1.15	12.99	14.14		Pre-Monsoon	.95	1.57	2.52
	Monsoon	.968	2.06	3.02		Monsoon	.56	.83	1.39
	Post-Monsoon	4.05	16.91	20.96		Post-Monsoon	.575	3.05	3.625
ARB	Annual	4.37	12.39	16.77	AS	Annual	6.08	2.643	7.51
	Winter	0.293	0	.29		Winter	0	0	0
	Pre-Monsoon	0	3.49	3.49		Pre-Monsoon	.141	0.77	0.911
	Monsoon	1.37	3.42	4.79		Monsoon	.123	.928	1.051
	Post-Monsoon	3.54	4.85	8.39		Post-Monsoon	3.36	2.61	5.97

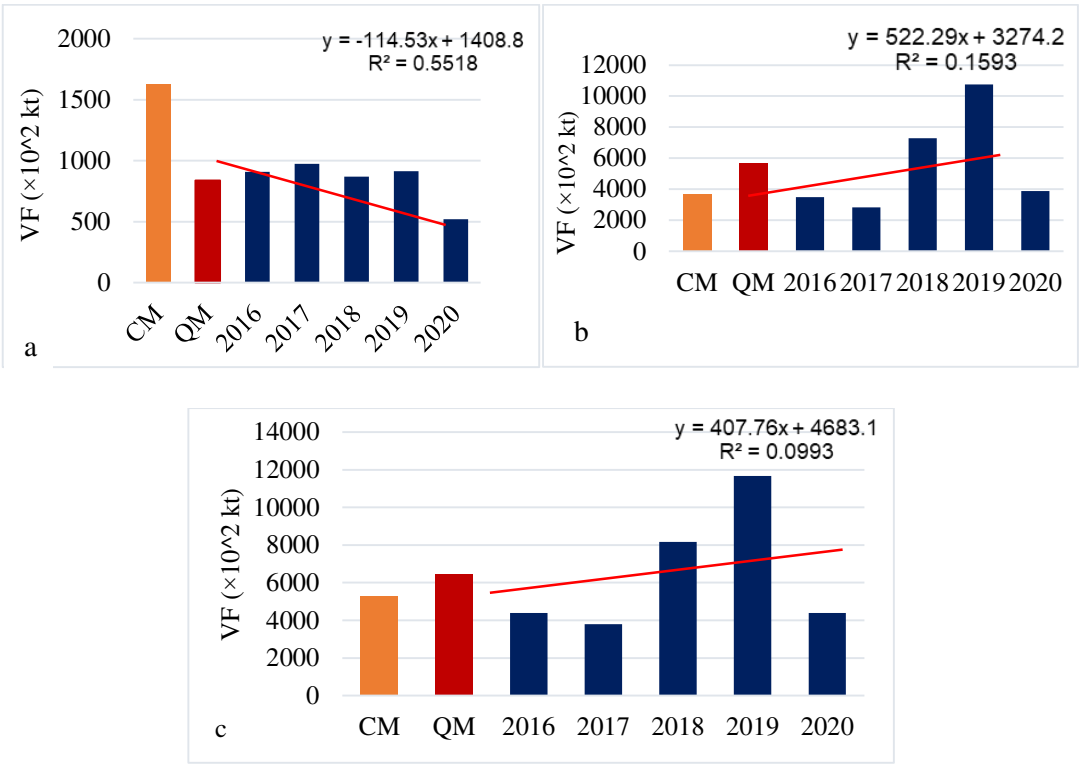

Fig.131-a) VF of cyclonic depressions in NIO b) VF of CS in NIO c) VF of total CDs in NIO

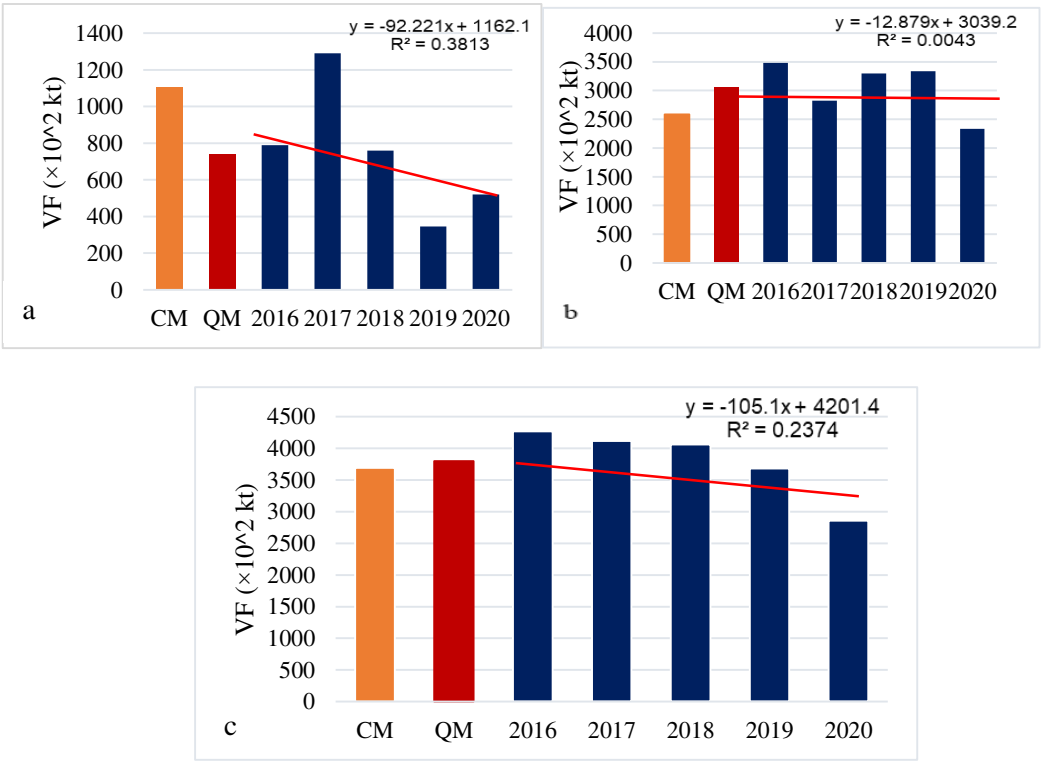

Fig.132-a) VF of cyclonic depressions in BOB b) VF of CS in BOB c) VF of total CDs in BOB

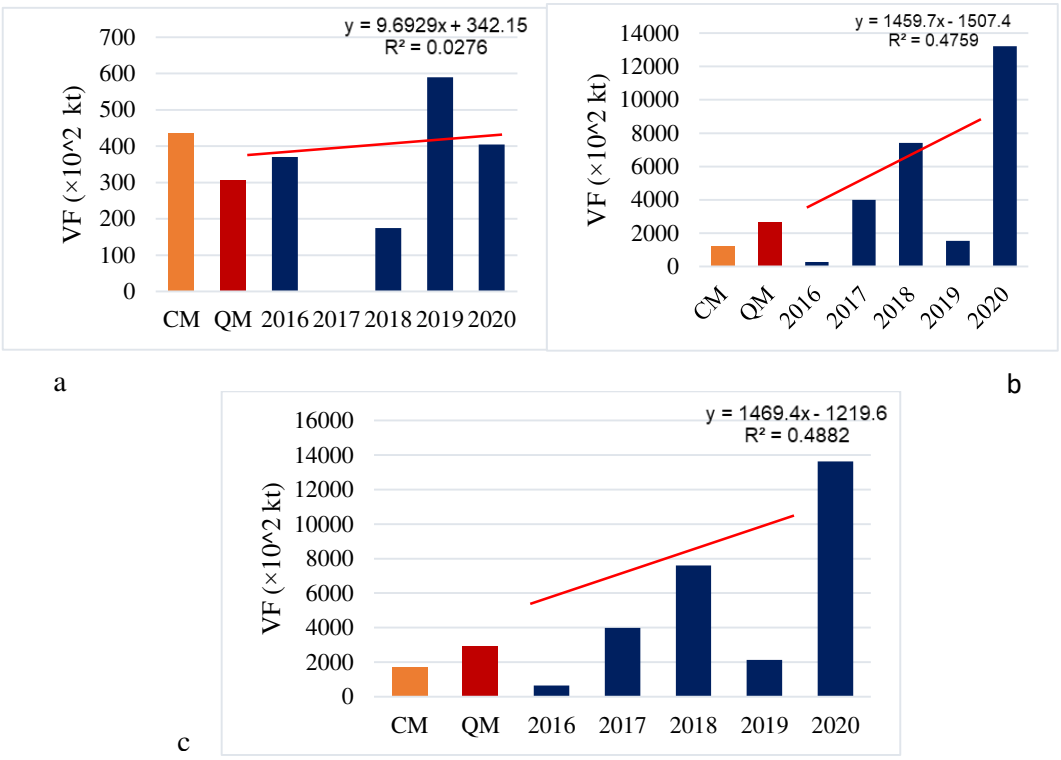

Fig.133-a) VF of cyclonic depressions in ARB b) VF of CS in ARB c) VF of total CDs in ARB

4.5.1(ii)Inter seasonal variation of mean Velocity Flux (VF) during CP and QP

Considering the BOB in the CP, the CS and Cyclonic depressions have higher VF in the post-monsoon season followed by the pre-monsoon. The value of VF for CD is lower compared to CS (Fig.134a). This same observation was made for QP also, but at a very lower value compared to QP (Fig.134b).Considering the CP in ARB, CS shows higher VF during the post-monsoon followed by the pre-monsoon and the monsoon, where as the CD shows higher value in the post-monsoon followed by the monsoon (Fig.135a) In ARB, the occurrence of more cyclonic depressions taking place during the monsoon period might be the reason for this. In QP, the VF for CD has increased with both having a higher value during the CP (Fig.135b). In NIO, during the CP and QP, the higher value of VF is evident for CS

than CD and is highest during the post-monsoon season, followed by the pre-monsoon and monsoon (Fig.136a and Fig.136b).

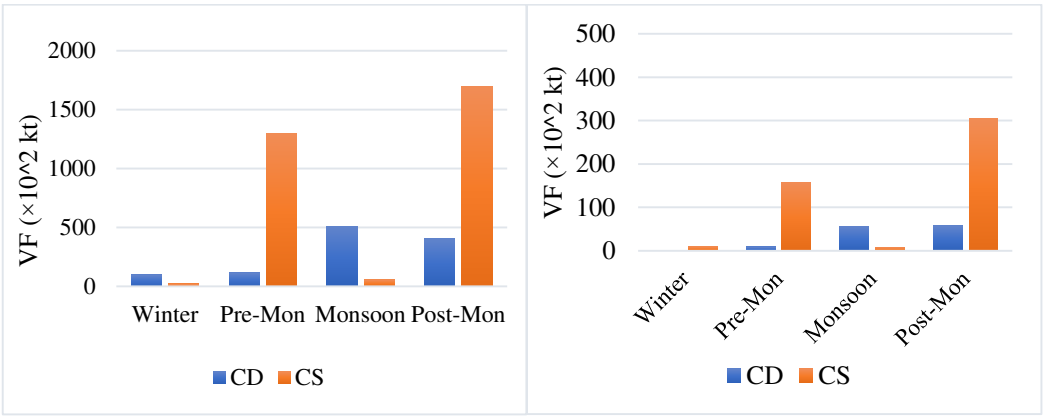

Fig.134 a) Variation of VF during CP in BOB b) Variation of VF during QP in BOB

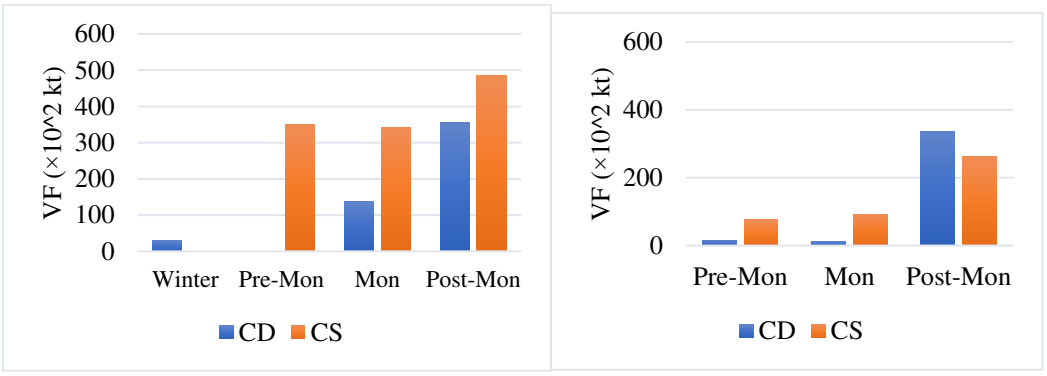

Fig.135 a) Variation of VF during CP in ARB b) Variation of VF during QP in ARB

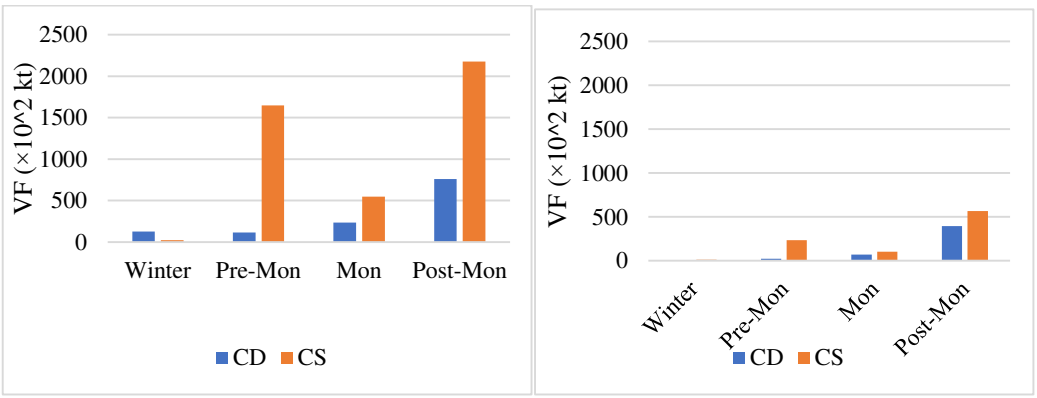

Fig.136 a) Variation of VF during CP in NIO b) Variation of VF during QP in NIO

4.5.2 Variation in mean Accumulated Cyclone Energy (ACE) in NIO

4.5.2 (i) Inter annual variation of ACE

The mean ACE of NIO during the climatological period (Table 2) is 20.83 104 ×10^4 kt^2 (4.64104×10^4 kt^2), with 14.30104×10^4 kt^2 (3.36104×10^4 kt^2) for BOB and 6.95104×10^4 kt^2 (1.36104×10^4 kt^2 for ARB for Cyclonic storms) (Cyclonic depressions). The ACE value is higher on BOB than on ARB, and the intraseasonal variation is greater in the BOB cyclonic disturbances. In comparison to the BOB and ARB, the BOB has a higher ACE for cyclonic storms in the Post Monsoon season than in the Monsoon season. The average intensity could be a factor in the increased ACE value in BOB. During the monsoon season, the ACE of tropical cyclones is higher in ARB than in BOB.

Considering the QP (Table 2), the annual ACE of CS is higher in NIO than in Cyclonic Depressions. Compared to AS and BOB, there is a slightly higher ACE for BOB, which infers that the ACE of ARB during recent years is increasing. Greater variation in intraseasonal variations can be seen in both BOB and ARB equally.

The overall changes in ACE during the entire study period for D, CS and total cyclonic disturbances in NIO (Fig.137a, Fig.137b and Fig.137c) indicate that D and DD show a significant negative trend whereas the ACE of cyclonic storms has a significantly increasing trend in recent periods. There is a significant increase in the QM than CM shows the overall increase in the ACE of cyclonic storms in recent periods. The total ACE has also had a positive trend in recent periods, with a higher value in QM than in CM. In the BOB, the D shows a negative trend with a higher value for CM than QM (Fig.138a), but the QM of CS shows a higher value than CM and a significant positive trend has been visible (Fig.138b) during recent years. When combining the total ACE of BOB, including all Cyclonic Depressions, shows a positive trend in recent years with QM having a higher value than CM (Fig.138c). So the ACE in BOB is increasing. In the ARB, the ACE of Cyclonic depression shows an a negative trend in recent years like that of BOB (Fig.139a). The CS and

total cyclonic disturbances of ARB have a significant positive trend in recent years, with a higher ACE in QM than in CM (Fig.139b and Fig.139c). It is very much evident that the ACE of ARB is significantly increasing. When the QP is taken into account, the annual ACE of CS in NIO is higher than in Cyclonic Depressions. Altogether, the ACE is increasing in BOB and ARB as well as NIO except for Cyclonic Depressions.

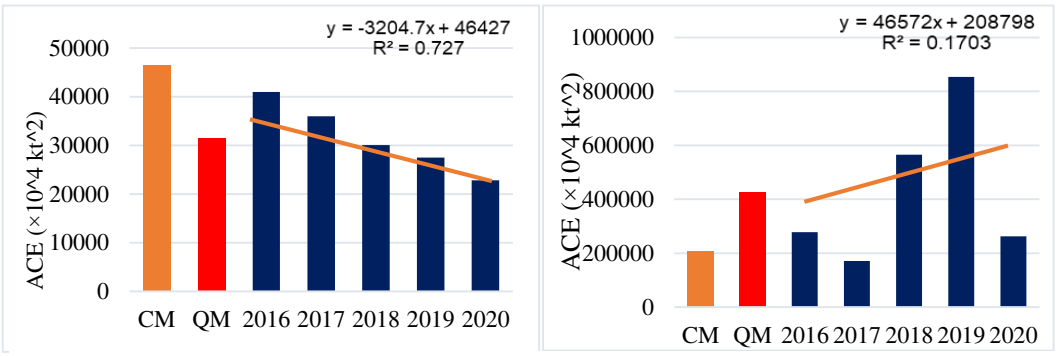

Fig.137 a)ACE of cyclonic depressions in NIO b) ACE of CS in NIO

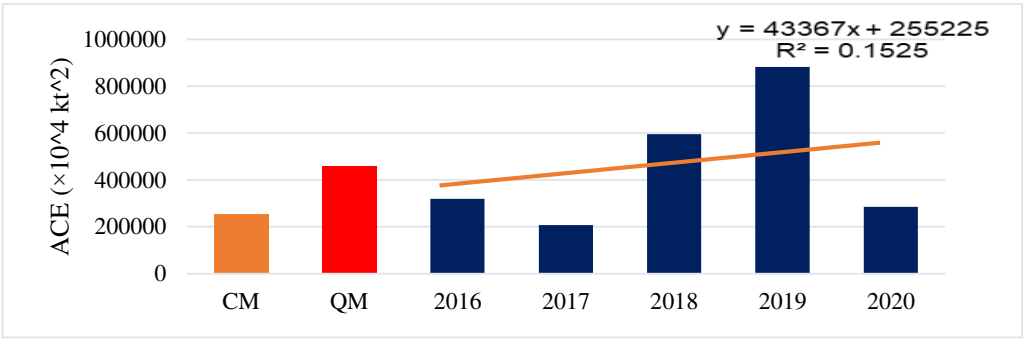

Fig.137 c) ACE of total CDs in NIO

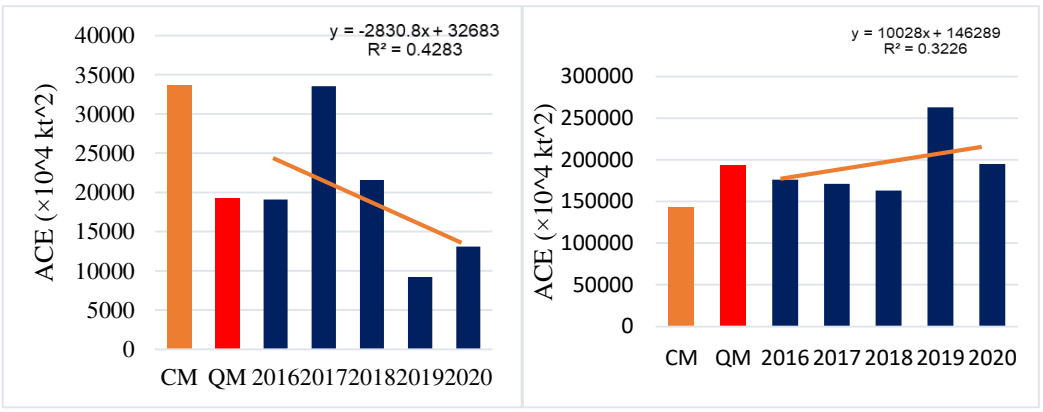

Fig.138 a) ACE of cyclonic depressions in BOB b) ACE of CS in BOB

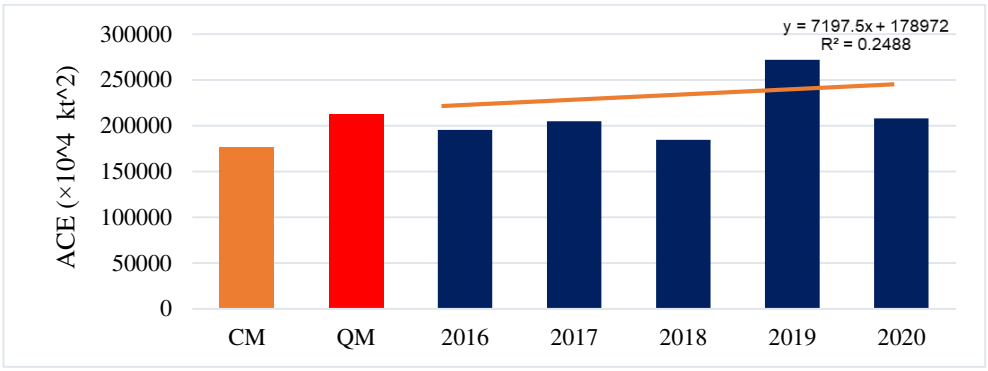

c) ACE of Total CDs in BOB

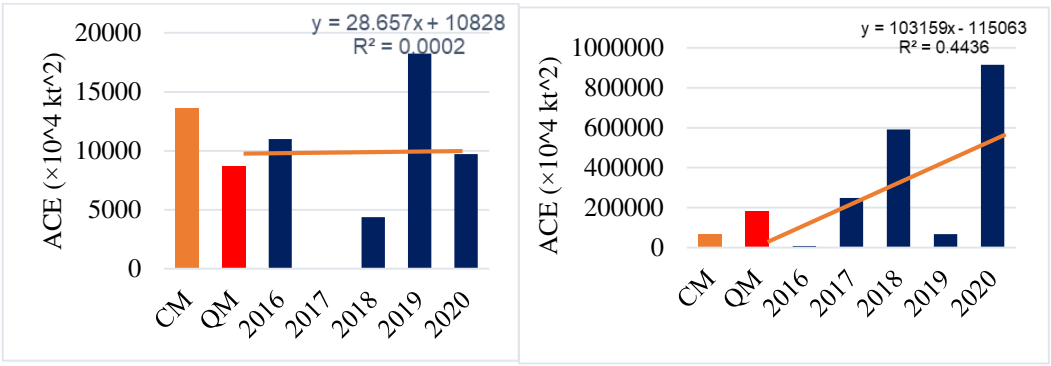

Fig.139 a) ACE of cyclonic depressions in ARB b) ACE of CS in ARB

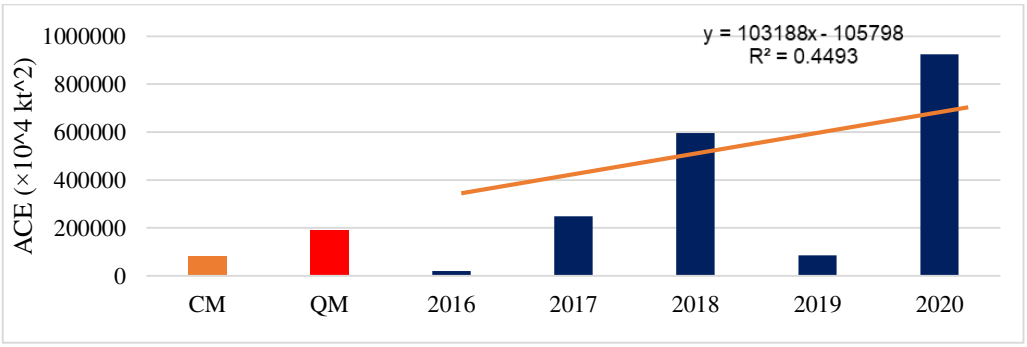

Fig.139 c) ACE of total CDs in ARB

Table 4.2 mean ACE (×10^4 kt) during CP and QP

Basin	CP	CD	CS	Total	Basin	QP	CD	CS	Total
NIO	Annual	14.64	20.83	25.47	NIO	Annual	3.14	4.62	6.76
	Winter	0.39	0.63	1.02		Winter	0	0.02	0.02
	Pre-Monsoon	0.32	9.81	10.13		Pre-Monsoon	0.34	1.75	2.09
	Monsoon	1.78	1.54	3.32		Monsoon	0.17	0.62	0.79
	Post-Monsoon	13.22	12.18	25.4		Post-Monsoon	1	3.519	4.51
BOB	Annual	12.36	16.30	29.66	BOB	Annual	1.93	2.36	4.32
	Winter	.30	0.63	0.93		Winter	0	0.02	0.02
	Pre-Monsoon	.32	7.27	7.59		Pre-Monsoon	.31	1.35	1.66
	Monsoon	1.36	0.14	1.5		Monsoon	0.14	0.02	0.16
	Post-Monsoon	11.85	9.62	21.47		Post-Monsoon	0.14	1.689	1.82
AS	Annual	1.36	6.95	8.31	AS	Annual	0.86	2.30	3.16
	Winter	.09	0	0.09		Winter	0	0	0
	Pre-Monsoon	0	2.54	2.54		Pre-Monsoon	0.03	0.4	0.43
	Monsoon	.42	1.40	1.82		Monsoon	.03	0.6	0.63
	Post-Monsoon	1.37	2.56	3.93		Post-Monsoon	0.86	1.830	2.69

4.5.2 (ii) Inter seasonal variation of mean Accumulated Cyclone Energy (ACE) during CP and QP

Considering the BOB in the CP,CS and Cyclonic depressions has a higer ACE on post-monsoon season followed by Pre monsoon. When compared to CS, the

value of ACE for CD is lower (Fig.140 a). During the QP, the ACE value of CS is observed to be higher (Fig.140 b). The ACE of cyclonic disturbances is almost non-existent in the QP. When compared to CP in ARB, CS has a similar high value during the pre-monsoon and post-monsoon seasons (Fig.141a). However, in QP, significant higher values were observed in the post-monsoon season, followed by the monsoon season (Fig.141b). ACE is higher for CS than CD in NIO during the CP and QP, and is highest during the post-monsoon season, followed by the pre-monsoon and monsoon seasons (Fig.142a and Fig.142b). When compared to CS, the ACE for cyclonic disturbances is negligible. When comparing AS and BOB, BOB has a slightly higher ACE, implying that ARB's ACE has been increasing in recent years. Greater intraseasonal variation can be seen in both BOB and AS equally.

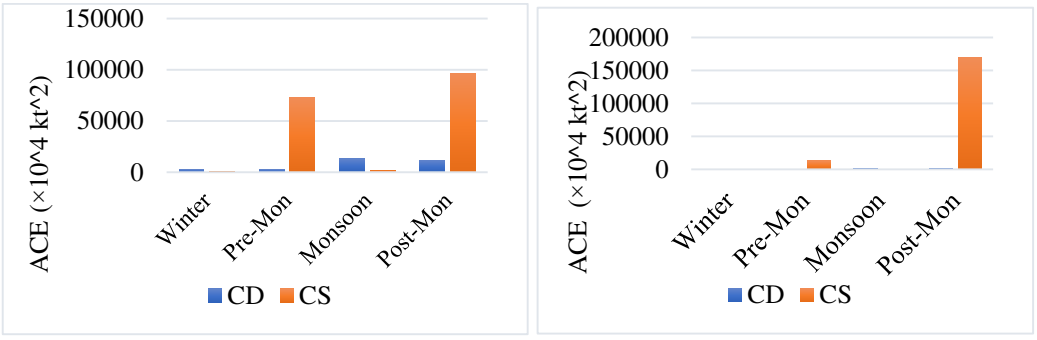

Fig.140 a) ACE of Cyclonic Depression in BOB during CP b)ACE of CS in BOB during QP

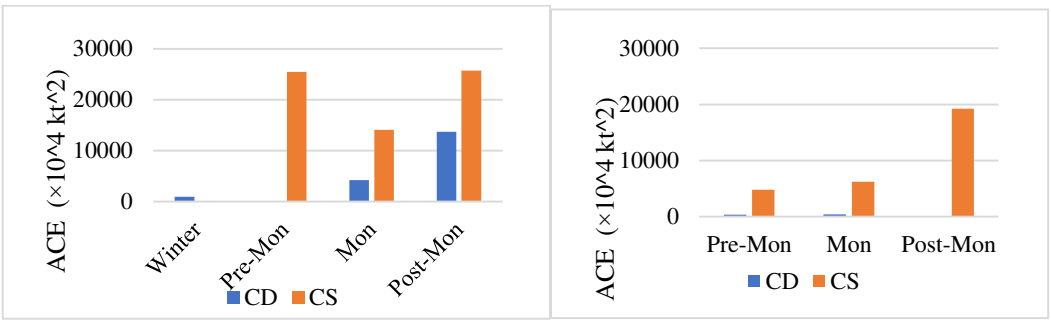

Fig.141 a)ACE of Cyclonic Depression in ARB during CP b)ACE of CS in ARB during QP

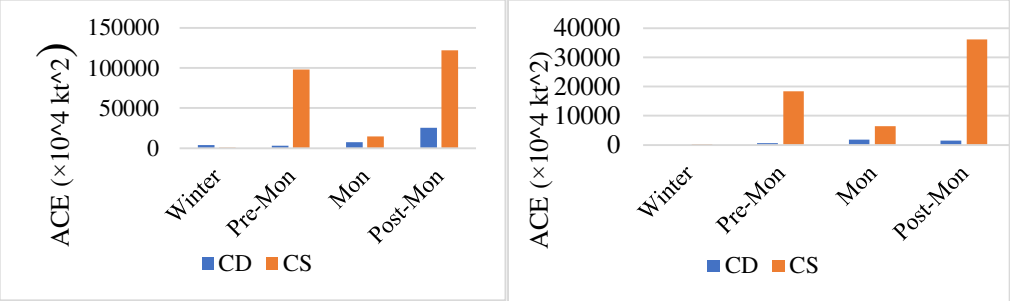

Fig.142 a) ACE of Cyclonic Depression in NIO during CP b)ACE of CS in NIO during QP

4.5.3 Variation in Power Dissipation Index (PDI) in NIO

4.5.3a Interannual variation of PDI

The mean PDI of NIO during the climatological period (Table4.5) is 14.68 106×10^6 kt^3 (0.87106×10^6 kt^3), which includes 9.55106×10^6 kt^3 (1.21106×10^6 kt^3) for BOB and 5.13106×10^6 kt^3 (0.45106×10^6 kt^3) for AS for Cyclonic storms (Cyclonic depressions). The PDI value is higher on BOB than in ARB, and the intraseasonal variation is greater in the BOB Cyclonic disturbances. When comparing the BOB and ARB, the BOB has a higher PDI for cyclonic storms in the post-monsoon and pre-monsoon seasons than in the monsoon season. Several studies have found that the average intensity duration and cyclogenesis play a significant role in the increased PDI value in BOB. ARB has a higher PDI value in the pre-monsoon season, followed by the monsoon and post-monsoon seasons.

The overall changes in PDI for D, CS, and total cyclonic disturbances in NIO (Fig.143a, Fig.143b, and Fig.143c) over the entire study period are shown below. The D and DD show a significant negative trend for recent PDI values, whereas the CM and QM do not show a significant difference. The PDI of cyclonic storms has been steadily rising in recent years. In NIO, there is a significant increase in the QM than CM, indicating an overall increase in the PDI of cyclonic storms in recent years. In recent years, the total PDI has also shown a significant upward trend, with a higher value in QM than in CM. In the BOB, the D exhibits a negative trend with a higher value for CM than QM (Fig.144a), but the QM of CS exhibits a higher

value than CM and a significant positive trend (Fig.144b) in recent years. When the total PDI of BOB, including all Cyclonic Depressions, is added together, it shows a positive trend in recent years, with QM having a higher value than CM (Fig.144c). As a result, it is clear that the PDI in BOB is rising. In ARB, the PDI for Cyclonic depression, like the BOB, has shown a downward trend in recent years (Fig.145a). In recent years, the CS and total cyclonic disturbances of ARB have shown a significant positive trend, with a higher PDI in QM than in CM (Fig.145b and Fig.145c). It is clear that the PDI of AS is increasing significantly. Altogether,the overall PDI of ARB, BOB and NIO with some exceptions for Cyclonic Depressions.

Table 4.3 The mean PDI (×10^6 kt) NIO during the CP and QP

Basin	Period	CD	CS	Total	Basin	Period	CD	CS	Total
NIO	Annual	0.87	14.68	15.56	NIO	Annual	0.85	16.98	17.84
	Winter	0.13	0.02	0.15		Winter	0	0.08	0.08
	Pre-Monsoon	0.09	6.78	6.87		Pre-Monsoon	0.09	1.65	1.74
	Monsoon	0.51	1.93	2.44		Monsoon	0.02	1.45	1.45
	Post-Monsoon	0.96	8.91	9.87		Post-Monsoon	0.49	14.18	14.67
BOB	Annual	1.21	9.55	10.75	BOB	Annual	0.51	14.94	15.45
	Winter	0.10	0.02	0.12		Winter	0	0.08	0.08
	Pre-Monsoon	.09	4.49	4.58		Pre-Monsoon	0.01	1.35	1.36
	Monsoon	.37	.03	0.4		Monsoon	0.03	1.05	1.08
	Post-Monsoon	0.36	7.21	7.57		Post-Monsoon	0.47	12.54	12.45
ARB	Annual	0.45	5.13	5.58	AS	Annual	0.25	1.46	2.14
	Winter	0.03	0	0.03		Winter	0	0	0
	Pre-Monsoon	0	2.29	2.29		Pre-Monsoon	0.08	0.3	0.38
	Monsoon	.14	1.90	2.04		Monsoon	0.01	0.4	0.41

	Post-Monsoon	0.6	1.7	1.6		Post-Monsoon	0.02	1.64	1.64

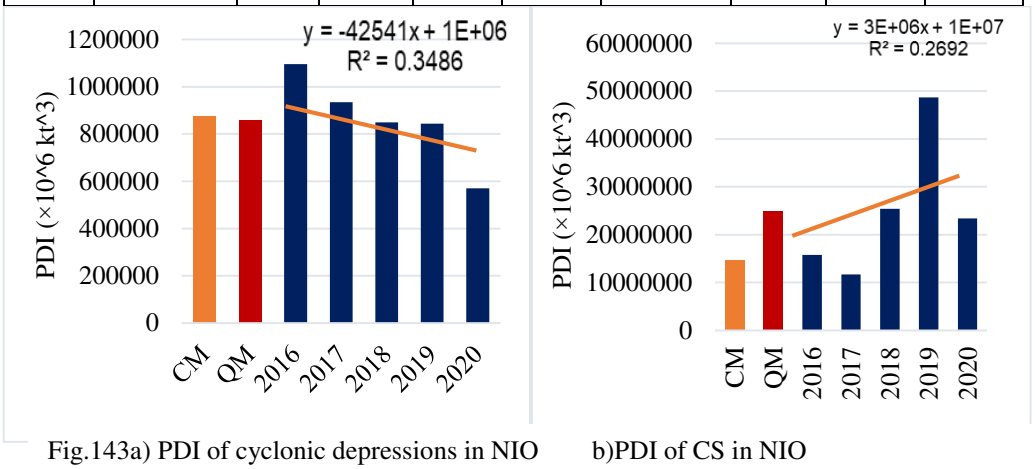

Fig.143a) PDI of cyclonic depressions in NIO b)PDI of CS in NIO

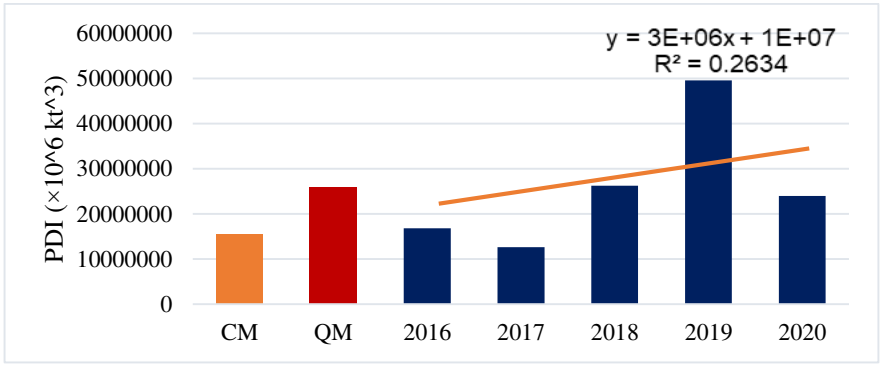

Fig.143 c) PDI of Total CDs in NIO

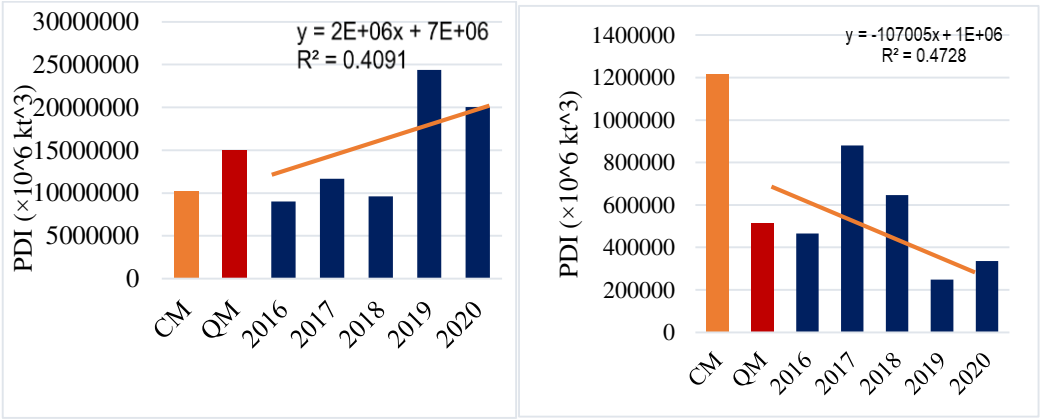

Fig.144a) PDI of cyclonic depressions in BOB b) PDI of CS in BOB

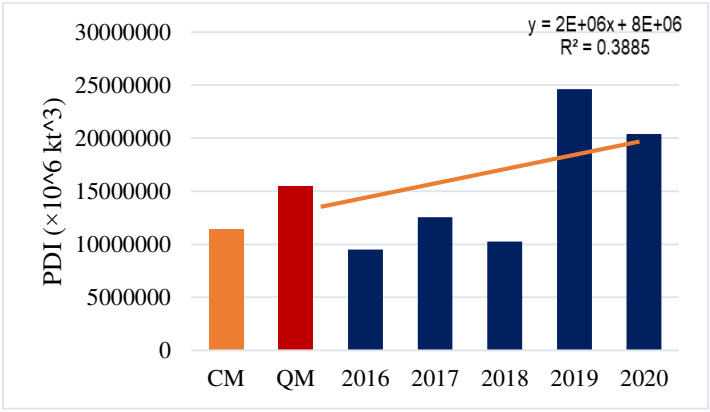

Fig.144 c) PDI of total CDs in BOB

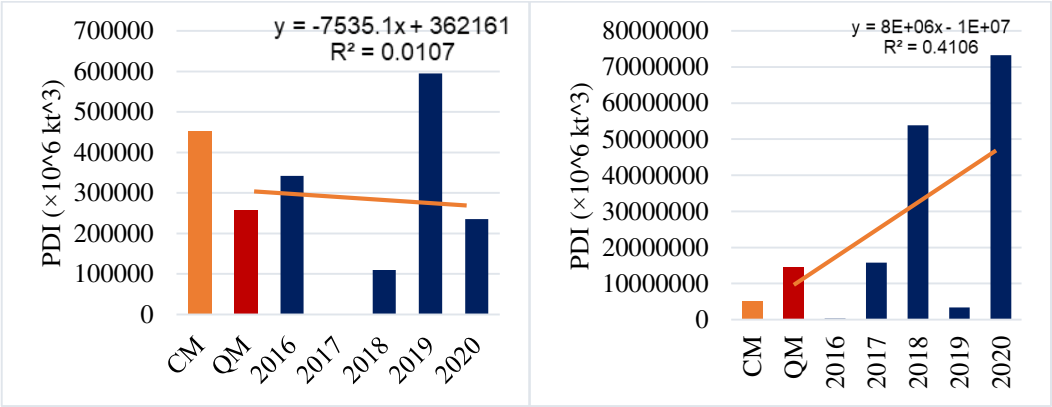

Fig.145a) PDI of cyclonic depressions in ARB b) PDI of CS in ARB

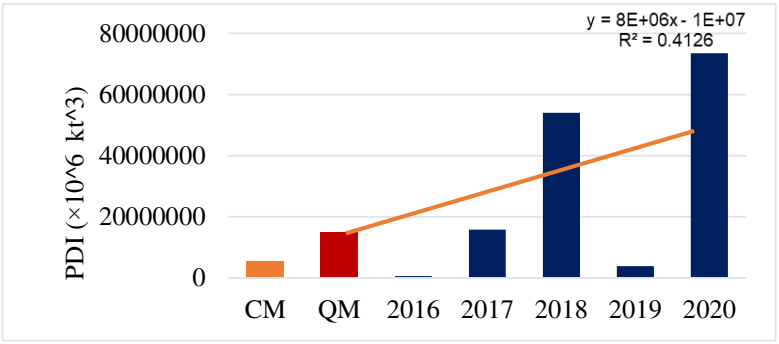

Fig.145 c) PDI of total CDs in ARB

4.5.3b Inter seasonal variation of Power Dissipation Index (PDI) during CP and QP

Considering the BOB, the post-monsoon season has a higher PDI in the CP, CS, and Cyclonic depressions, followed by the pre-monsoon season. When compared to CS, the value of VF for Cyclonic Depressions is lower (Fig.146a). During the QP, the PDI value of CS is observed to be higher (Fig.146b). The PDI of cyclonic disturbances is almost non-existent in the QP.

When the CP in ARB is considered, the CS has a similar high value during the pre-monsoon and post-monsoon seasons (Fi.147a). However, in QP, the post-monsoon season has a significantly higher value than the monsoon season (Fig.147b). When comparing the BOB and AS, the BOB has a higher PDI for cyclonic storms in the post-monsoon and pre-monsoon seasons than in the monsoon season. Overall, in NIO, during the CP and QP, the higher value of PDI is evident for CS than CD, with the highest value during the post-monsoon season, followed by the pre-monsoon and monsoon seasons (Fig.148a and Fi.148b). When compared to CS, the PDI for cyclonic disturbances is negligible.

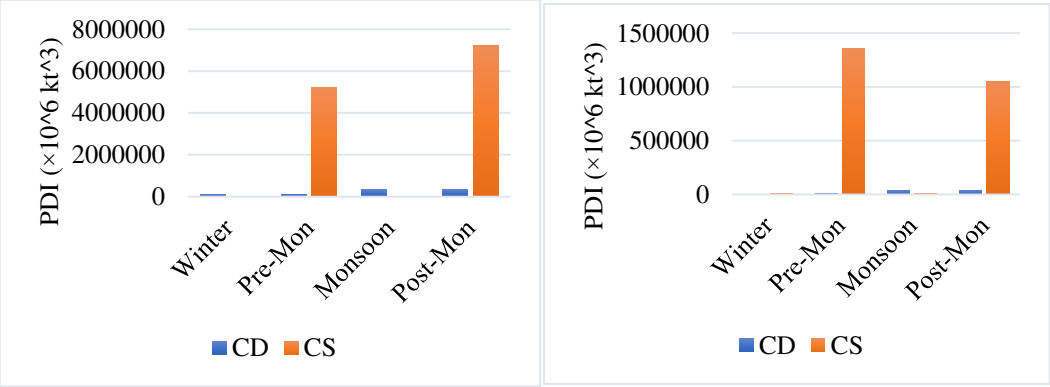

Fig.146 a) Interseasonal variation of PDI in BOB during CP b) Interseasonal variation of PDI in BOB during QP

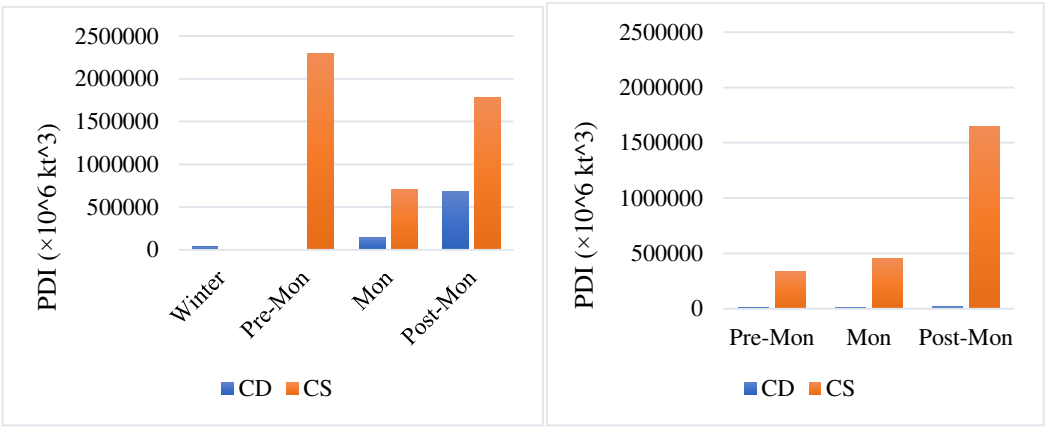

Fig.147 a)Interseasonal variation of PDI in ARB during CP b) Interseasonal variation of PDI in ARB during QP

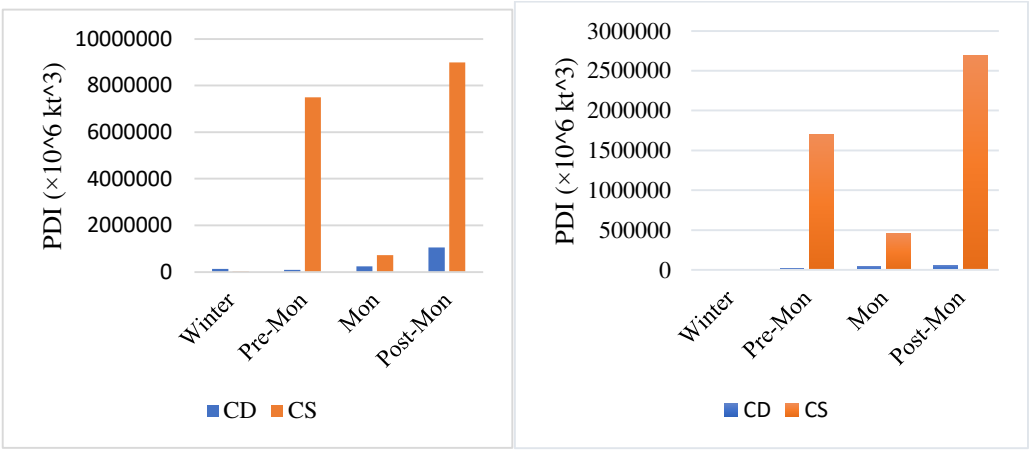

Fig.148 a)Interseasonal variation of PDI in NIO during CP b) Interseasonal variation of PDI in NIO during QP

4.6 Relationship of energy metrics with frequency, intensity and duration of CDs in CP and QP

4.6.1 Variation of energy metrics with frequency, duration and average intensity in BOB

The frequency of Cyclonic Depressions and CS that formed during the CP had a strong influence on the VF of Cyclonic depressions and Cyclonic storms in BOB. When the frequency rises, the VF rises, and vice versa for all CDs (Fig.149a and Fig.149b). Both ACE and PDI, which are the square and cube of cyclone wind speed, show a similar trend. The VF, ACE, and PDI are all highly dependent on the frequency of cyclones during the CP. In QP, the VF of cyclonic storms is frequency dependent (Fig.149c and Fig.149d), but the ACE and PDI are duration dependent (Table4). Overall, frequency is more dependent. In terms of duration, it also demonstrates a greater reliance on VF in the case of cyclonic depressions and cyclonic storms during the CP in BOB (Fig.150a and Fig.150b). VF in QP is highly dependent on duration (Fig.150c and Fig.150d). When the duration increases, so does the energy matrix. Except for QP, ACE and PDI follow the same pattern. In QP, ACE and PDI were negatively related to duration (Table 4). The average intensity of cyclonic depressions during the CP is not highly dependent on cyclonic depressions (Fig.151a), whereas cyclonic storms are highly dependent on cyclonic depressions (Fig.151b). In QP, the VF is more dependent on frequency and duration than on average intensity (Fig.151c and Fig.151d). The average intensity of cyclonic storms was highly correlated with ACE and PDI (Table4). Overall, the energy metrics in BOB is less dependent on average intensity than duration and frequency.

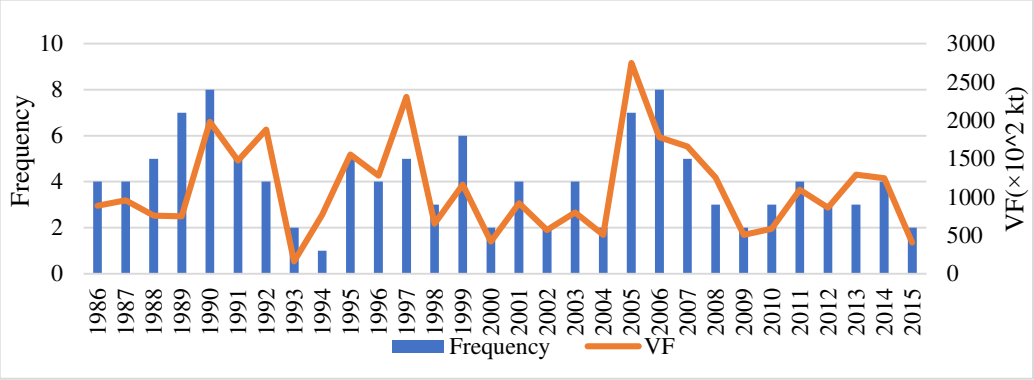

Fig.149a VF and frequency of cyclonic depressions in BOB during CP

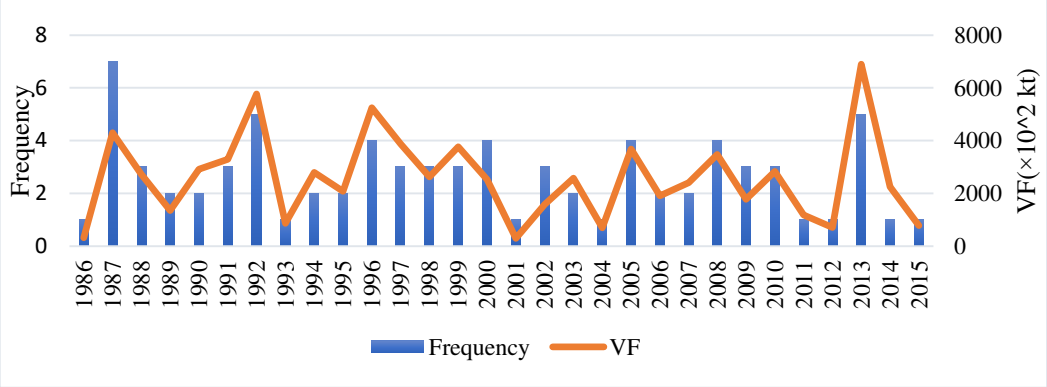

Fig.149b VF and frequency of CS in BOB during CP

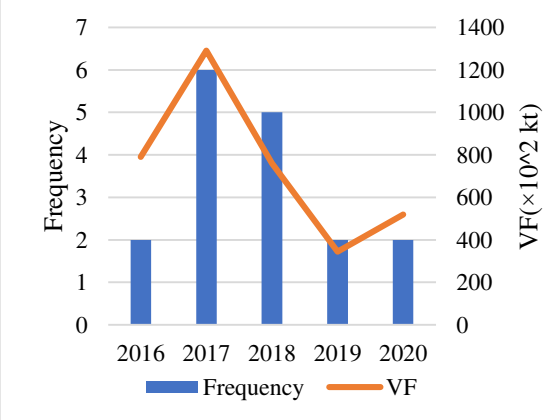

Fig.149c VF and frequency of cyclonic depressions in BOB during QP

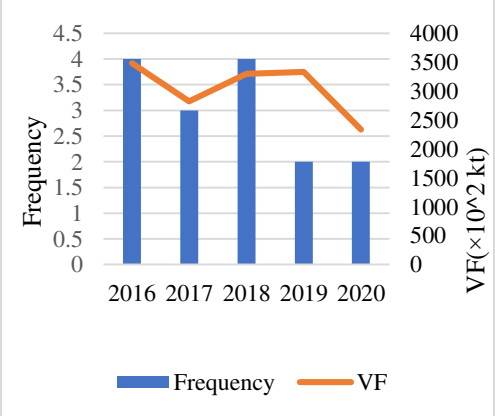

Fig.149d VF and frequency of CS in BOB during QP

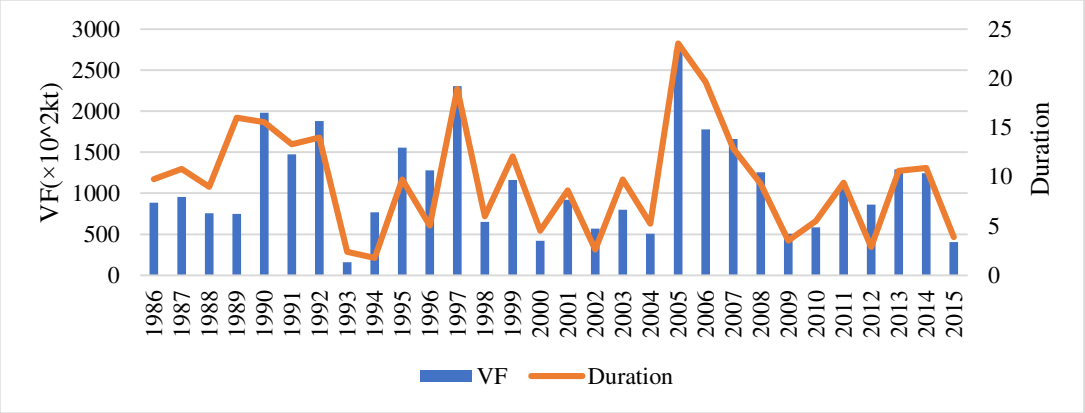

Fig.150a VF and duration of cyclonic depressions in BOB during CP

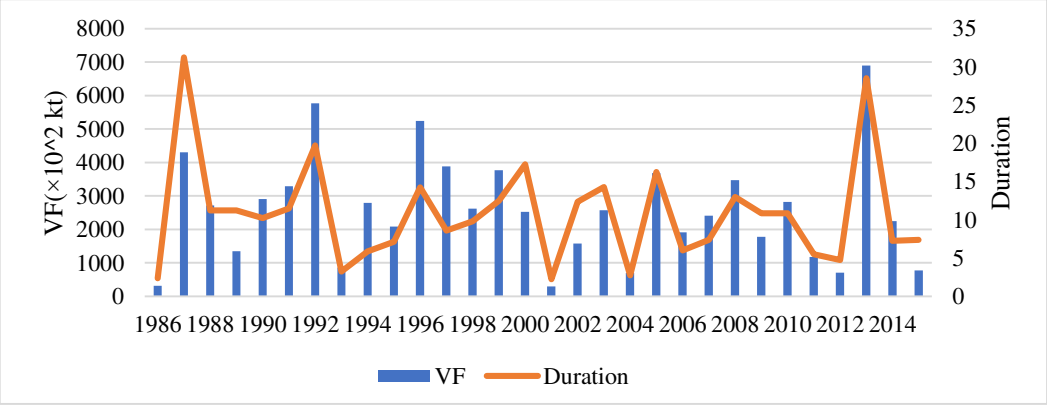

Fig.150b VF and duration of CS in BOB during CP

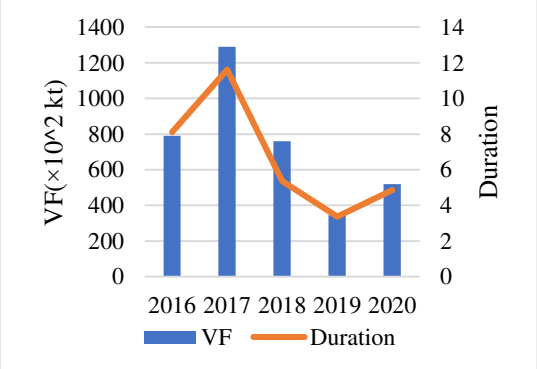

Fig.150c VF and duration of cyclonic depressions in BOB during QP

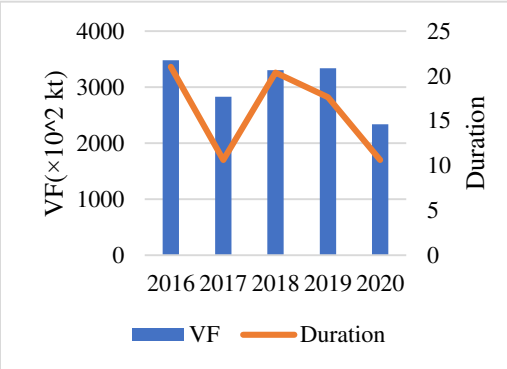

Fig.150d VF and duration of CS in BOB during QP

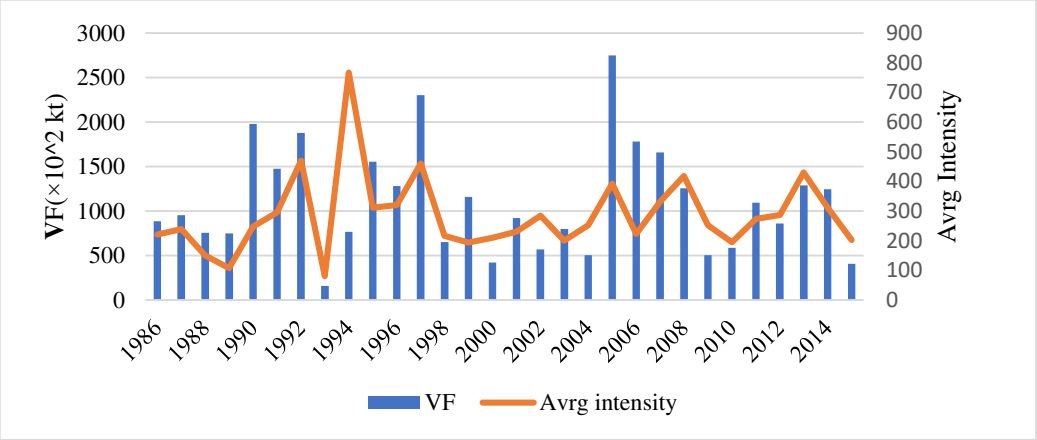

Fig.151a VF and average intensity of Cyclonic Depressions in BOB during CP

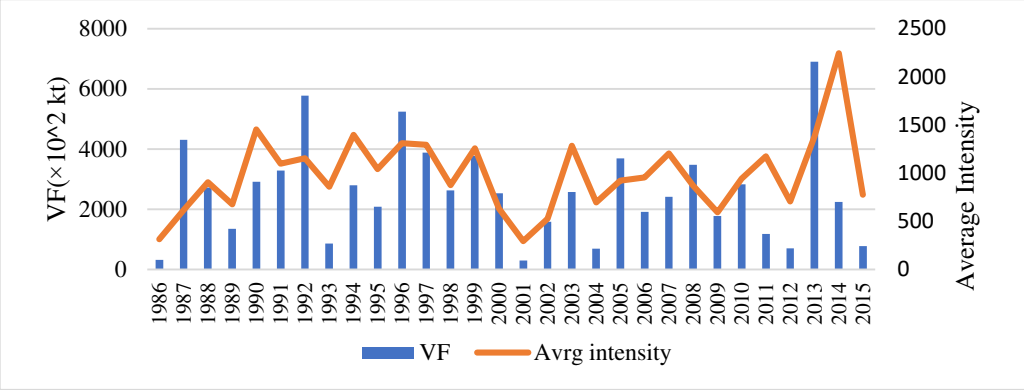

Fig.151b VF and average intensity of CS in BOB during CP

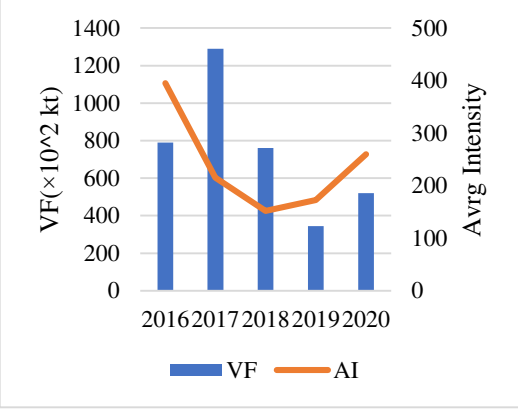

Fig.151c VF and average intensity of cyclonic depressions in BOB during QP

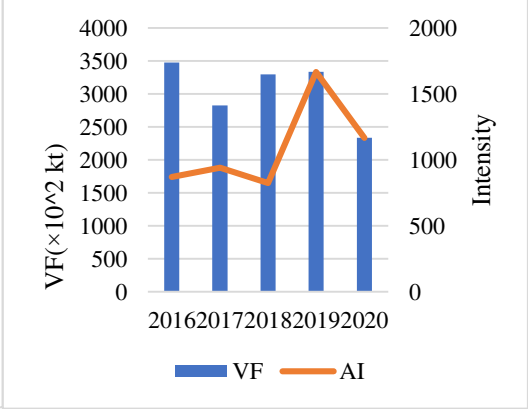

Fig.151d VF and average intensity of CS in BOB during QP

4.6.2 Correlation analysis of energy metrics in BOB

Table 4.4 - Correlation analysis of Spearman correlation test between the energy metrics with frequency, intensity and duration of cyclonic storms during CP

Column1	VF	ACE	PDI	Avrg. intensity	Duration
VF					
ACE	0.90****				
PDI	0.82****	0.98****			
Avrg. intensity	0.57***	0.70****	0.71****		
Duration	0.77****	0.61***	0.52**	0.16	
Frequency	0.84****	0.67****	0.56**	0.1	0.89****

The VF of CS has a highly significant positive correlation with frequency (0.84), duration (0.77), and average intensity (0.77). (0.57). The ACE has a strong positive correlation with average intensity (0.70), frequency (0.67), and duration (0.67). (0.61). The PDI is highly correlated with average intensity (0.71), frequency (0.56), and duration (0.56). (0.52). There is a significant positive correlation between frequency and duration (0.89).

Table 4.5 - Correlation analysis of Spearman correlation test between the energy matrix with frequency intensity and duration of cyclonic Storms during QP

Column1	Frequency	VF	ACE	PDI	AI
Frequency					
VF	0.47				
ACE	-0.79	0.1			
PDI	-0.95*	-0.4	0.7		
AI	-0.95*	-0.2	0.90*	0.90*	
Duration	0.73	0.87	-0.21	-0.67	-0.56

During the QP, VF of CS are negatively correlated with average intensity(-0.2) , positively correlated with duration (0.87) and frequency (0.47). ACE have significant positive correlation with average intensity(0.90) and negatively

correlated with duration (-0.21) and frequency (-0.79). The PDI showed a significant positive correlation with average intensity(0.90), and negative correlation with frequency (-0.95) and duration (-0.67).

Table 4.6.Correlation analysis of Spearman correlation test between the energy matrix with frequency intensity and duration of cyclonic depressions during CP

Column1	Frequency	VF	ACE	PDI	Avrg.intensity
Frequency					
VF	0.73****				
ACE	0.76****	0.98****			
PDI	0.69****	0.94****	0.96****		
Avrg.intensity	-0.02	0.61***	0.57**	0.63***	
Duration	0.87****	0.78****	0.78****	0.71****	0.17

During CP, VF ACE and PDI showed a overall positive trend. VF showed high significant positive correlation on Duration (0.78), Frequency(0.76) and average intensity (0.61). ACE showed a positive correlation for duration(0.78), frequency(0.76), and Average intensity (0.57). PDI positively correlated with duration (0.71), frequency (0.69) and average intensity (0.63).

Table 4.7- Correlation analysis of Spearman correlation test between the energy matrix with frequency intensity and duration of cyclonic depressions during QP

Column1	Frequency	VF	ACE	PDI	AI
Frequency					
VF	0.67				
ACE	0.89*	0.90*			
PDI	0.89*	0.90*	1.00****		
AI	-0.45	0.3	-0.1	-0.1	
Duration	0.67	1.00****	0.90*	0.90*	0.3

VF during QP showed significant positive correlation with duration(1), and positive correlation with frequency (0.67) and negatively correlated with average intensity (-0.45).

ACE was positively correlated with duration (.90), positively correlated with Frequency (0.89), and negatively correlated with average intensity (-0.45). PDI was highly correlated with duration (0.90) and frequency (0.89) and negatively correlated with average intensity (-0.1).

4.6.3 Variation of energy metrics with frequency, duration and average intensity in ARB

The frequency of Cyclonic Depressions formed during the CP did not show a significant dependence on the VF in ARB. But the CS showed a significant dependence on frequency. When the frequency rises, the VF rises, and vice versa for CDs, but some fluctuation from this trend between the years also visible (Fig.152a and Fig.152b). Both ACE and PDI, which are the square and cube of cyclone wind speed, show a similar trend. The VF, ACE, and PDI had a positive trend on frequency of cyclones during the CP but not much significant. In QP, the VF is less dependent on frequency than CP (Fig.152c and Fig.152d), ACE and PDI have also similar dependence (Table 4.9). Overall, frequency is less dependent on VF for ARB than BOB. In terms of duration, it also demonstrates a greater reliance on VF in the case of cyclonic depressions and cyclonic storms during the CP in BOB (Fig.153a and Fig.153b). VF in QP is highly dependent on duration (Fig.153c and Fig.153d). When the duration increases, so does the energy metrics. The VF of CS as well as Cyclonic Depressions was highly depend on Average Intensity during CP (Fig.154a and fig.154c), that of QP, the CS has a high dependence and Cyclonic Depressions did not show much dependence(Fig.154b and Fig.154d). The average intensity of cyclonic storms was highly correlated with ACE and PDI. Overall, the energy metrics in BOB is less dependent on frequency than duration and Average Intensity.

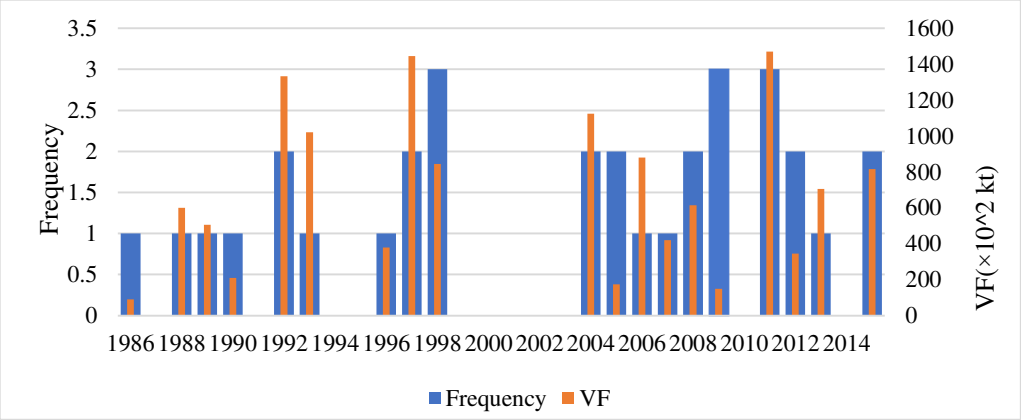

Fig.152a VF and frequency of cyclonic depressions in ARB during CP

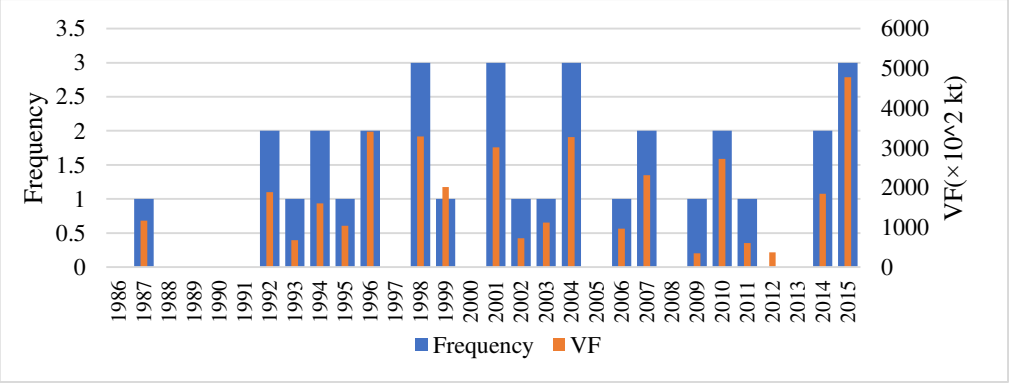

Fig.152b VF and frequency of CS in ARB during CP

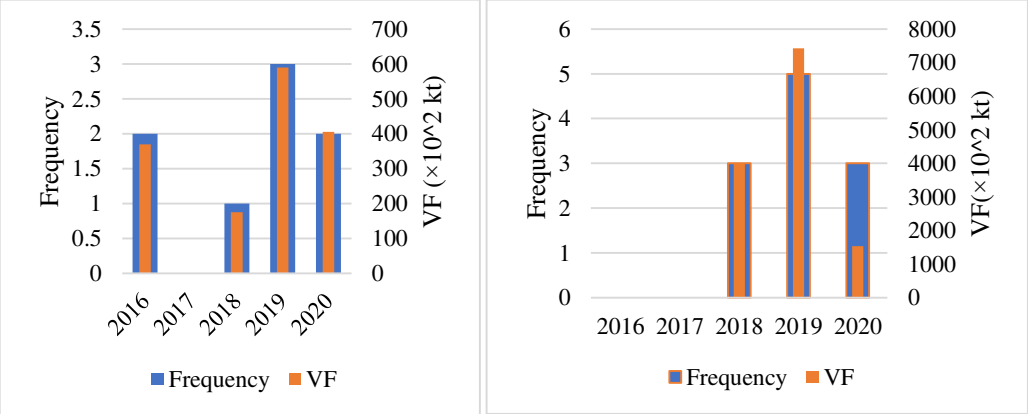

Fig.152c VF and frequency of cyclonic depressions in ARB during QP and Fig.152d VF and duration of CS in ARB during QP

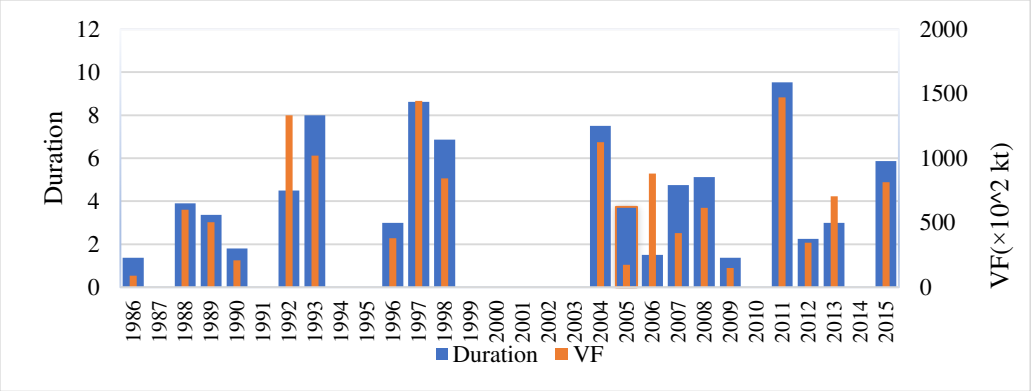

Fig.153a VF and duration of cyclonic depressions in ARB during CP

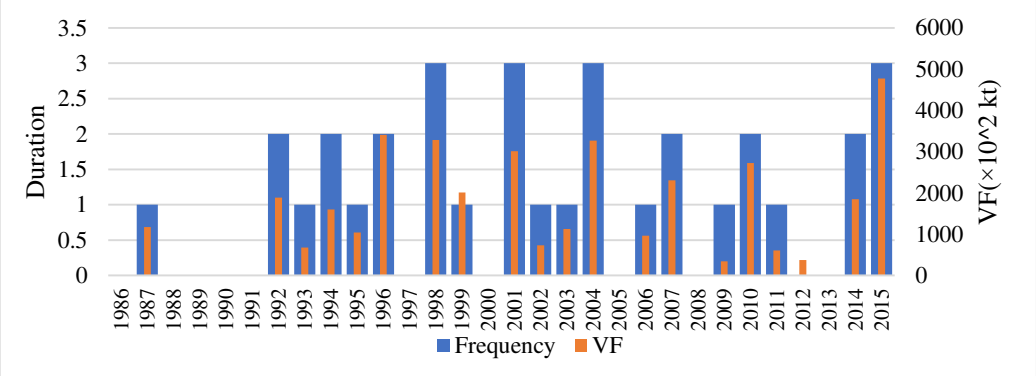

Fig.153b VF and duration of CS in ARB during CP

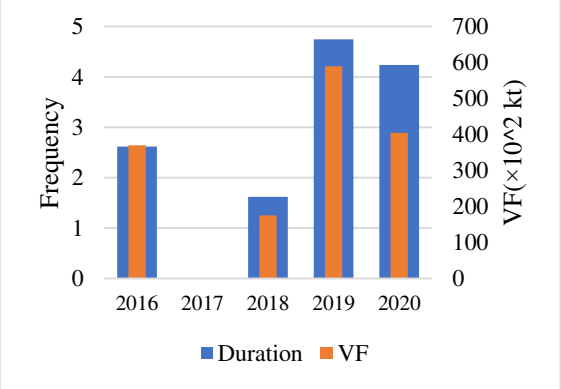

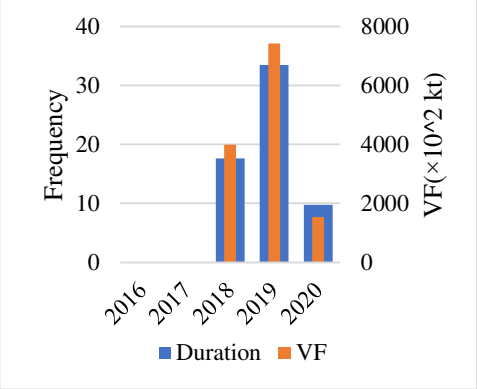

Fig.153c VF and duration of cyclonic depressions in ARB during QP and Fig.153d VF and duration of CS in ARB during QP

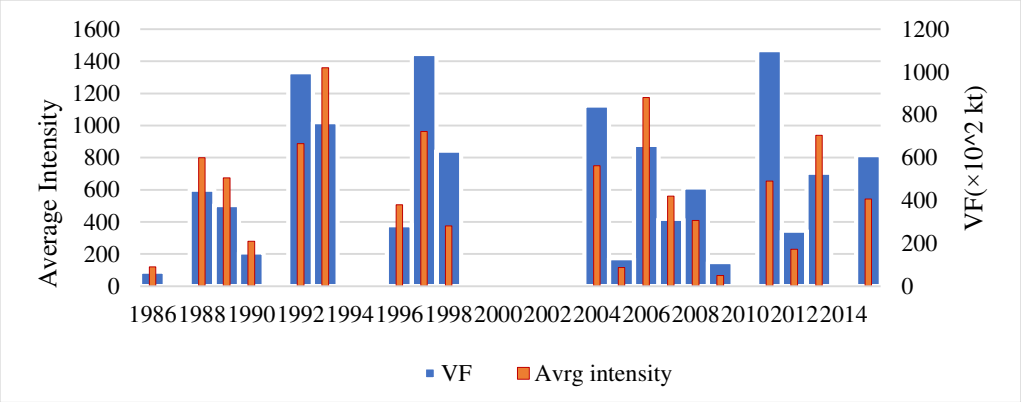

Fig.154a VF and average intensity of cyclonic depressions in ARB during CP

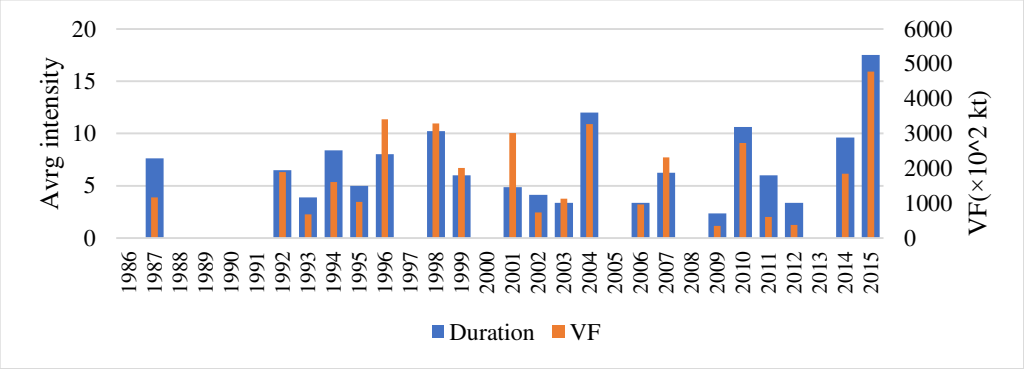

Fig.154b VF and average intensity of cyclonic depressions in ARB during CP

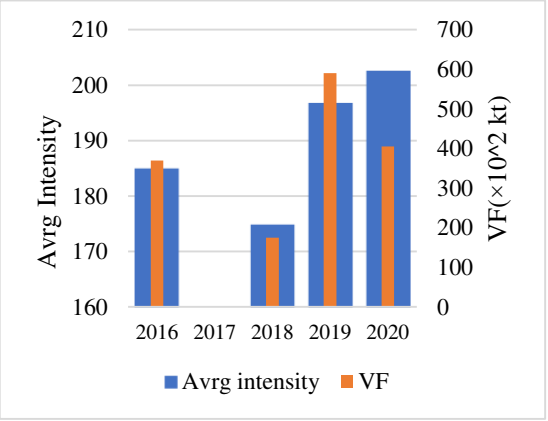

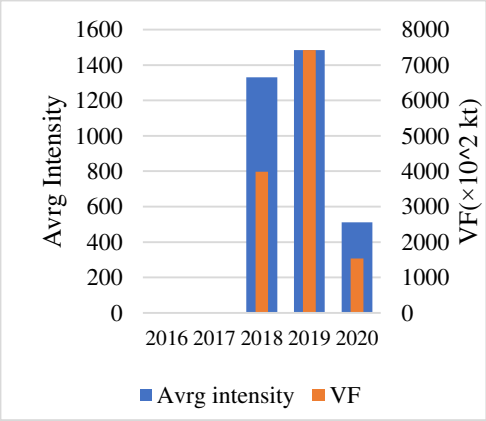

Fig.154c VF and average intensity of cyclonic depressions in ARB during QP and Fig.154d VF and average intensity of CS in ARB during QP

4.6.4 Correlation analysis of energy metrics in ARB

Table 4.9- Correlation analysis of Spearman correlation test between the energy metrics with frequency intensity and duration of CS during CP in ARB

Column1	VF	ACE	PDI	Avrg.intensity	Duration
VF					
ACE	0.90****				
PDI	0.84****	0.97****			
Avrg.intensity	0.74***	0.69**	0.69**		
Duration	0.78****	0.72***	0.64**	0.46*	
Frequency	0.87****	0.80****	0.71***	0.3	0.76****

The VF of CS had a significant positive correlation with Frequency (0.87), Duration (0.78 and Average Intensity (0.74).The ACE also highly correlated with frequency (0.71) followed by average intensity (0.69) and duration (0.64). PDI highly correlated with frequency (0.71), average intensity (0.69) and duration (0.64).

Table 4.10- Correlation analysis of Spearman correlation test between the energy metrics with frequency intensity and duration of CS during QP in ARB

Column1	Frequency	VF	ACE	PDI	Avrg.intensity
Frequency					
VF	0.87				
ACE	0.87	1.00****			
PDI	0.87	1.00****	1.00****		
Avrg.intensity	0.87	1.00****	1.00****	1.00****	
Duration	0.87	1.00****	1.00****	1.00****	1.00****

The VF, ACE and PDI of CS during QP is almost fully correlated with frequency, duration and average intensity.

Table 4.11- Correlation analysis of Spearman correlation test between the energy metrics with frequency intensity and duration of cyclonic depressions during CP in ARB

Column1	Frequency	VF	ACE	PDI	Avrg.intensity
Frequency					
VF	0.27				
ACE	0.23	0.99****			
PDI	0.22	0.97****	0.99****		
Avrg.intensity	-0.34	0.77***	0.79****	0.79****	
Duration	0.38	0.77***	0.72***	0.71***	0.44

VF, ACE and PDI of cyclonic depressions during CP did not show much correation with frequency whereas it is significantly correlated with duration and average intensity.

Table 4.12- Correlation analysis of Spearman correlation test between the energy metrics with frequency intensity and duration of cyclonic depressions during QP in ARB

Column1	Frequency	VF	ACE	PDI	Avrg.intensity
Frequency					
VF	0.95				
ACE	0.95	0.8			
PDI	0.95	0.8	1.00****		
Avrg.intensity	0.63	0.8	0.4	0.4	
Duration	0.95	1.00****	0.8	0.8	0.8

The VF, ACE and PDI of cyclonic depressions have a positive correlation with frequency and average intensity but not much significant. The VF was fully significantly correlated with duration whereas ACE and PDI are not much significant.

4.6.5 Variation of energy metrics with frequency duration and average intensity in NIO

The frequency of Cyclonic Depressions and CS formed during the CP showed a significant dependence on the VF in NIO (Fig.155a and Fig.155b). When the frequency rises, the VF rises, and vice versa for CDs, but some fluctuation from this trend between the years also visible .Both ACE and PDI, which are the square and cube of cyclone wind speed, show a similar trend. In QP, the VF of CS are fully correlated with Frequency (Fig.155c) whereas the Cyclonic Depressions not shown much (Fig.155d), ACE and PDI have also similar dependence. Overall, frequency has a high dependence on VF for NIO. In terms of duration, it also demonstrates a greater reliance on VF in the case of cyclonic depressions and cyclonic storms during the CP in BOB (Fig.156a and Fig.156b). VF in QP is highly dependent on duration (Fig.156c and Fig.156d). When the duration increases, so does the energy matrix. The VF of CS as well as cyclonic depressions have less dependence on average intensity during CP (Fig.157a and fig.157b), that of QP, the CS has a high dependence and Cyclonic Depressions did not show much dependence(Fig.157c and Fig.157d). The average intensity of cyclonic storms was not much correlated with ACE and PDI. Overall, the energy metrics in NIO, is less dependent on average intensity than frequency and duration.

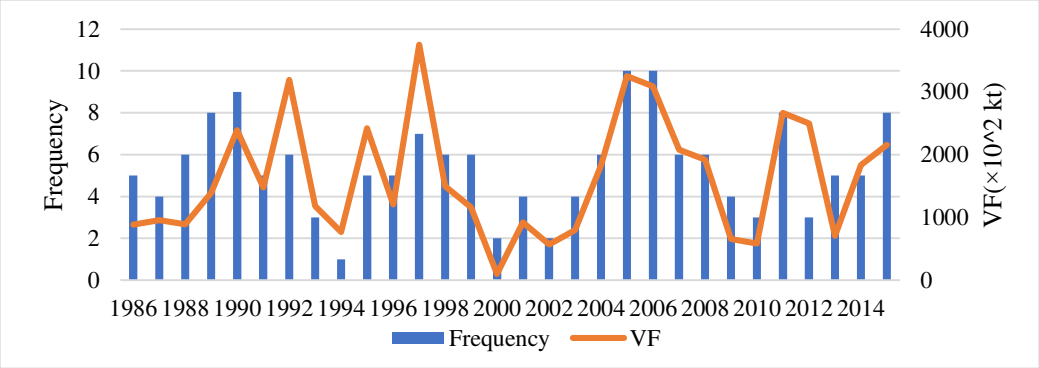

Fig.155a VF and frequency of cyclonic depressions in NIO during CP

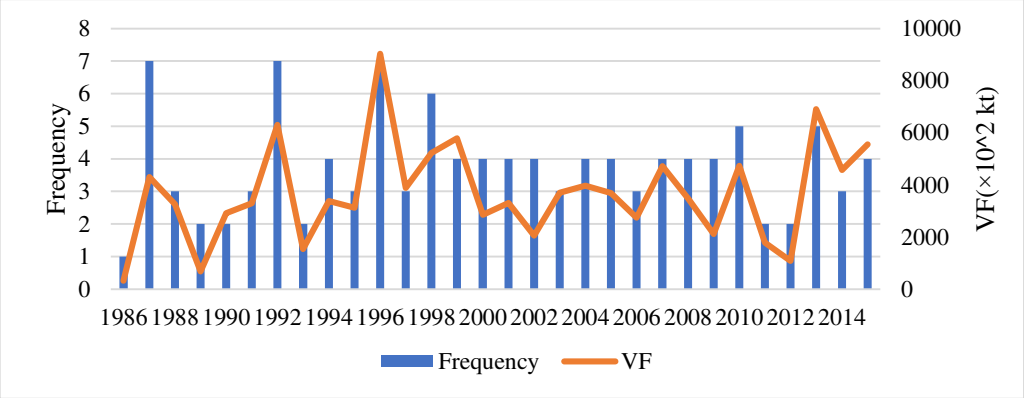

Fig.155b VF and frequency of cyclonic depressions in NIO during CP

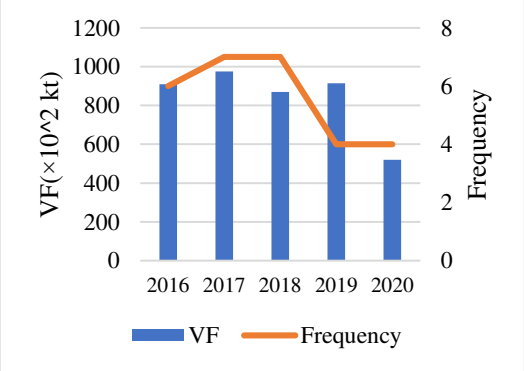

Fig.155c VF and frequency of cyclonic depressions in ARB during QP

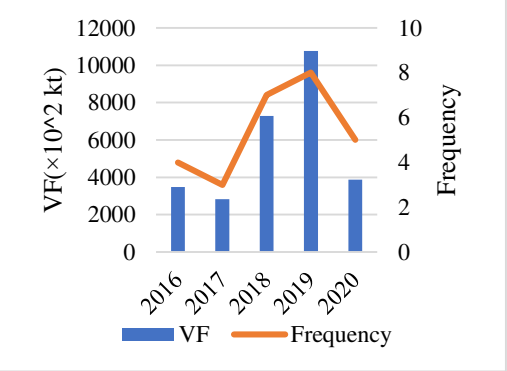

Fig.155d VF and frequency of CS in ARB during QP

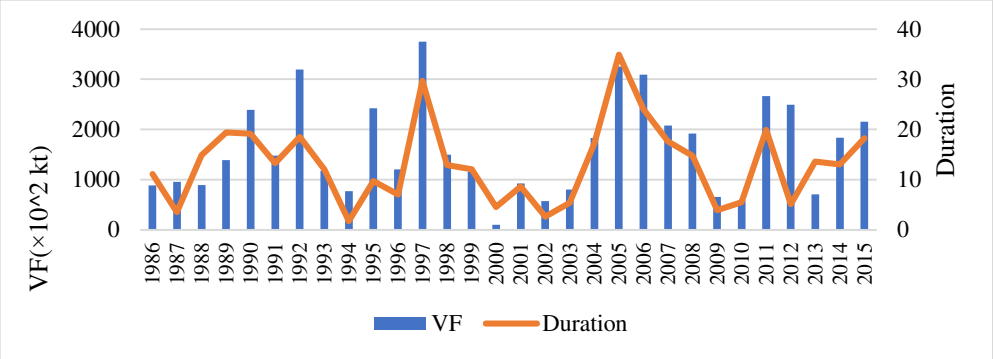

Fig.156a VF and duration of cyclonic depressions in NIO during CP

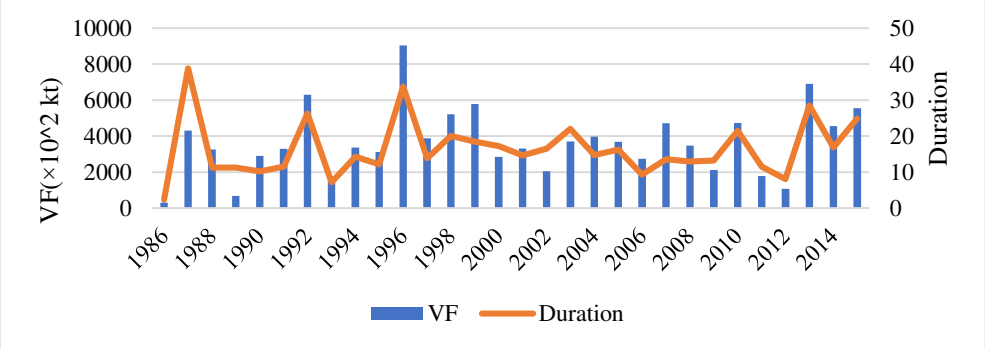

Fig.156b VF and duration of cyclonic depressions in NIO during CP

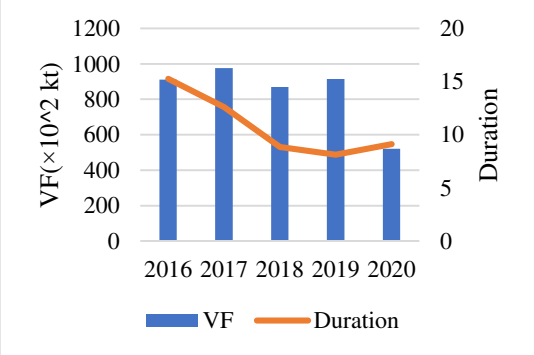

Fig.156c VF and frequency of cyclonic depressions in ARB during QP and

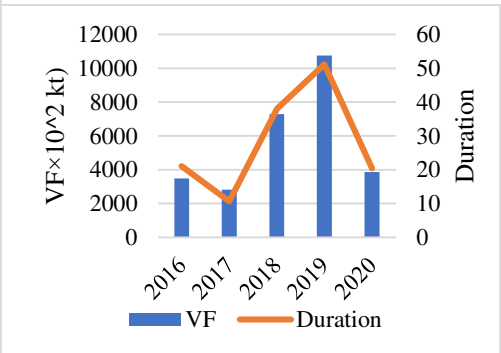

Fig.156d VF and frequency of CS in ARB during QP

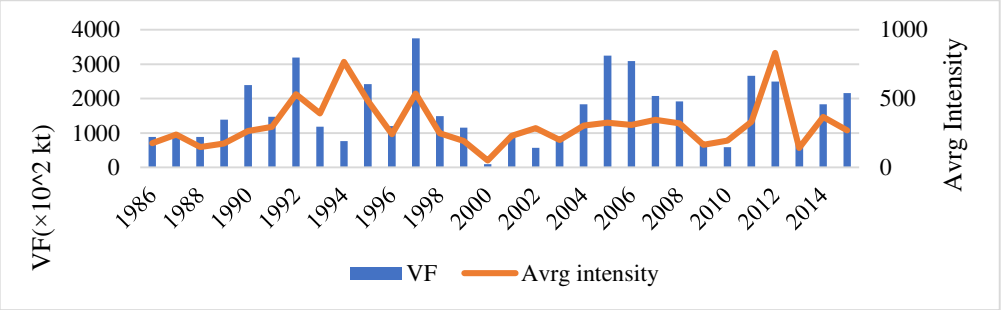

Fig.157a VF and duration of cyclonic depressions in NIO during CP

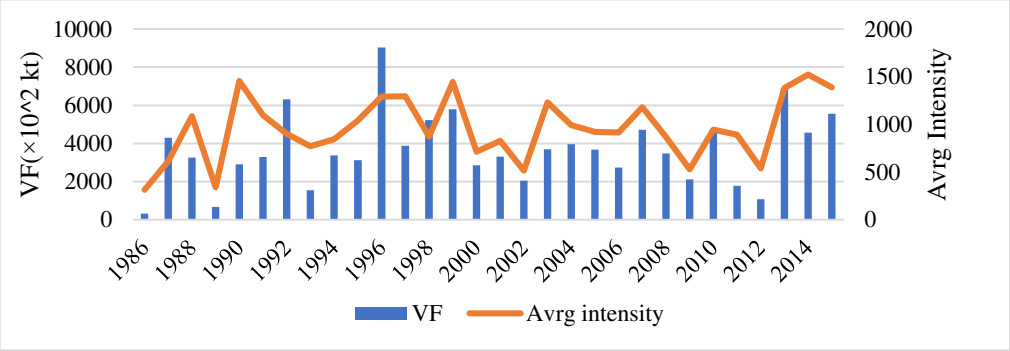

Fig.157b VF and duration of cyclonic depressions in NIO during CP

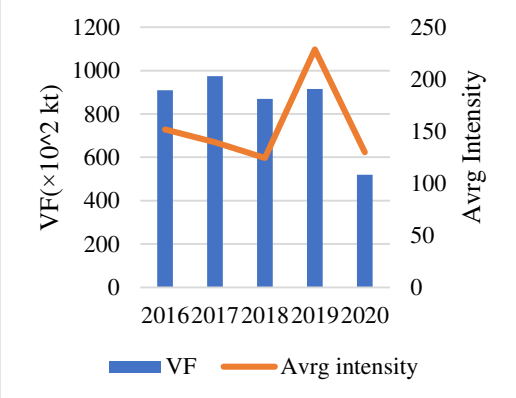

Fig.157c VF and frequency of Cyclonic Depressions in ARB during QP

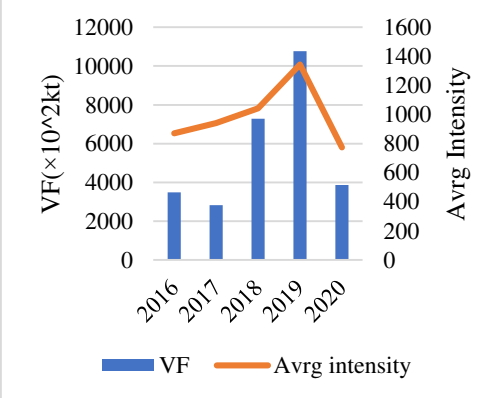

Fig.157d VF and frequency of CS in ARB during QP

4.6.6 Correlation analysis of energy metrics in NIO

Table 4.13- Correlation analysis of Spearman correlation test between the energy matrix with frequency intensity and duration of CS during CP in NIO

Column1	Frequency	VF	ACE	PDI	Avrg.intensity
Frequency					
VF	0.76****				
ACE	0.55**	0.88****			
PDI	0.43*	0.77****	0.94****		
Avrg.intensity	0.09	0.64***	0.77****	0.75****	
Duration.CS	0.84****	0.82****	0.56**	0.40*	0.31

The VF of CS had a significant positive correlation with frequency (0.76), duration (0.82) and average intensity (0.77). The ACE also highly correlated with frequency (0.55), average intensity (0.64) and duration (0.56).PDI correlated with frequency (0.43), average intensity (0.75) and Duration (0.40).

Table 4.14 - Correlation analysis of Spearman correlation test between the energy matrix with frequency intensity and duration of CS during QP in NIO

Column1	VF	Frequency	ACE	PDI	Avrg.intensity
VF					
Frequency	1.00****				
ACE	0.90*	0.90*			
PDI	1.00****	1.00****	0.90*		
Avrg.intensity	0.6	0.6	0.7	0.6	
Duration	0.90*	0.90*	1.00****	0.90*	0.7

VF of CS during QP was almost fully correlated with the frequency (1) and highly correlated with duration (90) followed by average intensity (0.6). PDI had a

high correlation with frequency and duration whereas less correlated with average intensity.

Table 4.15 - Correlation analysis of Spearman correlation test between the energy matrix with frequency intensity and duration of cyclonic depressions during CP in NIO

Column1	Frequency	VF	ACE	PDI	Avrg.intensity
Frequency					
VF	0.72****				
ACE	0.73****	0.99****			
PDI	0.72****	0.96****	0.98****		
Avrg.intensity	0.09	0.68****	0.67****	0.66****	
Duration	0.93****	0.74****	0.76****	0.76****	0.21

VF, ACE and PDI was highly correlated with frequency, duration and average intensity almost similarly.

Table 4.16 - Correlation analysis of Spearman correlation test between the energy matrix with frequency intensity and duration of Cyclonic depressions during QP in NIO

Column1	VF	Frequency	ACE	PDI	Avrg.intensity
VF					
Frequency	0.32				
ACE	0.5	0.63			
PDI	0.5	0.63	1.00****		
Avrg.intensity	0.6	-0.47	0.2	0.2	
Duration	0.1	0.32	0.7	0.7	0

During QP, none of the energy metrics did not show a significant correlation. Slight positive correlation was observed for VF, ACE and PDI.

4.7 Depth and cyclogenesis

When the average depth of cyclogenesis of CDs was compared to their occurrence in different seasons to see if there was any relationship between them, it was discovered that (Fig.158) the CDs with the greatest depth occurred during the winter season and the least during the monsoon season. Even though a small number of CDs are formed during the winter season, it has the highest depth of cyclogenesis. The average depth of cyclogenesis in the post-monsoon and pre-monsoon seasons is comparable to the other two seasons.

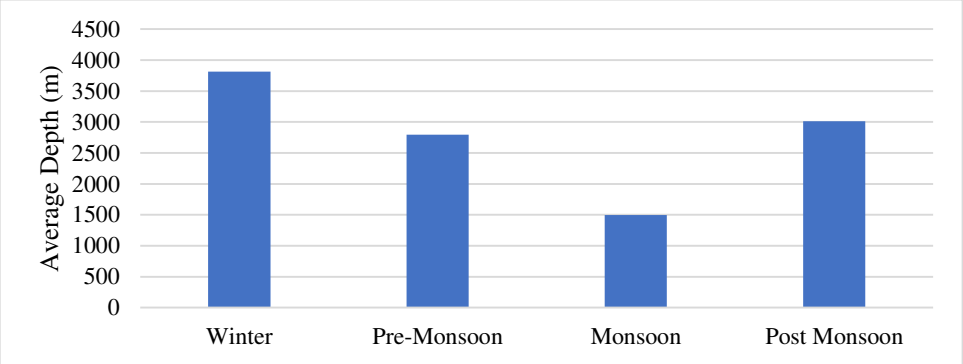

Fig.158 The Average depth of cyclogenesis in different Seasons

4.8 Morphology of ocean and cyclogenesis

The occurrence of CDs or Cyclogenesis on the various morphological features of the ocean during different seasons is depicted in Fig.159 a-d. The majority of CDs occurred in the fan region in all seasons except the monsoon season in which the cyclone was formed in shelf and fan region equally (Fig159a, Fig 159b). The Plateau, Escarpment, Canyons, Abyss, Guyots, Basins, and other regions where cyclogenesis occurred are significantly lower than the Fan region. Several environmental factors are a possible cause, which is not entirely unknown.

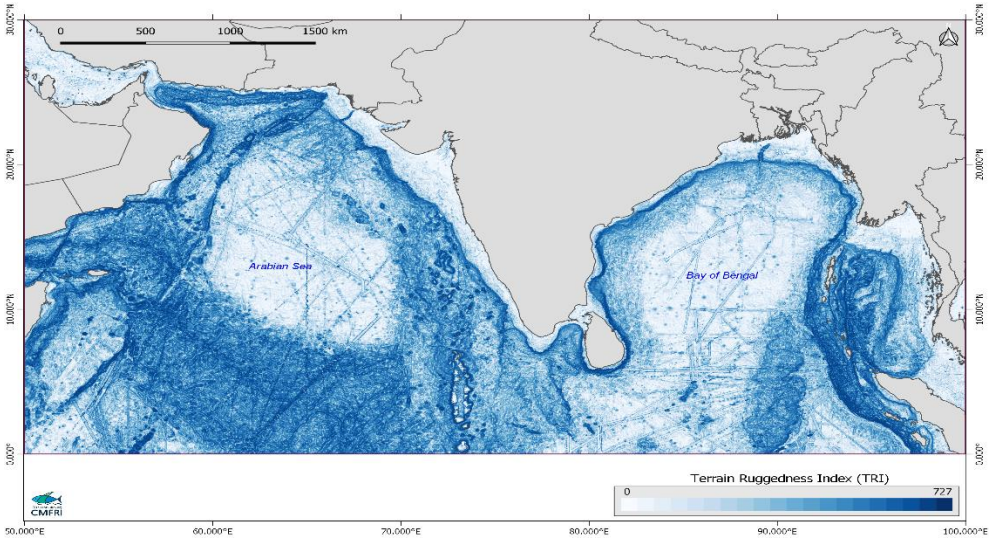

Fig.159a Morphology of NIO

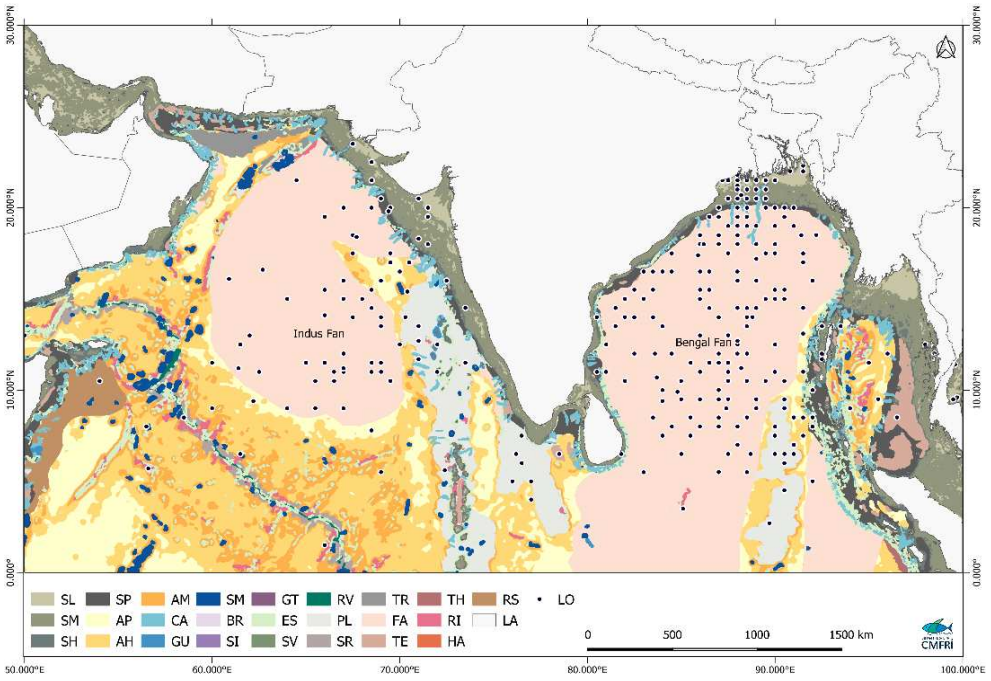

Fig.159b Location of cyclogenesis in NIO with respect to morphology

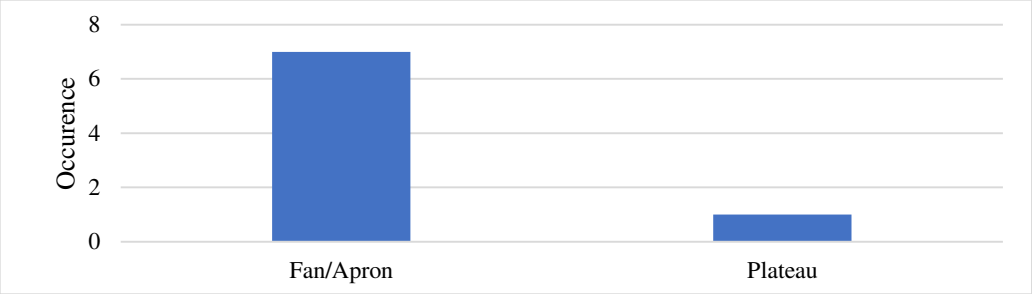

Fig.159 c Occurence of cyclogenesis and morphology in winter season

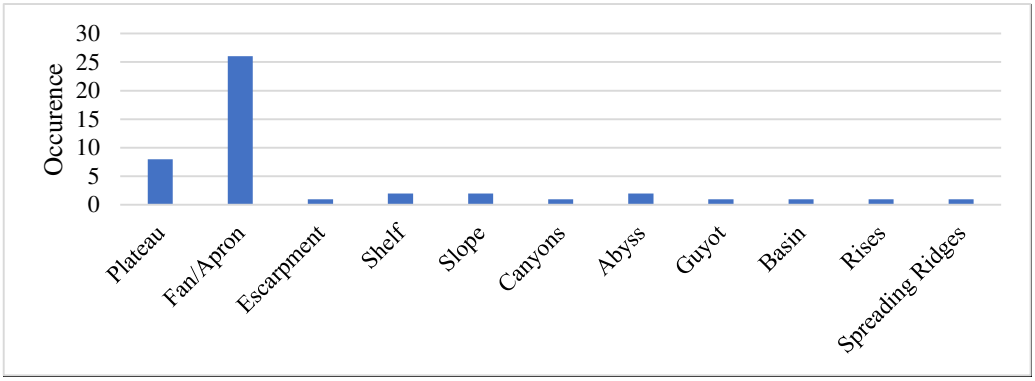

Fig.159 d Occurence of cyclogenesis and morphology in pre-monsoon season

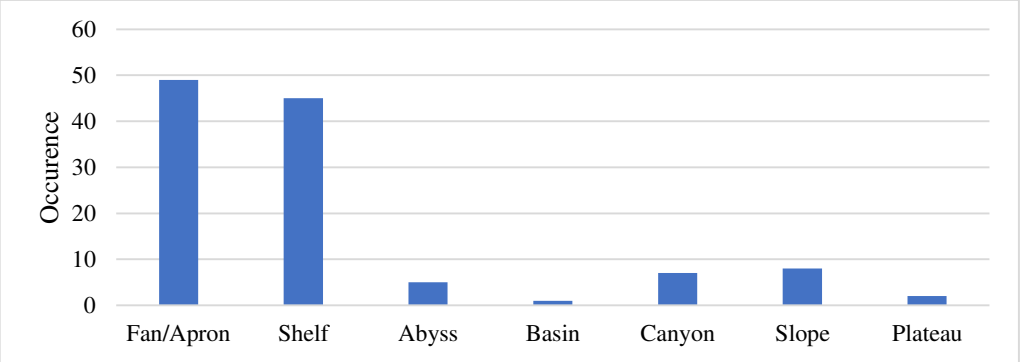

Fig.159 e Occurence of cyclogenesis and morphology in monsoon season

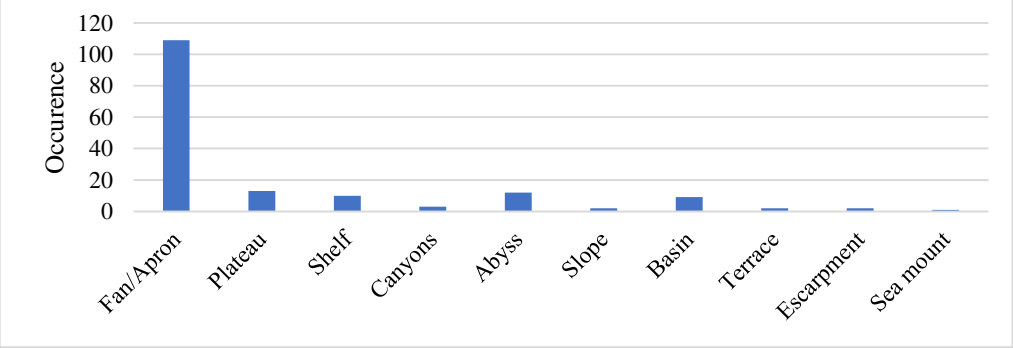

Fig.159 f Occurence of cyclogenesis and morphology in post-monsoon season

4.9 Impact of TC on major resources of Odisha coast

4.9.1 Variation of total catch and CPUE in the Odisha coast

The monthly catch of fishery resources and CPUE variation in 6 districts of Odisha coast during the study period 2007-2020 are shown in Fig.160a and Fig.160b. Higher catch is obtained at Jagatsinghpur whereas the remaining districts showed more or less similar catch with Kendrapara being the least. Almost all the district showed least catch in April and May. All the districts except Jagatsingpur obtained an average catch during other months whereas the Jagatsingpur Showed a highest catch. CPUE is also higher for Jagatsinghpur than other districts followed by Balasore, Puri, Bhadrak. CPUE showed a lowest value in May for all districts in Odisha. The least CPUE is is showed by Kendrapara and Puri. Table4.19 shows the gearwise total catch and CPUE in Odisha district. In jagatsingpur, the highest catch obtained through MDTN, MTN, OBGN, MGN and OBHL.

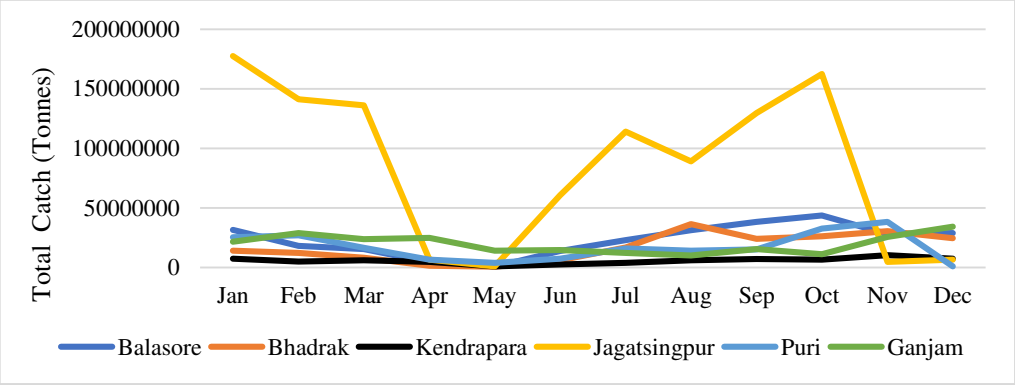

Fig.160 a Monthly total catch of 6 districts of Odisha during 2007-2020

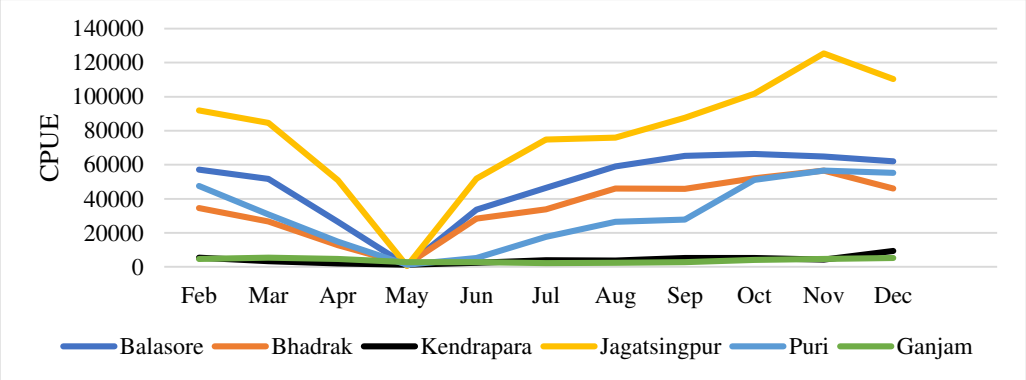

Fig.160 b Monthly CPUE of 6 districts of Odisha during 2007-2020

4.9.2 Species dissimilarity

The overall average dissimilarity of TCs during cyclonic month and respective months with no cyclones on the Odisha coast is depicted in Fig.161. Out of the twelve cyclones that hit on the Odisha coast, the Roanu, Amphan, and Viyaru contributed most to the overall average dissimilarity during the period 2007-2020. These cyclones are considered for further investigation. Table 13 depicts the overall average dissimilarity of three cyclones: Roanu, Viyaru, and Amphan between the months of A and A1, B and B1, C and C1, and D and D1. The table clearly shows that the OAD after the cyclone month for the three cyclones is decreasing. The OAD is higher during the cyclonic months, indicating that several factors caused by TC formation cause species dissimilarity. The OAD was decreased over the next few months, indicating that it is returning to normal. As a result, the formation of tropical cyclones results in a dissimilarity in species distribution.

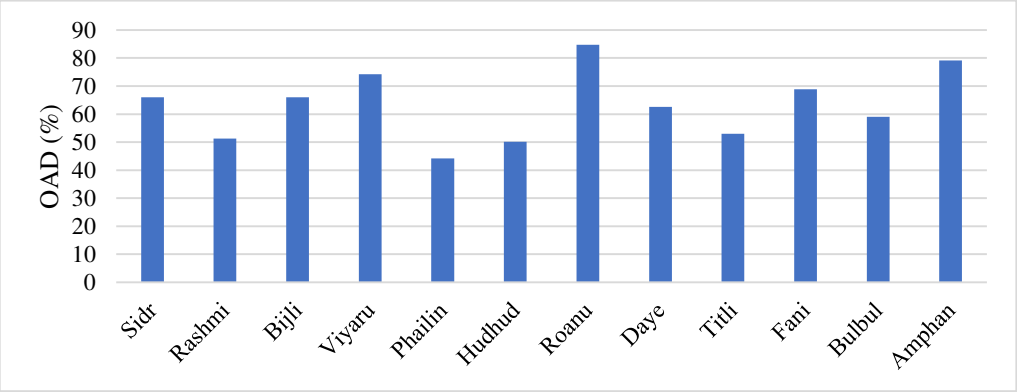

Fig.161 The OAD of the catches during the 12 cyclones in Odisha

Table 4.17.The overall average dissimilarity of three cyclones: Roanu, Viyaru, and Amphan between the cyclonic month and the respective month with no cyclones, the month just after the cyclonic month and the respective month with no cyclones, the second month after the cyclonic months and the respective months with no cyclones, and the third months after the cyclonic months and respective months with no cyclones.

Cyclones	A and A1	B and B1	C and C1	D and D1
Viyaru	74.23	57.16	52.14	46.71
Roanu	84.76	65.41	52.48	50.21
Amphan	79.11	67.09	59.98	49.74

4.9.2 a Viyaru

The CS Viyaru was formed in May 15, 2013.Table 4.18-4.22 depicts the species dissimilarity during the cyclone Viyaru with a cumulative percentage of up to 50% during the months A and A1, B and B1, C and C1, and D and D1. Because the OAD is higher during the months of A and A1, the five species that contributed the most to the OAD during this months is explored in detail.

The species dissimilarity during cyclone Viyaru up to 50 % cumulative percentage were contributed by 13 species during the cyclonic months(A) and the respective months with no cyclones (A1), 34 species during the next month after the cyclonic months (B) and the respective months with no cyclones (B1),47 species during the second months after the cyclonic month (C) and the respective months with no cyclones (C1) and 28 species during the third months after the cyclonic month (D) and the respective months with no cyclones (D1). The most important five species among this are given below (Table 4.18, Table 4.19, Table 4.20 and Table 4.21).

Sardinella longiceps, Sardinella fimbriata, Rastrelliger kanagurta, Thryssa dussumieri, and Johnius dussumieri contributed most to the dissimilarity. *Sardinella longiceps*, the most contributing species, showed a decrease in total catch during and after the cyclone Viyaru (Fig.162a), followed by *Sardinella fimbrita*, which also showed a slightly decreasing trend (Fig.162b) and also its catch decreased from normal. *Rastrelliger kanagurta* also showed a decreasing trend, but there was no significant drop in catch from normal (Fig.162c). *Thryssa dussumeiri* had a higher catch during the cyclone month, but no catch afterwards (Fig.162d). *Johnius dussumeiri* had a higher catch during the cyclone month as well, but it decreased in the following months (Fig.162e). All five species that contributed

more to the OAD during the cyclonic months had a negative catch trend, with *Thryssa dussumeiri* and *Johnius dussumeiri* having a higher catch during the cyclonic months.

Table 4.18 The species dissimilarity of important five species during cyclone Viyaru with a cumulative percentage of up to 50% during the cyclonic month and the respective month with no cyclones.

Taxon	Average dissimilarity	Contribution %	Cumulative %	Mean A	Mean A1
Sardinella longiceps	9.002	12.13	12.13	7.69	108
Sardinella fimbriata	6.14	8.27	20.4	398	705
Rastrelliger kanagurta	4.35	5.86	26.26	358	167
Thryssa dussumieri	3.22	4.33	30.59	249	8.05
Johnius dussumieri	2.32	3.13	33.72	192	25.8

Table 4.19 The species dissimilarity of important five species during cyclone Viyaru with a cumulative percentage of up to 50% during the next months after the cyclonic month and the respective months with no cyclones.

Taxon	Average dissimilarity	Contribution %	Cumulative %	Mean B	Mean B1
Sardinella longiceps	1.855	3.245	3.245	667	195
Johnius spp.	1.566	2.741	5.986	635	174
Pennahia anea	1.502	2.627	8.613	0	585
Stolephorus spp.	1.26	2.205	10.82	384	13.1
Metapenaeus dobsoni	1.238	2.166	12.98	560	234

Table 4.20 The species dissimilarity of important five species during cyclone Viyaru with a cumulative percentage of up to 50% during the second months after the cyclonic months and the respective months with no cyclones.

Taxon	Average dissimilarity	Contribution %	Cumulative %	Mean C	Mean C1
Pennahia anea	1.644	3.153	3.153	0	788
Solenocera crassicornis	1.314	2.52	5.673	0	607
Sardinella fimbriata	0.8639	1.657	7.33	494	493
Cynoglossus macrolepidotus	0.8394	1.61	8.94	0	393
Selar boops	0.838	1.607	10.55	0	383

Table 4.21 The species dissimilarity of important five species during cyclone Viyaru with a cumulative percentage of up to 50% during the third months after the cyclonic months and the respective months with no cyclones.

Taxon	Average dissimilarity	Contribution %	Cumulative %	Mean D	Mean D1
Pennahia anea	2.083	4.46	4.46	0	968
Trichiurus lepturus	1.486	3.181	7.641	968	278
Upeneus vittatus	1.284	2.748	10.39	123	719
Coilia dussumieri	1.243	2.661	13.05	577	0
Metapenaeus spp.	1.196	2.561	15.61	0	556

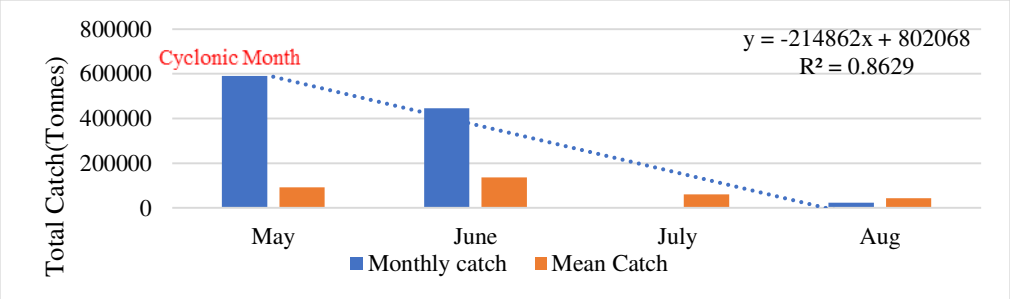

Fig.162a Variation in total catch of *Sardinella longiceps* during and after the cyclonic months and the respective months with no cyclones

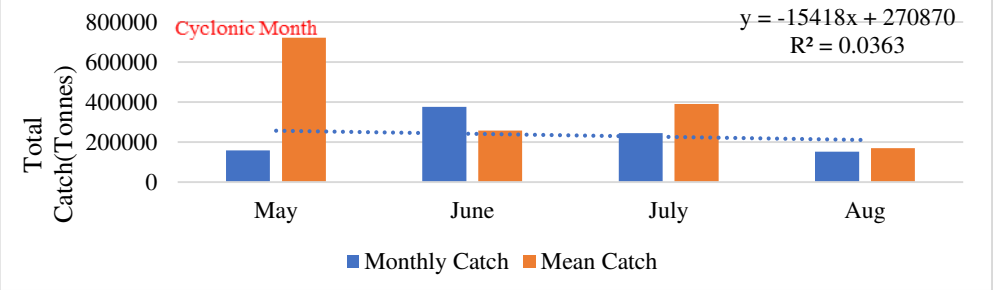

Fig.162b Variation in total catch of *Sardinella fimbriata* during and after the cyclonic months and respective months with no cyclone

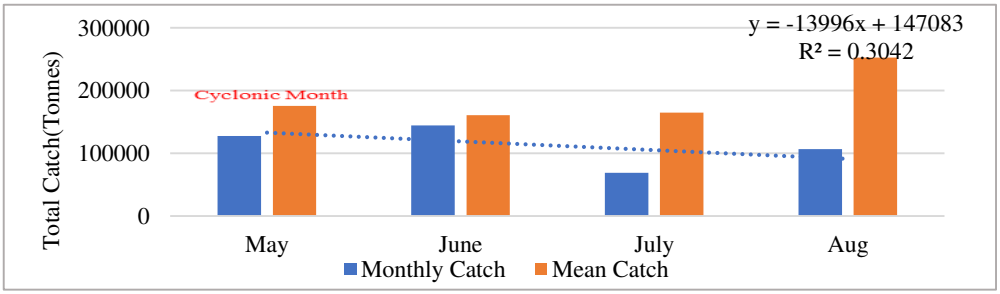

Fig.162c Variation in total catch of *Rastrelliger kanagurta* during and after the cyclonic months and the respective months with no cyclones

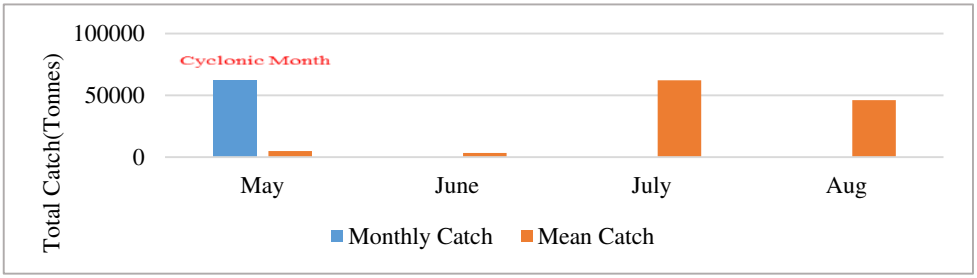

Fig.162d Variation in total catch of *Thryssa dussumeiri* during and after the cyclonic months and

the respective months with no cyclones.

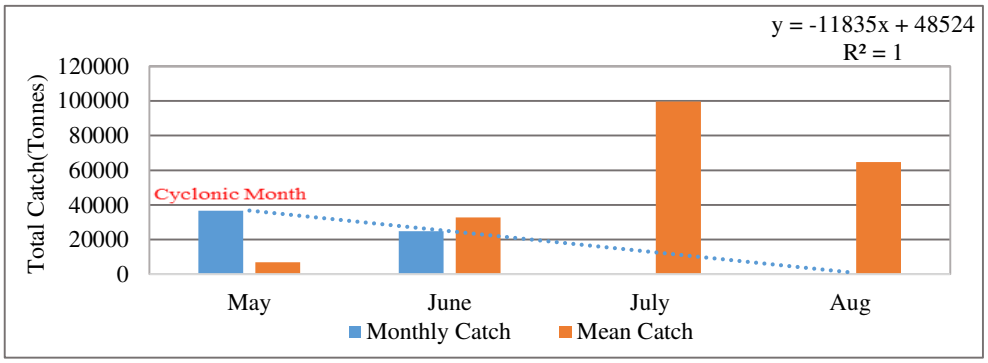

Fig.162e Variation in total catch of *Johnius dussumieri* during and after the cyclonic months and the respective months with no cyclones.

4.9.2b Roanu

The CS Roanu was formed in May 20, 2016.The OAD is higher during the cyclonic month (A) and the respective months with no cyclones (A1), the five species that contributed the most to the OAD during this months is explored in detail.

The species dissimilarity during cyclone Roanu up to 50 % cumulative percentage were contributed by 8 species during the cyclonic months(A) and the respective months with no cyclones (A1), 39 species during the next month after the cyclonic months (B) and the respective months with no cyclones (B1), 46 species during the second months after the cyclonic month (C) and the respective months with no cyclones (C1) and 28 species during the third months after the cyclonic month (D) and the respective months with no cyclones (D1). The most important five species among this are given below (Table 4.22, Table 4.23, Table 4.24 and Table 4.25).

Dussumieria spp., Rastrelliger kanagurta, Sardinella fimbriata, Megalaspis cordyla and Other Croakers are the species that contributed maximum to the dissimilarity during A and A1. *Dussumieria spp*., the most dissimilar species, showed a decreasing trend in total catch during and after cyclone Roanu with no

catch after the cyclone months (Fig.163a). *Rastrelliger kanagurta* had a positive trend with higher catch after the cyclone Roanu (fig.163b). *Sardinella fimbriata* showed a slight positive trend but the total catch is very much less from the normal (fig.163c). *Megalaspis cordyla* and Other croakers (fig.163d and Fig.163e) showed a positive trend. All the species except *Dussumieria* spp. showed a positive trend for the catch during the CS Roanu.

Table4.22 The species dissimilarity of cyclone Roanu with a cumulative percentage of up to 50% during the months cyclonic month (A) and the respective months with no cyclones (A1).

Taxon	Average dissimilarity	Contribution %	Cumulative %	Mean A	Mean A1
Dussumieria spp.	12.65	14.92	14.92	1.02	0
Rastrelliger kanagurta	10.44	12.32	27.25	962	167
Sardinella fimbriata	6.88	8.118	35.36	149	705
Megalaspis cordyla	3.049	3.598	38.96	245	0
Other Croakers	2.862	3.377	42.34	239	10.7

Table 4.23 The species dissimilarity of cyclone Roanu with a cumulative percentage of up to 50% during the next month after the cyclonic month (B) and the respective months with no cyclones (B1).

Taxon	Average dissimilarity	Contribution %	Cumulative %	Mean B	Mean B1
Escualosa thoracata	1.963	3	3	0	463
Pennahia anea	1.93	2.95	5.95	0	585
Sardinella spp.	1.645	2.515	8.466	298	198
Trichiurus lepturus	1.418	2.168	10.63	0	385
Sardinella fimbriata	1.365	2.087	12.72	234	423

Table4.24 The species dissimilarity of cyclone Roanu with a cumulative percentage of up to 50% during the second month after the cyclonic month (C) and the respective months with no cyclones (C1).

Taxon	Average dissimilarity	Contribution %	Cumulative %	Mean C	Mean C1
Rastrelliger kanagurta	1.484	2.828	2.828	959	253
Pennahia anea	1.444	2.751	5.579	0	788
Metapenaeus dobsoni	0.827	1.576	7.155	222	594
Kathala axillaris	0.799	1.523	8.678	549	179
Sepia spp.	0.775	1.477	10.15	437	72.6

Table 4.25 The species dissimilarity of cyclone Roanu with a cumulative percentage of up to 50% during the third months after the cyclonic month (D) and the respective months with no cyclones (D1).

Taxon	Average dissimilarity	Contribution %	Cumulative %	Mean D	Mean D1
Muraenesox spp.	4.074	8.113	8.113	0	1.65
Fungia fungitus	3.846	7.66	15.77	0	1.65
Kathala axillaris	1.287	2.564	18.34	926	196
Pennahia anea	1.076	2.142	20.48	0	629
Rastrelliger kanagurta	0.9536	1.899	22.38	929	380

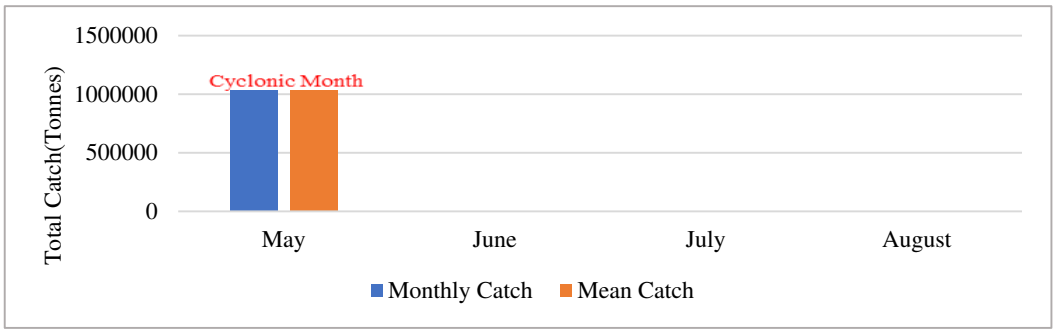

Fig.163a Variation in total catch of *Dussumieria spp*. during and after the cyclonic months (A) and the respective months with no cyclones (A1)

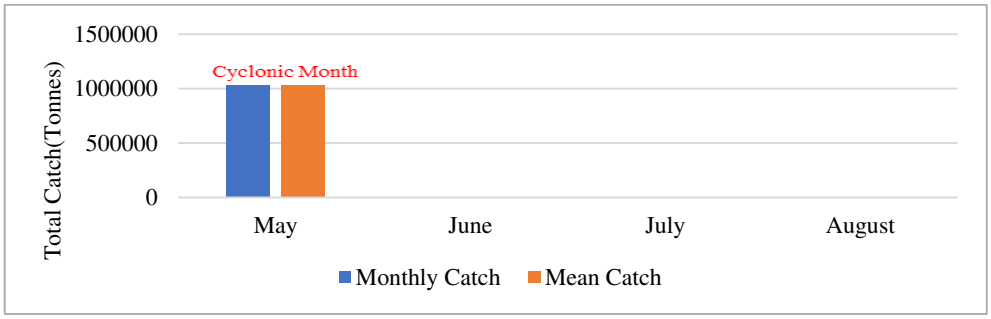

Fig.163b Variation in total catch of *Rastrelliger kanagurta* during and after the cyclonic months(A) and the respective months with no cyclones (A1)

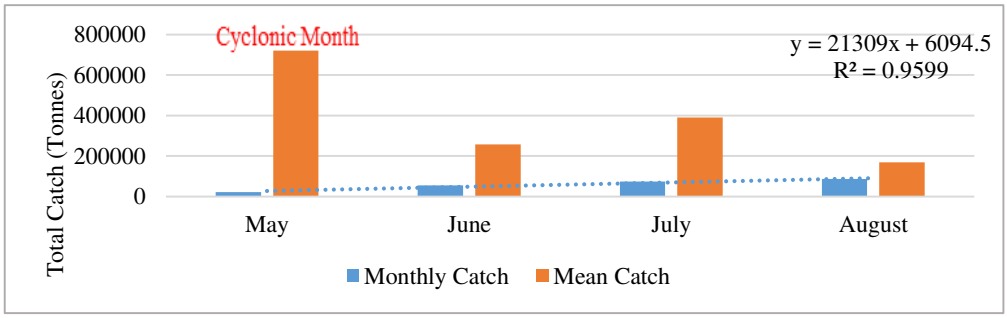

Fig.163c Variation in total catch of *Sardinella fimbriata* during and after the cyclonic months (A) and the respective months with no cyclones (A1)

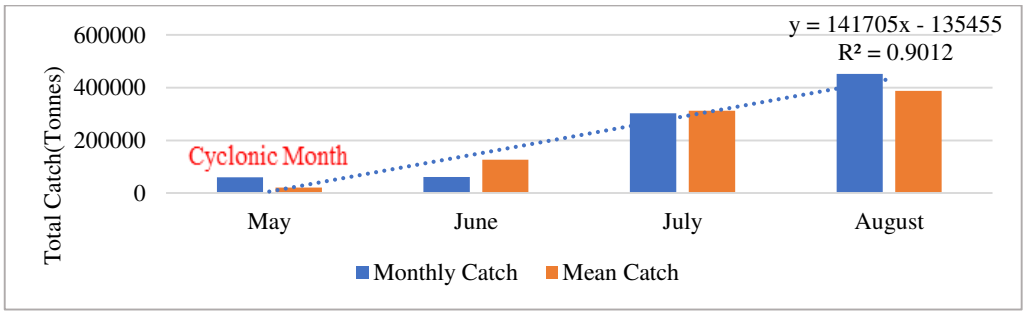

Fig.163d Variation in total catch of *Megalaspis cordyla* during and after the cyclonic months (A) and the respective months with no cyclones (A1)

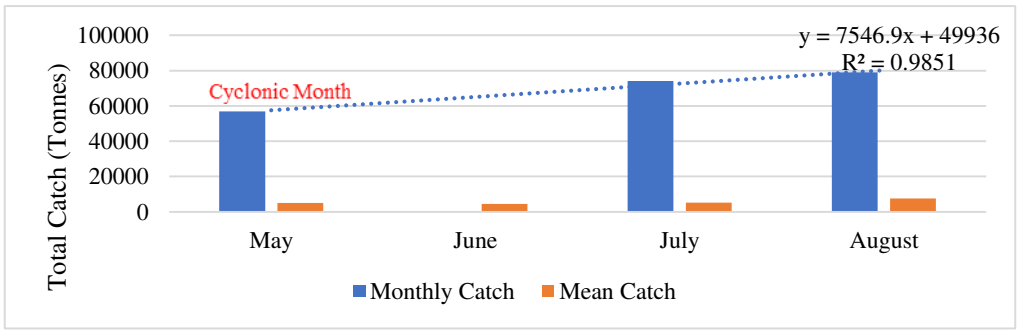

Fig.163e Variation in total catch of Other croakers during and after the cyclonic months (A) and the respective months with no cyclones (A1)

4.9.2c Amphan

The SuCS Amphan was formed in May 20, 2020. The OAD is higher during the cyclonic month (A) and the respective months with no cyclones (A1), the five species that contributed the most to the OAD during this months is explored in detail.

The species dissimilarity during cyclone Roanu up to 50 % cumulative percentage were contributed by 21 species during the cyclonic months(A) and the respective months with no cyclones (A1), 44 species during the next month after the cyclonic months (B) and the respective months with no cyclones (B1), 52 species during the second months after the cyclonic month (C) and the respective months with no cyclones (C1) and 51 species during the third months after the cyclonic month (D) and the respective months with no cyclones (D1). The most important five species among this are given below (Table 4.26, Table 4.27, Table 4.28 and Table 4.29).

Coilia dussumieri, Sardinella fimbriata, Harpadon nehereus, Plicofollis dussumieri, and *Escualosa thoracata* were the species that contributed most to the dissimilarity. *Coilia dussumieri*, the most dissimilar species, showed an increasing trend in total catch during and after cyclone Amphan. (Fig.164a). *Sardinella fimbriata* had a negative trend with higher catch after the cyclone Amphan (fig.164b). *Harpadon nehereus* showed a significant positive trend with the total catch is very much higher after the cyclonic month(fig.164c). *Plicofollis dussumieri* and *Escualosa thoracata* had a slight significant negative trend but the total catch of some months after the cyclonic month showed an increase (Fig.164d and Fig.164e). Altogether *Harpadon nehereus* and *Coilia dussumieri* showed an increase in catch after the occurrence of cyclone Amphan and others showed a negative trend.

Table 4.26 The species dissimilarity of cyclone Amphan with a cumulative percentage of up to 50% during the cyclonic months and the respective month with no cyclones.

Taxon	Average dissimilarity	Contribution %	Cumulative %	Mean A	Mean A1
Coilia dussumieri	10.7	13.52	13.52	1.38	1.85
Sardinella fimbriata	5.10	6.44	19.96	0.00	705
Harpadon nehereus	1.63	2.06	22.02	275	68.7
Plicofollis dussumieri	1.52	1.92	23.95	224	36.2
Escualosa thoracata	1.48	1.88	25.82	280	92.4

Table4.27 The species dissimilarity of Cyclone Amphan with a cumulative percentage of up to 50% during the next months after the cyclonic months (B) and the respective months with no cyclones (B1).

Taxon	Average dissimilarity	Contribution %	Cumulative %	Mean B	Mean B1
Stolephorus indicus	1.654	2.466	2.466	450	9.88
Pennahia anea	1.589	2.368	4.834	68.8	580
Escualosa thoracata	1.497	2.231	7.065	547	421
Leiognathus spp.	1.396	2.081	9.146	431	71.7
Setipinna taty	1.265	1.886	11.03	0	380

Table4.28 The species dissimilarity of Cyclone Amphan with a cumulative percentage of up to 50% during the second months after the cyclonic month (C) and the respective months without cylones (C1)

Taxon	Average dissimilarity	Contribution %	Cumulative %	Mean C	Mean C1
Uraspis uraspis	0.9968	1.662	1.662	1.07	351
Pennahia anea	0.9309	1.552	3.214	894	719
Penaeus indicus	0.9063	1.511	4.725	785	137
Sepiella inermis	0.883	1.472	6.197	675	36.8
Parapenaeopsis stylifera	0.8462	1.411	7.607	1.04	456

Table 4.29 The species dissimilarity of Cyclone Amphan with a cumulative percentage of up to 50% during the third months after the cyclonic months (D) and the respective months without cyclones (D1).

Taxon	Average dissimilarity	Contribution %	Cumulative %	Mean D	Mean D1
Pennahia anea	1.327	2.668	2.668	7.19	600
Solenocera crassicornis	0.8314	1.671	4.339	5.57	559
Tenualosa ilisha	7.95	1.60	5.937	305	686
Sardinella fimbriata	7.47	1.50	7.439	521	339
Lepturacanthus savala	7.46	1.50	8.94	273	470

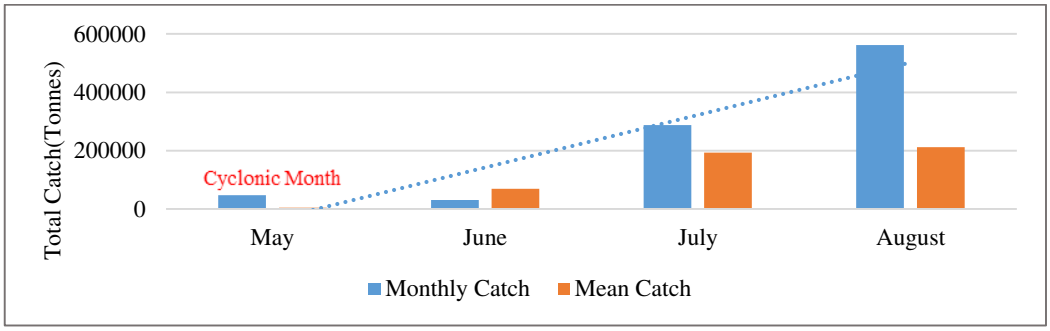

Fig.164a Variation in total catch of *Coilia dussumieri* during and after the cyclonic months and the respective months without cyclones.

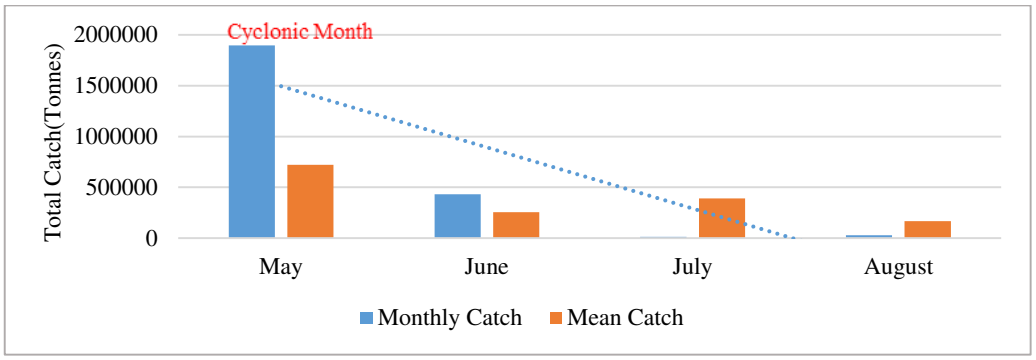

Fig.164b Variation in total catch of *Sardinella fimbriata* during and after the cyclonic months and the respective months without cyclones.

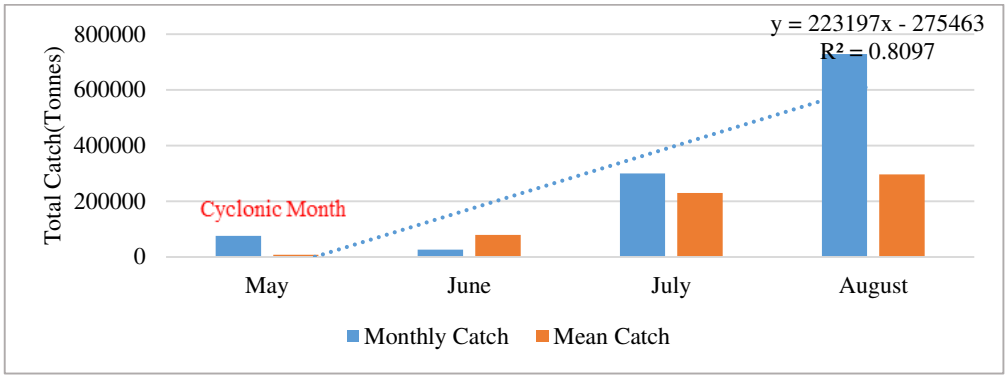

Fig.164c Variation in total catch of *Harpadon nehereus* during and after the cyclonic months months and the respective months without cyclones.

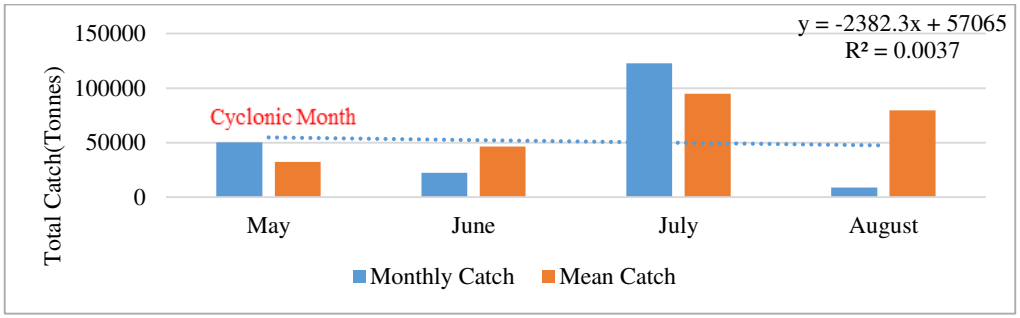

Fig.164d Variation in total catch of *Plicofollis dussumieri* during and after the cyclonic months and the respective months without cyclones.

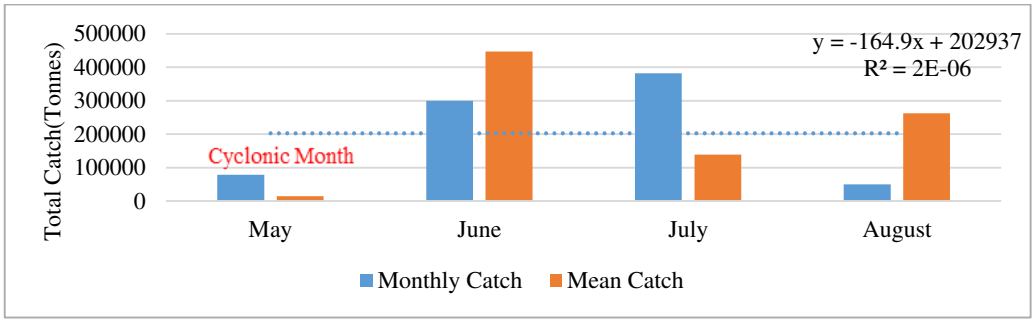

Fig.164d Variation in total catch of *Escualosa thoracata* during and after the cyclonic months and the respective months without cyclones.

4.10 Variation in chlorophyll a concentration

The variation in chl a for the three cyclones that contributed the most to OAD was investigated to see if there was an impact on ocean chl a content as a result of cyclone formation in area limited to 200 m contour along the Odisha coast. The climatological daily data were examined.

Fig.165a depicted the daily variation of chl a from before the formation of Cyclone Viyaru to 30 days later. It showed a slight positive trend, indicating that the chl a concentration increased following the formation of Cyclone Viyaru. The chl a value fluctuates, but overall there is a positive trend.

During Cyclone Roanu, the daily chl a variation was also a slightly positive trend (Fig.166a). Therefore, after the formation of cyclone Roanu, there is a slight increase in chl a.

A significant positive trend in both daily chl a concentration is clearly visible after the formation of Amphan (Fig.167a). Overall increase in the chl a concentration was observed.

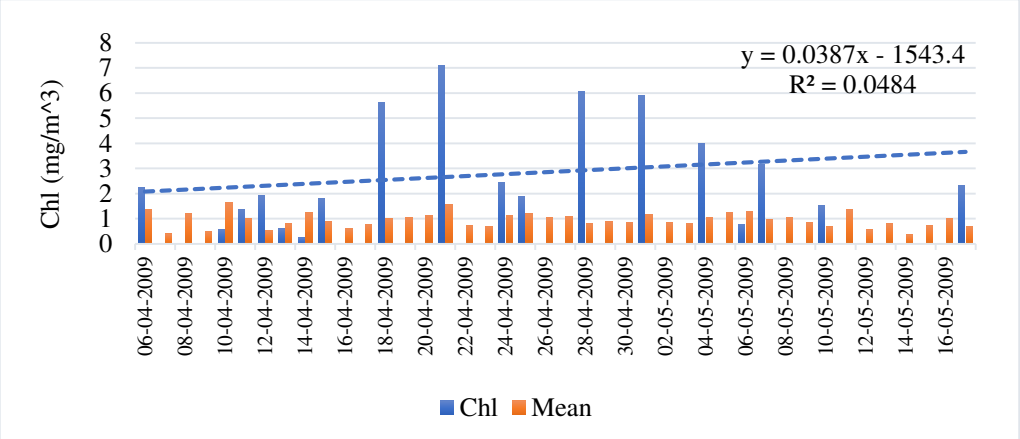

Fig.165a The variation of chl a during the cyclone Viyaru using daily data

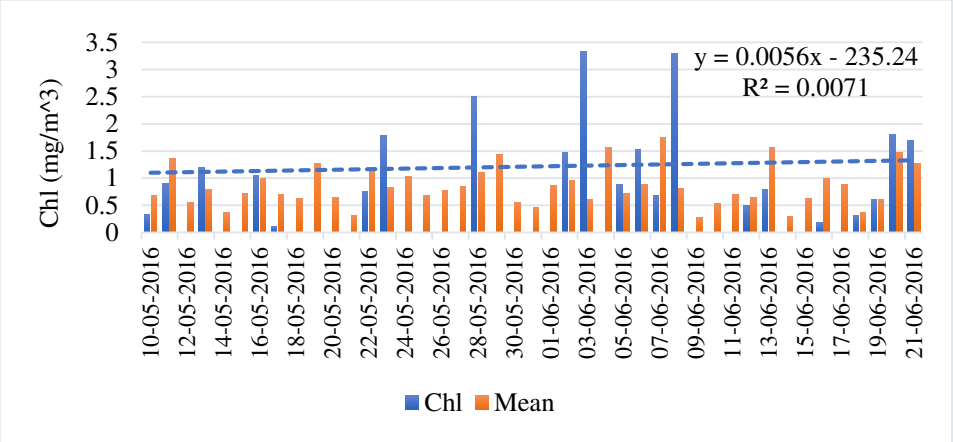

Fig.166 The variation of chl a during the cyclone Roanu using daily data

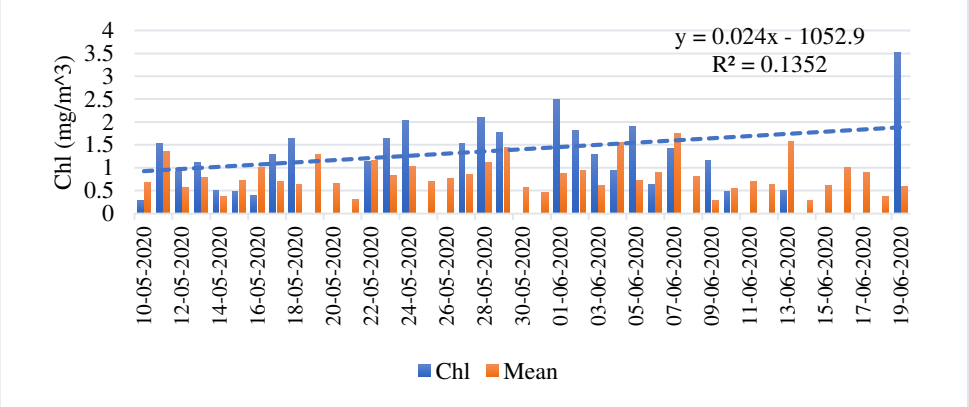

Fig.167a The variation of chl a during the cyclone Amphan using daily data

4.11 Impacts on major fishery resources

The CPUE variation of the economically important major five species on the Orissa coast was investigated. A general trend is observed for all species, with CPUE increasing during cyclonic events formed during October and November, whereas cyclones formed in April and May showed a negative trend for CPUE.

4.11.1 CPUE of *Sardinella fimbriata*

The yearly total catch variation of the species *Sardinella fimbriata* during 2007-2020 on the Odisha Coast is given in Fig.168a. It shows a slightly decreasing trend. The fluctuation in total catch between the years can be seen with a higher catch in 2020. The yearly CPUE showed a significant positive trend (Fig.168b) with a very higher value in 2020 compared to recent years. The catch and CPUE of *Sardinella fimbriata* show greater fluctuation during the period of cyclonic storms. Out of the twelve CS that we considered during the study period, CPUE showed a positive trend during the VSCS Bulbul and ESCS Sidr (Fig.169 and Fig.170), both of which were formed in the Nov. CPUE showed a negative trend during CS Roanu and ESCS Fani, both of which were in May (Fig.171 and Fig.172). In general, it could be stated that the cyclones which formed during Oct-Nov resulted in a positive trend in CPUE and those which formed in April-May showed a negative trend.

During Bulbul, CPUE showed a positive trend for OBGN and MDTN (Fig.173a and Fig.173b), which contributed more to the CPUE than NM. Other gears like OBRS, MTN, and NM also contributed towards CPUE but show a negative trend (Fig.173c, Fig.173d, Fig.173e,). Some catch was contributed by OBHL did not show any trend. During Sidr, OBGN and NM contributed more, showing a slightly positive trend, followed by MTN, which shows a slightly negative trend (Fig.174a, Fig.174b, Fig.174c). OBGN contributed more to the CPUE at the time of cyclone Roanu, which shows a positive trend, followed by MDTN and NM, which showed a negative trend (Fig.175a, Fig.175b, Fig.175c). During Fani, some catch were contributed by OBBN, which did not show any

significant trend. MDTN and OBGN contributed more toward CPUE followed by OBRS, but all showed a significant negative trend (Fig.176a, Fig.176b, Fig.176c). A few contributions were also given by MGN, NM and OBGN, but did not show any significant trend.

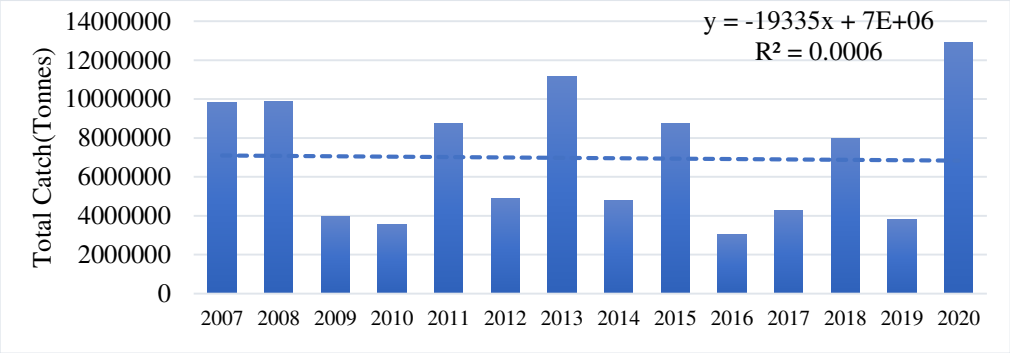

Fig.168a The yearly total catch variation of the species *Sardinella fimbriata* during 2007-2020 along the Odisha Coast.

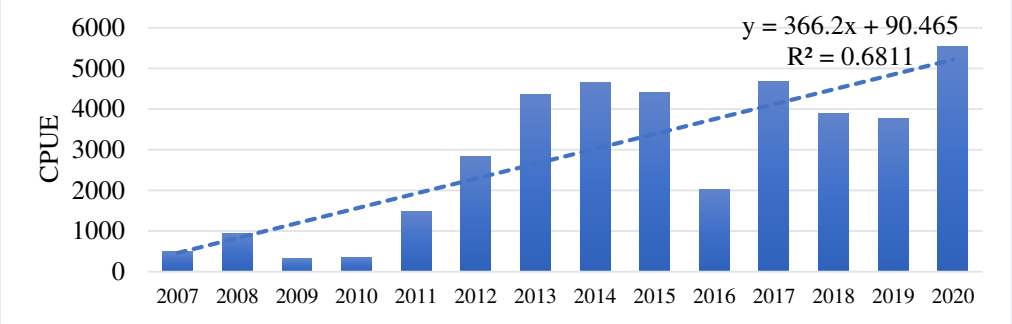

Fig.168b The yearly CPUE variation of the species *Sardinella fimbriata* during 2007-2020 along the Odisha Coast

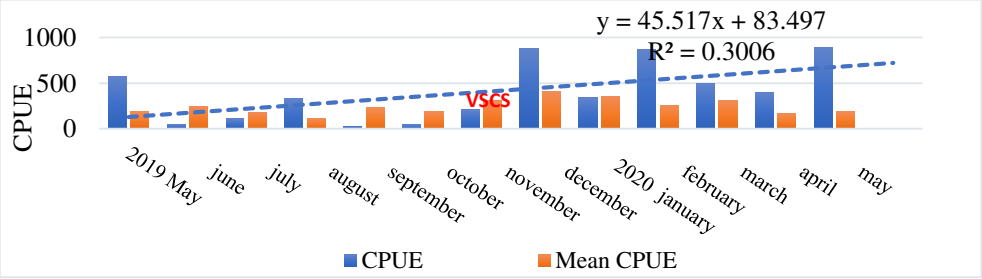

Fig.169 The CPUE variation of the species *Sardinella fimbriata* during the cyclone Bulbul

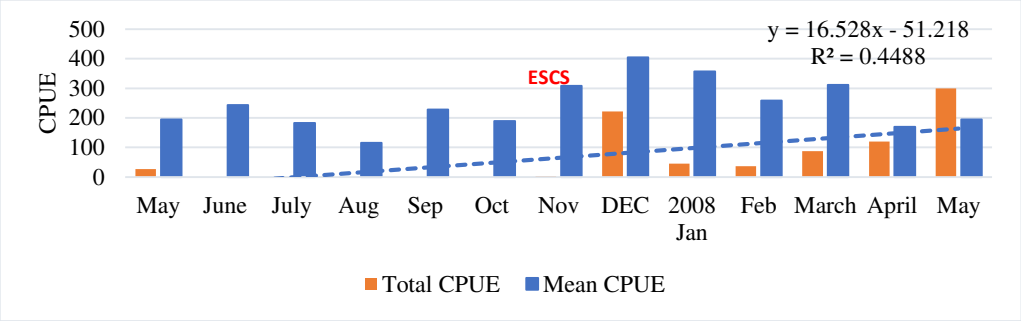

Fig.170 The CPUE variation of the species *Sardinella fimbriata* during the cyclone Sidr

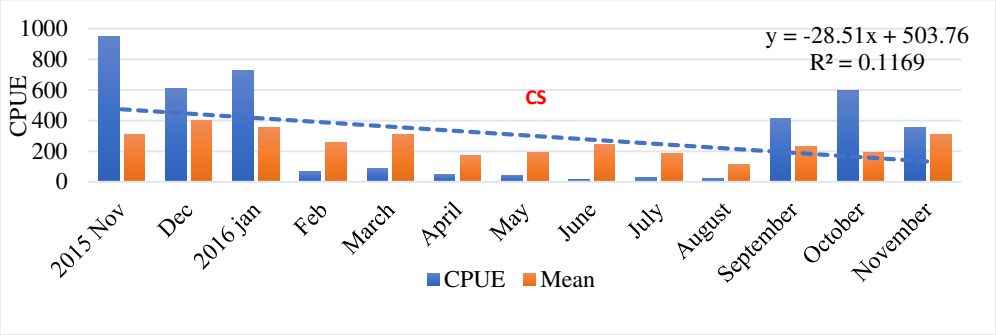

Fig.171 The CPUE variation of the species *Sardinella fimbriata* during the cyclone Roanu

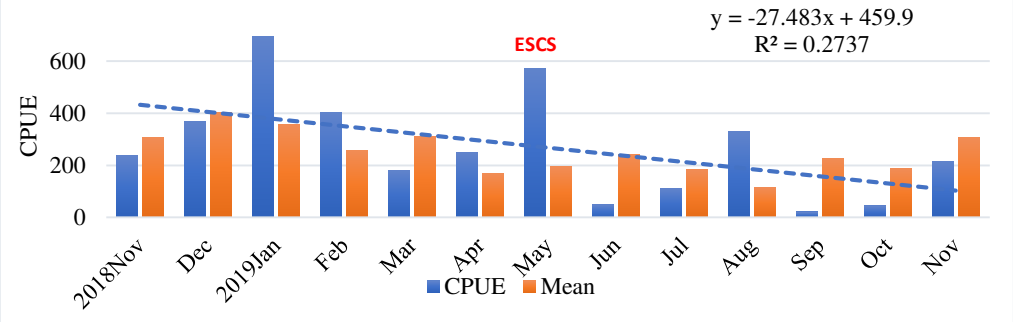

Fig.172 The CPUE variation of the species *Sardinella fimbriata* during the cyclone Fani

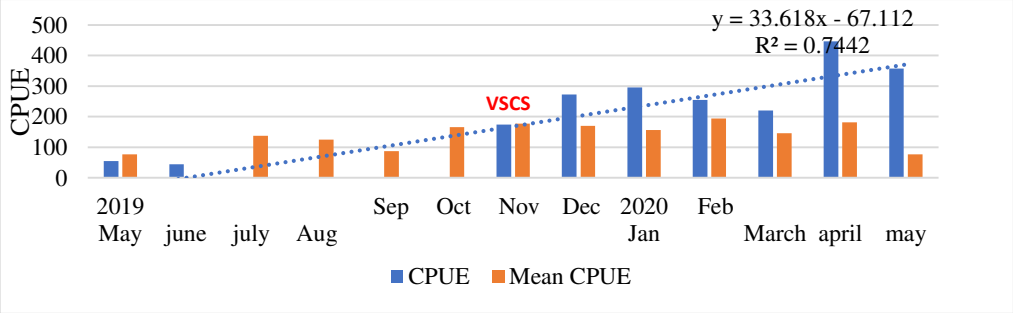

Fig.173a CPUE of OBGN during Bulbul

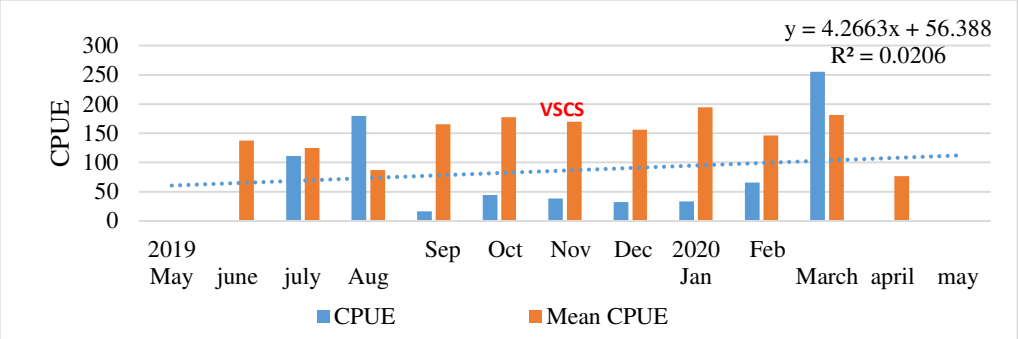

Fig.173b CPUE of MDTN during Bulbul

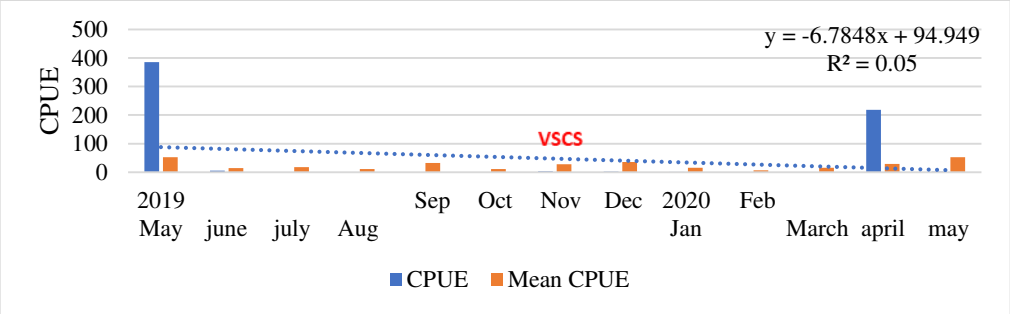

Fig.173c CPUE of MTN during Bulbul

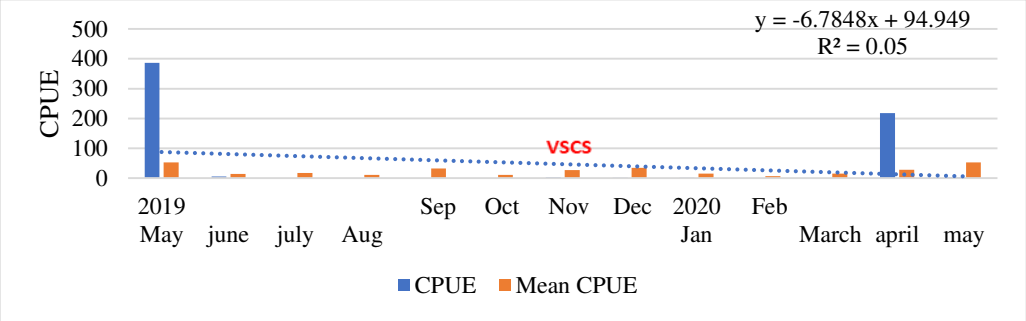

Fig.173d CPUE of NM during Bulbul

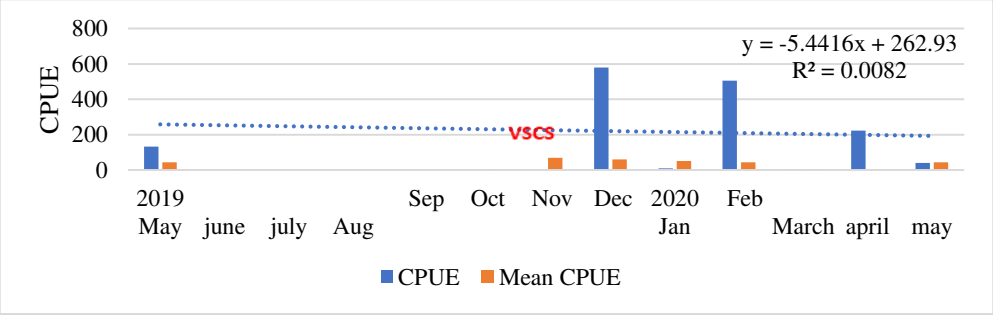

Fig.173e CPUE of OBRS during Bulbul

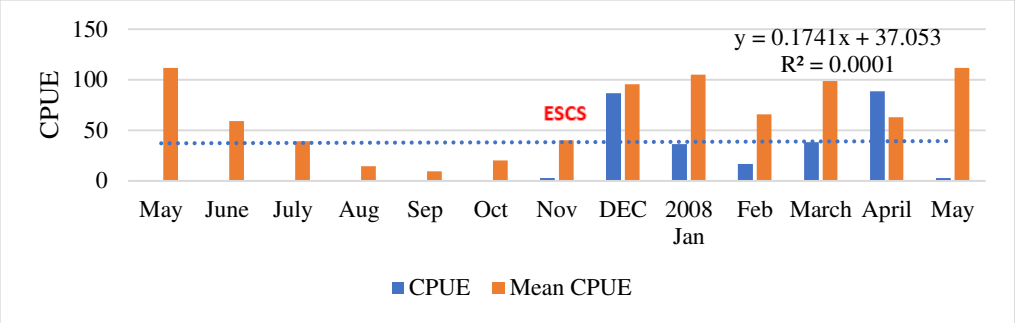

Fig.174a CPUE of OBRS during Sidr

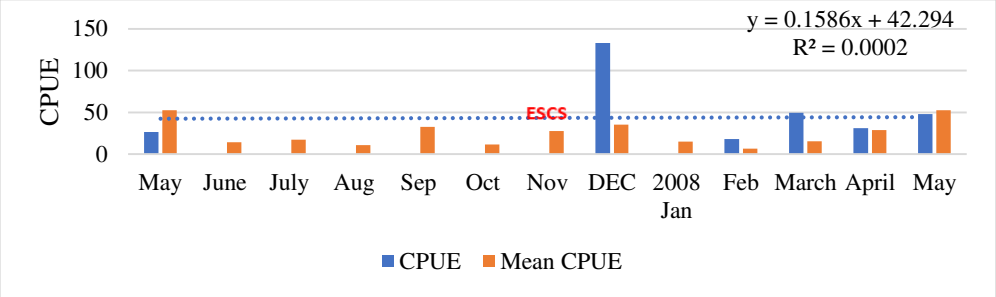

Fig.174b CPUE of NM during Sidr

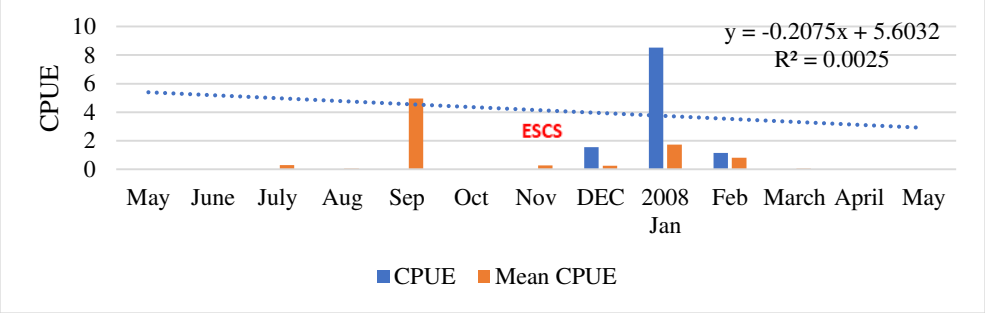

Fig.174c CPUE of MTN during Sidr

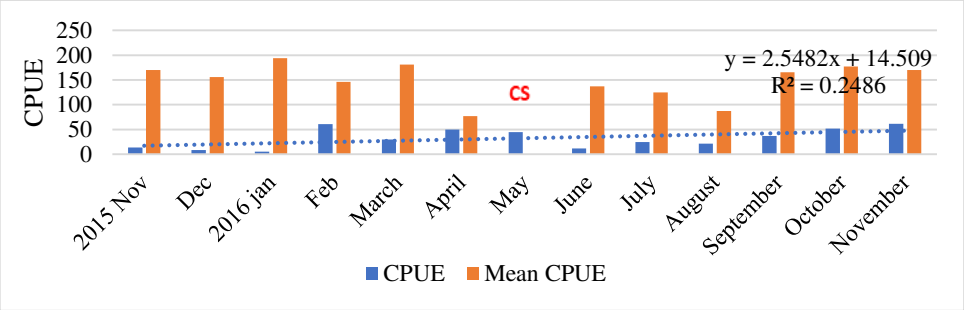

Fig.175a CPUE of OBGN during Roanu

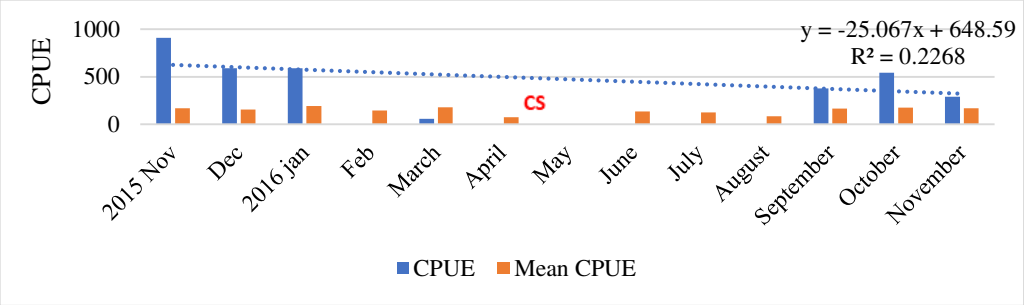

Fig.175b CPUE with MDTN during Roanu

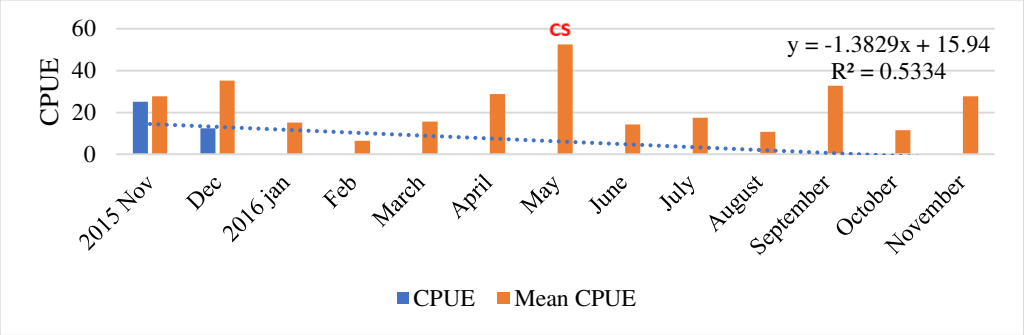

Fig.175c CPUE with NM during Roanu

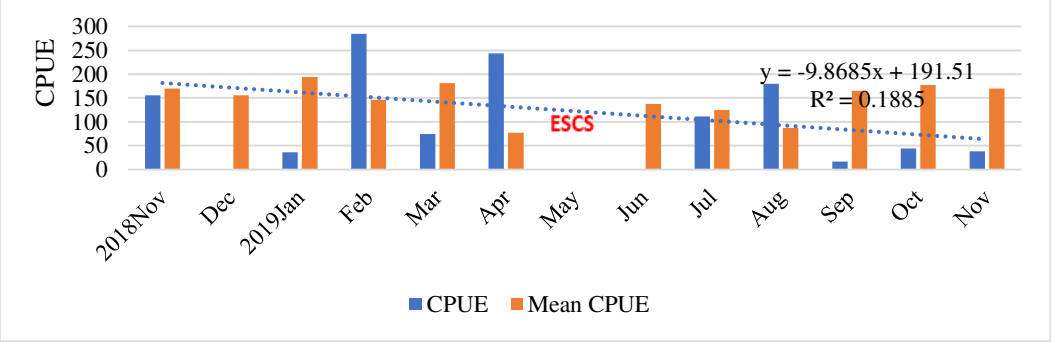

Fig.176a CPUE with MDTN during Fani

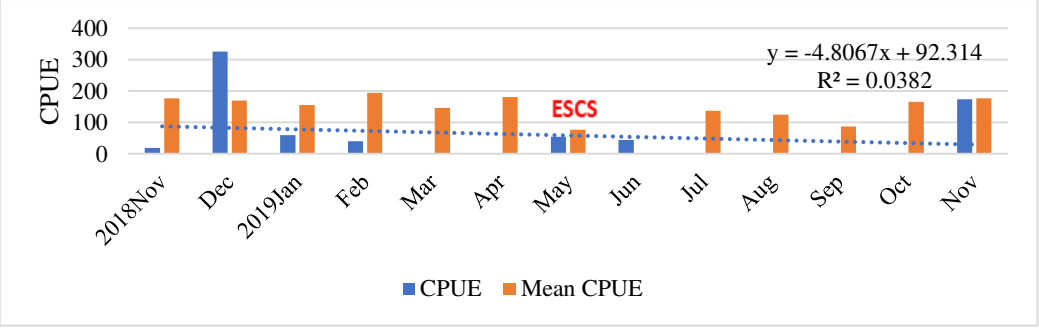

Fig.176b CPUE with OBGN during Fani

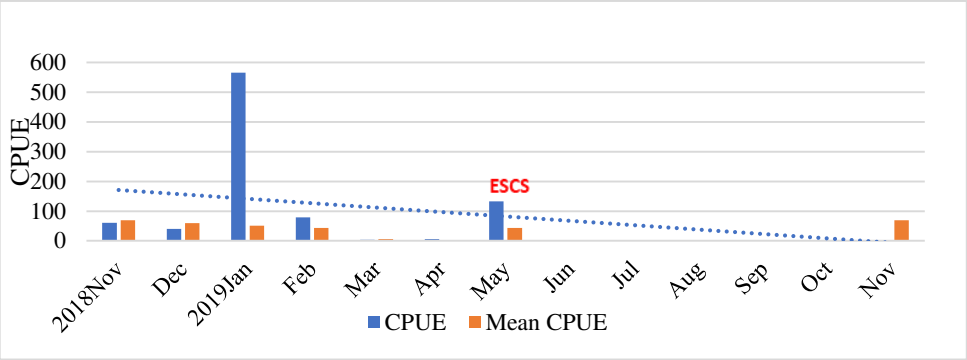

Fig.176c CPUE of OBRS during Fani

4.11.2 CPUE of *Rastrelliger kanagurta*

The annual variation in total catch and CPUE of Rastrelliger kanagurta were showed in Fig.177a and Fig.177b. During the study period 2007-2020, total catch did not show any trend, remaining relatively constant throughout the years, whereas CPUE showed a positive trend. ESCS Philin and CS Rashmi, both of which formed in October, had a positive impact on the species (Fig.178 and Fig.179), whereas CS Bijli and SuCS Amphan, both of which formed in April, had a negative impact (Fig.180 and Fig.181).

The CPUE after cyclone Philin increased significantly, owing primarily to MDTN, OBGN, and MTN, all of which showed a significant positive trend, followed by NM (Fig.182a, Fig.182b, Fig182c and Fig.182d), which showed a slightly decreasing trend. The catch during Cyclone Rashmi was primarily contributed by MDTN and MTN, which demonstrated a positive trend (Fig.183a and Fig.183b). NM and OBGN contributed a small percentage (Fig.183c and Fig.183d), but it showed a negative trend. MDTN and MTN contributed to the catch during cyclone Bijli (Fig.184a and Fig.184b), both of which contributed to the decrease in catch after the cyclone. During Amphan, CPUE showed a negative trend in MDTN, MGN, OBGN, and OBRS, but its total catch after the cyclone is increasing (Fig.185a, Fig.185b, Fig.185c and Fig.185d).

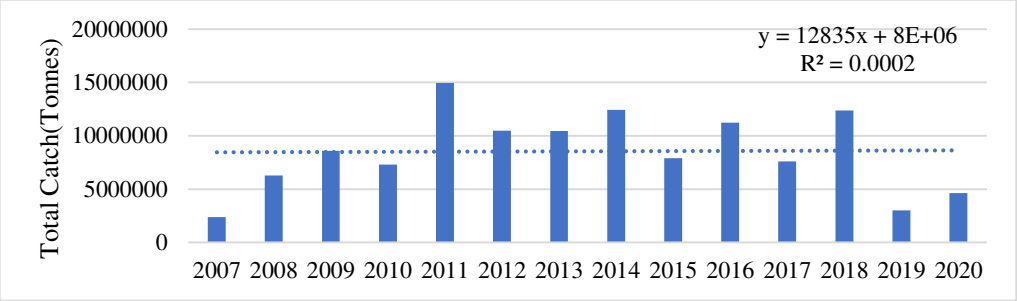

Fig.177a The yearly total catch variation of the species *Rastrelliger kanagurta* during 2007-2020 along the Odisha Coast

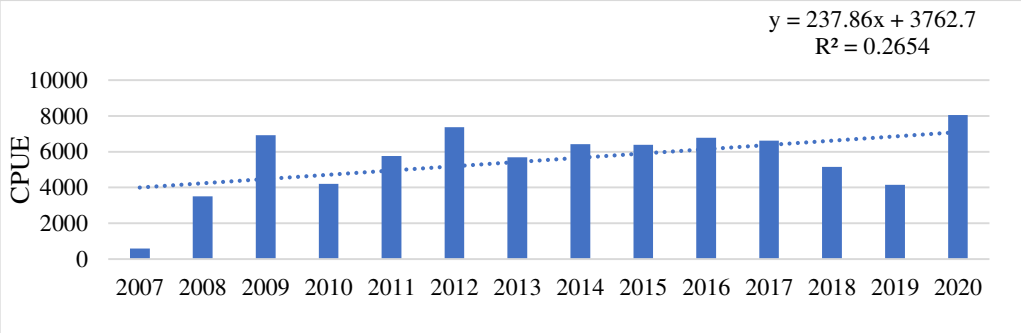

Fig.177 Yearly CPUE variation of the species *Rastrelliger kanagurta* during 2007-2020 along the Odisha Coast

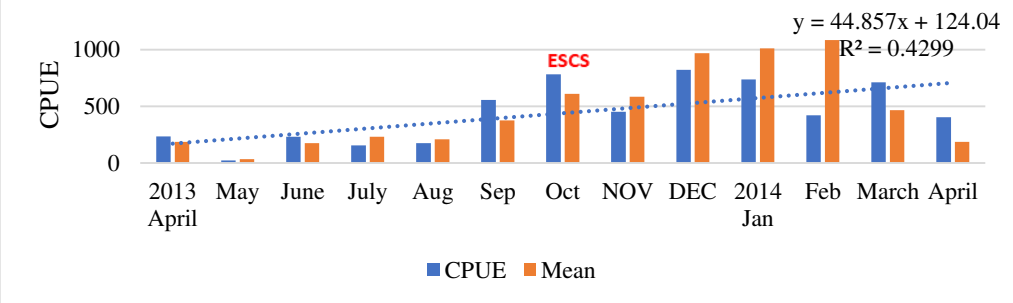

Fig.178 The CPUE variation the species *Rastrelliger kanagurta* during the cyclone Phailin

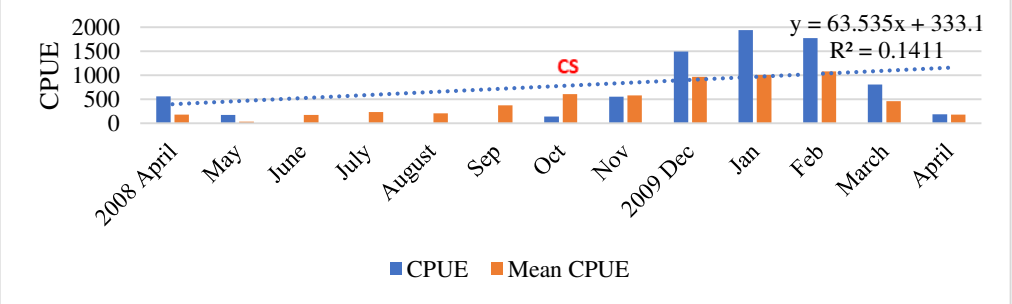

Fig.179 The CPUE variation the species *Rastrelliger kanagurta* during the cyclone Rashmi

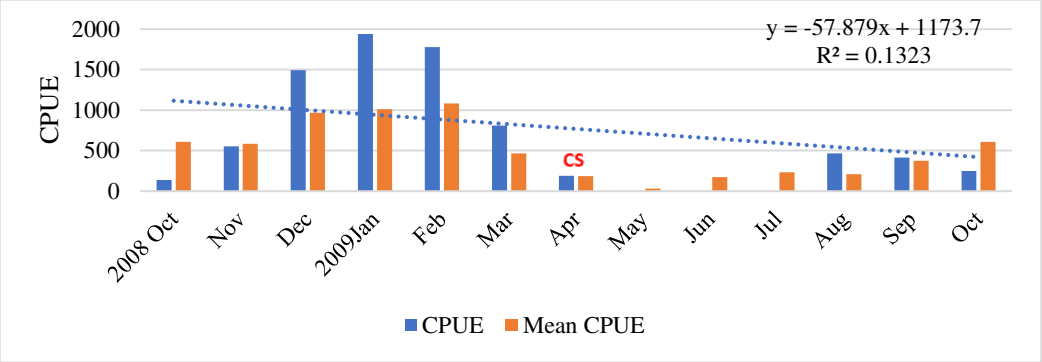

Fig.180 The CPUE variation the species *Rasrelliger kanagurta* during the cyclone Bijli

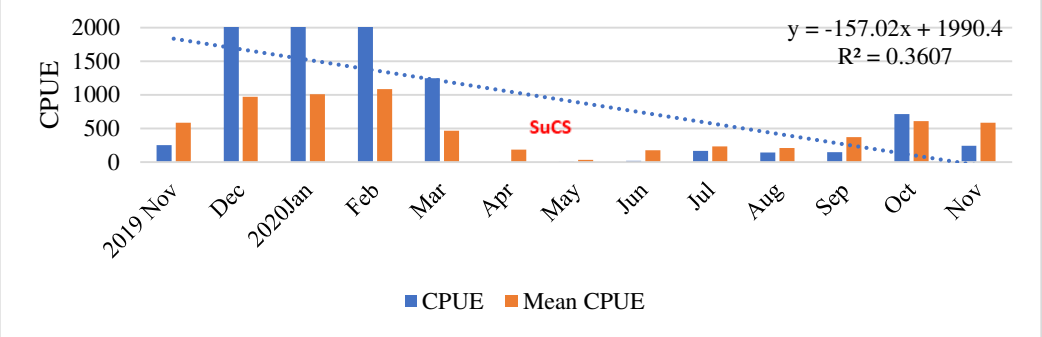

Fig.181 The CPUE variation the species *Rasrelliger kanagurta* during the cyclone Amphan

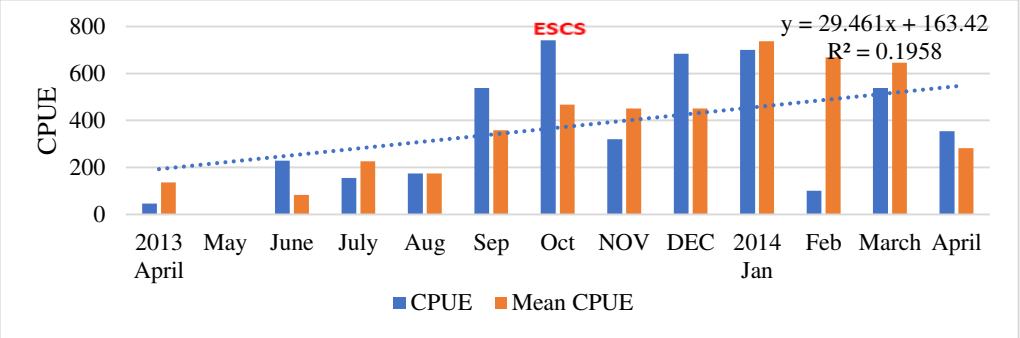

Fig.182 a CPUE of MDTN during Phailin

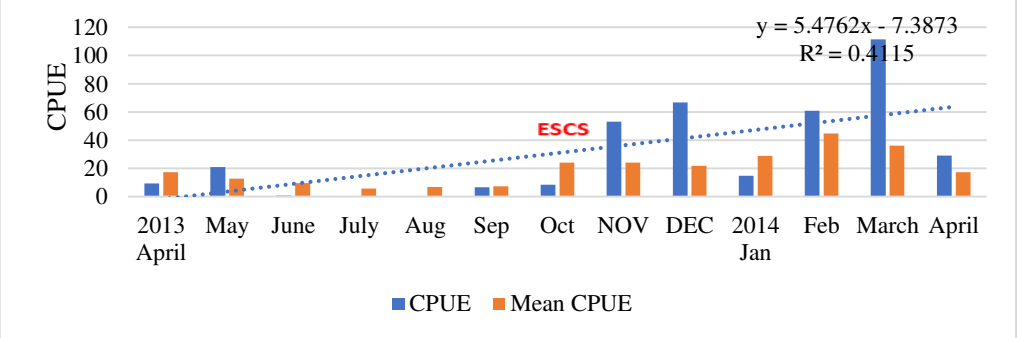

Fig.182b CPUE with OBGN during Phailin

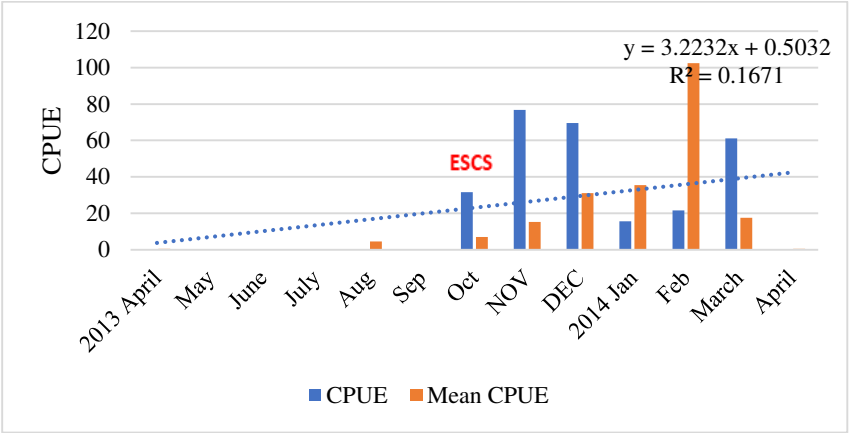

Fig.182c CPUE with MTN during Phailin

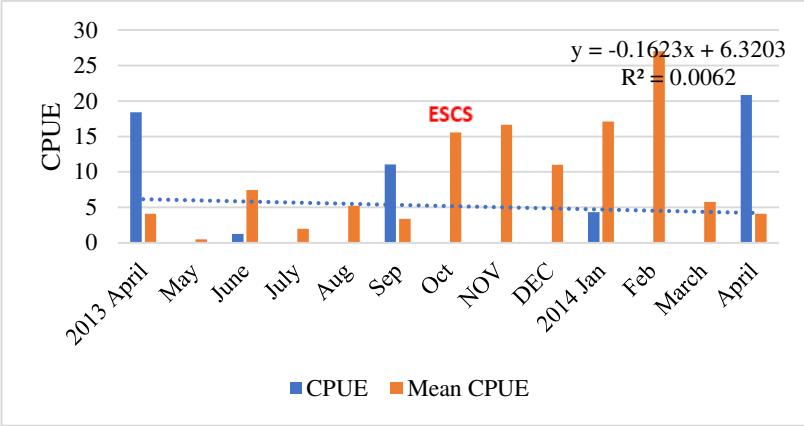

Fig.182d CPUE with NM during Phailin

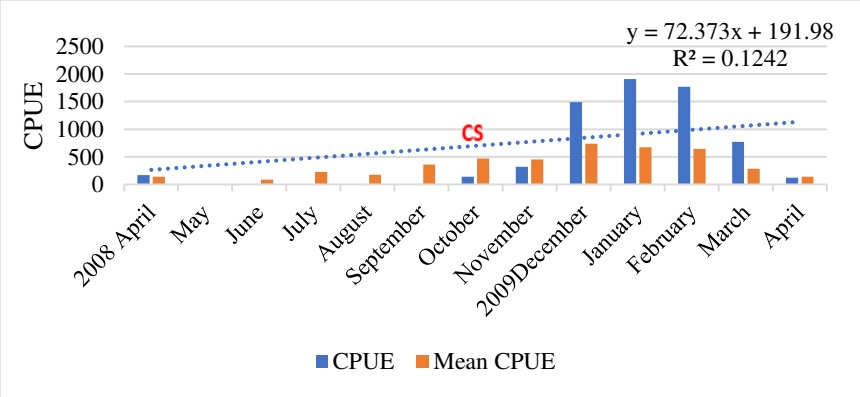

Fig183.a CPUE of MDTN during Rashmi

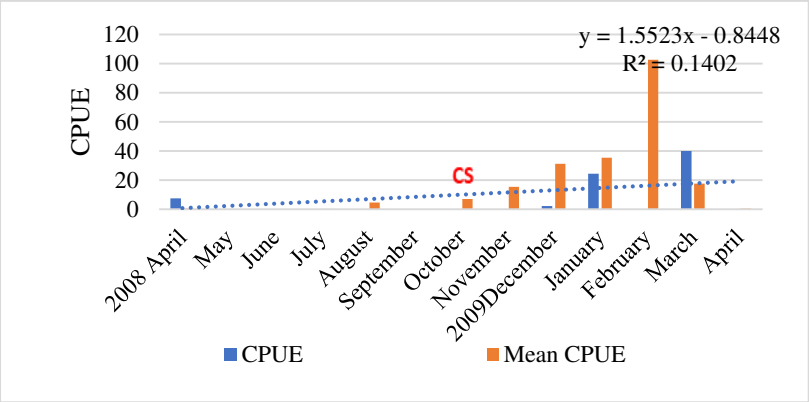

Fig.183.b CPUE of MTN during Rashmi

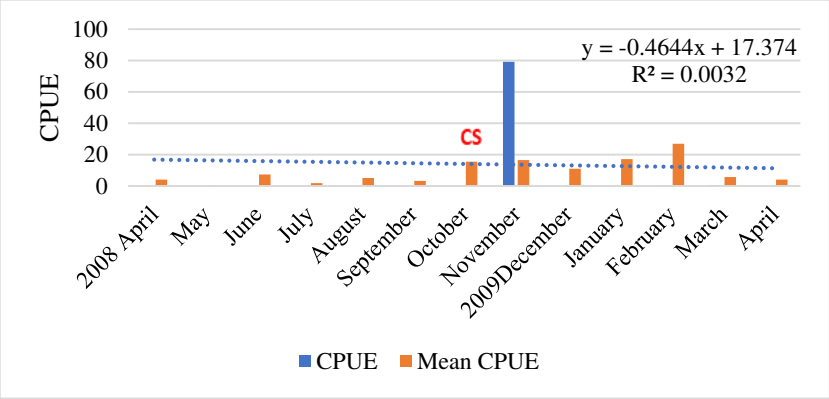

Fig183.c CPUE of NM during Rashmi

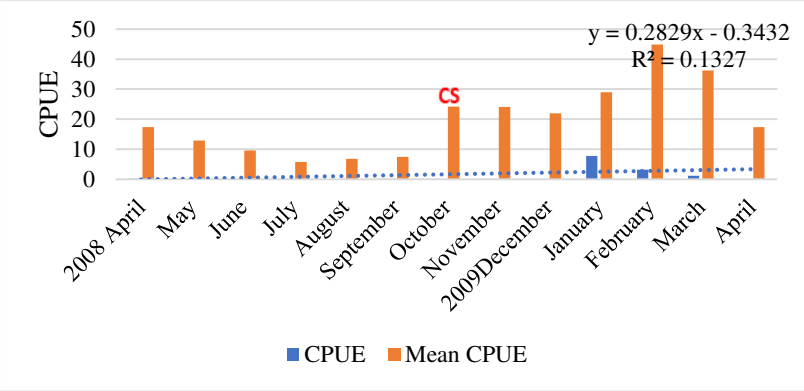

Fig.183.d CPUE of OBGN during Rashmi

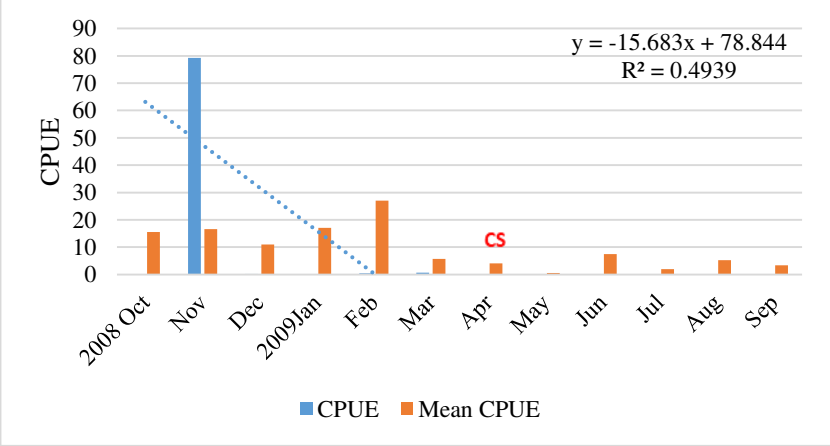

Fig184.a CPUE of NM during Bijli

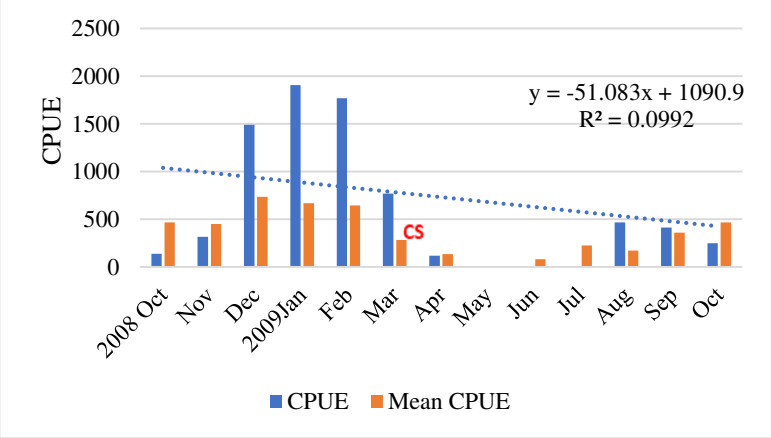

Fig.184.b CPUE of MDTN during Bijli

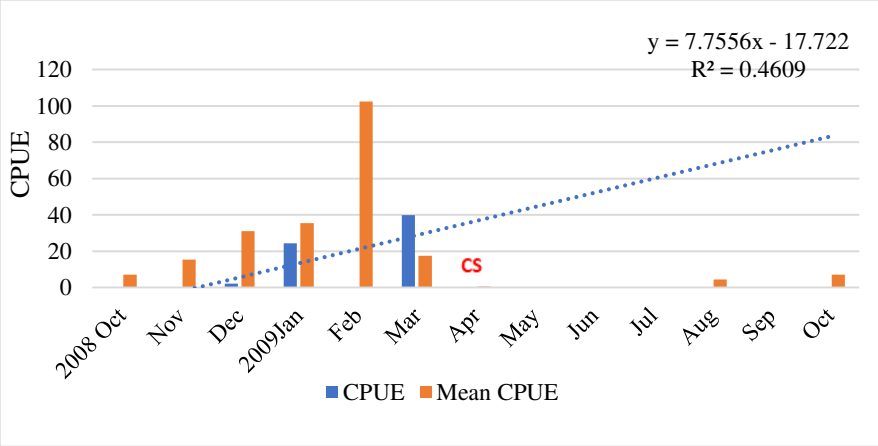

Fig.184c CPUE of MTN during Bijli

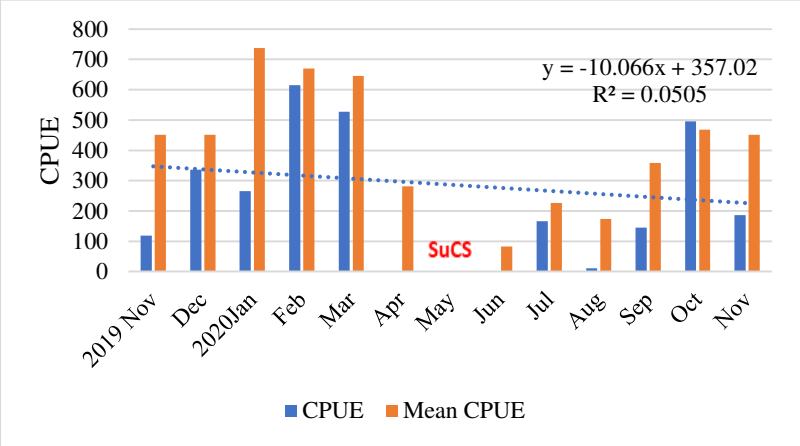

Fig.185a CPUE of MDTN during Amphan

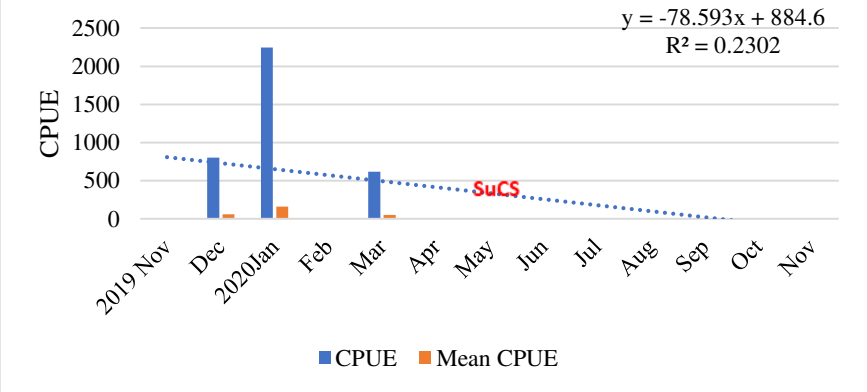

Fig.185b CPUE of MGN during Amphan

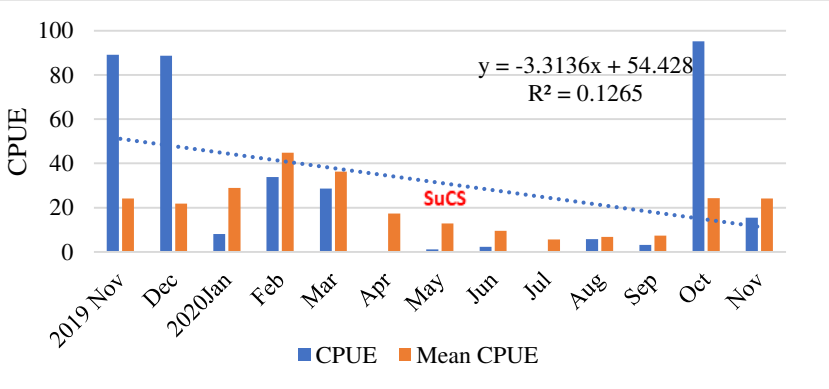

Fig.185c CPUE of OBGN during Amphan

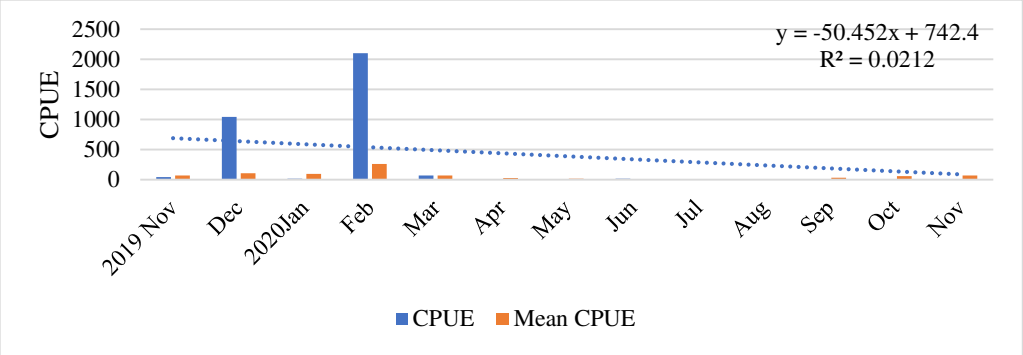

Fig.185b CPUE with OBRS during Amphan

4.11.3 CPUE of *Trichurus lepturus*

The yearly variation of total catch and CPUE of *Trichurus lepturus* during the study period 2007-2020 was given in Fig.186.a and Fig.186b. Both showed a decreasing trend. Out of the twelve cyclones that hit the Odisha coast, Sidr and Rashmi had a positive trend for the CPUE for T.lepturus, whereas the CPUE for Bijli and Viyaru had a negative impact (Fig.187, Fig.188,Fig.189, Fig190). During the Sidr, OBGN, MDTN, and MTN contributed most to the total CPUE. remaining by NM, which showed a negative trend, and some contributed by OBRS, which did not show any trend. OBGN, NM, MDTN contributed more to the CPUE during the cyclone Rashmi, followed by MTN, which showed a negative trend. OBHL and MGN also contributed some but did not show any trend. Bijli showed an overall negative trend for CPUE with MDTN contributing more to CPUE followed by MTN OBGN and NM, but all of these showed a negative trend compared to previous CPUE. MGN, OBRS, OBHL also contributed but did not show any significant trend. MDTN and OBGN contributed to the CPUE during Viyaru but showed a negative trend. A small contribution was made by NM and MTN. The other two species, L.*savala* and T.*ilisha*, also showed more or less similar general trends to these species.

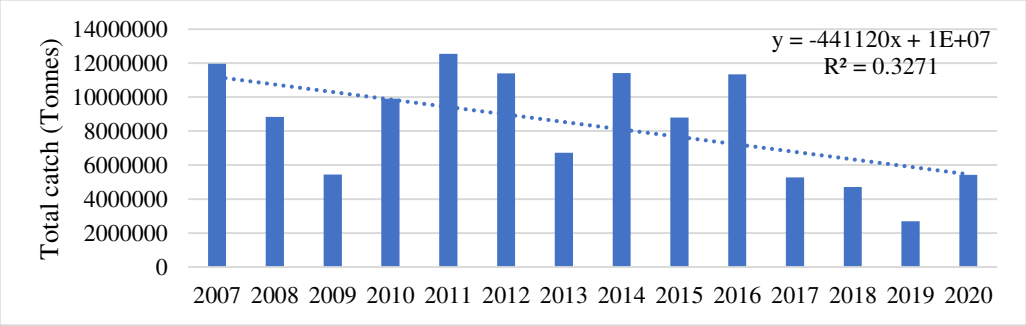

Fig.186 a The catch variation of *Trichurus lepturus*

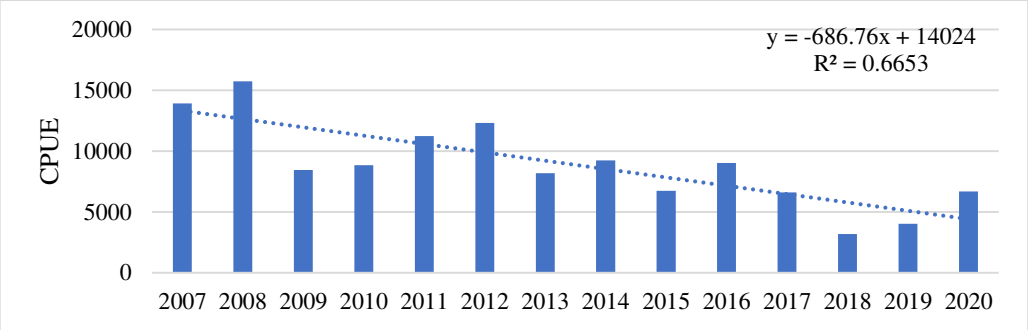

Fig.186 b CPUE of *Trichurus lepturus*

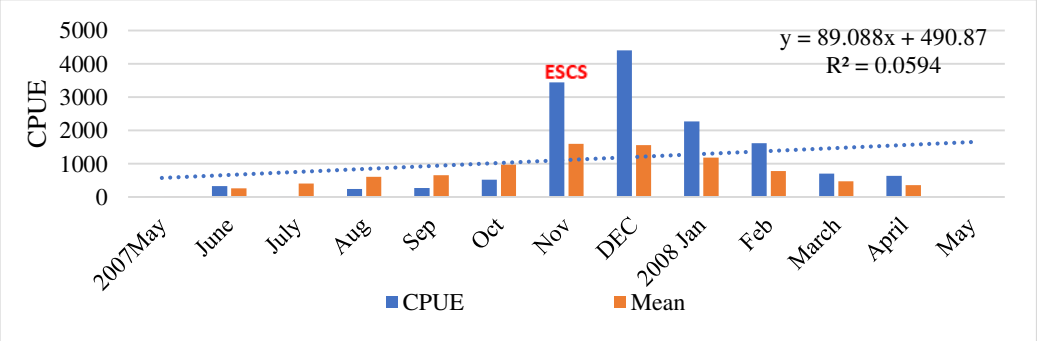

Fig.187 The CPUE variation of the species *Trichurus lepturus* during the cyclone Sidr.

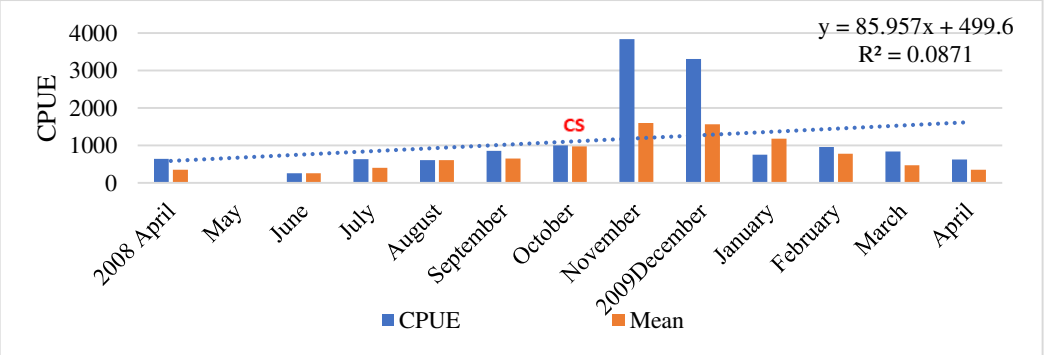

Fig.188 The CPUE variation of the species *Trichurus lepturus* during the cyclone Rashmi

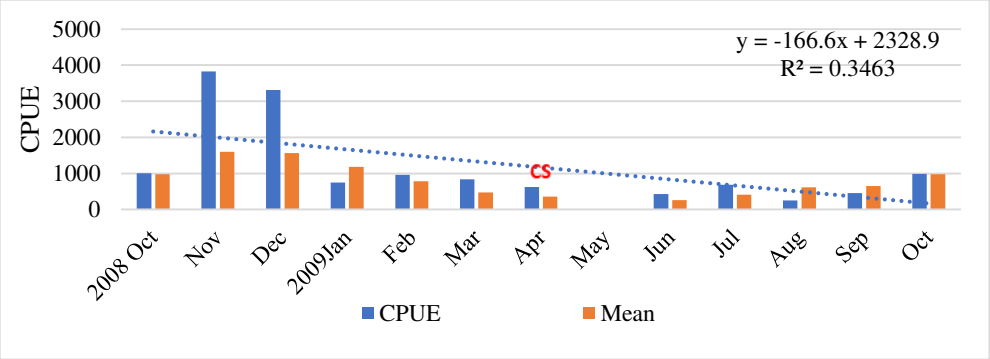

Fig.189 The CPUE variation of the species *Trichurus lepturus* during the cyclone Bijli

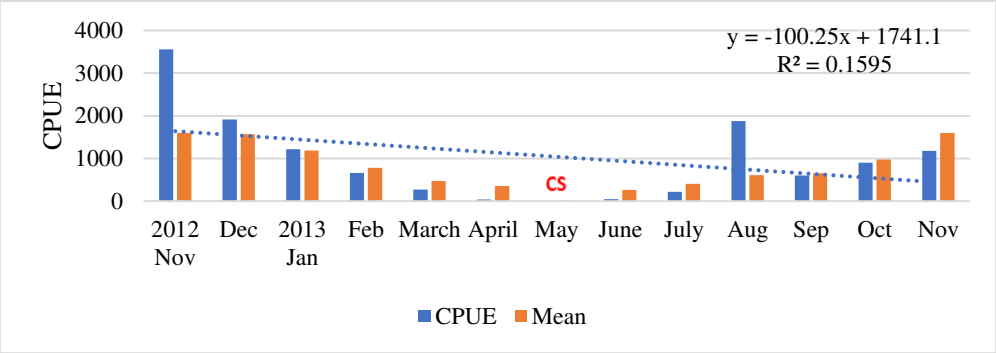

Fig.190 The CPUE variation of the species *Trichurus lepturus* during the cyclone Viyaru

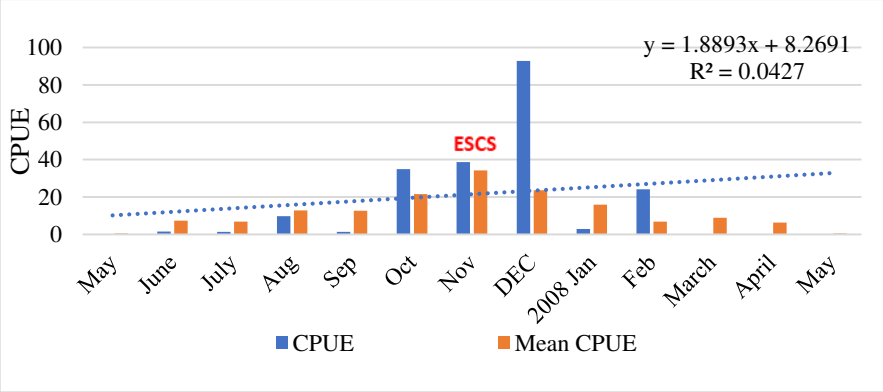

Fig.191a CPUE with OBGN during Sidr

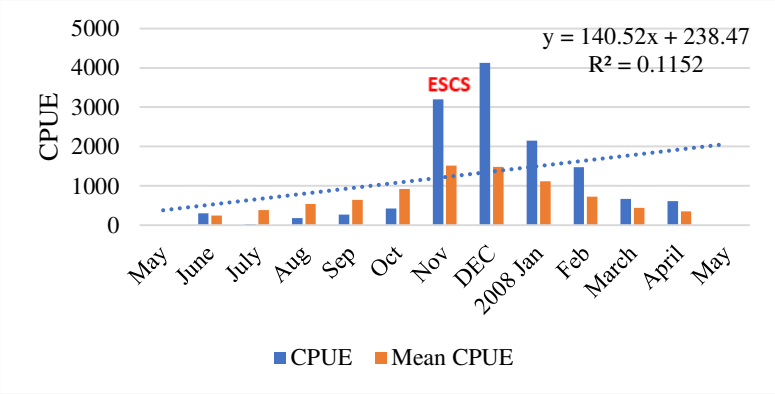

Fig.191b CPUE with MDTN during Sidr

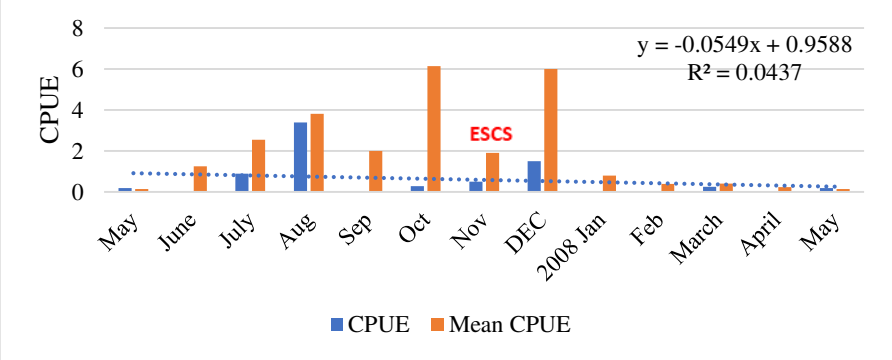

Fig.191c CPUE with NM during Sidr

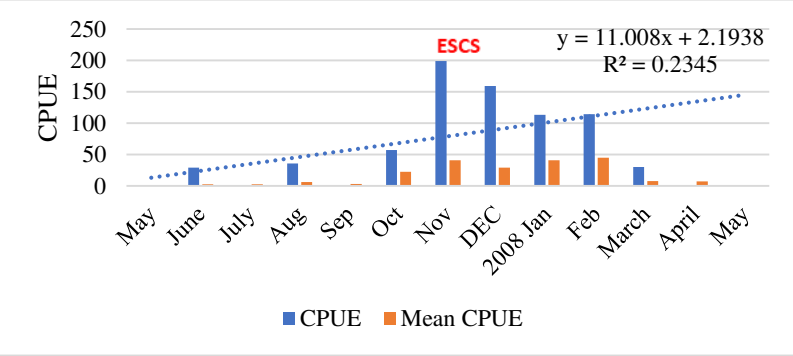

Fig.191d CPUE with MTN during Sidr

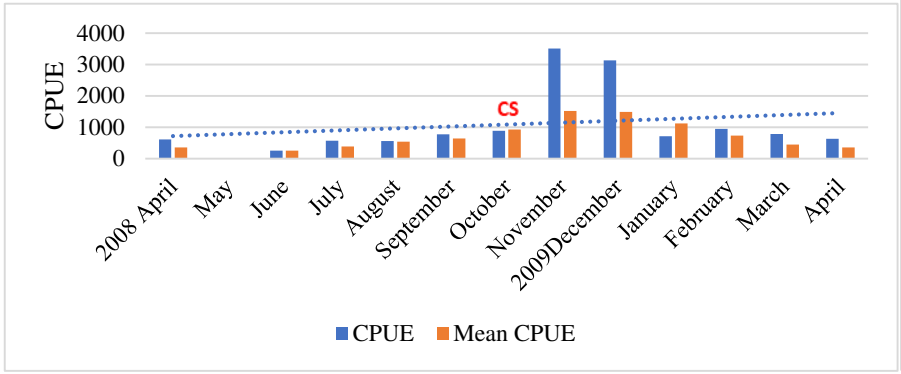

Fig.192a CPUE with MDTN during Rashmi

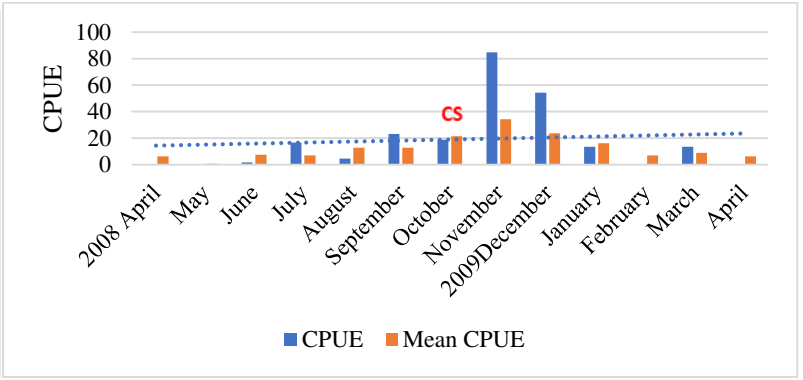

Fig.192b CPUE with OBGN during Rashmi

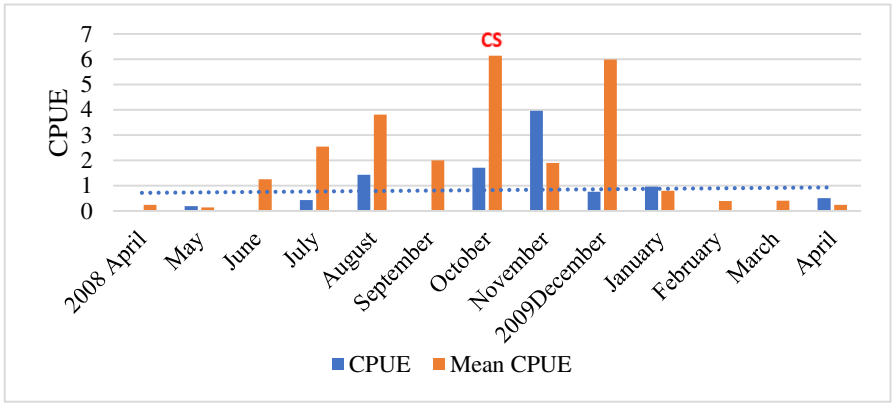

Fig.192c CPUE with NM during Rashmi

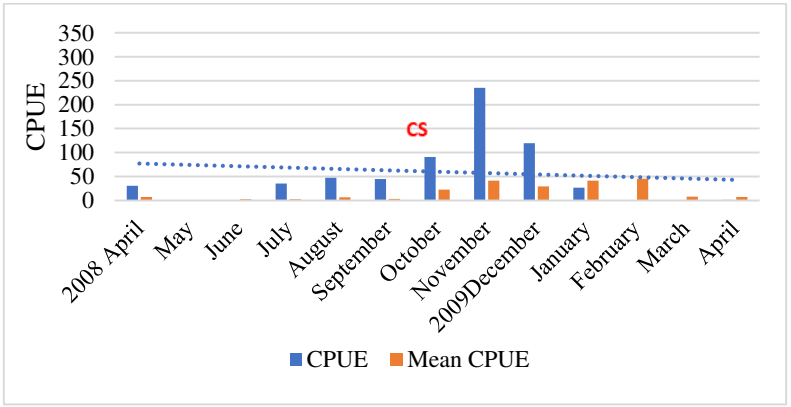

Fig.192d CPUE with MTN during Rashmi

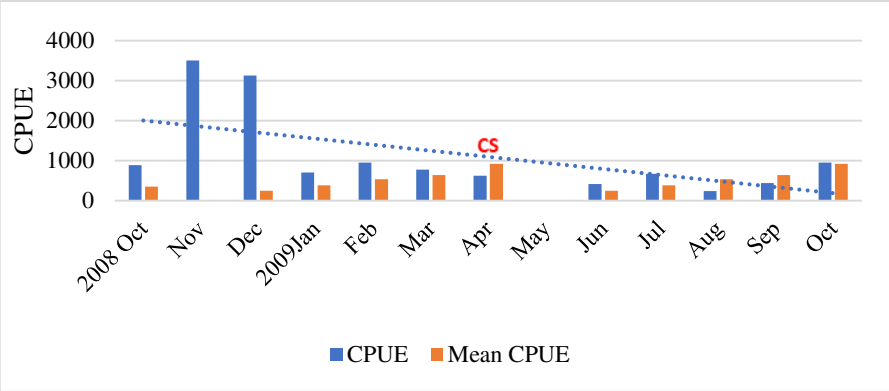

Fig.193a CPUE with MDTN during Bijli

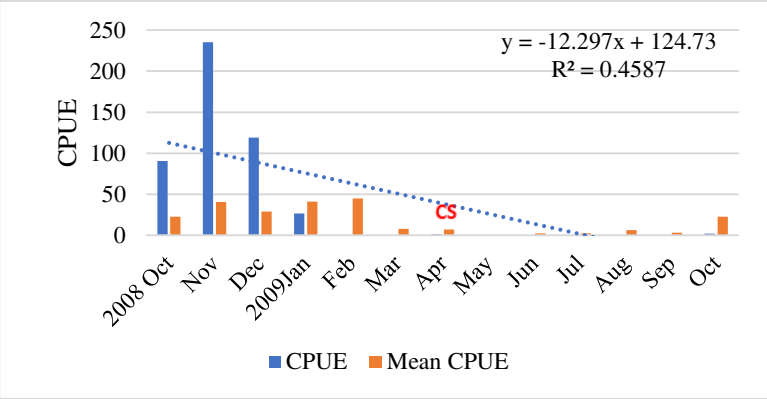

Fig.193b CPUE with MTN during BIJLI

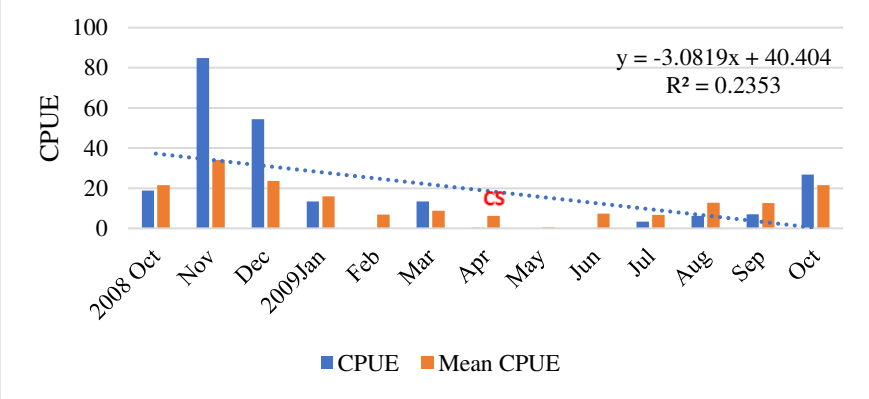

Fig.193a CPUE with OBGN during Bijli

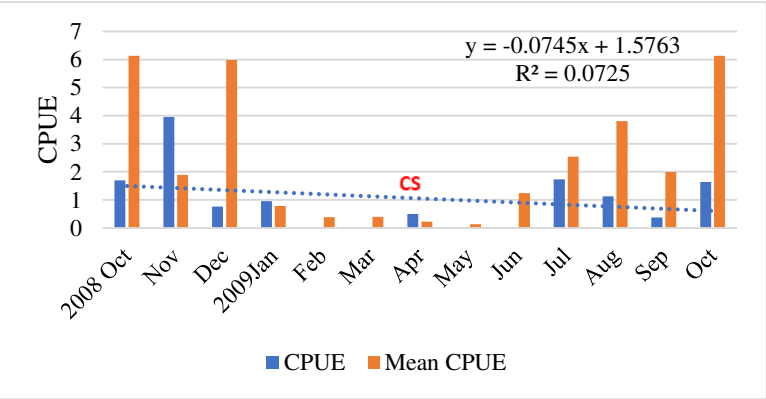

Fig.193b CPUE with NM during BIJLI

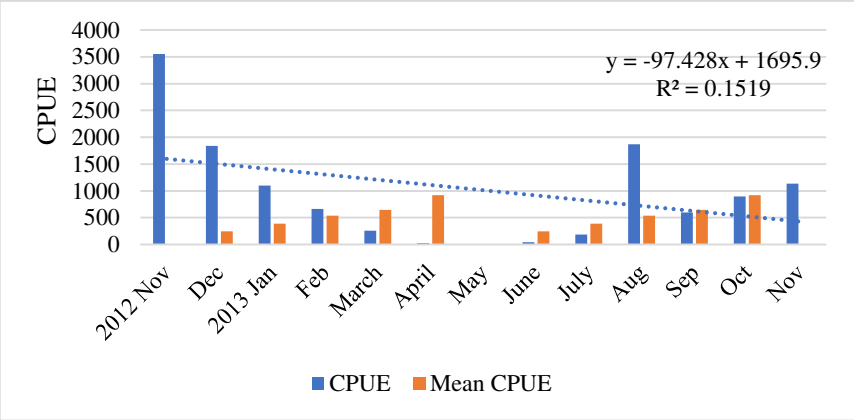

Fig.194a CPUE with MDTN during Viyaru

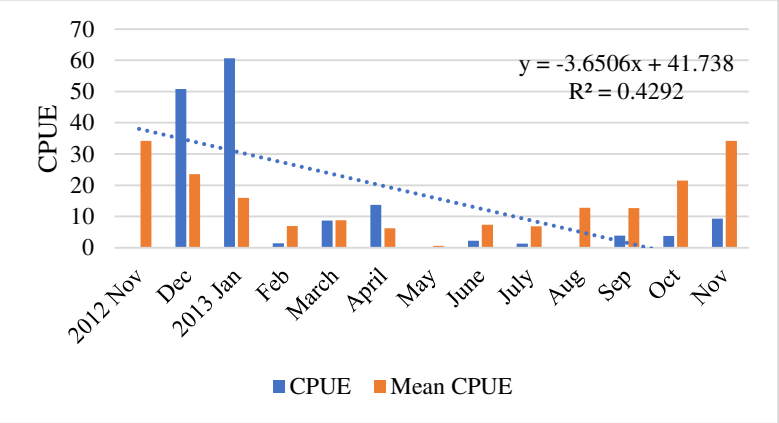

Fig.194b CPUE with OBGN during Viyaru

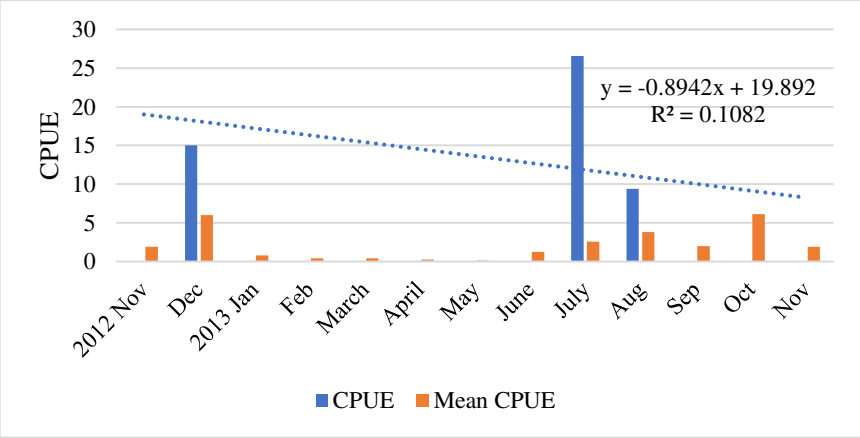

Fig.194c CPUE with NM during Viyaru

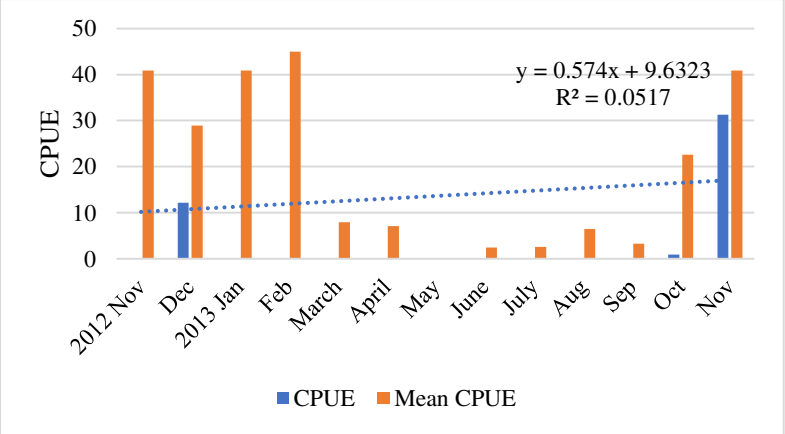

Fig.194d CPUE with MTN during Viyaru

CHAPTER 5

DISCUSSION

A tropical cyclone (TC) is one of the most potentially destructive extreme events, causing severe damage to life and property in the nation (Sebastian *et al*., 2015). Considering the Northern Indian Ocean (NIO), it accounts for 8% of global Tropical Cyclones. More cyclones form in the Bay of Bengal than in the Arabian Sea, and the ratio of their respective frequencies is about 4:1 (Singh *et al.,* 2000). This study focused on the spatio-temporal variation of CDs in NIO. The long-term changes in the spatio-temporal patterns of CDs were analyzed and their impacts on the major marine fish resources of Odisha coast were also assessed.

5.1 Spatial distribution of TC in NIO

The spatial distribution of CDs along the NIO was studied. The annual distribution of CDs indicates that TCs formed throughout the NIO and made landfall along the shores of India, Bangladesh, Myanmar, Sri Lanka, and Oman. Studies made by Hussain *et al*., (2011) point out the impacts of TC on coastal regions of india. He observed that storm surges associated with severe tropical cyclones pose a threat to the majority of the countries surrounding the North Indian Ocean. The study could observe that the location of origin of the majority of CDs produced were between 5° N-20° N latitude. Similar results were reported by Bhardwaj *et al*., (2019) which highlighted the spatial distribution of CS along the NIO region.

Seasonal distribution of the CDs indicates that during the winter, the frequency of CDs is significantly lower, and the majority of them are generated in BOB. During the pre-monsoon season, CDs become more common, and their genesis location shifts northward (Bhardwaj *et al*., (2019). During this season, the majority of CDs were generated between 5 and 15 degrees latitude. This genesis location has shifted north again and the frequency also increased during the monsoon season, with the majority of them forming between 15-20 degrees latitude in both BOB and AS. Cyclogenesis locations have a poleward shift in almost all

global basins (Bishnupriya *et al*.,2019). In the last decade, there has been a high probability of a shift in cyclogenesis location (within 93–100^{o}E), migrating towards the eastern sector in BOB and this shift in cyclogenesis has a relation with SST (Bishnupriya *et al*., 2019). During the post-monsoon season, the frequency of CDs increases dramatically, forming in all regions of the NIO, including BOB and ARB. The entire eastern and western shores are affected by landfall.

The monthly distribution indicates that from January to August, the average genesis location of TCs shifted northward, then southward continuously. The smallest number of CDs could be seen in February and March, while the highest frequency could be seen in October and November followed by April and May. The results reported by Bhardwaj *et al*., (2019) which corroborates this findings includes During two peak TC seasons, a wide range of genesis locations and tracks was observed (pre- and post-monsoon seasons). During the premonsoon season, most TCs tracked northward and made landfall along the coasts of Bangladesh and Myanmar, whereas TCs during the post-monsoon season affected the entire coast of BOB. The monthly spatial pattern of BOB TCs revealed that genesis locations and tracks almost exactly followed the Sun's northward and southward shifting. From January to July, the mean genesis location of TCs shifts northward, then continues to move southward.

5.2 Temporal distribution of TC in NIO

It is clear from this study that there has been little increase in the frequency of CDs in NIO when considering CP and QP, but it is not much significant whereas the area affected by CDs has increased in recent years. This slight increase in the frequency were contributed by cyclonic depressions and not by cyclonic storms. The frequency and area affected by the intense cyclones increased in the NIO during the CP. Webster *et al*., 2005 examined Category 4 – 5 hurricanes (maximum sustained winds (1-minute average) >= 115 knots) for all TC basins over the previous 30 years and discovered that their numbers nearly doubled between a previous (1975 – 1989) and a more recent (1990 – 2004) 15-year period

When analysing the BOB and ARB separately, a similar trend in frequency and intensity was observed for BOB like the NIO, but it could be noted that there was an increase in the frequency and area affected by the CDs of AS. Tropical storm activity in the ARB has a bimodal annual frequency distribution, with peaks during the pre- and post-monsoon seasons. The frequency of intense cyclones were found to be increasing in NIO. During 1979–2015, the ARB experienced an average of 1.7 (0.6 during the pre-monsoon season and 0.9 during the post-monsoon season) tropical storms (lifetime maximum surface wind speed 17.5ms1) per year, accounting for only about 2% of global storm frequency. Several climate models have been used to project future climate, and the results generally indicate that the frequency of weak (intense) storms will decrease (increase) globally in the future (Murakami *et al*., 2017). Murakami et al; used a 60-km-mesh atmospheric model to perform multi physics and multi SST ensemble climate projections under the IPCC A1B scenario14. The results showed that during the post-monsoon season, the mean locations of tropical storms may shift westwards over the North Indian Ocean, resulting in an increased (decreased) frequency of tropical storms over the ARB (Bay of Bengal). As previously discussed, Evan et al; reported that the recent increase in anthropogenic aerosols increased TC intensity over the ARB due to a weakening of vertical wind shear.

During the summer monsoon, which accounts for the greatest number of intense cyclones, the frequency of tropical cyclones in the North Indian Ocean has increased. The rising trend has been caused primarily by a decrease in vertical wind shear. As a result, the future evolution of North Indian Ocean storm activity will be heavily influenced by the warming of the sea surface waters as well as vertical wind shear (Munikrishna., 2009).

Considering the monthly distribution, NIO experiences the most cyclonic disturbances in October-November which is the post-monsoon season followed by pre-monsoon and monsoon. The least in January-February and March which is the winter Season. Bhardwaj *et al.,* 2019 reported that the maximum number of TCs was formed during the post-monsoon (about 64%) followed by pre-monsoon (about

21%), monsoon (about 11%), and winter (about 4%) season in BOB. In ARB, maximum CDs formation take place during the post-monsoon followed by Monsoon and Pre-Monsoon. Previous studies (Singh *et al*., 2001; Singh 2007; Srivastav *et al*., 2000) have found an increase in the frequency of intense TCs in NIO during high TC activity months, namely November and May, using IMD's existing dataset. Cyclone and severe cyclone frequencies exhibit bimodal behaviour, peaking in May and November. Total cyclonic disturbances are most common in October, followed by November, August, and September (Tyagi *et al*., 2009).

When compared to CP, the frequency of CDs over NIO was decreasing during QP. Considering the BOB and ARB, the BOB exhibits a similar trend to the NIO, but the frequency of CDs in ARB is increasing in QP rather than CP, with a 20% increase in total cyclonic disturbances, including a 20% increase in Cyclonic Depressions and a 34% increase in Cyclonic Storms.

5.3 Variation of TC energy metrics in NIO

When compared to ARB, higher VF is visible in BOB for cyclonic storms in both the Pre-Monsoon and Post-Monsoon seasons. It may be due to the fact that the average VF mainly depends on the number, duration and intensity of CDs and TCs and these are higher over the BOB than over the ARB (Mohapatra *et al*., 2016). VF is significantly higher in both BOB and ARB during the Post-Monsoon season, which could be attributed to the increased frequency and intensity of cyclones at that time. Mohapatra *et al*., 2016 showed that the VF of Cyclonic depressions and CS is significantly higher during the post monsoon season than during the pre-monsoon and monsoon seasons over the BOB and NIO due to higher frequency, duration, and average intensity of TCs during the post monsoon season. He also showed that there is no statistically significant difference in mean VFs across seasons for both CDs and TCs. Taking the VF over QP into account, there is an increase in the annual VF over NIO, BOB, and AS. The frequency and average intensity of TC increased during the QP. It can be understood from the result that the overall changes in VF for total cyclonic disturbances in NIO over the entire

study period revealed an increase in QM rather than CM, indicating an overall increase in VF of cyclonic storms. The CS and total cyclonic disturbances of AS have shown a positive trend, with QM having a higher VF than CM. More or less similar trend is observed for both ACE and PDI. In comparison to the BOB and ARB, the BOB has a higher ACE for cyclonic storms in the Post Monsoon season than in the Monsoon season. The average intensity could be a factor in the increased ACE value in BOB. During the monsoon season, the ACE of tropical cyclones is higher in AS than in BOB (Mohapatra *et al*., 2016). In NIO, The PDI of cyclonic storms has been steadily rising in recent years. There is an increase in the QM than CM, indicating an overall increase in the PDI of cyclonic storms in recent years. The significant increase in power dissipation over the last 30 years or so could be attributed to storms becoming more intense on average and/or surviving at high intensity for longer periods of time. The overall increase in net power dissipation is being driven by the duration and peak intensity trends (Emmanuel, 2005).

The study conducted by Bishnupriya *et al.*, (2016) reported a significant increase in PDI and ACE in 2005-2015 when compared to the 1980s where in the last four decades, the decadal variability in PDI has increased nearly sixfold.

Some studies linked this increase in energy metrics to climate change too. Increasing SST is another factor which contributed for the rise. In theory, for every 1℃ increase in tropical ocean temperature, peak wind speed should increase by about 5%. Given the observed increase of only about 0.5 C, peak winds should have increased by only 2–3 percent, and power dissipation by 6–9 percent. When combined with the expected increase in storm lifetime, a total increase in PDI of around 8–12 percent would be expected, falling far short of the observed change (Emmanuel, 2005). Contradiction to this observation, Maneesha *et al*., (2011) find out that SST alone is not a driving parameter for the climatic variability of cyclones in NIO.

While evaluating the relationship of energy metrics with the frequency intensity and duration of cyclones, the results showed a higher dependence on frequency and duration and less dependence on intensity. Murakami *et al.,* (2014)

demonstrated that a positive increase in TC genesis frequency is the primary contributor to the overall increase in ACE and PDI. Other factors, such as track length and intensity, appear to be minor.

The VF of Cyclonic depressions and Cyclonic storms in BOB showed a high dependence on the Frequency and Duration of D and CS that formed during the CP whereas the intensity does not show much dependence. Taking the QP into account, the annual ACE of CS in NIO is higher than in Cyclonic Depressions. When comparing ARB and BOB, BOB has a slightly higher ACE, implying that ARB's ACE has been increasing in recent years. Greater intra-seasonal variation can be seen in both BOB and AS equally. Mohapatra et al., (2019) found that when VF, ACE, and PDI are compared, the VF and PDI per year are more dependent on intensity, whereas the ACE per year is more but equally dependent on intensity and duration of TC over the NIO. All three annual metrics discussed above are relatively less dependent on the frequency of TC genesis over the NIO. The overall changes in ACE for D, CS, and total cyclonic disturbances in NIO over the entire study period show that D and DD have a significant negative trend, whereas ACE of cyclonic storms has a significant increasing trend in recent periods.

Wind, rain, and storm surge caused by tropical cyclones cause significant damage to life and property in countries bordering the North Indian Ocean, particularly the Bay of Bengal (Smitha *et al.,* 2005). The impact of increase in this energy metrics implies the increase in the associated phenomenas like rainfall, storm surges etc. The destruction along with the tropical cyclones therefore increases. The tropical cyclones Sidr (November 2007) and Aila (May 2009) in Bangladesh, as well as Cyclone Nargis (May 2008) in Myanmar's Irrawaddy delta, demonstrated how devastating storm surges can be on coastal areas. All of these cyclonic events killed people and harmed the livelihoods, socioeconomic systems, and environments of Bangladeshi coastal communities (Munshi *et al*; 2014). On September 30, 2007, a northeast–southwest oriented trough occurred from Andhra to the south Orissa coast, which intensified into a low pressure system (1002 mb)

and was centred over the Visakhapatnam region, causing heavy rainfall during the 4–5th of October 2007 (Maneesha *et al*., 2011).

5.4 Morphology of ocean and cyclogenesis

It was assumed that the ocean floor was completely flat before scientists invented sonar. In fact, the ocean floor contains the tallest mountains and deepest canyons, which are far taller and deeper than any landform found on the continents. The same tectonic forces that form geographical features such as volcanoes and mountains on land also form similar features at the ocean's bottom. In this study, we observed that the location of cyclogenesis has some association with the morphological feature of ocean floor and it was discovered that 87% CDs in winter, 56% CDs in pre-Monsoon, 42% CDs during monsoon and 67% CDs during post-monsoon are formed over fan region followed by the shelf with 5% during pre-monsoon, 38% during monsoon and 8% in post-monsoon.

Fans are characterised as "a relatively smooth, fan-like depositional feature that typically slopes away from the outer termination of a canyon or canyon system. Fans are located offshore from the base of the continental slope and overlap and form part of the continental rise and shelf is a zone adjacent to a continent (or around an island) that extends from the low water line to a depth where there is usually a significant increase in slope towards oceanic depths (Harris *et al*;2014).

This could be due to the contiguous and vast extent of Fan area providing the favourable conditions for cyclogenesis and the uniform water mass over the Fan area could be a factor to this. Literature dealing with this aspect of cyclogenesis is nil indicating that this is a topic with great potential for future research.

5.5 Impact of TC on major resources of Odisha coast

5.5a Impact of TCs on catch and CPUE

The impact of CDs along Odisha coast including the districts Jagatsingpur, Balasore, Bhadrak, Kendrapara, Puri and Ganjam were studied. The analysis indicated that, the impact on total catch and effort varied between the cyclone

affected districts. During the CDs, there were loss in fishing days due to the rough sea conditions as well as catch and effort declined due to other land based destruction and damages.

The northern districts of Odisha State, such as Bhadrak and Balasore, were the most vulnerable, with storm tides exceeding 7.0 m. The Ganjam district has the lowest vulnerability, while districts in the central region such as Puri, Jagatsinghpur, and parts of Kendrapara experienced storm tides ranging from 2.8 to 4.0 m. The cross-shore inundation clearly shows that the districts of Jagatsinghpur, Kendrapara, and Bhadrak are extremely vulnerable to storm surge inundation during cyclone landfall. The maximum cross-shore extent of inundation in Kendrapara district is approximately 65 km for a maximum sustained wind speed of 140 knots (during landfall). The combined effect of storm tide and inundation clearly shows that the districts of Kendrapara and Bhadrak are among the most vulnerable along the Odisha coast. The coastal belts of Jagatsinghpur, Kendrapara, Bhadrak, and Balasore are low-lying areas that are not only vulnerable to coastal inundation, but also to river flooding from major riverine systems.

5.5b Resource abundance and assemblage

Roanu, Amphan, and Viyaru were the three cyclones that contributed the most to the overall average dissimilarity of the twelve cyclones that hit the Odisha coast between 2007 and 2020. The CPUE of different gears operated were found to be impacted in different ways in the analysis, indicating that resource assemblages distant from the coastline also underwent changes after the cyclones.

The OAD is higher during the cyclonic months, indicating that the cyclone has impacts on the species assemblages, either directly or indirectly. The OAD decreased over the next few months, indicating that it is returning to normal. So, the study could infer that the cyclones affects the species distribution in turn affecting the overall dissimilarity of the catches. Furthermore, there was a lot of variation in the species assemblage depending on the gears. An increasing trend in the ocean chlorophyll a content was also observed. The availability of nutrients

limits the amount of chlorophyll in the upper layer of tropical oceans. As a result, oceanic processes that can bring nutrients into the euphotic zone are critical. Nutrient injection into the surface layer with near-zero nutrient concentration results in strong phytoplankton blooms with 5–8 mg m23 surface chlorophyll-a concentrations (Smitha *et al.,* 2005). Satellite chlorophyll observations (Subrahmanyam et al., 2002) has discovered that phytoplankton blooms occurred in response to an Arabian Sea cyclone in May 2001. The strong winds that accompany cyclones mix water to deeper depths and thus induct nutrients into the mixed layer, resulting in high chl a during the clear sky period that usually follows a cyclone (Vinayachandran *et al*., 2003).

Similarly, cyclone Sidr increased the Chl a to the right of the cyclone track by more than four times in the central Bay of Bengal after the cyclone passed (Maneesha *et al*., 2011). Strong winds associated with cyclones churn up the upper ocean, resulting in the vertical entrainment of cold and nutrient-rich waters to the surface along the cyclonic track. Increased nutrient input has been linked to increased phytoplankton biomass in the presence of cyclones/supercyclones (Sarma *et al*., 2019). Madhu *et al.,* (2002) also noted enhanced nutrient concentrations (nitrate by 1 μM) and the consequent increase in primary production (by 21 to 955 mgC m−2 d−1) in the south western Bay of Bengal by the super cyclone of 1999. For about two weeks, the nutrients enhanced by the episodic heavy rainfall event supports the phytoplankton.

Several other studies indicated that there was a non-increase in chl a concentrations after the cyclones. Study conducted by Sarma *et al*., (2019) indicated that cyclones suppressed nutrient input through vertical mixing in the coastal Bay of Bengal due to strong stratification and convergence, and increased TSM load, resulting in a decrease in phytoplankton biomass and production. It was also discovered that fishery catch decreased significantly after the VSCS Hudhud hit the Visakhapatnam coast due to low plankton concentration. Not only the intensity of the cyclone, but also the soil characteristics of the zone where the cyclone hits, influence the biological response to the cyclone in the coastal region. According to

their findings, the VSCS Hudhud did not increase primary production, unlike other cyclones that formed in the Bay of Bengal, because it crossed a major city, as opposed to other cyclones that crossed fertile lands (Sarma *et al*., 2019).

The CPUE variation in ecocnomically important five species such as *Sardinella fimbriata, Rastrelliger kanagurta, Trichurus lepturus, Lepuracanthus savala and Tenulosa ilisha* in the Odisha coast were studied. A general positive trend was observed for all species, with CPUE increasing during cyclonic events formed in October and November, whereas cyclones formed in April and May showed a negative trend for CPUE. This means there is a both positive and negative effect on the fisheries resources due to the formation of tropical cyclones. Positive effects may due to the increase in fish abundance due to phytoplankton blooms which serves as food for most of the pelagic fish species. The CPUE variation of the economically important major five species on the Orissa coast was also investigated. A general trend was observed for all species, with CPUE increasing during cyclonic events formed in October and November, whereas cyclones formed in April and May showed a negative trend for CPUE. This was in tune with the trends showed for landing of the studied fish resources.

Stronger storms are found to amplify disturbance regimes, affecting coastal and shallow fish habitats, access to fish stocks, and, as a result, fishing effort. More extreme rainfall patterns will increase variability in terrestrial nutrient enrichment of marine ecosystems, influencing coastal productivity as well as the distribution and abundance of fish stocks. (Johnson *et al*., 2010).

CHAPTER 6

SUMMARY

The primary interest of the project titled Spatio-temporal variation of TCs in NIO and its impacts on major marine fish resources is an attempt to investigate the spatial and temporal variations of tropical cyclone (TC) activity in the Northern Indian Ocean (NIO) and understanding how storms interact with marine fishery sector. The information generated from the study can evolve into adaptive action and help to reduce the vulnerability of those dependent on fisheries for their livelihood. The study found significant impacts on fish resources, and the environment, indicating the need for increased preparedness among coastal communities. The details are summarised below.

Spatial distribution of CDs

The spatial distribution of CDs along the NIO was studied. The majority of CDs were produced between 5° N-20° N latitude. Seasonal distribution indicates that during the winter, the frequency of CDs is significantly lower, and the majority of them were generated in BOB. During the pre-monsoon season, CDs were more common, and their genesis location shifted northward .This genesis location had shifted north again, and the frequency had also increased again during the monsoon season. During the post-monsoon season, the frequency of CD increased dramatically, forming in all regions of the NIO, including BOB and ARB. The entire eastern and western shores are affected by landfall. The monthly distribution indicates that from January to August, the average genesis location of TCs shifted northward, then southward continuously. The smallest number of CDs could be seen in February and March, while the highest frequency could be seen in October and November followed by April and May

Temporal distribution

The frequency of CDs in NIO does not show much increase. When analysing the BOB and AS separately, a similar trend for frequency and intensity was observed for BOB like the NIO, but it is surprising to note that there was an increase

in the frequency and area affected due to the CDs of ARB. The energy metrics of NIO such as VF, ACE and PDI showed an increasing trend in NIO. These enery metrices were more dependent on frequency and duration than average intensity.

With regard to the ocean floor morphology, the majority of CDs occurred in the fan region in all seasons except the monsoon season in which the cyclone was formed in shelf and fan region equally.

Impact on fisheries sector

Analysis of impact of TCs in the five districts of Odisha (Balasore, Bhadrak, Kendrapara, Jagatsingpur, Puri and Ganjam) indicated that the impact on catch and catch per unit effort (CPUE) varied between districts and gears. Higher catch was obtained at Jagatsinghpur whereas the remaining districts showed more or less similar catch with Kendrapara being the least. Almost all the district show least catch in April and May. CPUE is also higher for Jagatsinghpur than other districts followed by Balasore, Puri, Bhadrak. CPUE showed a lowest value in May for all districts in Odisha. The least CPUE was reported from Kendrapara and Puri.

Species dissimilarity and resource abundance

Because the Odisha coast witnessed the greatest number of cylones along the Indian coast, it was chosen for this investigation to determine the impacts of cyclones on marine fish resources. The 12 cyclones that hit the Odisha coast during the study period were examined. The three cyclones that contributed the most to the overall average dissimilarity among the twelve cyclones that hit the Odisha coast between 2007 and 2020 were Roanu, Amphan, and Viyaru. The OAD after the cyclonic month for the three cyclones were found to be decreasing. The OAD was higher during the cyclonic months, indicating that TC formation had an impact on species dissimilarity. The OAD was found to be decreasing in the next few months, indicating that it was returning to normal and it impacts were not long term.

While evaluating the chl a concentration in response to these three cyclones, they showed a slight positive trend, indicating that the chl a concentration increased in response to the formation of TCs.

The CPUE variation of the economically important major five species including *Sardinella fimbriata, Rastrelliger kanagurta, Trichurus lepturus, Lepuracanthus savala* and *Tenulosa ilisha* on the Odisha coast was investigated. A general trend was observed for all species, with CPUE increasing during cyclonic events formed in October and November, whereas cyclones formed in April and May showed a negative trend for CPUE.

General conclusion

The study indicates that the occurrence of CDs in NIO are increasing with a major increase in higher frequency and intensity for intense cyclones. Comparing the ARB and BOB, more occurrence of CDs is evident for BOB than ARB, but the analysis during the Climatological Period indicates that the number and intensity of CDs in ARB are increasing. The relation with morphology of oceanic basin indicates occurrence of most of the cyclones in Fan region may be due to the vast extent of Fan area providing the favourable conditions for cyclogenesis.

The relationship between the occurrence of CDs and its positive and negative impacts with the fisheries sector was studied. The environmental changes which is the changes in Chl a concentration was brought through this study. However this extreme event have a high impact on resources and also the community, infrastructure which clearly indicates a need for adaptive action to reduce the impact and increase the resilience capacity of the fishers.

REFERENCES

Adriaan, D. R., Myron, P., Georg, H., Engelhard, C.2009.Resolving the effect of climate change on fish populations.*J.Mar.Sci*.66(7):1570-1583.

Bardwaj, P., Singh, O.2019. Climatological characteristics of Bay of Bengal tropical cyclones: 1972–2017.*Theor.Appl.Climatol.*139(0):615-629.

Bishnupriya, S., Prasad, K. B.2016. Assessment on historical cyclone tracks in the Bay of Bengal, east coast of India.*Int. J. Climatol*.36(0): 95–109.

Bishnupriya, S., Prasad, K. B.2018. Multi-hazard risk assessment of coastal vulnerability from tropical cyclones A GIS based approach for the Odisha coast.*J.Environ.Manage*.206 (0):1166-1178.

CMFRI Annual Report 2018-2019. http://210.212.232.211:8080/jspui/flipdocs/267/mobile/index.html#p=1

Das, Y.2018. Parametric modeling of tropical cyclone wind fields in India. *Nat Hazards.* 93(0), 1049–1084 . https://doi.org/10.1007/s11069-018-3340-x

Delesalle, B., Pichon, M., Frankignoulle, M., Gattuso, J. P.1993. Effects of a cyclone on coral reef phytoplankton biomass, primary production and composition (Moorea Island, French Polynesia).*J.Plankton Res*.15(12): 1413–1423.

Demestre, M., Sanchez, P., Abello, P.2000. Demersal fish assemblages and habitat characteristics on the continental shelf and upper slope of the north-western Mediterranean.*J.Mar.Biolog*.*80*(6):pp.981-988.

Dutta, S., Lanvin, B., Paua, F.2004. The global information technology report 2003-2004: Towards an equitable information society. Oxford University Press, USA. p.290.

Emmanuel, K.2005.Increasing destructiveness of tropical cyclones over the past 30 years. *Nat*. 436(0).doi:10.1038/nature03906

Eric, K. W., Johnny, C. L. 2011.Interannual variations of tropical cyclone activity over the north Indian Ocean.*Int.J.climatol*.32(6) :819-830.

Evan, A. T., Camargo, S. J.2011. A climatology of Arabian Sea cyclonic storms. *J. Clim*. 24(0):140–158.

Flugel, H.1972. Pressure-animals. *Mar. Ecol*. 18(1), pp.1407-1450.

Food and Agriculture Organisation (FAO). 2018. Impact of disasters and crises on agriculture and food security, 2017. Rome, p.143.

Friedrich, A. S., Julian, P.M.2001.The monsoon circulation of the Indian Ocean.*Prog. Oceanogr.*51(1):1-123.

Fritz, E.S.1974. Total diet comparison in fishes by Spearman rank correlation coefficients. *Copeia*. 20(0):210-214.

Furnas, M., Mitchell, A., Skuza, M., Brodie,J.2005. In the other 90%: phytoplankton responses to enhanced nutrient availability in the Great Barrier Reef Lagoon. 51(1-4): 253–265. doi:10.1016/j.marpolbul.2004.11.010

George, G., Jayasankar, J., Shah, P., Joseph, T., Raj, M. S., Shafeeque, M., Platt, T., Sathyendranath, S.2019. How Oceanography Influences Fishery Biology? - A Case of Distribution Differences in Carnivorous and Planktivorous Fishes along the Coastal Waters of Eastern Arabian Sea. ICAR-CMFRI, pp. 319-352.

Global Climate Risk Index 2020

Gray, W. M.1968. Global View of the Origin of Tropical Disturbances and Storms. *Monthly Weather Review*, 96(10):669-700.

Harris, P.T.2014. Geomorphology of the oceans, Marine Geology, http://dx.doi.org/10.1016/ j.margeo.2014.01.01

Holland, G.J., Belanger, J.I., Fritz, A.2010. A Revised Model for Radial Profiles of Hurricane Winds. 138(12):4393-4401. https://doi.org/10.1175/2010MWR3317.1

Hobday, A. J., Poloczanska, E. S., Matear, R. J.2008.Implications of climate change for Australian fisheries and aquaculture: A preliminary assessment. Report to the Department of Climate Change, Canberra.

Hussain, M. A., Abbas, S., Ansari, M. R. K.2011.Persistency Analysis of Cyclone History in Arabian Sea. *The Nucleus.* 48(4) :273-277.

Jenny, L. E., Atallah, E. H.2010. Environmental impacts on tropical cyclone structure and intensity change. https://hal.archives-ouvertes.fr/hal-00962278

Johnson, J. E., Welch, D. J.2010. Marine Fisheries Management in a Changing Climate: A Review of Vulnerability and Future Options. *Rev. Fish. Sci.*18(1):106–124.

Knutson, T. R., Mcbride, J. I., chan, J., Emanuel, K., Holland, K., landsea, C., held, I., Kossin, J. P., Srivastava, A. K., Sugi, M. 2010.Tropical cyclones and climate change.*Nat.Geosci*.113(0):157-163.

Krishnan, R. J., Sanjay, C. G.2020. Assessment of Climate Change over the Indian Region, A Report of the Ministry of Earth Sciences (MoES), Government of India.

Leitao, F., Maharaj, R. R., Vieira, V. M. N. C. S., Teodosio, A., Cheung, W. W. L. 2018.The effect of regional sea surface temperature rise on fisheries along the Portuguese Iberian Atlantic coast. *Aquat.Conserv.: Mar.Freshw.Ecosyst.* 28(6):1351–1359.

Madhu, N. V., Maheswaran, P. A., Jyothibabu, R., Sunil V. R. V., Balasubramanian, T., Gopalkrishnan, T., Nair, K. K. C.2002.Enhanced biological production off Chennai triggered by October 1999 super cyclone (Orissa); *Curr. Sci*. 82(0).1472–1479.

Maneesha, S., Manasa, R. B.2015. Impact of SST on Tropical Cyclones in North Indian Ocean. *Procedia.Eng*.1116(0):1072-1077.

Maneesha, K., Sarma, V. V. S. S., Reddy, N. P. C., Sadhuram, Y., Murty, T. V. R., Kumar, M. D.2011.Mesoscale atmospheric events promote phytoplankton blooms in the coastal Bay of Bengal. *J. Earth Syst. Sci.* 120; 1–10.

McAdie, C. 2007. Tropical Cyclone Climatology. National Hurricane Center.

McKinnon, A. D., Meekan, M. G., Carleton, J. H., Furnas, M. J., Skirving, D. W. 2003. Rapid changes in shelf waters and pelagic communities on the southern Northwest Shelf, Australia, following a tropical cyclone. *Cont.Shelf.Res*. 23(1):93-111.

Michael, G. S., Nampoothiri G.1993. The western boundary current of the seasonal subtropical gyre in the Bay of Bengal. https://doi.org/10.1029/92JC02070.

Mohapatra, M., Vijay Kumar, V. 2017. Interannual variation of tropical cyclone energy metrics over North Indian Ocean. *Clim Dyn.* 48(0), 1431–1445.

Munikrishna, K. 2009. Intensifying tropical cyclones over the North Indian Ocean during summer monsoon—Global warming. *Glob.Planet Change*.

Munshi, K. R., Thomas, W. S.2014. The Perception and Impact of Natural Hazards on Fishing Communities of Kutubdia Island, Bangladesh.*Geographical Review*.104(1), 71-86, DOI: 10.1111/j.1931-0846.2014.12005.x

Murakami, H., Gabriel, A., Vecchi., Underwood, S.2017.Increasing frequency of extremely severe cyclonic storms over the Arabian Sea. *Nat.Clim.Change*.7(0):885–889.

Nayak, S. R., Sarangi, R. K., Rajawat, A. S.2001. Application of IRS-P4 OCM data to study the impact of cyclone on coastal environment of Orissa. *Curr.Sci*. 80(0):1208–1212.

Naylor, E. Atkinson, R. J.1972. Pressure and the rhythmic behaviour of inshore marine animals. *In Symposia of the Society for Experimental Biology* .26(0), pp.395-415.

National Fisheries Development Board (NFDB), 2019. About Indian Fisheries, Department of Fisheries, Ministry of Fisheries, Animal Husbandry & Dairying, Gov. of India.: http://nfdb.gov.in/about-indian-fisheries.htm

Poiner, I. C., Conacher, N., Loneragan, R., Kenyon., Somers, I. F.1993.Effects of cyclones on seagrass communities and penaeid prawn stocks of the Gulf of Carpentaria. Final Report, FRDC Projects 87/16 and 91/45. CSIRO Marine Laboratories. Cleveland, OH: CSIRO Division of Fisheries

Prasannakumar, S. R., Roshin, P., Jayunarvekar, P. K.2009. Response of the Arabian Sea to global warming and associated regional climate shift .*Mar.Environ. Res*.68(5):217-222.

Rana, A. S., Zaman, Q., Afzal, M., Haroon, M. A.2014.Characteristics of sea surface temperature of the Arabian Sea Coast of Pakistan and impact of tropical cyclones on SST. *Pak. J.Meteorol*. 11(21).

Royer, J.F., Chauvin, F., Timbal, B. 1998. A Gcm Study of the Impact of Greenhouse Gas Increase on the Frequency of Occurrence of Tropical Cyclones. *Climatic Change.* 38(0):307-343.

Richards., Laura, J., Schnute, J. T.1992. Statistical Models for Estimating CPUE from Catch and Effort Data. *Can. J. Fish. Aquat.* 49(7);1315–1327.

Riddle, M. J.1988.Cyclone and bioturbation effects on sediments from coral reef lagoons. *Estua. Coast. Shelf Sci*.27(6):687-695.

Sainsbury, N. C., Genner, M. J., Saville, G. R.2018. Changing storminess and global capture fisheries. *Nature. Clim. Change.*8(0):655–659.

Sarma, V. V. S. S., Srinivas, T. N. R., Kumari, V. R., Prasad, M. H. K., Dalabehera, H. B.2019. Suppressed biological production in the coastal waters off Visakhapatnam, India under the impact of the very severe cyclonic storm Hudhud. *J. Earth Syst. Sci*.128:142.

Sebastian, M., Behera M., R. 2015. Impact of SST on Tropical Cyclones in North Indian Ocean. *Procedia Eng*. 116(0): 1072-1077.

Shetye, S. R., Gouveia, A. D., Shenoi, S. S. C., Sundar, D., Michael, G. S., Nampoothiri, G. 1993. The western boundary current of the seasonal subtropical gyre in the Bay of Bengal. *J. of Geophys. Res.* 98(C1), 945.

Singh, O. P. 2010. Recent Trends in Tropical Cyclone Activity in the North Indian Ocean. *Indian Ocean Tropical Cyclones and Climate Change*: 51-54

Singh, O.P., Khan T. M. A., Rahman, S.2001.Has the frequency of intense tropical cyclones increased in the North Indian Ocean. *Curr Sci*. 80:575–580.

Singh, O.P. 2007. Long-term trends in the frequency of severe cyclones of Bay of Bengal: observations and simulations. *Mausam.* 58(0):59–66.

Smitha, A. K. H., Rao, D., Sengupta. 2006. Effect of May 2003 tropical cyclone on physical and biological processes in the Bay of Bengal. *Int. J. Remote Sens.* 27(23), 5301-5314.

Spentza, E., Chicaud, B.2012. Parametric Modelling of Cyclonic Winds For Quick Location Assessment. The Twenty-second International Offshore and Polar Engineering Conference.

Srinath, M., Kuriakose, S., Mini, K. G. 2005. Methodology for the estimation of marine fish landings in India. CMFRI Special publication, 86, pp.1-57.

Srivastav, A. K., Sinharay, K. C. 2000. Trends in the frequency of cyclonic disturbances and their intensification over Indian Seas. *Mausam* .51(0):113–118.

Subrahmanyam, B., Rao, K. H., Rao, N. S., Murthy, V. S. N., Sharp, R. J.2002. Influence of a tropical cyclone on chlorophyll_a concentration in the Arabian Sea. *Geophys. Res. Lett*. 29(0). DOI:10.1029/2002GL015892.

Thomas, A., Pringle, P., Pfleiderer, P., Schleussner, C.2018.Tropical Cyclones: Impacts, the link to Climate Change and Adaptation. *climateanalytics.org.*

Tyagi, A., Bandyopadhyay, B. K., Mohapatra, M. 2009. *Monitoring and Prediction of Cyclonic Disturbances Over North Indian Ocean by Regional Specialised*

Meteorological Centre, New Delhi (India): Problems and Prospective. Indian Ocean Tropical Cyclones and Climate Change, 93–103.

Vinayachandran, P. N., Simi, M.2003. Phytoplankton bloom in the Bay of Bengal during the northeast monsoon and its intensification by cyclones. *Geophys. Res. Lett*. 30(11):1572, doi:10.1029/2002GL016717, 2003.

Webster, P. J., Holland, J. A., Curry., Chang. 2005. Changes in tropical cyclone number, duration, and intensity in a warming environment. *Science*.309(5742): 1844–1846.

Zhang, Q., Zhang, W., Lu, X., Chen, Y. D.2011. Landfalling tropical cyclones activities in the south China: intensifying or weakening . Int.J.climatol. 32(12):1815-1824.

Spatio-temporal variation of Tropical Cyclones in Northern Indian Ocean and its impact on marine fisheries

by

Gopika Gopi

(2016-20-025)

THESIS

Submitted in partial fulfilment of the requirements for the degree of

B.Sc. – M.Sc. (Integrated) Climate Change Adaptation

Faculty of Agriculture

Kerala Agricultural University

COLLEGE OF CLIMATE CHANGE AND ENVIRONMENTAL SCIENCE

VELLANIKKARA, THRISSUR – 680

656 KERALA, INDIA

2021

ABSTRACT

One of the most significant effects of climate change is the occurrence of extreme weather events. As a result of global climate change, weather events have become more intense in recent years. The current study is an attempt to look into the spatial and temporal distribution of CDs in NIO during the climatological period 1986-2015 and the following quinquennial period 2016-2020 based on the IMD best track data. An attempt was also made to find out the impacts of the CDs in the marine fisheries sector. A large variability in the frequency and intensity of the CDs formed in the NIO was observed. When compared to CP, the frequency of CDs over NIO was decreasing during QP. Considering the Bay of Bengal (BOB) and Arabian Sea (ARB), the BOB exhibits a similar trend to the NIO, but the frequency of CDs in ARB is increasing in QP rather than CP, with a 20% increase in total cyclonic disturbances, including a 20% increase in cyclonic depressions and a 34% increase in cyclonic storms and intensity also increased in QP. A large increase in the frequency of intense cyclones was witnessed with the formation of more no. of CDs in the post-monsoon season followed by pre-monsoon and monsoon. The majority of CDs were produced between the latitudes of 5° N and 20° N. Altogether, BOB region witnessed a higher number of CDs compared to ARB in terms of frequency and Intensity. But in recent years an increase in the frequency and intensity of CDs in ARB was visible. The interseasonal and interannual variations of VF, ACE, and PDI for the NIO as a whole, as well as the BOB and ARB during the study period were also investigated. VF showed an increasing trend in AS and NIO and a decreasing trend in BOB. The ACE was found increasing in BOB, ARB and the whole NIO region except for cyclonic depressions. The overall PDI of ARB, BOB and NIO with some exceptions for cyclonic depressions. These energy metrics were highly dependent on frequency and duration and less dependent on Average Intensity. Monthly catch of fishery resources and CPUE variation in six districts of Odisha coast during the period 2007-2020 were also assessed. Higher catch was obtained at Jagatsinghpur whereas the remaining districts reported less landings with Kendrapara being the least. The SIMPER test revealed that the species that comprised the total catch were nearly identical, but with either low abundance or

complete absence. The three cyclones which contributed to the OAD in Odisha coast during 2007-2020 are Viyaru, Roanu and Amphan. The catch variation of economically important five species such as *Sardinella fimbriata, Rastrelliger kanagurta, Trichurus lepturus, Lepturacanthus savala* and *Tenulosa ilisha* in Odisha coast was studied which revealed the increase and decrease in their catch due to the impact of cyclones during 2007-2020. The chlorophyll concentration immediately after the formation of the cyclones showed an increase but a decrease was also observed after a few cyclones. The information generated from the study can help evolve adaptive action plans and help to reduce the vulnerability of those dependent on marine fisheries for their livelihood.